Title
The time has come: of GIGANTEA paralogs and grass circadian clocks

Author
Bendix, Claire

Publication Date
2015

Peer reviewed|Thesis/dissertation

The time has come: of GIGANTEA paralogs and grass circadian clocks

By

Claire Leah Bendix

A dissertation submitted in partial satisfaction of the

requirements for the degree of

Doctor of Philosophy

in

Plant Biology

in the

Graduate Division

of the

University of California, Berkeley

Committee in charge:

Frank Harmon, Chair
Sarah C. Hake
David A. Weisblat

Fall 2015

Abstract

The time has come: of GIGANTEA paralogs and grass circadian clocks

by

Claire Leah Bendix

Doctor of Philosophy in Plant Biology

University of California, Berkeley

Professor Frank Harmon, Chair

This work addresses the function of two circadian clock genes in maize, namely *gigantea1* (*gi1*) and *gi2*, as well as the larger question of the role that circadian clock genes play in grass species. Previous work on the plant circadian clock has primarily focused on the model genetic system, *Arabidopsis thaliana*, and the current conception of the clock has been constructed on the basis of this work. Arabidopsis is, however, evolutionary distant from monocot species, such as the grass *Zea mays* (maize), that are grown as crops. Furthermore, many crop plants have convoluted domestication histories that have resulted in complex genomes containing remnants of entire duplicated genomes. Circadian clock genes are proposed to be preferentially retained after whole genome duplications, and to evolve altered roles when duplicate gene copies persist in genomes.

GIGANTEA (*GI*) is a plant-specific gene that is conserved across vascular plants and plays a central role within plant circadian and developmental processes. Most plants only have one copy, but maize has two, which are both expressed. One approach taken to investigate the roles of the *gi* genes was to generate *gi* mutants in maize and evaluate their impacts on clock gene expression, developmental phenotypes, and disease resistance. This analysis showed that *gi1* and *gi2* have differential effects on clock gene expression, *gi2* may play a role in disease resistance, and that phenotypic effects of either mutant are minor compared to the Arabidopsis *gi* mutants.

A second approach was to heterologously express maize GI proteins in yeast to identify protein interaction partners. First, a set of predicted protein interaction partners were computationally identified on the basis of known Arabidopsis GI interactors. Both maize GI proteins were found to interact with homologs of known Arabidopsis interactors in maize, and in some cases, GI1 and GI2 had different interaction strengths. Second, GI1 and GI2 were used as baits in yeast two-hybrid screens against a library generated from maize cDNA to identify putative novel interacting partners. The screen identified a number of novel interaction partners, and found that each GI preferentially interacts with a different set of protein types.

Finally, evolutionary trees were elucidated in order to computationally identify orthologs of known circadian clock genes in all three species. In conjunction with this, a comprehensive RNA-Seq timecourse of reference inbred lines for maize, sorghum, and

Setaria was performed. This allowed the identification of a number of genes likely involved in the maize circadian clock. Preliminary computational analysis of this extensive dataset indicates that circadian orthologs between the species retain similar phases. For individual genes, altered expression patterns have been found between the species, which could indicate functional innovation.

These lines of evidence suggest that genes within the circadian clock have evolved novel properties across plant species. The work presented here shows that even conserved clock genes have altered functionality in monocots. The catalog of maize circadian genes will provide a starting point for further research of the maize circadian clock. Through evolution and domestication, important monocot crop species contain multiple copies of core circadian genes, meaning that crop clocks have diverged from the model based on the Arabidopsis circadian clock. The circadian clock plays important roles in growth, stress responses, and defense against pathogens, and so continued research directly focused on crop circadian clocks will aid agricultural efforts to breed resilient high-yield crops.

Dedication

For my grandmothers, Jane Bendix and Gertrud Flückiger

Table of Contents

Chapter One: Circadian clock genes universally control key agricultural traits 1
Abstract 1
Introduction 1
The circadian clock 1
Overview of flowering time control 3
A brief introduction to featured crops 4
***PRR* genes 5**
Eudicots 6
Monocots 6
***GI* genes 8**
Eudicots 9
Monocots 9
EC genes: *ELF3*, *ELF4*, and *LUX* 11
Eudicots 11
Monocots 12
Conclusions and Future Perspectives 14
Circadian clocks in abiotic stress responses 14
Circadian clocks in plant defense 15
Circadian clocks in hybrid vigor 16
Figures 18
Tables 19

Chapter Two: Genetic and phenotypic effects of *gigantea1* and *gigantea2* transposon insertion lines in maize 23
Abstract 23
Introduction 23
gi1 and *gi2* expression and *gi* insertion mutant characteristics 25
Results 26
The expression of core and output circadian clock genes is altered in *gi* insertion mutants 26
In BC3 plants, *gi1* mutant alleles cause early flowering under LD conditions but not SD conditions 27
In BC3 plants, loss of *gi1* function alters the timing of vegetative phase change and increases plant height 28
In BC5/BC6 plants, flowering time phenotypes in LD conditions are reduced and height phenotypes are eliminated 29
BC5/BC6 mutant plants have altered amounts of chlorophyll 30
BC5/BC6 mutant plants have altered disease resistance phenotypes 30
Transgenic expression of *gi1,* and to a lesser extent *gi2,* complements the flowering phenotype of an *atgi* null mutation 30
Discussion 31
Materials and Methods 35

Plant materials 35
Growth conditions for genetic analyses and timecourse sampling strategies 35
Sample collection, first-strand cDNA preparation and real-time quantitative PCR (RT-qPCR) 36
Growth and flowering time phenotyping 37
Chlorophyll measurement 38
Disease resistance measurements 38
Construction of Arabidopsis transgenic lines and flowering time analysis 38
Figures 40
Supplemental Figures 63
Supplemental Tables 74

Chapter Three: GI1 and GI2 protein interaction partners 76
Abstract 76
Introduction 76
Results 78
Conservation between maize gi1 and gi2 and AtGI 78
Pairwise yeast two hybrid assays: dilution series 79
Pairwise yeast two hybrid assays: liquid culture assay using ONPG 79
Yeast two hybrid library screen 80
Discussion 81
Materials and Methods 83
Protein alignments and visualization 83
Pairwise yeast two hybrid assays 83
Yeast two hybrid library screen 84
Figures 85
Tables 97
Supplemental Figures 103
Supplemental Tables 110

Chapter Four: Bioinformatic identification and characterization of maize circadian clock genes and grass circadian gene expression 111
Abstract 111
Introduction 111
Results 113
Diversity and evolution of circadian clock genes in grasses 113
LHY and *RVE* genes 114
PRR genes 115
GI genes 117
Evening complex genes: *ELF3, ELF4,* and *LUX* 118
ZTL, FKF1, and LKP2 genes 120
RNA-Seq reveals the diel expression patterns of grass genes 121
RNA-Seq rhythmic analysis 121
Discussion 122
Materials and Methods 125
Creation of protein lists and tree building 125
Naming maize genes and finding protein domains 126
RNA-Seq Experiment 126

Figures **128**
Tables **182**
Supplemental Figures **191**
References **194**

Acknowledgements

Thanks to my advisor, Frank Harmon, and all Harmon lab members past and present. Thanks also to my qualifying exam committee and my thesis committee, especially to Sarah Hake and David Weisblat, who served on both committees and provided me with support and enthusiasm throughout my PhD.

A special thanks goes to my mentors, Barbara Baker and Sheila McCormick. Barbara made me feel welcome in Berkeley when I first arrived, and has supported me in so many ways over the years. Sheila has provided me with advice about writing, grants, and my career, all with her characteristic humor and directness.

Thank you to my classmates Megan Cohn and Jake Brunkard, who are great friends and excellent scientists. I started this program thinking it would be a lonely endeavor, and it is all thanks to you that it hasn't been.

Thank you to my family for everything. You all know what academic work is like, and your advice and perspectives have helped keep me going. Thank you to my mother, who has cheered for me, commiserated with me, and sent me treats. Thank you to my sister, for the laughter, the distractions, and the help in making decisions. Thank you to my father, who has edited my proposals, strategized with me, and reminded me that this is a "hunting license" worth having.

Thank you to Aaron Sluis, who has been there through all the science and the feelings about science. Thank you for keeping me as sane as possible, and encouraging me to worry less and enjoy more.

Chapter One: Circadian clock genes universally control key agricultural traits

The following chapter is a modified version of an article published in *Molecular Plant* (Bendix et al., 2015).

Abstract

Circadian clocks are endogenous timers that enable plants to synchronize biological processes with daily and seasonal environmental conditions in order to allocate resources during the most beneficial times of day and year. The circadian clock regulates a number of central plant activities, including growth, development, and reproduction, primarily through controlling a substantial proportion of transcriptional activity and protein function. This review examines the roles that alleles of circadian clock genes have played in domestication and improvement of crop plants. The focus here is on three groups of circadian clock genes essential to clock function in *Arabidopsis thaliana*: *PSEUDO-RESPONSE REGULATORs*, *GIGANTEA*, and the evening complex genes *EARLY FLOWERING 3*, *EARLY FLOWERING 4*, and *LUX ARRHYTHMO*. Homologous genes from each group underlie quantitative trait loci that have beneficial influences on key agricultural traits, especially flowering time but also yield, biomass, and biennial growth habit. Emerging insights into circadian clock regulation of other fundamental plant processes, including responses to abiotic and biotic stresses, are discussed to highlight promising avenues for further crop improvement.

Introduction

The circadian clock

The endogenous circadian clock generates approximately 24-hour rhythms and confers this rhythmic behavior on a wide range of key plant processes (for reviews, see (Baldwin and Meldau, 2013; Golembeski et al., 2014; Harmer, 2009; Nagel and Kay, 2012). A fundamental role of clock-generated rhythms is to anticipate daily and seasonal environmental cycles, which allows the plant to optimize internal processes with respect to external conditions. In this way, the circadian clock provides a fitness advantage (Dodd et al., 2005; Green et al., 2002; Michael et al., 2003). Up to this point, the majority of the work on the plant circadian clock has been done with the model plant *Arabidopsis thaliana.* The information below outlines the current understanding of the Arabidopsis circadian system.

As a master controller of plant gene expression, the circadian clock regulates more than 30% of the Arabidopsis transcriptome (Covington et al., 2008; Harmer et al., 2000; Michael et al., 2008). The clock controls a similar proportion of the transcriptome in rice, papaya, maize, soybean, and poplar (Filichkin et al., 2011; Hayes et al., 2010; Hoffman et al., 2010; Khan et al., 2010; Marcolino-Gomes et al., 2014; Zdepski et al., 2008). Genes subject to circadian clock regulation are central to many important physiological processes (Figure 1.1), including flowering time (Park et al., 1999; Yu et al., 2008), phytohormone synthesis and signaling (Covington and Harmer, 2007;

Covington et al., 2008; Goodspeed et al., 2012), growth control (Nozue et al., 2007), metabolic activities (Bläsing et al., 2005; Graf et al., 2010; Gutiérrez et al., 2008; Hong et al., 2013; Ni et al., 2009), abiotic stress responses (Legnaioli et al., 2009; Liu et al., 2013), and plant-pathogen interactions (Wang et al., 2011b; Yang et al., 2015a; Zhang et al., 2013).

At the molecular level, the core circadian clock is made up of genes that interact through a series of transcriptional and post-transcriptional feedback loops to create rhythmic gene expression (Fogelmark and Troein, 2014; Hsu and Harmer, 2014). Although core circadian clock genes are expressed throughout the day, distinct morning, day, and evening transcriptional phases exist, and each phase represents the activity of multiple core circadian clock proteins (Figure 1.1).

CIRCADIAN CLOCK ASSOCIATED1 (CCA1) and LATE ELONGATED HYPOCOTYL (LHY) are two key transcription factors that are expressed and active at dawn (Green and Tobin, 1999; Schaffer et al., 1998; Wang and Tobin, 1998). These partially redundant MYB transcription factors are members of the larger *REVEILLE* (*RVE*) gene family, which also contains the principal clock activators RVE8, RVE6, and RVE4 (Chaudhury et al., 1999; Kuno et al., 2003; Rawat et al., 2009, 2011; Zhang et al., 2007). Within the promoters of target genes, CCA1 and LHY recognize two related cis-regulatory sequences known as the evening element (EE) and the CCA1-binding site (CBS) (Carre and Kay, 1995; Harmer et al., 2000; Wang et al., 1997). During the morning, CCA1 and LHY repress expression of evening expressed genes, including *TIMING OF CAB EXPRESSION1* (*TOC1*), *LUX ARRHYTHMO* (*LUX*), *EARLY FLOWERING 3* (*ELF3*), and *EARLY FLOWERING 4* (*ELF4*) (Alabadí et al., 2001; Hazen et al., 2005; Kikis et al., 2005), and at the same time promote the expression of *PSEUDO-RESPONSE REGULATOR* (*PRR*) gene family members *PRR9* and *PRR7* (Farré et al., 2005).

Sequential expression of *PRR* genes over the course of the day imposes transcriptional repression on other *PRR* family members and additional core clock genes (for review, see (Farré and Liu, 2013)). CCA1- and LHY1-stimulated peak expression of *PRR9* occurs in the morning and is soon followed by *PRR7* at midday (Matsushika et al., 2000). PRR9 and PRR7 act together in a feedback loop to suppress expression of *CCA1* and *LHY* in the late morning (Farré and Kay, 2007; Nakamichi et al., 2010). Afternoon accumulation of PRR5 represses *PRR9*, *PRR7,* and *RVE8* expression (Matsushika et al., 2000; Nakamichi et al., 2012; Rawat et al., 2011). Evening accumulation of TOC1 maintains repression of *CCA1*, *LHY*, and earlier-expressed *PRR*s; in addition, TOC1 activity feeds back to repress its own expression (Gendron et al., 2012; Huang et al., 2012). PRR3 binds to and stabilizes TOC1 protein in the vasculature (Para et al., 2007), but its role within the clock is not yet completely established.

The evening complex (EC) is a trimeric protein assembly composed of LUX, ELF3, and ELF4 (Nusinow et al., 2011). LUX is a MYB-like transcription factor (Hazen et al., 2005; Onai and Ishiura, 2005), while ELF3 and ELF4 are each unique plant-specific proteins without conserved functional domains (Doyle et al., 2002; Hicks et al., 2001). The EC represses expression of *PRR9, PRR7, GIGANTEA (GI)*, and *NIGHT LIGHT-INDUCIBLE AND CLOCK-REGULATED1* (*LNK1)* in the late evening (Chow et al., 2012; Dixon et al., 2011; Helfer et al., 2011; Herrero et al., 2012; Kolmos et al.,

2009; McWatters et al., 2007). The EC represses itself near dawn through inhibition of *LUX,* which allows the clock regulatory cycle to repeat the next day (Helfer et al., 2011).

RVE8 activates evening expressed genes in opposition to CCA1 and LHY (Rawat et al., 2011). RVE8 protein peaks in the afternoon, although its transcript has dawn-phased expression. Binding of RVE8 to EE sequences activates expression of *TOC1*, *PRR5, PRR9, GI, LUX,* and *ELF4* (Farinas and Mas, 2011; Hsu et al., 2013; Rawat et al., 2011). RVE8 activity is partially redundant with RVE4 and RVE6 (Hsu et al., 2013). *LNK1* and *LNK2* are also expressed at dawn, and have slightly delayed protein expression. Both LNK1 and LNK2 proteins physically interact with RVE transcription factors and act as co-activators for RVE8 and RVE4 in the upregulation of *PRR5* and *TOC1* transcription (Xie et al., 2014).

An important post-transcriptional event is control of TOC1 and PRR5 protein accumulation by the combined activities of ZEITLUPE (ZTL) and GI (Demarsy and Fankhauser, 2009; Ito et al., 2012). ZTL is an F-box protein that serves as a clock-specific blue light photoreceptor (Kim et al., 2007b; Somers et al., 2000). GI is a large plant-specific protein that is a scaffold for multiple protein complexes (Fowler et al., 1999; Huq et al., 2000; Park et al., 1999). Activation of ZTL by light promotes interaction with GI and this protects both from degradation by the 26S proteasome (Kim et al., 2007b). Once the ZTL-GI complex associates with TOC1 or PRR5, the PRR protein is degraded by the 26S proteasome (Fujiwara et al., 2008; Kiba et al., 2007; Kim et al., 2007b; Más et al., 2003). Similarly, GI protein accumulation is controlled by complex formation with ELF3, which induces GI degradation by the 26S proteasome (Yu et al., 2008).

The timing of gene expression and the regulatory relationships within the core oscillator are essential for maintaining circadian rhythms. Together, circadian clock genes form a highly interconnected regulatory network (Fogelmark and Troein, 2014; Hsu et al., 2013; Pokhilko et al., 2012) that influences a wide range of plant signaling and metabolic pathways (Figure 1.1).

Overview of flowering time control

Flowering time is regulated by both internal and external cues, which are integrated to ensure correct timing of this critical developmental decision. In *Arabidopsis*, the vernalization, autonomous, and photoperiodic pathways together determine flowering time, with the contribution of each dependent on the genetic background of the plant (for review, see (Shim and Imaizumi, 2015)). These signaling networks converge on three main floral integrators: *LEAFY* (*LFY*), *SUPPRESSOR OF OVEREXPRESSION OF CO 1* (*SOC1*), and *FLOWERING LOCUS T* (*FT*) (Koornneef et al., 1998; Pajoro et al., 2014). Because of the well-defined regulatory association between the circadian clock and the photoperiodic flowering pathway (Johansson and Staiger, 2015; Song et al., 2013), the discussion here is limited to the signaling networks involved in this pathway.

Arabidopsis assesses day length, or photoperiod, through circadian clock regulation of key flowering time genes. The two primary genes involved are *CONSTANS* (*CO*), a zinc-finger transcription factor (Putterill et al., 1995), and *FT* (Kobayashi et al., 1999; Turck et al., 2008). CO is a transcriptional activator stabilized by light that is expressed in the leaf and induces the expression of *FT* in long day (LD) conditions (Kobayashi et al., 1999). FT protein is a small transcriptional co-factor, which

acts as a mobile florigen that is expressed in leaves, moves into the phloem, and travels to the shoot apical meristem to induce the transition from vegetative to reproductive development (Corbesier et al., 2007; Jaeger and Wigge, 2007; Turck et al., 2008). Many and varied genes are involved in photoperiodic flowering across different species, yet *FT* homolog floral promotion activity appears to be conserved (for reviews, see: (Andrés and Coupland, 2012; Ballerini and Kramer, 2011; Greenup et al., 2009)). In some species, other cues are required before photoperiodic cues can be perceived: for example, temperate cereals require vernalization (Shrestha et al., 2014). While perception of and response to these cues are important, a full discussion of these pathways is beyond the scope of this review.

A brief introduction to featured crops

The crops featured here include representatives of both eudicots and monocots (Table 1.1), two major vascular plant clades that have evolved independently for over 100 million years (Chaw et al., 2004). The primary eudicots discussed are *Brassica rapa* L., sugar beet (*Beta vulgaris* ssp. *vulgaris*), soybean (*Glycine max*), pea (*Pisum sativum*), and lentil (*Lens culinaris*). *B. rapa* is a diploid relative of Arabidopsis. Subspecies of *B. rapa* are widely cultivated, have diverse growth habits, and encompass considerable natural variation (Lou et al., 2011). Cultivated sugar beet likely descends from the European wild beet (*Beta vulgaris* ssp. *maritime*) (Jung et al., 1993), which has a wide latitudinal distribution and correspondingly varied vernalization requirements (Dijk et al., 1997). Sugar beet is a biennial crop that requires vernalization and subsequent long day (LD) photoperiods to flower (Bell and Bauer, 1942). Soybean is a diploid legume species originally from East Asia that is now widely grown across the Americas. Soybean flowers in short day (SD) photoperiods and seminal work on photoperiodism utilized soybean (Garner and Allard, 1920, 1922). Pea and lentil are also diploid members of the legume family, and were domesticated early in human history. The wild forms of both species require LD conditions for flowering, but selection of alleles that allow SD flowering produced varieties now used as spring crops (Weller and Ortega, 2015; Weller et al., 2012).

The monocot crops discussed are rice (*Oryza sativa*), barley (*Hordeum vulgare*), wheat (*Triticum* sp.), sorghum (*Sorghum bicolor*), and maize (*Zea mays* ssp. *maize*). Rice was domesticated in Asia and today is a staple crop grown around the world. There are two main varieties: short-grained *japonica* and long-grained *indica* (Callaway, 2014). Flowering of rice is stimulated by SD conditions (Chandraratna, 1953). Barley occurs in two main forms: the winter type requires vernalization, and is cold-tolerant, but sensitive to SD, while the spring type does not require vernalization, cannot tolerate cold, and is insensitive to SD conditions (von Zitzewitz et al., 2005). Wheat has a complex domestication history, and multiple wheat varieties are still used in agriculture today: diploid einkorn wheat (*Triticum monococcum*), hexaploid bread wheat (*Triticum aestivum*), and tetraploid emmer wheat (*Triticum turgidum* ssp. *dicoccum*). Wheat is generally classified as a LD plant and it was the major Green Revolution crop, providing one of the first examples of improved yields with modern breeding technology (Borlaug, 1983; Pingali, 2012; Zhang et al., 2014). Sorghum is a drought-tolerant diploid grass, and ancestrally a SD plant (Garner and Allard, 1923; Quinby and Karper, 1945). Maize is also a diploid grass that is both an important crop plant as well as a model organism for biological research (Strable and Scanlon, 2009). Maize was domesticated in Mexico

from the wild progenitor teosinte (*Zea mays* ssp. *parviglumis*) (Beadle, 1939; Benz, 2001; Galinat, 1983; Iltis, 1983), which is a SD plant (Emerson, 1924), and tropical maize inbreds commonly exhibit accelerated flowering in SD (Galinat and Naylor, 1951; Kuleshov, 1933). Recent advances in sequencing technologies are providing genetic insights into modern crop species, facilitating efforts to improve crop traits (Olsen and Wendel, 2013; Renny-Byfield and Wendel, 2014).

This review describes alleles of circadian clock genes that have been shown to directly influence key crop traits (Table 1.1). It is organized by gene group beginning with the *PRR* gene family, then the *GI* genes, and ending with the EC genes. Throughout, eudicot crop plants are discussed first, as these closer relatives of Arabidopsis are expected to have circadian clocks similar to this model, followed by monocot crop plants, which form the bulk of the crop species grown worldwide. Finally, we introduce promising avenues for future research on circadian clock genes in crop species based on recent work in Arabidopsis and *Brassica oleracea*.

PRR genes

The *PRR* gene family is a major contributor to the clock system in Arabidopsis, with five genes (*TOC1, PRR3, PRR5, PRR7*, and *PRR9*) serving as clock components (Farré and Liu, 2013). The Arabidopsis *PRR*s contribute to many clock-associated functions, including flowering time regulation (Nakamichi et al., 2007, 2012), clock temperature compensation and entrainment (James et al., 2012; Salomé and McClung, 2005; Salomé et al., 2010), response to photosynthetic sugar (Haydon et al., 2013), maintenance of mitochondrial homeostasis (Fukushima et al., 2009; Nakamichi et al., 2009a), heat shock response (Karayekov et al., 2013), cold stress response (Nakamichi et al., 2009b, 2012), oxidative stress response (Liu et al., 2013), and the regulation of stomatal conductance (Liu et al., 2013).

All PRR proteins contain a pseudo-response regulator domain and a CCT (CO, COL, and TOC1) motif (Makino et al., 2000; Mizuno and Nakamichi, 2005; Putterill et al., 1995; Strayer et al., 2000). The pseudo-response regulator domain shares homology with the receiver domain of response regulators from two-component signal transduction systems, but key residues normally involved in signaling are substituted in the PRR proteins (Makino et al., 2000; Mizuno and Nakamichi, 2005; Putterill et al., 1995; Strayer et al., 2000). The CCT motif is shared with CONSTANS-LIKE (COL) family transcription factors, which includes the flowering time protein CONSTANS (CO) (Makino et al., 2000; Mizuno and Nakamichi, 2005; Putterill et al., 1995; Strayer et al., 2000).

*PRR*s likely evolved from true response regulators with evolutionary analysis indicating that the *TOC1* clade diverged first, followed by the clade containing *PRR5* and *PRR9*, and most recently the clade containing *PRR3* and *PRR7* (Satbhai et al., 2011). In monocots, gene duplication events produced *PRR37* and *PRR73,* which are phylogenetically and syntenically similar to Arabidopsis *PRR7*, as well as *PRR59* and *PRR95,* which are similar to Arabidopsis *PRR5* (Takata et al., 2010).

Eudicots

B. rapa has eight *PRR* genes, of which five are orthologs of the *AtPRRs* and three are retained duplicates (Kim et al., 2007a, 2012). *BrPRR*s are under circadian control and are expressed in a sequential wave similar to the Arabidopsis PRR genes (Kim et al., 2012). When mapped to chromosomes, *BrPRR*s were found to be close to loci that affect flowering-time (Kim et al., 2012). A pioneering genomic study in *B. rapa*, which investigated the consequences of genome fractionation (i.e., gene loss or retention during diploidization of the triplicated genome following whole-genome duplication) for circadian clock genes, showed that *BrPRR* genes, as well as *BrREV* and other circadian-clock-associated genes, have been preferentially retained in comparison with neighboring genes, core eukaryotic genes, and a set of genes chosen at random (Lou et al., 2012).

In sugar beet, bolting locus *B* is a major genetic factor responsible for the switch from an annual to a biennial growth habit in modern cultivars (Abegg, 1936; Boudry et al., 1994). The gene underlying this locus is a *PRR* gene named *BOLTING TIME CONTROL 1* (*BvBTC1*). *BvBTC1* is a member of the clade containing *AtPRR3* and *AtPRR7*, but appears to correspond to a third copy of an ancestral *PRR. BvBTC1* RNA interference (RNAi) lines have unaltered circadian gene expression (Pin et al., 2012), supporting the idea that *BvBTC1* may not be involved in the sugar beet circadian clock. Instead, *BvBTC1* may fulfill *CO* function together with the zinc-finger transcription factor *BvBBX19*, recently identified as the basis of bolting locus *B2* (Dally et al., 2014). Sugar beet has two *FT* genes: *BvFT1,* which functions as a floral repressor, and *BvFT2*, which functions as a canonical floral activator (Pin et al., 2010). In annuals, *BvFT1* expression is constitutively low, while in biennials, *BvFT1* is initially expressed at a high level that is then gradually reduced by vernalization. On the other hand, *BvFT2* is induced in LD conditions in both annuals and biennials. *BvBTC1 RNAi* lines in an annual background show *BvFT* expression profiles characteristic of biennial plants (Pin et al., 2012). When vernalized, *BvBTC1 RNAi* plants are stunted and have a delayed flowering phenotype similar to that of *BvFT2 RNAi* plants. Biennial cultivars carry *Bvbtc1,* a recessive allele that appears to produce a functional gene product capable of regulating *BvFT* genes, yet requires vernalization for activity (Pin et al., 2012).

PRR genes have been identified in other eudicot crops, but these remain functionally uncharacterized. In the papaya (*Carica papaya*) genome, members of all three *PRR* clades are present in an expanded gene family, while other light- and circadian-related genes are proportionally underrepresented compared with the poplar or Arabidopsis genomes (Ming et al., 2008). The *CpPRR* genes appear to be regulated by the same time-of-day specific cis-regulatory elements found in promoters of circadian clock-regulated genes in Arabidopsis (Zdepski et al., 2008). These findings provide tantalizing evidence that circadian clock genetics of less tractable crop plants have diverged from the Arabidopsis model.

Monocots

Rice has five *PRR* genes, all of which are under circadian control. *OsPRRs* are expressed in a sequential wave that differs from the Arabidopsis *PRR*s in that *OsPRR73* and *OsPRR37* peak together first, followed by a shared peak of *OsPRR95* and *OsPRR59* (Murakami et al., 2003). Expression of *OsPRR1* peaks in the evening in a pattern analogous to Arabidopsis *TOC1* (Murakami et al., 2003).

Recent work showed that *OsPRR37* is the gene underlying the *Heading date 2* (*Hd2*) QTL present in rice cultivars grown across northern regions of Asia and Europe (Koo et al., 2013). The strong *Hd2* alleles present in photoperiod-insensitive *indica* and *japonica* rice cultivars correspond to mutant alleles of *OsPRR37*. In addition to *Hd2*, *japonica* cultivars grown at the northern limit of rice cultivation (40-53° N) also have early flowering alleles of *Ghd7*/*Hd4* (Koo et al., 2013). Naturally occurring *Ghd7/Hd4* alleles have pleiotropic effects on yield, growth, and flowering time, and non-functional alleles are present in rice planted for short growing seasons (Xue et al., 2008). Thus, worldwide expansion of rice cultivation to high latitude areas selected for mutation of both *OsPRR37* and *Ghd7*, likely due to the very early flowering conferred by this combination of alleles (Koo et al., 2013).

Crosses between winter and spring barley identified the *Photoperiod-H1 (Ppd-H1*) QTL that governs LD photoperiod sensitivity (Laurie et al., 1995). The gene underlying *Ppd-H1* is a *PRR37* gene (*HvPRR37*) (Turner et al., 2005). A mutation in the *HvPRR37* CCT domain (*ppd-H1)* causes late flowering and alters expression of flowering time genes in ways consistent with the late flowering phenotype, including reduced expression of *HvCO* and *HvFT* (Campoli et al., 2012; Turner et al., 2005). *HvPRR37* has rhythmic expression patterns similar to *AtPRR7*, but may have a limited role in the circadian oscillator as the hypomorphic *ppd-H1* allele minimally affects the expression patterns and levels of putative core circadian clock genes (Campoli et al., 2012).

A characteristic of Green Revolution wheat varieties is earlier flowering (Borlaug, 1983; Pingali, 2012). The photoperiod-insensitive *Ppd-D1a* allele is the major source of early flowering for hexaploid wheat (*Triticum aestivum)* (Worland et al., 1998). A comparative genomic study found the *Ppd-D1a* allele affects a *TaPRR37* gene that is in a genomic location syntenic with *HvPRR37* (Beales et al., 2007). Sequencing of the *Ppd-D1a* allele revealed a 2-kilobase pair (kb) deletion upstream of the *Ppd-D1* gene. This polymorphism has two effects on *Ppd-D1* expression: 1) a delay in timing of expression that results in peak transcript levels coinciding with the dark period of a long day instead of the light period, and 2) the use of an altered transcriptional start site (Beales et al., 2007). Early flowering in plants carrying the *Ppd-D1a* allele is associated with increased *TaFT1* expression. This may be the result of reduced peak *TaCO1* expression in *Ppd-D1a* plants, or a direct effect of the shift in *Ppd-D1* peak expression (Beales et al., 2007). Therefore, *Ppd-D1* represses flowering and its activity appears be light dependent.

Two other *TaPRR37* homeologs are present in the hexaploid wheat genome, *Ppd-A1* and *Ppd-B1*. Polymorphisms that cause altered transcriptional regulation of each gene are associated with photoperiod-insensitive alleles (Seki et al., 2011; Shaw et al., 2013). The *Ppd-A1a* allele is a deletion of 1 kb upstream from the gene (Shaw et al., 2013), and the *Ppd-B1a* allele has an upstream insertion of 300 base pairs (Seki et al., 2011). Together, the photoperiod-insensitive alleles *Ppd-D1a, Ppd-A1a*, and *Ppd-B1a* account for quantitative differences in flowering times and yields. Lines carrying multiple photoperiod-insensitive alleles flower earlier than lines carrying single alleles. Moreover, these alleles act additively to increase levels of *TaFT1* expression (Shaw et al., 2012). This indicates that the three *TaPRR37* genes act together to inhibit flowering via direct or indirect repression of *TaFT1* expression

Sorghum has six historically identified maturity loci, *Ma_{1-6}* (Quinby, 1966, 1967, 1975; Quinby and Karper, 1945; Rooney and Aydin, 1999). Recessive early flowering *ma_1* alleles were crucial in sorghum domestication (Quinby, 1966, 1967, 1975) and its adaptation to temperate regions (Quinby, 1974; Smith and Frederiksen, 2000); on the other hand, dominant late flowering *Ma_1* alleles have been important in more recent breeding efforts to generate lines for biofuel production (Mullet et al., 2014). The gene underlying *Ma_1* is a *PRR37* gene (*SbPRR37*) (Murphy et al., 2011). *SbPRR37* expression is circadian clock regulated in a photoperiod-dependent waveform: in SD conditions, *SbPRR37* peaks during the morning, while in LD or constant light (L/L) conditions, a morning and an evening peak are present. The morning-phased peak is a conserved characteristic seen in *PRR37* genes of other grasses (Beales et al., 2007; Turner et al., 2005) and *AtPRR7* (Mizuno and Nakamichi, 2005), but the evening-phased peak appears to be unique to *SbPRR37*. This light-dependent evening expression is associated with repression of flowering under LD conditions through increased *SbCO* expression that, in turn, represses the florigen genes *SbFT*, *SbZCN8*, and *SbZCN12* (Murphy et al., 2011).

In the crop plant species highlighted here, the primary role of the *PRR* family genes appears to be control of flowering time. The *PRR* genes appear to have diverse roles in their contribution to flowering across species; however, the role of *PRR* genes in regulation of florigen gene expression correlates well with ancestral photoperiod behavior of that species (Shrestha et al., 2014). A question that has yet to be widely addressed is whether *PRR* genes influence other responses of crop plants to their environment, such as reactions to temperature cues.

GI genes

The first mutant alleles of *GI* were identified in screens for late flowering mutants in Arabidopsis (Koornneef et al., 1991; Rédei, 1962). Subsequent work demonstrated that *AtGI* is required for normal circadian rhythms, photoperiodic flowering time, and blue light signaling (for review, see (Crepy et al., 2007)). The circadian clock regulates expression of the *AtGI* transcript and the protein levels oscillate accordingly (Fowler et al., 1999; Huq et al., 2000; Park et al., 1999). AtGI physically interacts with other proteins to modify their stability or activity (Kim et al., 2007b; Park et al., 2013; Yu et al., 2008), and likely associates with DNA to modify transcription (Sawa and Kay, 2011; Song et al., 2014). In photoperiodic flowering pathways, AtGI acts directly and indirectly to stimulate flowering primarily by promoting *CO* and *FT* expression (Park et al., 1999; Sawa and Kay, 2011; Sawa et al., 2007; Song et al., 2014; Suárez-López et al., 2001). *AtGI* is also involved in regulation of carbohydrate metabolism (Dalchau et al., 2011), phytohormone signaling (Penfield and Hall, 2009; Tseng et al., 2004), fruit set (Brock et al., 2007), and stress responses to stimuli including cold (Cao et al., 2005), karrikin (Nelson et al., 2010), herbicide (Qian et al., 2014), drought (Riboni et al., 2013), and salt (Park et al., 2013).

Orthologs of *AtGI* are present in all characterized vascular plant genomes and the proteins are highly conserved across the entire length of the protein. Beyond vascular plants, a GI protein acts to promote a LD-dependent growth phase transition in a non-vascular plant, the liverwort *Marchantia polymorpha* (Kubota et al., 2014).

Eudicots

LATE BLOOMER 1 (LATE1) is an ortholog of *AtGI* from pea (Hecht et al., 2007). *late1* mutants flower later, for a longer time, and branch more when grown under normally inductive LD conditions. A strong decrease in expression of *FTL*, a pea homolog of *FT* (Hecht et al., 2007), is associated with the delayed flowering of *late1* plants. This effect on *FTL* expression is similar to the lower *FT* expression observed in Arabidopsis *gi* mutants (Suárez-López et al., 2001). The *CO* ortholog, *PsCOLa,* does not have altered expression, and likely does not have a role in flowering time regulation in legumes (Hecht et al., 2011; Weller and Ortega, 2015; Wong et al., 2014). At the genetic level, *LATE1* is important for proper circadian clock function. Like Arabidopsis *gi* mutants (Martin-Tryon et al., 2007), *late1* plants display reduced amplitude and phase advances in the rhythmic expression of the putative clock genes *PsLHY, PsTOC1,* and *PsELF4*. In addition, *LATE1* is required for normal amplitude circadian rhythms in both L/L and constant dark (D/D) conditions (Liew et al., 2009). These findings indicate that *LATE1* has the same range of functions as *AtGI*.

The *E* series of maturity loci, *E1-8,* regulate flowering time and the length of the reproductive phase in soybean (Bernard, 1971; Bonato and Vello, 1999; Buzzell, 2011; Cober and Voldeng, 2001; Cober et al., 2010; McBlain and Bernard, 1987). Of these, the *E1-E4* and *E7* loci are responsible for photoperiodic control of flowering time (Watanabe et al., 2012; Weller and Ortega, 2015; Zhai et al., 2014). Mapping of the *E2/FT2* locus showed that the responsible gene is *GmGIa*, a soybean homolog of *AtGI* (Watanabe et al., 2011; Weller and Ortega, 2015). The *E2* locus enhances the photoperiod response, contributes to early flowering, and is involved in latitudinal adaptation (Jiang et al., 2014; Weller and Ortega, 2015). Plants carrying an *e2* allele flower early and have increased expression levels of *GmFT2a*, a soybean *FT* homolog (Watanabe et al., 2011). This indicates *GmGIa* has a repressive role in flowering. Including *GmGIa*, soybean has three *GmGI* genes, but four expressed transcripts have been described (Li et al., 2013). It remains unclear what contribution the other two *GmGI* genes make to flowering time and whether any of the *GmGI* genes are important for circadian clock function.

The role of *GI* homologs has also been examined in other eudicot crops, including tomato (*Solanum lycopersicum*), potato (*Solanum tuberosum*), and radish (*Raphanus sativus*). A comparative analysis of Solanaceae transcriptomes indicated a role for *GI* in tomato seed germination and potato tuber formation (Rutitzky et al., 2009). In tomato seeds, *SlGI* is upregulated by red light, but not far red light (Rutitzky et al., 2009), indicating *SlGI* may contribute to germination as *AtGI* does in Arabidopsis (Penfield and Hall, 2009). Potato *GI* (*StGI*) is more highly expressed in LD than SD in a phyB-dependent manner and may be involved in tuber formation (Rodríguez-Falcón et al., 2006; Rutitzky et al., 2009). Another example comes from radish, where reducing expression of *RsGI* results in late-flowering plants with short stature that produce more radish biomass (Curtis et al., 2002).

Monocots

Rice GI (*OsGI*) function is well studied with regard to its contribution to flowering time and the circadian clock (for review, see (Izawa, 2012)). Transgenic overexpression of *OsGI* produces photoperiod-independent late flowering that is accompanied by increased expression of *Hd1*, a rice *CO* homolog, and reduced expression of *Hd3a*, a

rice FT homolog (Hayama et al., 2003). Two independent *OsGI* mutant alleles, *osgi-1* and *osgi-2*, delay flowering under SD photoperiods but not in LD conditions (Izawa et al., 2011). The photoperiod-specific flowering time phenotype of these mutants is due to the primary role of OsGI in promoting *Hd1* expression (Shrestha et al., 2014). Since *Hd1* upregulates *Hd3a* in SD but serves as its repressor in LD (Kojima et al., 2002; Yano et al., 2000), the flowering time phenotype of the *osgi* alleles reflects the photoperiod dependent activity of *Hd1.*

OsGI is also important for proper regulation of genes within and outside the rice circadian clock. Both *osgi-1* and *osgi-2* cause downregulation of *OsLHY* (Izawa et al., 2011), yet *OsPRR1* is upregulated and its rhythms are dampened. *OsPRR59* and *OsPRR95* also exhibit damped rhythms and higher expression, while *OsPRR73* and *OsPRR37* are largely unaffected. Thus, OsGI appears to repress expression of evening expressed *OsPRR1*, *OsPRR59*, and *OsPRR95*, but not day expressed *OsPRR73* and *OsPRR37*. In addition, loss of *OsGI* activity causes transcriptome-wide changes in gene expression: 75% of >27,000 expressed genes in field-grown plants have altered expression in the *osgi-1* background (Izawa et al., 2011). Furthermore, different amplitude and phase are apparent for a set of over 6,000 rhythmically expressed genes. Loss of OsGI in *osgi-1* plants cause pleiotropic changes in metabolism and development of field grown plants, including increased starch content, decreased chlorophyll content, and reduced vegetative growth (Izawa et al., 2011). *osgi-1* plants also have longer panicles, increased panicle and spikelet numbers, and increased grain number. However, *osgi-1* does not positively affect overall grain yield because the grains of mutant plants are lighter than those of wild type plants (Izawa et al., 2011).

Barley *GI* (*HvGI*) appears to play a limited role in flowering time. Initial genetic mapping did not show association between *HvGI* and known flowering time QTLs or photoperiod genes (Dunford et al., 2005). Later work with a wild barley backcross population linked *HvGI* to a flowering time QTL in that population (Wang et al., 2010). In this case, the effect on flowering time was small and disappeared in wild barley introgression lines. In addition, a genome-wide association study found 19 heading date QTLs in a panel of 200 spring barley lines, one of which mapped to the *HvGI* locus (Pasam et al., 2012).

The maize genome has two *GI* genes, *Zmgi1* and *Zmgi2*, and *Zmgi1* is consistently expressed more highly than *Zmgi2* (Hayes et al., 2010; Mendoza et al., 2012; Miller et al., 2008). Analysis of the expression of circadian clock genes in *Zmgi1* and *Zmgi2* mutants shows that *Zmgi1* regulates the expression of core circadian clock genes, while *Zmgi2* regulates circadian output genes (Chapter Two). In the backcross three generation, *Zmgi1* mutant plants undergo vegetative phase change earlier, flower earlier, and grow taller than non-mutant plants in LD conditions (Bendix et al., 2013). These plants also have increased expression of *constans of Zea mays1* (*conz1*), a maize *CO* homolog (Meng et al., 2011; Miller et al., 2008), and *Zea mays CENTRORADIALIS 8* (*ZCN8*), a maize *FT* homolog (Danilevskaya et al., 2008; Lazakis et al., 2011; Meng et al., 2011). The observed phenotypes are largely lost in later backcross generations, and are not apparent in *zmgi2* mutant plants (Chapter Two). Both *zmgi1* and *zmgi2* appear to be functionally similar to *AtGI*, as transgenic expression in a null *atgi* mutant restores normal flowering time and growth habit (Bendix et al., 2013, Chapter Two).

Studies across eudicot and monocot crop plants provide evidence of conserved function for *GI* genes in regulation of flowering time. As with the *PRR* genes, whether *GI* genes promote or inhibit flowering varies by species, and is linked to the ancestral growth habit of the plant in question. In general, GI promotes flowering in long day plants and inhibits flowering in short day plants. The pleiotropic effects on metabolism and development caused by loss of *OsGI* indicate a broader contribution to multiple key agronomic traits, possibly linked to a significant change in circadian clock function. This possibility is supported by strong alterations in circadian gene expression of *GI* mutants. *GI* genes are also linked to growth processes throughout the plant life cycle in other crop plants, including maize, tomato, and radish.

EC genes: *ELF3*, *ELF4*, and *LUX*

In Arabidopsis, the *LUX*, *ELF3*, and *ELF4* genes were first identified in separate genetic screens as mutants affecting the circadian clock, photomorphogenesis, or the photoperiodic flowering response (Doyle et al., 2002; Hazen et al., 2005; Khanna et al., 2003; Onai and Ishiura, 2005; Zagotta et al., 1996). As expected for proteins that function as a complex, single and double mutants of *ELF3*, *ELF4*, and *LUX* have comparable circadian clock, growth, and flowering time phenotypes (Nusinow et al., 2011). The EC is an integral part of the circadian clock (Dixon et al., 2011; Helfer et al., 2011; Thines and Harmon, 2010) and a direct regulator of genes that control plant growth processes (Nusinow et al., 2011). EC genes are also implicated in shade avoidance processes (Coluccio et al., 2011; Jiménez-Gómez et al., 2010), water transport in the root (Takase et al., 2011), osmotic stress response (Habte et al., 2014), response to UV-B stress (Takeuchi et al., 2014), and senescence inhibition (Sakuraba et al., 2014).

Eudicots

Four pea loci that affect flowering under SD conditions are *HIGH RESPONSE TO PHOTOPERIOD (HR/QTL3)*, *DIE NEUTRALIS (DNE*), *STERILE NODES (SN)*, and *PHOTOPERIOD RESPONSE (PPD)* (King and Murfet, 1985; Murfet, 1971, 1973; Taylor and Murfet, 1996). Alleles at each locus shorten the length of the reproductive phase, reduce basal branching, and cause early flowering in SD conditions.

A pea ortholog of *ELF3* (*PsELF3*) underlies *HR*, as well as a major photoperiodic flowering QTL identified in crosses between wild and cultivated pea accessions (Weller et al., 2012). Spring cultivars harboring the mutant allele of *HR (hr)* display early flowering, reduced branching, and insensitivity to red/far-red light ratios at the end of the day. The *hr* allele harbors a frame-shift mutation near the end of the first exon of *PsELF3* that results in a severely truncated transcript. Heterologous expression of wild type *PsELF3* in a null *atelf3* background complements the mutant phenotype, but expression of the *hr* allele does not (Weller et al., 2012). The *hr* allele is present across many domesticated pea germplasms, and likely played an important role in breeding pea to have a spring-flowering habit (Weller and Ortega, 2015).

In closely related lentil, a QTL that controls flowering in SD conditions is tightly linked with an ortholog of *PsELF3* (Sarker, 1999; Weller et al., 2012). Sequencing of *LcELF3* in lines with an early flowering allele of this QTL revealed a synonymous mutation at the splice acceptor site for exon 3 (Weller et al., 2012). This mutation results in an exon-skipping event that produces a truncated transcript with a modified reading

frame. Thus, photoperiodic flowering in lentil also depends on the activity of an EC protein.

DNE is a pea ortholog of *AtELF4* (Liew et al., 2009). In SD conditions, plants with the *dne* loss of function allele have increased expression of *FTL*. In addition, loss of *DNE* function modifies behavior of the pea circadian clock, primarily under diurnal conditions. In SD, LD, L/L, and D/D conditions, expression of the clock genes *PsTOC1*, *LATE1*, and *PsPRR59* is perturbed (Liew et al., 2009), but none of the alterations observed are major, and they are not consistent between genes. In contrast, *atelf4* mutants have profoundly altered clocks with reduced accuracy in period and a propensity for arrhythmicity (Doyle et al., 2002). Thus, *DNE* may be involved in the circadian clock, but in a less central role than *AtELF4*.

Identification of *SN* revealed it to be the *LUX* ortholog of pea (Liew et al., 2014). Similar to plants carrying *dne* alleles, plants with *sn* alleles are early flowering, insensitive to photoperiod, and have increased expression of the pea *FT* genes *FTa1*, *FTa2*, *FTc*, and *PIM*, but not *FTL* (Liew et al., 2014). Multiple naturally occurring *sn* alleles exist in pea, and were likely used to expand the range of pea cultivation in the United States (Liew et al., 2014). It should, however, be noted that *sn* alleles only exist in the subset of pea lines that already carries the *hr* mutation (Weller and Ortega, 2015).

sn plants grown under SD and D/D conditions have altered expression of clock genes, but as in *dne* plants the perturbations are neither major nor consistent across genes (Liew et al., 2014). Under L/L conditions, a more consistent alteration of expression is seen: most circadian genes exhibit advanced peak expression and altered amplitude. Both amplitude and rhythmicity of *SN* are reduced in a *hr* mutant background grown in L/L, whereas *DNE* expression appears unaltered. This may indicate a different regulatory relationship exists between EC genes in pea than that seen in Arabidopsis.

Monocots

The rice genome has two *ELF3* orthologs, *OsELF3-1* and *OsELF3-2* (Murakami et al., 2007). Multiple independent alleles that modify *OsELF3-1* activity are known, including two identified as QTLs, *early flowering 7 (ef7)* (Saito et al., 2012) and *heading date 17 (hd17)* (Matsubara et al., 2012); two insertion mutants, the transposon insertion allele *oself3* (Yang et al., 2013) and the T-DNA insertion allele *oself3-1* (Zhao et al., 2012)*;* and transgenic RNAi lines (Zhao et al., 2012). The strong knockout alleles *ef7* and *oself3* each cause late flowering regardless of photoperiod (Yang et al., 2013; Yuan et al., 2009). Similarly, the *oself3-1* line is late flowering under both natural LD (>14h light) and SD (<10h light) conditions (Zhao et al., 2012). On the other hand, the *Hd17 QTL* in Japanese 'Nipponbare' rice cultivars is a weak loss of function allele that produces a later flowering phenotype only in LD conditions (Matsubara et al., 2012). Regardless of the allele, the strong *OsELF3-1* mutants cause high expression of *Ghd7* and *Hd1* along with concomitant low expression of *Hd3a* (Saito et al., 2012; Zhao et al., 2012). In addition to lower *Hd3a* expression, analysis of *oself3-1* and RNAi lines found reduced expression of *Ehd1* (Zhao et al., 2012), a flowering time promoter (Doi et al., 2004). These results demonstrate that loss of *OsELF3-1* disrupts photoperiod-dependent control of key flowering time genes, which produces a photoperiod-insensitive flowering phenotype.

In addition to its role in flowering time, *OsELF3-1* is involved in light-dependent regulation of circadian clock genes (Zhao et al., 2012). The *oself3-1* mutant causes

higher amplitude expression of *OsGI* and *OsPRR*s in diurnal conditions (Zhao et al., 2012). In contrast, this mutant exhibits dampened rhythms for *OsPRR*s and *OsGI* expression in L/L conditions, as well as loss of *OsLHY* rhythmicity (Zhao et al., 2012). Similar phenotypes are seen in *oself3* plants grown in diurnal and L/L conditions, indicating disrupted clock function when *OsELF3-1* activity is absent (Yang et al., 2013). Characterization of *OsELF3-1* RNAi lines confirms that *OsELF3-1* is required for sustained rhythmic expression of *OsLHY* and *OsPRR* in L/L conditions (Zhao et al., 2012).

The contribution of *OsELF3-2* to flowering time or the circadian clock remains unclear. The *osef3* allele is a T-DNA insertion in *OsELF3-2* (Fu et al., 2009). *osef3* plants are late flowering in both SD and LD conditions. On the other hand, additional T-DNA insertion alleles of *OsELF3-2* do not have measurable defects in flowering time (Zhao et al., 2012). The reason for this discrepancy is not yet known.

EAM8 is a barley ortholog of *ELF3* (*HvELF3)* (Faure et al., 2012). The barley *early maturity* (*eam*) loci have been used to breed cultivars for short growing seasons around the world because they confer reduced or nonexistent responses to photoperiod (Laurie et al., 1995; Lundqvist, 2009; Zakhrabekova et al., 2012). Cultivars carrying early flowering *eam8/mat-a* alleles are grown at high latitudes (Börner et al., 2002), and plants with *eam8* mutant alleles have high expression levels of *Ppd-H1*, *HvCO,* and *HvFT1*. In addition, *eam8* mutants have disordered circadian gene expression analogous to *atelf3* mutants (Hicks et al., 1996). Circadian genes, such as *HvCCA1, HvTOC1,* and *HvGI*, display reduced expression levels and altered timing of expression in *eam8* mutants: these effects on expression become especially apparent under L/L conditions (Faure et al., 2012). Dampened rhythmic expression for output genes is also present in *eam8*, indicating significant clock disruption (Faure et al., 2012).

EAM10 is a barley ortholog of *LUX, HvLUX1* (Campoli et al., 2013). Like *eam8* alleles, *eam10* alleles cause early flowering independent of photoperiod. This phenotype is linked to increased expression of *HvFT* in SD conditions. *eam10* alleles also disrupt rhythmic expression of core clock and output genes. Stem elongation in *eam10* is more rapid than in wild type (Campoli et al., 2013), like in arrhythmic *atelf3*, *atelf4*, and *atlux* mutants (Doyle et al., 2002; Hazen et al., 2005; Khanna et al., 2003; Liu et al., 2001; Onai and Ishiura, 2005; Reed et al., 2000). *HvLUX1* and *HvELF3* may act in the same pathway to regulate *Ppd-H1,* as *AtLUX* and *AtELF3* regulate *AtPRR7* and *AtPRR9* (Chow et al., 2012; Dixon et al., 2011; Helfer et al., 2011). Thus, it seems that adaptation of barley varieties to short growing seasons involved selection of EC gene alleles that cause early flowering by rendering the circadian clock nonfunctional (Faure et al., 2012).

In wheat, fine mapping of early flowering QTLs has been enabled by the identification of syntenic regions among grasses (Mayer et al., 2011). KT3-5 is a photoperiod-insensitive early flowering accession of *Triticum monococcum* (einkorn or diploid wheat) (Gawroński et al., 2014). *earliness per se 3 (eps-3A^m)* is the early-heading locus responsible for photoperiod insensitivity in KT3-5. *eps-3A^m* was mapped to a gene called *WPCL1*, which is an ortholog of *AtLUX* (Gawroński et al., 2014). Early flowering in KT3-5 plants is accompanied by elevated expression of *TmFT*, *Ppd-1, WCO1,* and *TmHd1* (Mizuno et al., 2012). In addition, KT3-5 plants with the *eps-3A^m* allele have a severely perturbed clock characterized by a long and irregular period

under L/L conditions (Gawroński et al., 2014). Interestingly, the KT3-5 accession out-performs the wild type accession in warmer temperatures, but KT3-5 is unable to phenotypically adjust to different environmental conditions (Gawroński et al., 2014).

These findings demonstrate that EC genes are important for circadian clock function across evolutionarily distant crop plants. Mutant alleles in EC genes are sufficient to disrupt normal clock function in pea, rice, and wheat. In most cases, the flowering time phenotypes observed in plants carrying these mutant alleles appear to result from disrupted rhythms arising from impaired circadian clocks; however, a more in-depth understanding of the regulatory connections between flowering time regulatory pathways and circadian clocks in each species is needed to fully appreciate the mechanisms underlying each flowering phenotype.

Conclusions and Future Perspectives

At present, Arabidopsis represents the best-studied plant circadian clock system. Over the past decade, the seminal findings in this model plant have been used to link circadian clock gene function to agronomic traits across many eudicot and monocot crops (Table 1.1). Looking to the future, emerging areas of research show circadian clock involvement in other key plant activities, especially plant-environment interactions. Since the circadian clock coordinates the expression of large numbers of important genes controlling agriculturally relevant traits, points of circadian clock control represent hubs of important transcriptional networks. Modification of these hubs by mutation of individual circadian clock genes has the potential for systemic effects that produce beneficial agronomic traits. The areas highlighted below are where future work in crop species is expected to be beneficial for agriculture.

Circadian clocks in abiotic stress responses

Research has repeatedly linked the circadian clock to abiotic stress responses (for review, see (Grundy et al., 2015)). The clock is involved in regulating multiple stress response pathways, and mutation or overexpression of circadian clock components affects plant stress tolerance and acclimation ability. In turn, the clock is regulated by the presence of abiotic stress, which causes alternative splicing of clock gene transcripts and leads to clock protein degradation.

One promising future avenue of research is the link between the circadian clock and drought response. The phytohormone abscisic acid (ABA) is essential for drought stress response and acts through several physiological mechanisms, including regulation of stomatal closure (for review, see (Yoshida et al., 2014). ABA treatment induces *TOC1* expression and, in a feedback loop, TOC1 attenuates ABA signaling and directly regulates expression of ABA signaling genes (Legnaioli et al., 2009). *toc1* mutant plants exhibit increased survival in water-limited conditions due to reduced water loss that is accomplished by reduced stomatal opening. Other clock genes have also been linked to drought tolerance, including the *PRR*s (Nakamichi et al., 2009b), *GI* (Fornara et al., 2015; Park et al., 2013), and *LKP2* (Miyazaki et al., 2015).

Reactive oxygen species (ROS) are toxic by-products of photosynthesis and respiration that can lead to cellular damage at high levels. ROS stress occurs under drought conditions, as plants often limit water loss by closing stomata, which reduces gas exchange and increases photorespiration (Grundy et al., 2015; Miller et al., 2010). ROS also serve as a cue to coordinate signal transduction networks associated with

ROS homeostasis and stress (Mittler et al., 2004), and ROS-scavenging enzyme production peaks at midday when oxidative stress is highest (Lai et al., 2012). *CCA1* controls genes involved in production, response, and transcriptional regulation of ROS in Arabidopsis (Lai et al., 2012). When grown in ROS stress-inducing conditions, *CCA1* overexpressing (*CCA1-ox)* plants are better able to attenuate ROS stress and show higher expression of ROS controlling genes (Lai et al., 2012). In addition, plants carrying mutations in circadian clock genes are hypersensitive to ROS (Grundy et al., 2015), indicating that a functional clock is necessary for the ROS stress response.

Circadian clocks in plant defense

The circadian clock aids plant defense by preparing defense responses in anticipation of likely pathogen attack. There are two broad classes of defense responses, which are primary or basal resistance and secondary or *R*-gene mediated resistance. A mutant screen in Arabidopsis identified novel genes involved in *R*-gene-mediated resistance elicited by *Hyaloperonospora arabidopsidis* (downy mildew) (Wang et al., 2011b). These *R*-genes are regulated by circadian clock control through *CCA1* to increase in expression before dawn, the time at which downy mildew disperses its spores. In *cca1* mutant plants, resistance to downy mildew is compromised, and *R*-gene expression is greatly reduced. In contrast, *CCA1-ox* plants have enhanced resistance to downy mildew (Wang et al., 2011b), thus demonstrating the importance of CCA1 in stimulating the defense response.

The “defense at dawn” behavior is also evident in responses against a virulent strain of the bacterial pathogen *Pseudomonas syringae* pv.*tomato* (*Pst* DC3000) (Bhardwaj et al., 2011). In this case, basal defense in the form of callose deposition at the cell wall is activated in the morning. The morning-specific resistance response is abolished in arrhythmic *CCA1-ox* and *elf3-1* mutants (Bhardwaj et al., 2011). Further work showed that together *CCA1* and *LHY* regulate both basal and R-gene-mediated defense, and that activation of defense responses in turn feeds back to regulate the clock (Zhang et al., 2013). A recent study in tomato showed that plants infected with *Pst* DC3000 had high resistance in the morning, and increased susceptibility in the evening (Yang et al., 2015b). Treatment with red light at night significantly increased resistance, and resulted in increased accumulation of salicylic acid (SA), and the transcription of defense-related genes, in part due to induced expression of circadian clock genes (Yang et al., 2015b). Finally, sudden ROS overproduction, one of the first defense responses, is not only under circadian control but stronger in the morning (Korneli et al., 2014).

These studies indicate that the clock acts to coordinate defense responses by accounting for both plant susceptibility and pathogen activity. Moreover, a single alteration to a clock gene potentiates significant changes to defense responses. These findings are already being used to detect infections that are otherwise difficult to study, such as Paulownia witches’ broom disease (Fan et al., 2014), and could provide a simple means to alter defense responses that would not require altering hormone pathways or inserting suites of *R*-genes.

A functional circadian clock is also important for defense against insect herbivores. Arabidopsis plants are more resistant to the generalist herbivore *Trichoplusia ni* (cabbage looper) when both plants and insects are entrained to the same L/D cycles than when the plants are entrained 12 hours out of phase with the

herbivores (Goodspeed et al., 2012). Furthermore, arrhythmic *CCA1-ox* plants are less resistant than wild type. Clock-mediated herbivore resistance is linked to rhythmic accumulation of the major plant defense phytohormone jasmonic acid (JA), which controls accumulation of anti-herbivore metabolites called glucosinolates. Circadian clock-driven accumulation of JA and glucosinolates ensures maximum levels of these compounds are produced just before the afternoon, which is the peak feeding time of the cabbage looper (Goodspeed et al., 2012).

Circadian clock regulation of JA and glucosinolates also enables vegetables and fruits to defend against insect herbivory after harvest. Cabbage heads (*Brassica oleracea)* maintain circadian rhythms and rhythmic accumulation of glucosinolates after harvest (Goodspeed et al., 2013). These rhythms are sufficiently robust for harvested heads of cabbage to show greater resistance to cabbage looper herbivory when both are entrained to the same L/D cycles. Other foods demonstrate this same phenomenon after harvest, including spinach, sweet potatoes, and blueberries (Goodspeed et al., 2013).

Circadian clocks in hybrid vigor

Hybrids grow larger and more vigorously than their inbred parents. This effect is known as hybrid vigor or heterosis, and is associated with higher photosynthetic rates, along with modification of carbohydrate and starch metabolism. Heterosis has also been linked to improved disease resistance: hybrid Arabidopsis plants have increased resistance to *Pst* DC3000 as a result of increased SA biosynthesis (Yang et al., 2015a).

To take advantage of the positive effects of heterosis, most crop plants are grown as hybrids or are polyploids. Despite its widespread use in agriculture, the mechanisms underlying heterosis are incompletely understood (Schnable and Springer, 2013). In Arabidopsis, circadian clock activity has been implicated in metabolic vigor, both in stable allopolyploids and segregating F_1 hybrids (Ni et al., 2009). In allopolyploids, the expression of genes involved in photosynthesis, starch, and sugar metabolism is increased from midday to evening. These genes are normally repressed by *CCA1*, and their increase in expression is the result of midday-specific *CCA1* repression that arises from chromatin modification at the *CCA1* promoter. Arabidopsis F_1 hybrids show a similar regulatory connection between diminished *CCA1* activity and increased expression of metabolic genes that results in greater metabolic activity (Ni et al., 2009). Moreover, manipulating *CCA1* expression in non-hybrid Arabidopsis plants to be similar to the hybrid pattern recapitulates hybrid expression behavior for chlorophyll and starch synthesis genes, as well as analogous enhancement of metabolic activity (Ni et al., 2009).

Furthermore, a distinct parent-of-origin effect in heterosis is correlated with CHH methylation sites in *CCA1* promoter regions. The effect appears to be established in developing embryos, and increased metabolic vigor is seen when the maternal copy of *CCA1* is repressed (Ng et al., 2014). This finding provides intriguing links to parental conflict theories of imprinting (Ng et al., 2014). Although the effect on other circadian genes has not yet been established, the epigenetic modulation of *CCA1* in hybrids provides a promising mechanism that could be implemented in crop plants that cannot be easily hybridized.

Circadian clock genes represent powerful tools to alter single or multiple traits simultaneously and their potential for application is just beginning to be understood.

Exploiting clock-regulated activities, such as those highlighted above, and existing circadian clock gene alleles holds the potential for breeding crops better adapted to diverse environments and buffered against the fluctuations inherent to climate change.

Figures

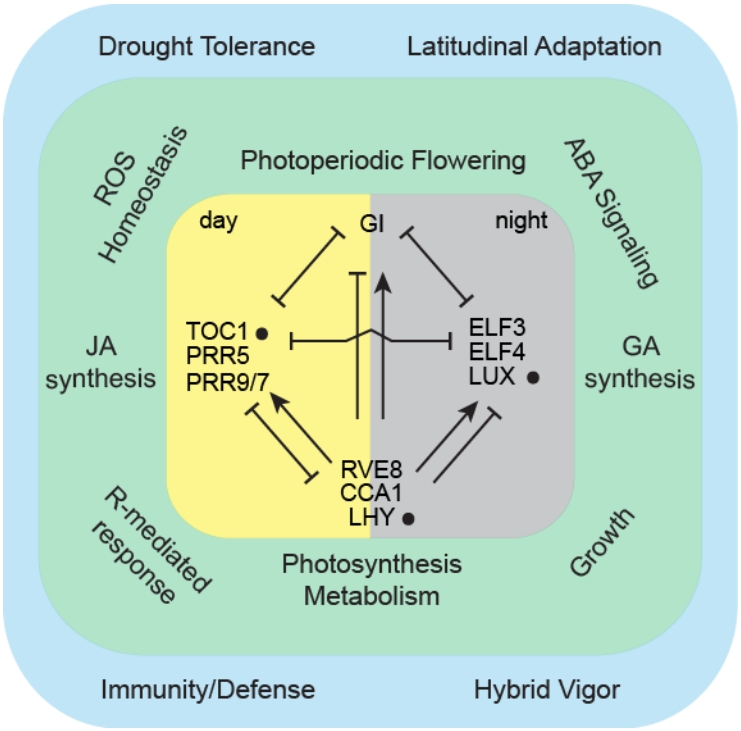

Figure 1.1. The plant circadian clock contributes to multiple agronomic traits. The central area represents the regulatory interactions within the core circadian clock, and is adapted from the F2014 model (Fogelmark and Troein, 2014). The yellow highlighted area represents day, and the grey area night. Lines with blunt arrows indicate inhibition, while lines with pointed arrows indicate activation. Solid circles next to *TOC1*, *LUX*, and *LHY* stand for feedback inhibition. The green shaded region shows signaling and physiological pathways that are directly controlled by circadian clock genes or the rhythmic output of the circadian clock itself. The blue shaded area contains traits influenced by clock-regulated pathways.

Tables

Species	QTL/Locus	Gene in species	Arabidopsis homolog(s)	Role/Trait	References
Eudicots					
B. vulgaris ssp. vulgaris	*B*	*BvBTC1*	*PRR7/PRR3*	biennial growth habit; CO function	Pin et al., 2012; Dally et al., 2012
	–[1]	*BvPRR7*	*PRR7*	–[2]	Pin et al., 2012
G. max	*E2/FT2*	*GmGIa*	*GI*	flowering time regulation	Watanabe et al., 2011
P. sativum	−	*LATE1*	*GI*	circadian clock function; flowering time regulation	Hecht et al., 2007; Liew et al., 2009
	HR/QTL3	*HR*	*ELF3*	circadian clock function; flowering time regulation; light response	Liew et al., 2009; Weller et al., 2012
	DNE	*DNE*	*ELF4*	circadian clock function; flowering time regulation	Liew et al., 2009; Weller et al., 2012
	SN	*SN*	*LUX*	circadian clock function; flowering time regulation	Liew et al., 2009; Weller et al., 2012
L. culinaris	*HR*	*HR*	*ELF3*	flowering time regulation	Liew et al., 2009; Weller et al., 2012

Species	QTL/Locus	Gene in species	Arabidopsis homolog(s)	Role/Trait	References
Monocots					
O. sativa	–	*OsPRR1*	*TOC1*	–	Murakami et al., 2003; Koo et al., 2013
	Hd2	*OsPRR37*	*PRR3/PRR7*	flowering time regulation	Murakami et al., 2003; Koo et al., 2013
	–	*OsPRR73*	*PRR7/PRR3*	–	Murakami et al., 2003; Koo et al., 2013
	–	*OsPRR59*	*PRR5/PRR9*	–	Murakami et al., 2003; Koo et al., 2013
	–	*OsPRR95*	*PRR9/PRR5*	–	Murakami et al., 2003; Koo et al., 2013
	–	*OsGI*	*GI*	flowering time and growth regulation; circadian clock function	Hayama et al., 2003; Izawa et al., 2011
	ef7/hd17	*OsELF3-1*	*ELF3*	light-dependent circadian clock regulation; flowering time regulation	Zhao et al., 2012; Yang et al., 2013
	–	*OsELF3-2*	*ELF3*	–	Zhao et al., 2012; Yang et al., 2013
H. vulgare	*Ppd-H1*	*HvPRR37*	*PRR3/PRR7*	flowering time regulation	Turner et al., 2005; Campoli et al., 2012

Species	QTL/Locus	Gene in species	Arabidopsis homolog(s)	Role/Trait	References
H. vulgare	–	*HvGI*	*GI*	limited flowering time regulation	Dunford et al., 2005; Wang et al., 2010; Pasam et al., 2012
	eam8/mat-a	*EAM8*	*ELF3*	circadian clock function; flowering time regulation	Faure et al., 2012
	eam10	*EAM10*	*LUX*	circadian clock function; flowering time regulation	Campoli et al., 2013
T. aestivum	–	*Ppd-D1*	*PRR3/PRR7*	flowering time regulation	Beales et al., 2007; Seki et al., 2011; Shaw et al., 2012; Shaw et al., 2013
	–	*Ppd-A1*	*PRR3/PRR7*	flowering time regulation	Beales et al., 2007; Seki et al., 2011; Shaw et al., 2012; Shaw et al., 2013
	–	*Ppd-B1*	*PRR3/PRR7*	flowering time regulation	Beales et al., 2007; Seki et al., 2011; Shaw et al., 2012; Shaw et al., 2013
T. monococcum	*eps-3A^m*	*WPCL1*	*LUX*	circadian clock function; flowering time regulation	Mizuno et al., 2012; Gawronski et al., 2014

Species	QTL/Locus	Gene in species	Arabidopsis homolog(s)	Role/Trait	References
S. bicolor	Ma_1	*SbPRR37*	*PRR3/PRR7*	flowering time regulation	Murphy et al., 2011
Z. mays	–	*Zmgi1*	*GI*	circadian clock function; limited flowering time regulation	Miller et al., 2008; Mendoza et al., 2013; Bendix et al., 2013
	–	*Zmgi2*	*GI*	clock output regulation	Miller et al., 2008; Mendoza et al., 2013; Bendix et al., 2013

Table 1.1. Circadian clock genes associated with key agronomic traits. A – in the QTL/Locus column indicates there is no known QTL/Locus associated with the gene, while a – in the Role/Trait column indicates the function of the gene is unknown.

Chapter Two: Genetic and phenotypic effects of *gigantea1* and *gigantea2* transposon insertion lines in maize

The following chapter includes a modified version of an article published in *Plant, Cell & Environment* (Bendix et al., 2013) excerpts from an article published in *Maydica* (Mendoza et al., 2012), and unpublished data.

Abstract

GIGANTEA (GI) is a circadian clock-associated gene directly involved in the control of growth, flowering time, and developmental transitions in the model dicot species *Arabidopsis thaliana*. The role of the circadian clock in regulating growth in monocots remains ambiguous, however, and the function of *GI* in monocot development remains uncharacterized. Maize has two paralogous *GI* genes, of which *gigantea1* (*gi1*) is more highly expressed than *gi2*. To understand the role of *gi1* and *gi2* in the regulatory networks of the maize circadian clock system, transposon insertion mutants were evaluated for changes in circadian gene expression, flowering time, growth phase, and growth control. Changes in core circadian gene expression were found in *gi1* mutants, and small flowering time effects were observed in *gi1* and *gi2* mutant lines. This indicates that maize *gi1* plays a role within the maize circadian clock, that maize *gi2* does not, and that neither copy on its own has as wide-reaching a physiological effect as *AtGI.*

Introduction

In Arabidopsis, *GIGANTEA* (*AtGI*) encodes a component of the core clock oscillator (Rubio and Deng, 2007), and is required for normal circadian rhythms. The circadian clock regulates expression of the *AtGI* transcript, which peaks in the evening (Fowler et al., 1999), and AtGI protein levels closely follow the oscillation of the transcript (David et al., 2006; Huq et al., 2000; Park et al., 1999). Arabidopsis *gi* (*atgi*) null mutants (Martin-Tryon et al., 2007) have altered expression of other core clock components, which is characterized by reduced amplitude and phase advances. The short period effect becomes more pronounced when the mutants are assayed after transfer to constant conditions (Martin-Tryon et al., 2007). This indicates that AtGI normally acts to maintain the phase of clock gene expression, and to a lesser extent the amplitude.

AtGI was originally identified in a screen for supervital mutants which were all found to be late-flowering (Koornneef et al., 1991; Rédei, 1962), and delayed flowering under inductive photoconditions is the most striking phenotype of *atgi* mutants, and in fact. Under inductive conditions, *atg*i null mutants regularly flower after producing over 35 leaves in comparison to 8 leaves produced by wild type (Martin-Tryon et al., 2007). Under non-inductive conditions, wild type plants produce a similar amount of leaves to *atgi* nulls, while *atgi* flowering behavior remains the same (Martin-Tryon et al., 2007). *AtGI* acts to regulate photoperiodic flowering in ways that are biochemically distinct from its function within the clock (Mizoguchi et al., 2005), but it is often thought of as a floral integrator linking clock function to flowering time.

One way in which *AtGI* induces flowering in long-day photoperiods (LD) is by regulating miR172 accumulation (Jung et al., 2007). This microRNA promotes flowering

by repressing *APETALA2 (AP2)*-type transcription factors that inhibit both floral activator and flower development genes (Aukerman and Sakai, 2003; Yant et al., 2010). miR172 is abundant in *Arabidopsis* plants grown in LD, but much less abundant in plants grown in short-day photoperiods (SD). Null *atgi* mutants exhibit low miR172 levels in LD that are comparable with to the levels in of SD-grown wild-type (WT) plants, indicating that *AtGI* contributes to miR172 accumulation in LD photoperiods. AtGI also has a number of post-transcriptional roles in governing the core CO-FT flowering module, which will be discussed in more detail in the next chapter.

As well as promoting the transition to flowering, miR172 participates in vegetative phase change pathways that regulate the timing of the developmental transition from the vegetative juvenile to vegetative adult phases (Huijser and Schmid, 2011; Li and Zhang, 2016). It remains to be determined whether phase change is altered in *atgi* mutants.

Null *atgi* mutants also have altered light responses and elongated growth habits as seedlings (Araki and Komeda, 1993; Fowler et al., 1999; Huq et al., 2000; Rédei, 1962). Both of these phenotypes are linked to the role *AtGI* plays in light signaling, which is again distinct from its role within the circadian clock (Oliverio et al., 2007). Wild-type Arabidopsis seedlings stop elongating their hypocotyls and become photosynthetic (de-etiolate) in response to far-red, red, or blue light (Chen et al., 2004). In null *atgi* mutants grown under continuous red or blue light, seedlings grow a long hypocotyl and do not de-etiolate. Moreover, *atgi* mutants are hyposensitive to far red light pulses. It has been shown that AtGI positively regulates the very low fluence response pathway of phyA, and is necessary for the gating of this response by the clock (Oliverio et al., 2007). This regulation is likely connected to the reduced dormancy seen in *atgi* mutants.

Other *atgi* mutant characteristics include abiotic stress tolerance, increased starch levels, and increased chlorophyll. The latter two processes remain largely uncharacterized, as do many other roles that *AtGI* has been found to have (Mishra and Panigrahi, 2015).

AtGI homologs appear to have comparable functions across the species in which they have been studied, especially in eudicots. *Brassica rapa GI (BrGI*) mutants exhibit altered circadian rhythms, are late flowering, and have abiotic stress tolerance (Xie et al., 2015). In *Pisum sativum, LATE1* gene is an ortholog of Arabidopsis *GI* (Hecht et al., 2007), which when mutated causes photoperiod-insensitive late flowering, reduced seedling de-etiolation responses, and altered expression of putative circadian clock genes. In monocots, rice *OsGIGANTEA* (*OsGI*) is necessary for proper circadian clock regulation of three-quarters of rhythmically expressed genes (Izawa et al., 2011). The *osgi* mutant is late-flowering under inductive photoperiods, and has increased starch levels. On the other hand, *osgi* mutants have decreased chlorophyll levels and reduced vegetative growth, distinguishing the *osgi* mutants from the large, deep-green *atgi* mutants. All of these *GI* genes are able to complement *atgi* mutants when transgenically expressed, perhaps indicating that varied phenotypes are due to variation in interaction partners rather than alterations in the *GI* genes themselves.

The maize genome contains two *gigantea* (*gi*) homeologs, originally named as *gigantea of zea mays 1a/b* (Miller et al., 2008), now designated *gi1* and *gi2* for clarity. These *gi* homeologs arose from the tetraploidy event in the maize ancestor that occurred approximately 5–12 million years ago (Gaut and Doebley, 1997; Swigonová et

al., 2004). During subsequent evolution, the maize genome has retained two distinct subgenomes, maize 1 subgenome and maize 2 subgenome that have experienced different levels of fractionation (gene loss) (Schnable et al., 2011). The maize 1 subgenome is less fractionated and generally more strongly expressed than the maize 2 subgenome. *gi2* is present on the maize 1 subgenome, whereas *gi1* is on the maize 2 subgenome (Schnable and Freeling, 2011). The expression of these *gi* homeologs is circadian-regulated (Khan et al., 2010), and diurnal expression of each is greater in leaves than immature ears (Hayes et al., 2010). Aside from this limited description, these genes are largely uncharacterized.

To better understand the role of *GI* in maize and its regulatory pathways, mutants of the *gi1* and *gi2* genes were evaluated for their effect on circadian gene expression and developmental processes, including flowering time and vegetative phase change. Mutants in *gi1* had a similar effect on circadian gene expression as *atgi* mutants, demonstrating both phase advances and reduced amplitude. The *gi2* mutants did not show this effect. In the initial generations, *gi1* mutants flowered earlier in LD photoperiods, underwent earlier vegetative phase change, and grew taller than wild-type plants. These phenotypes, however, disappeared with sufficient introgression: both *gi1* and *gi2* mutants are not phenotypically different from their wild-type siblings in any significant way. These findings indicate that maize *gi1* plays a role within the maize circadian clock, maize *gi2* does not, and that neither has as wide-reaching a physiological effect as *AtGI.*

gi1 and *gi2* expression and *gi* insertion mutant characteristics

The expression of *gi1* and *gi2* is rhythmic, with peak transcript levels at 12 hours after dawn (ZT12) in long day conditions. Of the two genes, *gi1* is expressed more highly than *gi2,* with transcript levels approximately 6-fold higher at ZT12 (Figure 2.1.A).

From the Trait Utility System for Corn (TUSC) collection of *Mutator* (*Mu*) transposon lines, two independent *Mu* transposon insertion alleles were identified in *gi1* and one *Mu* insertion allele in *gi2* (Figure 2.1.B). All three alleles were introgressed into the stiff-stalk temperate inbred A632, a maize line of high agronomic importance (Liu et al., 2003). For initial experiments, A632 was used as a wild-type reference. After crossing the lines to A632 for 5-6 generations to remove any background *Mu* transposons from the original TUSC lines and to ensure genetic uniformity, non-mutant sibling lines were used as references. The experimental results presented here include assays of these mutants at two separate backcross stages, namely at backcross 3 (BC3) and at backcross 5 or 6 (BC5/BC6) (Supplemental Figure 2.1).

The first insertion allele in *gi1* (*gi1-m1*) is located 2,495 base pairs (bp) downstream from the transcription start site, in exon 7. The second insertion allele in *gi1* (*gi1-m2*) is 1,453 bp downstream from the beginning of the gene and in exon 2, which is part of the 5'UTR. In both insertion alleles, the transcripts produced have aberrant transcriptional start sites and are interrupted by the *Mu* insertion. The *gi1-m1* allele also has a high level of splicing errors (Mendoza et al., 2012). Both *gi1* alleles reduce *gi1* expression level while maintaining rhythmicity, and due to the presence of *Mu* in their transcripts are unlikely to produce many functional protein products.

The insertion allele in *gi2* (*gi2-m1*) is close to the end of the transcript, in exon 15. It is at the tail end of the coding sequence rather than the 3'UTR. This means that transcript produced from this allele will contain *Mu* sequence at its end, and will likely

have altered amino acids downstream of the insertion. Transcript characterization has not been done *gi2-m1* mutant plants.

Results

The expression of core and output circadian clock genes is altered in *gi* insertion mutants

In order to fully test the effects of *gi* insertion mutants on circadian genes, insertion lines were assayed under diurnal conditions as well as constant light conditions. The diurnal assays were done with homozygous BC3 plants, while the constant light assays were primarily done with homozygous BC5/BC6 plants (Supplemental Figure 2.1).

When grown in long day (LD) conditions in the greenhouse, *gi* insertion mutants show altered expression levels of circadian clock genes relative to A632 (Figure 2.2). Rhythmicity of clock gene expression is maintained in all lines, although expression shape is altered in some genes. The expression level of *gi1* is reduced throughout the timecourse in *gi1-m1* (FH340) plants, and reduced in the trough in *gi1-m2* (FH342) plants, while *gi2-m1* (FH359) plants show expression levels comparable to wt. Interestingly, a different pattern is seen in the expression level of *gi2.* Here, both *gi1-m1* (FH340) and *gi1-m2* (FH342) have increased peak expression levels, while *gi2-m1* (FH359) levels are reduced throughout. This could indicate that a compensatory mechanism is in place to increase *gi2* expression in the absence of *gi1*, but that no such mechanism exists for *gi1*.

For *lhy1*, peak expression is reduced in *gi1-m2* (FH342) and *gi2-m1* (FH359), but not *gi1-m1* (FH340), while for *lhy2*, *gi1-m1* (FH340) and *gi2-m1* (FH359) show reduced peak expression. Both *gi1-m2* (FH342) and *gi2-m1* (FH359) have broader peaks in both *lhy* expression peaks that begin already at ZT24 and continue to ZT27. The expression of *toc1a* is comparable across all lines, although there is a slight increase in expression seen in the insertion mutant lines at the peaks. *cat3* expression is similar across all lines except at the peaks, yet *cab* expression is increased throughout in *gi1-m1* (FH340) and *gi1-m2* (FH342) (Figure 2.2). These results show that in some cases, *gi* insertion lines result in reduced expression and phase advances. This expected effect, however, is not seen for all genes or present in all lines.

When grown in short day (SD) conditions in the greenhouse, *gi* insertion mutants again show altered expression levels of circadian clock genes and some altered expression shapes relative to A632 (Figure 2.3). Overall, gene expression levels in SD are substantially lower than in LD across all four lines. The expression level of *gi1* is reduced in all insertion lines throughout the timecourse, including in *gi2-m1* (FH359). The expression level of *gi2* is again quite different from that of *gi1*, and here only the FH359 has decreased expression. *gi1-m1* (FH340) and *gi1-m2* (FH342), in contrast have increased expression of *gi2* and a peak shifted slightly earlier, to ZT8. Here there appears to be a more complicated interrelation between *gi1* and *gi2* expression levels.

The expression of *prr73* is very distinct between the lines; *gi1-m1* (FH340) and *gi1-m2* (FH342) have increased expression throughout, while *gi2-m1* (FH359) is similar to wt. Both *lhy1* and *lhy2* show similar expression patterns among all four of the lines. In contrast, all three insertion lines show an increase in *toc1a* expression with an earlier start of peak expression, while *toc1b* expression appears to be similar across all lines.

Interestingly, *cat3* expression shows a similar increase and shift of peak from ZT12 to ZT8 in the insertion lines. The most striking difference can be seen in *cab1* expression levels, where a 2-fold increase in expression can be seen throughout the day in *gi1-m1* (FH340) and *gi1-m2* (FH342). These results indicate that under SD conditions, increases in circadian gene expression are present while the phase advances seen in some genes under LD remain consistent. In addition, *prr73* and *toc1a*, which weren't tested in LD, are significantly affected by *gi* expression changes.

Next, gene expression was tested under constant light (LL) conditions. A preliminary timecourse with a limited number of BC2/BC3 plants showed that the rhythmicity of entrained genes is mostly maintained, and that the alterations in gene expression seen in diurnal conditions continue to be present (Supplemental Figure 2.2). These results indicated that the altered expression seen in insertion lines under diurnal conditions becomes more apparent in free running conditions.

A 48-hour timecourse of BC5/BC6 plants in LL demonstrated the full extent of the clock alterations (Figure 2.4). As before, the plants were entrained in LD conditions (16 hours light; 8 hours dark), and then released into constant light for 3 days, with sampling beginning after the first full day in constant light. In both *gi1* mutant lines, the expression of *gi1* was reduced, and the peak expression time shifted about 3 hours earlier than in their wild type sibs. *gi2* expression is quite similar between mutant and wild type lines, although the *gi1m1* mutant shows an early peak, and becomes more arrhythmic during the third day in constant light. In contrast, the *gi2m1* mutant has no difference in *gi1* or *gi2* expression level, indicating that the mutant is not able to substantially alter expression level or timing of either *gi. prr73* expression differs across all three mutant lines, with *gi1m1* and *gi2m1* showing a high peak at the beginning of day 2 in LL, while gi1m2 has the clearest peak at the beginning of day 3. Interestingly, the *gi1m1* mutant shows closely spaced peaks and an increased expression level relative to the *gi1m1* wild type.

The disruption of the clock becomes particularly apparent in the two *lhy* genes. Both *lhy1* and *lhy2* have decreased expression levels and rhythmicity in the *gi1m1* mutant. The *gi1m2* mutant maintains rhythmicity, but has increased peak and decreased trough expression. The *gi2m1* mutant has minor peak timing alterations, but otherwise little noticeable change in comparison to the wild type. The expression levels of *cab1* tell a similar story, showing significant alterations in the *gi1m1* mutant, and less severe alterations in the *gi1m2* mutant. The *gi2m1* mutant appears somewhat altered at the beginning of day 3, but otherwise very similar to the wild type line. The *toc1* genes have increasing peak expression from the second to the third day, with both *gi1* mutants having higher and earlier peaks (by about 3 hours) than their wild type counterparts. The *gi2m1* mutant also shows increased expression at the peak on the second day, but not altered timing. *cat3* expression also increases on the second day. Here, *gi1m1* shows substantially increased expression, while *gi1m2* just shows a slightly earlier peak. Interestingly, this is the gene where the most difference is seen between *gi2m1* and its wild type sibling: peaks are later by about 6 hours and much higher.

In BC3 plants, *gi1* mutant alleles cause early flowering under LD conditions but not SD conditions

To determine whether *gi1* participates in regulation of maize flowering time, BC3 homozygous lines carrying both *gi1* mutant alleles were evaluated over two summers in

the field and in greenhouse LD and SD conditions. Plants grown in the field (LD) carrying either *gi1* mutant allele flowered with fewer leaves than A632 (Figure 2.5.A). *gi1-m1* (FH340) plants exhibited the greatest reduction in leaf number, with mutant plants producing an average of 19, while *gi1-m2* (FH342) plants had 20 leaves, and A632 plants made 21 leaves.

The contribution of *gi1* to maize flowering time was also examined in SD conditions in the greenhouse and compared with plants grown in LD conditions at the same time. SD elicited earlier flowering in the A632 inbred, with plants grown in SD having an average of two fewer leaves than in LD (Figure 2.5.A). Both *gi1* mutant alleles produced an average leaf number close to that of A632 in the SD photocycles (Figure 2.5.A), and neither *gi1* mutant allele had an additional positive effect on flowering time.

To determine whether misregulation of flowering time genes contributed to the early flowering phenotype of BC3 *gi1* mutants, the expression levels of the floral regulators *zea mays centroradialis8* (*zcn8*), an *FT*-like floral activator (Meng et al., 2011), and *constans of zea mays1* (*conz1*), a *CONSTANS*-like gene (Miller et al., 2008) were assayed. A comparison of *zcn8* and *conz1* expression in LD and SD timecourses shows that *conz1* is rhythmic and increased at the time of peak expression in the *gi1* insertion lines under both conditions (Figure 2.5.B). In LD conditions, there is a narrow peak at ZT12 in the *gi1* mutants, which is not mirrored in A632. In SD conditions, the *conz1* peak begins at ZT8 and extends through to ZT28 across all lines. *zcn8* expression is low and arrhythmic in LD conditions, while in SD conditions, *zcn8* expression is 2- to 6-fold higher in all lines and somewhat rhythmic. Both genes are expressed more rhythmically in SD across all lines examined, which may indicate that SD conditions drive rhythmicity in these flowering time genes.

When expression levels of the mutant lines were plotted relative to A632, the differences in expression levels became clearer (Figure 2.6). Across genotypes, *zcn8* accumulation increased throughout development, yet at each stage was elevated in the *gi1-m1* mutant (FH340) relative to A632 (Figure 2.6.A). There is higher *zcn8* expression in *gi1-m1* (FH340) and *gi1-m2* (FH342) plants that is consistent with the early flowering phenotype of mutant plants. Both mutant lines also showed increased *conz1* expression, suggesting that the higher expression of *conz1* may be responsible for increased *zcn8* expression. The increase in expression of *zcn8*, however, was weaker in SD, despite similarly increased *conz1* levels.

In BC3 plants, loss of *gi1* function alters the timing of vegetative phase change and increases plant height

The timing of vegetative phase change was evaluated in *gi1* mutants to determine whether *gi1* is involved in this developmental transition. In *gi1-m1* (FH340) plants, the transition occurred up to two leaves sooner than in A632 or *gi1-m2* (FH342) plants (Figure 2.7.A).

A potential mechanism by which this *gi1* mutant allele may have affected phase change was by altering accumulation of miR172, like *AtGI* does (Jung et al., 2007), or by altering miR156 accumulation, which is known to be involved in vegetative phase change. However, this appeared to not be the case for the *gi1* mutant alleles: evaluation of miR172 and miR156 levels by Northern blot did not reveal substantial differences in accumulation of these small RNAs in whole seedlings between the A632 inbred and the *gi1* mutants (Figure 2.7.C). Therefore, *gi1* appears to contribute to regulation of

vegetative phase change through another mechanism.

An increase in height phenotype was apparent in young plants, and most obvious after flowering. V8–V9 stage mutant plants were already visibly taller than A632 plants, and after flowering, plants carrying either *gi1* insertion allele were significantly taller than A632 (Figure 2.7.B). Consistent with the other phenotypes described here, the *gi1-m1* (FH340) plants had a large increase in height, while *gi1-m2* (FH342) plants induced a lesser increase in height.

In BC5/BC6 plants, flowering time phenotypes in LD conditions are reduced and height phenotypes are eliminated

In order to test whether the flowering time phenotypes seen in BC3 plants persisted in later generations, BC5/BC6 plants were examined in LD conditions in the field. These lines were grown in the greenhouse during the winter to propagate known genotypes for the following field season, and were also assayed for phenotypes in that time. Although the assay was done with very few plants (n= 2-9, depending on line), no differences in flowering time were seen between homozygous mutant and homozygous non-mutant siblings within the same line (Supplemental Figure 2.3)

Under LD conditions in the field, the BC5/BC6 lines show no significant differences in flowering time between mutant and non-mutant siblings (Figure 2.8). This is especially apparent within the large grow-outs of a single BC5/BC6 segregating line for each insertion mutant (CB05, CB08, and CB27), although the other segregating lines showed similar trends. Although there are some significant differences between homozygous lines, these lines were small due to poor field conditions: the non-mutant *gi2-m1* (CB40) line consists of 4 individuals, while the *gi2-m1* mutant (CB44) line CB44 is only 3. The differences seen between homozygous BC6 *gi1-m1* lines may be truly significant (n>=12 per genotype), yet the fact remains that a similar trend is not seen in the larger segregating *gi1-m1* line (CB05, n>=23 per genotype).

Double mutant lines containing *gi1-m1* and *gi1-m2* were grown in the field concurrently with single mutant lines. As well as CB25, the large segregating parental population descended from a *gi2-m1* (FH359) by *gi1-m1* (FH340) cross, multiple selfed and sibbed offspring of CB25 were grown out. Unfortunately, all but one of these lines (CB47) was segregating for either insertion, making characterization challenging. By grouping measurements according to the state of each allele, an intriguing indication that heterozygosity is important for flowering time emerged (Figure 2.9). Overall, the range of leaf count data for the double lines is fairly limited, with the exception of the homozygous CB47 line, and so these differences are likely to be genotype-linked (Supplemental Figure 2.4). Further work with genetically uniform lines would need to be done to confirm these findings.

The absence of a height phenotype is quite apparent when BC5/BC6 plants are grown in the field (Figure 2.10). There are no significant differences seen within any of the segregating populations. In the homozygous lines, the only differences are seen in lines carrying *gi1-m1* insertions, and these are fairly small. As with flowering time, this effect was already seen in the greenhouse that previous winter. In contrast to the flowering time measurements, the range of height measurements of the individual double lines was quite variable and line-specific (Supplemental Figure 2.4). In the larger segregating CB25 line, no genotype-dependent height phenotype was apparent.

BC5/BC6 mutant plants have altered amounts of chlorophyll

The same BC5/BC6 lines used in the LL timecourse were analyzed for chlorophyll amount. *gi1-m1* mutant (CB51) plants had significantly ($p < 0.05$) more chlorophyll a, chlorophyll b, and total chlorophyll than non-mutant CB38 plants (Figure 2.11). There was no visible or statistical difference in chlorophyll amount between *gi1-m2* non-mutant (CB54) and *gi1-m2* mutant (CB42) plants. *gi2-m1* mutant (CB44) plants, on the other hand, appeared to have increased chlorophyll in comparison to *gi2-m1* non-mutant (CB43) plants, but the statistical tests remained non-significant at p-values of about 0.13. Chlorophyll tests on individual plants were also done, and yielded similar though non-significant results (Supplemental Figure 2.5).

BC5/BC6 mutant plants have altered disease resistance phenotypes

In the genetic analysis, it was shown that the *gi* insertion lines disrupted the maize circadian clock. Multiple papers have shown that a functional clock is important in disease resistance processes, and so we decided to test the *gi* mutants.

The most striking differences between mutant and wild type lines were seen in the Southern Leaf Blight (SLB) assays (Figure 2.12). The *gi1-m1* mutant line (CB39) was more resistant throughout the measuring period than either its wild type sib line (CB38), or the inbred line A632. The CB42 line, carrying the weaker *gi1-m2* mutation, was similar to both its wild type sib (CB40) and A632. The *gi2-m1* mutant line (CB44) had increased susceptibility throughout the measurement period (Supplemental Figure 2.6). When both mutations are present in at least one copy, the *gi1-m1* mutation appears to outweigh that of the *gi2-m1* mutation (Supplemental Figure 2.7).

No clear difference in susceptibility could be seen when the same lines were inoculated with Northern Leaf Blight (NLB) or Grey Leaf Spot (GLS) (Figure 2.12). A632 was somewhat more susceptible to NLB earlier on, but final scores were similar across all lines.

Transgenic expression of *gi1,* and to a lesser extent *gi2,* complements the flowering phenotype of an *atgi* null mutation

To establish that *gi1* encodes a protein that is comparable in function with its *Arabidopsis* homolog, *gi1* was tested for its ability to rescue the *atgi-201* loss-of-function mutant. Plants carrying the *atgi-201* allele have a severe delay in flowering under LD conditions (Jung et al., 2007; Martin-Tryon et al., 2007), which was used to assess phenotypic complementation. Stable transgenic lines were established in *atgi-201* that carried a fusion construct of the *AtGI* native promoter and either the maize *gi1* CDS (*AtGIp::gi1*) or the Arabidopsis *GI* CDS (*AtGIp::AtGI*) (Figure 2.13.A). Two independent, homozygous T3 lines with expressed transgenes were identified for each transgenic construct (Figure 2.13.A) and these were tested for rescue of the flowering phenotype of *atgi-201*.

The *AtGIp::gi1* construct effectively complemented the flowering defect of the *gi-201* mutant, as did the *AtGIp::AtGI* construct (Figure 2.13.B). *atgi-201* plants grown in LD produced over five times the number of rosette leaves at flowering (Figure 2.13.B), and required an average of 43 more days to reach flowering than WT plants. In contrast, two representative *AtGIp::gi1* lines flowered with a total number of leaves that was no different from WT plants (Figure 2.13.B). A similar degree of complementation was apparent in plants carrying the *AtGIp::AtGI* construct. Plants from both transgenic

lines and WT reached flowering after a similar number of days in LD. The effective substitution of *gi1* for *AtGI* demonstrated that GI1 has biochemical attributes that approximate its *Arabidopsis* homolog.

Stable transgenic lines carrying a fusion construct of the maize *gi2* mRNA sequence under the Arabidopsis *GI* native promoter were also established in *gi-201* (Supplemental Figure 2.8). These lines demonstrated varied phenotypes, with some being more *gi-201*-like and others being more WT-like. This range of phenotypes could be due to several factors, including differences between GI1 and GI2 proteins, differences in the genomic context of the T-DNA insertion affecting expression, or the use of the *gi2* mRNA versus the *gi1* CDS, since the maize mRNA transcript might be inefficiently processed in Arabidopsis. In either case, the WT-like plants indicate that *gi2* is capable of complementing the late flowering time phenotype, but because the *gi2* lines could not be effectively compared to the other minigene constructs, this line of inquiry was not pursued further.

Discussion

These results demonstrate that the maize *gi1* gene fulfills many similar roles to its homolog *AtGI. gi1* regulates core circadian genes, and in early backcrosses, *gi1* mutants had flowering time phenotypes. The *gi2* gene regulates circadian output genes, and both *gi* mutants have increased chlorophyll levels. Both maize *gi* mutants also have altered responses to disease, although *gi1-m1* increases resistance, while *gi2-m1* increases susceptibility. When heterologously expressed in Arabidopsis, both *gi* genes are able to complement *AtGI* mutant phenotypes, but to differing degrees. Overall, the *gi1* gene is more similar to *AtGI*, both in terms of gene expression regulation and phenotypes. The *gi2* gene, while still retaining some *AtGI*-like characteristics, appears more divergent.

The LD and SD timecourse results indicate that the absence of either *gi1* or *gi2* affects the expression level and timing of maize circadian clock genes without altering their rhythmicity. An increase in *gi2* expression is seen under both conditions in *gi1* insertion lines, while a decrease in *gi1* expression is only seen in the *gi2* insertion line under SD conditions. Overall, SD conditions seem to have a larger impact on expression timing, with many genes showing peaks shifted slightly earlier. This indicates that peak expression is linked to the timing of dawn and dusk. Finally, *cab1* expression is substantially increased in *gi1* insertion lines under LD and SD, indicating there is an effect on photosynthesis.

The LL timecourse results indicate that the *gi1* insertion lines disrupt the maize circadian clock. In some cases, this disruption is similar to *atgi* mutants, in that reduced amplitude of expression and an earlier peak is seen. In others, however, increased expression or altered peak and trough duration are present, indicating a different mechanism of *gi* action is present in maize than in *Arabidopsis.* As for *gi2,* the insertion line does not appear to have much of an effect on clock gene expression, which could be due to the mutant allele being weaker. Overall, *gi1* mutants affect most core clock genes as well as the output gene *cab1,* which encodes a subunit of LHCII, in LL, indicating that *gi1* acts similarly to *AtGI* in that it is involved both in the clock and light regulation. The *gi2* mutant, on the other hand, only has a strong effect on expression of the output gene *cat3.* This could indicate that *gi2* primarily acts to regulate genes

outside of the core clock, and perhaps has taken on a greater share of the non-clock functions known from *atgi.*

Another intriguing possibility is that *gi2* may be more involved in the temperature-regulated clock. In *Arabidopsis, AtCAT3* expression is temperature rather than light-responsive, and separate oscillators regulated by the different cues have been proposed (Michael et al., 2003). *AtCAT3* mRNA expression is dusk-phased, and unlike *AtCAT2*, there is no circadian gating in its response to light (Zhong, 1998). A study done in maize comparing pigment-deficient mutants to their wild-type siblings showed that *cat3* oscillation was the same in both and therefore did not require photosynthetic processes (Acevedo et al., 1991). Moreover, when these plants were grown in LL or DD, *cat3* transcript was continually expressed at a high level. Another study compared *cat3* entrainment to *cab*, and showed that *cat3* required a full LD (or DL) cycle to entrain where *cab* required only one transition from L to D (or D to L) (Boldt and Scandalios, 1995), further supporting the idea that *cat3* is temperature-regulated.

BC3 and BC5/ BC6 plants carrying *Mu* transposon insertion alleles were phenotypically characterized, with strikingly different results. Both *gi1* mutant alleles decreased the total number of leaves produced by BC3 plants, indicating an earlier transition to floral development than seen in normal plants. The *gi1* mutants also showed increased expression of *zcn8*, a FT-like gene that likely embodies an FT-like florigen activity (Meng et al., 2011), and *conz1*, a CO-like gene. Interestingly, plants with the *gi1-m1* allele had an average leaf number in SD that was indistinguishable from that in LD, indicating that the *gi1* mutant does not make a major contribution to flowering in SD photoperiods.

BC3 *gi1* mutant plants grew taller than normal A632 individuals, which demonstrated that *gi1* functions to restrict growth. *Arabidopsis gi* mutants also display elongated morphology (Araki and Komeda, 1993; Rédei, 1962), which appears to be the combined effects of *atgi* mutation on light and phytohormone signaling pathways, as well as alterations in circadian rhythms (Huq et al., 2000; Martin-Tryon et al., 2007; Mizoguchi et al., 2005; Oliverio et al., 2007; Tseng et al., 2004). Similarly, *gi1* is likely an important contributor to phytochrome-mediated light signaling pathways in maize, as taller plants are common when reduced phytochrome activity is conditioned by either mutation (Sawers et al., 2002; Sheehan et al., 2007) or shade conditions (Dubois and Brutnell, 2011).

The congruent positive effects of *gi1* mutation on maize growth and phase change suggest that elevated gibberellin (GA) activity may be present in *gi1* mutants. AtGI represses the activity of SPINDLY (SPY) (Tseng et al., 2004), a regulator of GA signaling that has both positive and negative effects on hypocotyl elongation: it both promotes hypocotyl elongation in the absence of AtGI and represses GA signaling which would also promote hypocotyl elongation in the absence of SPY (Jacobsen and Olszewski, 1993; Tseng et al., 2004). The earlier vegetative phase change seen in *gi1-m1* mutant plants would be consistent with this idea, as GA is known to promote vegetative phase change in maize (Evans and Poethig, 1995), but this was not examined at the protein level.

In part, further GA characterization was not done because the phenotypic results from both field- and greenhouse-grown BC5/BC6 plants indicate that the altered height phenotypes seen in BC3 plants were likely due to a heterotic effect that disappeared

with increased backcrossing. Although two of the original TUSC mutant lines had A632 as a parent, the other 50% of their genetic background was not A632. Crossing these lines into A632 likely resulted in metabolic vigor and increased growth (Duvick, 2001; Ni et al., 2009; Zanoni and Dudley, 1989). The lack of a height phenotype in BC5/BC6 plants furthermore indicates that there is no functional link between maize *gi* genes and growth, and possibly that there is also no link between the maize circadian clock and growth. Recent papers have demonstrated that this link is lacking in other grasses (Matos et al., 2014), indicating this fundamental role of the *Arabidopsis* circadian clock may not exist in grasses.

The reduction of the flowering time effect over the generations is likely also due to the disappearance of a heterotic effect. The expression of flowering time genes in BC5/BC6 was not tested due to the lack of a flowering time phenotype, but they may still be altered in insertion lines. It is surprising though, that the loss of *gi* expression should have such a small effect on flowering time, given *gi* mutant characteristics in other species. The *osgi* mutant also has a number of phenotypes that differed from *AtGI* mutant phenotypes (Izawa, 2012; Izawa et al., 2011), indicating that grass *GIs* may be fundamentally different.

Another factor that could play a role in the reduced phenotype seen as the genetic background becomes more uniform is the level of photoperiod sensitivity within the A632 inbred line. Recent studies have shown that many temperate maize inbreds have been bred to have reduced photoperiod sensitivity in order to have broader growing ranges, and so crosses to tropical inbred lines might show increased flowering time responses. Multiple maize inbred lines are used to characterize developmental mutants, as maize lines are genetically diverse and different phenotypes are seen depending on genetic background. During the course of this work, therefore, the mutants were also crossed to the temperate inbred lines A619, B73, Mo17, Ms71, and W22. These lines were chosen for agronomic importance, as well as a wider representation of genetic background, generation time, growth habit, and phenotype (Liu et al., 2003). These outcrosses occurred at a different rate, meaning that they were not comparable to the A632 background lines at the times the assays occurred. This material is, however, available for future studies of the effect of the insertion, and could provide further insight into the phenotypic effects of *gi* mutations.

The *gi1-m1* and *gi1-m2* double mutant lines provided intriguing evidence that the *gi* mutants may primarily affect flowering time when in a heterozygous state. Given that *AtGI* primarily affects flowering via protein-protein interactions, this could indicate that the *gi* insertion lines produce defective proteins unable to interact with flowering time proteins. Another possibility is that a GI homo- or heteromer of some number is needed for some of these interactions, and an imbalance in functional *gi* products no longer allows these to be made at the same rate. *In vitro,* AtGI has been shown to form tetramers (Black et al., 2011), although no functional characterization or *in vivo* verification of this exists. Further characterization of the double mutant lines will be needed to verify these results, as the segregating nature of most of the lines means that once the measurements are divided by genotype the sample sizes are quite small. As mentioned above, other maize inbred lines could provide stronger flowering time results, and construction of double mutant lines in these would also be worthwhile.

Despite the limited phenotypes seen in sufficiently introgressed mutants, multiple

QTL studies have identified either *gi1* or its region as being of importance to maize flowering time and domestication. Joint linkage analysis of the maize Nested Association Mapping (NAM) population found that many small effect QTL have additive effects on maize flowering time (Buckler et al., 2009). In this study, *gi1* was not directly implicated as contributing to a specific QTL affecting flowering time; however, a locus on chromosome 8 at 18.3 centimorgans (cM) was identified in a subset of tropical inbreds. This QTL delays flowering in all lines with the allele, and is distinct from the strong *vgt1* and *vgt2* QTLs located further downstream on this chromosome (Buckler et al., 2009; Salvi et al., 2007; Vlăduţu et al., 1999). The positions of the markers used to pinpoint this QTL (at 18.4 and 57.5 cM) bracket the *gi1* gene, so *gi1* (at 44.5 cM) is one candidate for the gene underlying this QTL. In another study, Hufford *et al*. identified likely domestication and improvement genes based on genome-wide resequencing of a large number of improved maize lines, landraces and wild accessions (Hufford et al., 2012). In this analysis, *gi1* was identified as a candidate improvement gene. Therefore, some aspect of *gi1* function appears to have contributed to at least one key improvement trait.

Testing chlorophyll content of BC5/BC6 lines provided a phenotypic result consistent with *atgi* mutant phenotypes. *gi1-m1* mutants had significantly more chlorophyll than their wild type siblings, and *gi2-m1* mutants also had increased levels. This indicates that maize *gis* are still linked to chlorophyll levels, although the mechanics behind this remain unclear.

The results from the disease resistance test provided an interesting possibility that the *gi* genes in maize may be involved in disease resistance processes. It is likely that this effect is not direct, but instead a result of the way in which the clock is disrupted in *gi* mutants. Studies in *Arabidopsis* and other species have demonstrated that the circadian clock primarily acts to correctly time disease resistance events (Wang et al., 2011b; Zhang et al., 2013). A recent study showed that *AtGI* mutants had increased resistance to *Fusarium oxysporum* infection, potentially indicating direct involvement of *AtGI* in disease resistance processes (Lyons et al., 2015). It is therefore possible either that the *gi* genes directly regulate disease resistance processes, or that the phenotypes seen are the result of the altered clock gene expression timing in *gi* mutants. Further work to characterize this effect would be needed to draw firm conclusions, however, as only one of the three diseases tested showed visible differences between the lines.

Expression of *gi1* and, to an extent, *gi2* was capable of complementing the flowering delay of an Arabidopsis *gi* loss-of-function allele (Figure 2.13), which shows that GI1 and GI2 can make the correct protein-protein interactions to integrate into this heterologous signaling system. This indicates that the GI proteins in maize are sufficiently conserved between dicots and monocots to have cross-species functionality, and are able to regulate dicot flowering time processes. The flowering time system in monocots, however, has diverged over evolutionary time (Ballerini and Kramer, 2011): although maize gis have the same domains, their interaction partners and regulatory networks could be entirely different.

In the context of what is known of *GI* mutants in other plants, these findings support the idea that *GI* genes have different effects in monocots than they do in dicots. Dicot *GI* mutants appear to have similar genetic effects to *AtGI* and the same strong phenotypic effects. In contrast, monocot *GI* mutants have similar genetic effects, but the

phenotypic effects are reduced, opposite to those seen in dicots, or practically undetectable. Flowering time is an especially good example of this, as monocots use multiple different regulatory systems than dicots to promote flowering (Ballerini and Kramer, 2011; Buckler et al., 2009). *AtGI,* which has such extensive flowering time effects in Arabidopsis*,* appears to have been entirely sidelined in favor of other genes and systems in monocots. While other backgrounds, double mutants, and phenotypic measurements may yet prove maize *gi1* and *gi2* to have important physiological roles, these results show that clock gene functions characterized in Arabidopsis will need to be re-thought in monocots.

Materials and Methods

Plant materials

Dr. Sarah Hake at the Plant Gene Expression Center (Albany, CA, USA) generously provided maize inbred A632. Dr. Robert Meeley at Pioneer Hi-Bred International, Inc. (Johnson, IA, USA) screened the Trait Utility System for Corn (TUSC) population for *Mutator* (*Mu*) insertions in *gi1* and *gi2*, and provided putative mutant seed through Agricultural Research Service Cooperative Research and Development agreement number 58-3K95-7-1225-M.

The TUSC population was created by the Pioneer Hybrid company beginning in 1992, and carries the high copy number *Mutator* (*Mu*) transposon (Hake and Bennetzen, 2009; Meeley and Briggs, 1995). The collection was generated in two main phases, the PV03 phase and the BT94 phase, and so each stock has a population designator that represents its origin. The PV03 phase represented ~350 inbred by *Mu* crosses using about 65 different standard *Mu* lines. A mixture of inbred females was used, largely on the basis of which were ready to cross, and so this portion of the TUSC population has a highly heterogeneous background. The BT94 phase has less diversity, as all *Mu*-carrying plants were crossed to females of a single hybrid line, namely Pioneer 3394. The TUSC population contains mutant alleles for nearly 90% of the genes targeted, but because *Mu* is high copy number, mutants of interest often contain a number of background mutations. Standard practice in dealing with these maize stocks is to cross them to inbred lines for five or six generations in order to reduce the complication of having background insertions.

gi1 mutant alleles were *gi1-m1::Mu3* and *gi1-m2::Mu1* (Mendoza et al., 2012)*,* and the *gi2* mutant allele was *gi2-m1.* The parental inbred background of the gi1-m1 and gi1-m2 insertions is primarily A632, while that of the gi2-m1 insertion is CJ27. Each allele was backcrossed to A632 five or more times. At different stages in backcrossing, plants were sib-crossed or selfed to develop homozygous lines, which were then used in genetic and phenotypic assays (Supplemental Figure 2.1).

Growth conditions for genetic analyses and timecourse sampling strategies

SD for gene expression experiments was provided by a growth chamber that provided a 3:1 mix of cool white fluorescent and incandescent white light at 300 µmol m^{-1} s^{-1}. For both SD and LD experiments, daytime temperature was 28 °C and nighttime temperature was 22 °C.

For gene expression in both LD and SD, the plants were sampled at V-stage 6. Two punches were taken from each individual at each timepoint, one from the youngest

fully expanded leaf (L6), and one from the next-youngest leaf. Punches began 8cm away from leaf tip or if tip missing, 6cm from break. Per genotype, 10-12 most robust-appearing individuals used, or if fewer than 10 germinated, all used. Before collecting tissue, settings were altered to constant light and constant daytime temperature, and collection began at ZT27 on Day 2. A repeat-sampling strategy was employed, with each subsequent timepoint taken closer to the base of the leaf than the previous one.

For the preliminary LL timecourse on BC3 plants, 2 V7 A632 plants, 5 V6 gi1-m2 plants, and 3 V7 gi2-m1 plants were sampled. Plant pots were moved from the greenhouse into a growth chamber set to constant light, and sampling was begun 24 hours after that transition. The same repeat-sampling strategy as above was used to take two punches taken per plant every timepoint for gi1-m2 and gi2-m1, and three were taken for A632. The LD and LL gene expression results for BC3 plants are the results of two single timecourses, while those for SD are the amalgamated results of three separate timecourses (SD1, SD3, SD5).

For the LL timecourse on BC5/BC6 plants, a walk-in growth chamber was used that provided white light at about 440 µmol photosynthetically active radiation (PAR) m^{-1} s^{-1} at shelf level and about 698 µmol PAR m^{-1} s^{-1} at top height of plants. Plants were germinated and grown in LD conditions (16h L:12 h D) with daytime temperatures between 26°C and 28°C (depending on shelf) and nighttime temperatures of 22 °C. Before collecting tissue, settings were altered to constant light and constant daytime temperature, and collection began at ZT27 on Day 2. 18 punches were taken at each timepoint using a 4 mm Uni-Core punch, and new plants were sampled every timepoint except the last two. The lines used were CB38, CB42, CB51, CB43, CB44, and CB54. Due to lower rates of germination, a different number of punches and plants was used for CB38 (9 punches, 2 plants) and CB42 (18 punches, 1 plant), but all other lines were 6 punches and 3 plants per timepoint.

Sample collection, first-strand cDNA preparation and real-time quantitative PCR (RT-qPCR)

Plant tissue for RT-qPCR was harvested with a 2.5 or 4.0 mm Uni-Core punch, collected in a 1.5 mL microcentrifuge tube, and immediately frozen in liquid N_2. A green light-emitting diode (LED) light was used for collection during dark periods. Samples were pulverized with 3.2 mm stainless steel beads using nylon adapters chilled with liquid N_2 in a MixerMill 301.

For the first timecourses, total RNA was purified with Plant RNA Reagent, and for the later timecourses with TRIzol, both according to the manufacturer's recommendations. Initially, contaminating DNA was removed from 5 ug total RNA with the TURBO DNA-free kit, and first-strand cDNA was prepared from 1.6 ug of DNase-treated RNA with the Maxima Universal First-Strand cDNA Synthesis kit. Later, the manufacturer altered the Maxima kit to be compatible with an initial 2 minute dsDNAse removal step, and so this was used subsequently. Initially, the resulting cDNA was diluted 1:5 prior to use, later only 1:4.

RT-qPCR used EvaGreen dye and the listed primers (Supplemental Table 2.1) in a CFX96 RT-PCR Detection System. Briefly, two technical replicate RT-qPCR reactions received 2 uL each of diluted first-strand cDNA and consisted of 1X Ex Taq buffer, 1X EvaGreen dye, 0.2 mm dNTP mix, 5% vol/vol DMSO, 0.05 mg ml^{-1} BSA, 0.01% vol/vol

Tween-20 and 0.3 mM of each primer. Thermocycling conditions were a step of 95 °C for 3 min, then 40 cycles of 95°C for 10s, 60°C for 30s, and 75 °C for 10 s (detection of EvaGreen at this step), followed by a melt curve starting at 60 °C ramping up to 95 °C in 0.5 °C increments that were 10 s each. Ct values were calculated with the regression function in the Bio-Rad CFX Manager Software from reactions exhibiting a single melting peak at the melting temperature of the specific RT-qPCR product. The gene *GRMZM5G816228* was used as the normalization transcript in initial RT-qPCRs, because it is broadly expressed in leaves at moderate levels and transcript levels do not fluctuate over time (Khan *et al*. 2010). Later RT-qPCRs used the gene *GRMZM2G064954,* which was found to fluctuate even less in an RNA-Seq dataset. Expression values were calculated according to the formula: Expression level = $2^{\wedge}(Ct^{normalizer} - Ct^{gene})$.

Growth and flowering time phenotyping

SD photoperiod experiments for flowering time in BC3 plants were performed in a greenhouse with approximately 12 h of natural daylight in February and March 2012. LD conditions in the greenhouse for flowering time experiments and gene expression experiments in BC3 plants were the same except the light period was extended to 16 h in the evening with supplemental light composed of an equal mix of light from Ecolux® Lucalox® High-Pressure Sodium ED18 and Multi-Vapor® Quartz Metal Halide ED37 lamps. LD conditions in the greenhouse for phenotyping of BC5/BC6 plants were approximately 12h of natural daylight between November 2014 and January 2015. Natural light was extended to 16 h in the evening with supplemental light composed of red and blue LEDs.

Field phenotyping assays were done on the Gill tract in Albany, California during the summers of 2011, 2012, and 2015, and on the University of California, Davis campus during the summer of 2012. At Gill tract, plants were sown in two to three trails separated by five to seven days starting in late May or early June. Plants in Davis were sown mid-May. At this latitude, day length ranged between 14 and 15 h over the course of the experiment.

Leaf number was counted after completion of silking and anthesis and the count included all leaves on the main stalk with the cotyledon counting as number 1. Flowering time was measured as the total number of leaves on the main stalk of the plant. Leaf number was chosen as a metric to study *gi* function, because *gi1* was expected to act early in flowering time regulation, namely at the point of transition from new leaf initiation to floral development (Sawa and Kay, 2011; Sawa et al., 2007). In addition, silking and anthesis are dependent on environmental conditions (Araus et al., 2012), and were considered less likely to be under clock regulation.

The timing of vegetative phase change was based on the loss of juvenile epicuticular wax from leaves (Evans and Poethig, 1995). The first leaf completely lacking visual evidence of juvenile waxes was counted as the first adult leaf. Plant height was measured after onset of silking and anthesis as the distance in cm from prop roots to the flag leaf with measuring poles calibrated to the half-cm. All phenotype results were plotted and analyzed using GraphPad Prism. Error bars used include the standard error of the mean (SEM), and the range. The type of error bar used is indicated below the graph in the figure legend.

Chlorophyll measurement

The lines used to measure chlorophyll were CB38, CB42, CB51, CB43, CB44, and CB54. Leaf punches were taken at mid leaf (equidistant from midrib and leaf margin) with a 4.0 mm Uni-Core punch, immediately put into 1 ml DMSO, and then incubated in a water bath at 65° C for 30 minutes. Then, 164.4 ul of each sample (as well as blanks) were transferred into wells of a Corning 96 Well UV Plate. Measurements of the samples were taken at A645 and A663 using a plate reader. Then, these measurements were adjusted to a 1 cm path length using the equation (sample-blank) / 0.5 cm (Warren, 2008), whereby 'blank' is an average of two measurements.

The adjusted measurements were used to calculate chlorophyll content using Arnon's equations (Richardson et al., 2002), as follows: Chlorophyll a (grams per liter) = 0.0127 * A663 – 0.00269 * A645; Chlorophyll b (grams per liter) = 0.0229 * A645 – 0.00468 * A663; Total chlorophyll (grams per liter) = 0.0202 * A645 + 0.00802 * A663. The obtained values were then adjusted from grams per liter to mg per cm^2 using the equation (Chlorophyll * 1000) / (Leaf punch area * Leaf punch number).

Two sets of chlorophyll measurements were made. The first set was pooled samples of 2 punches each from 3 plants, and four pools were taken per line. The second set was 2 punches from 1 plant, and three individual measurements were made per line. As some punches ended up stuck to sides of tubes, the variable 'Leaf punch number' represents the actual number of punches in the DMSO, which varied across samples. All results were plotted and analyzed using GraphPad Prism. Unpaired two-tailed t-tests were done to compare the mean results of mutant and non-mutant sibs to each other.

Disease resistance measurements

Disease tests were done in collaboration with the lab of Peter Balint-Kurti over two consecutive summers in 2014 and 2015 in Clayton, North Carolina and Blacksburg, Virginia. In 2014, BC3 plants were sent, and in 2015 BC5/BC6 plants were sent. Sufficient seed was sent for two biological replicates planted and inoculated at different times, and in some cases different fields. The response to three separate diseases was tested: Southern Leaf Blight (SLB), Northern Leaf Blight (NLB), and Grey Leaf Spot (GLS). Disease incidence was visually assessed on separate dates, and often by different people. In cases where multiple people assessed the same plants on the same day, an average score was plotted. Scoring was done on a scale of 1-9 for SLB and GLS with 9 being resistant, and on a scale of 0-100 for NLB with 0 being resistant. All results were plotted and analyzed using GraphPad Prism.

Construction of Arabidopsis transgenic lines and flowering time analysis

Arabidopsis transgenic lines were constructed by Dr. Frank Harmon and Desirée Stanley. Schematics of the transcriptional fusions between the *AtGI* promoter and the *gi1*/*AtGI* coding sequences (CDS) are outlined in Figure 2.13. The *gi1* CDS was amplified (Supplemental Table 2.1) from cDNA made from A632 leaf samples with Phusion DNA High-Fidelity DNA polymerase. The Arabidopsis *GI* CDS was amplified from cDNA made from whole 7-day-old seedlings (Supplemental Table 2.1). The *AtGI* promoter, which corresponded to genomic region from -1 to -2310 base pairs upstream of the Arabidopsis *GI* transcription start site, was amplified from genomic DNA with

primers that added a *NotI* site to the 3′-end of the fragment (Supplemental Table 2.1). All fragments were subcloned into the pENTR/D-TOPO vector. After verifying the DNA sequences by Sanger sequencing using the BigDye kit, the *AtGI* promoter fragment was cloned upstream of each CDS with *NotI*. Each *promoter::CDS* fusion was moved into the pEARLEYGATE301 binary vector (Earley et al., 2006) using LR Clonase II to make the corresponding expression construct.

Constructs were transformed into Arabidopsis *atgi-201* plants with *Agrobacterium* strain GV3101 by floral dip (Clough and Bent, 1998). Arabidopsis *atgi-201* seed was obtained from the Arabidopsis Biological Resource Center at The Ohio State University as germplasm name SALK_092757 (Alonso et al., 2003). Primary transgenic plants (T1 generation) were selected with 18 mg ml^{-1} DL-phosphinothricin on plates with 0.8% agar and 1X MS (Murashige and Skoog, 1962) medium in the LD conditions described later. Two representative T3 lines homozygous for a single *AtGIp::gi1* or *AtGIp::AtGI* insertion were selected for flowering time analysis. Flowering time was measured for plants grown in LD conditions with 16 h light followed by 8 h darkness at 23 °C in a Conviron growth chamber. Cool white fluorescent bulbs provided illumination at 50 µmol m^{-2} s^{-1}. Rosette leaves were counted when the inflorescence reached 1 cm in height and this date was counted as the day of flowering.

Expression of *AtGI* transcript and *gi1* transcript was evaluated 8 h after dawn in 1-week-old WT, *atgi-201* and T3 transgenic plants grown on plates in LD conditions as described earlier. Whole plants were harvested from plates, collected in a 1.5 mL microcentrifuge tube, and immediately frozen in liquid N_2. cDNA was made from total RNA extracted from these plants as described earlier. Expression of *gi1* and *AtGI* in these samples was measured as the number of transcript molecules present in an aliquot of cDNA. This method was chosen to allow quantitative comparison of expression across all genotypes and lines, because *gi1* is not an endogenous Arabidopsis transcript. Standard curves of Ct values versus transcript number were constructed for *gi1*, *AtGI* and *AtPP2A* with the corresponding purified RT-qPCR product as template. *AtPP2A* served as normalization standard (Shin et al., 2007). Standard curves were calculated from a serial 1:2 dilution series spanning 1×10^7 to 7.81×10^4 single-stranded DNA molecules, which encompassed the range of Ct values observed with the experimental samples. The number of transcript molecules in samples was determined from the standard curve based on the Ct value from RT-qPCR reactions performed as described earlier. To account for technical variation, *gi1* and *AtGI* expression is presented as the ratio of their transcript number to that of *AtPP2A*.

Figures

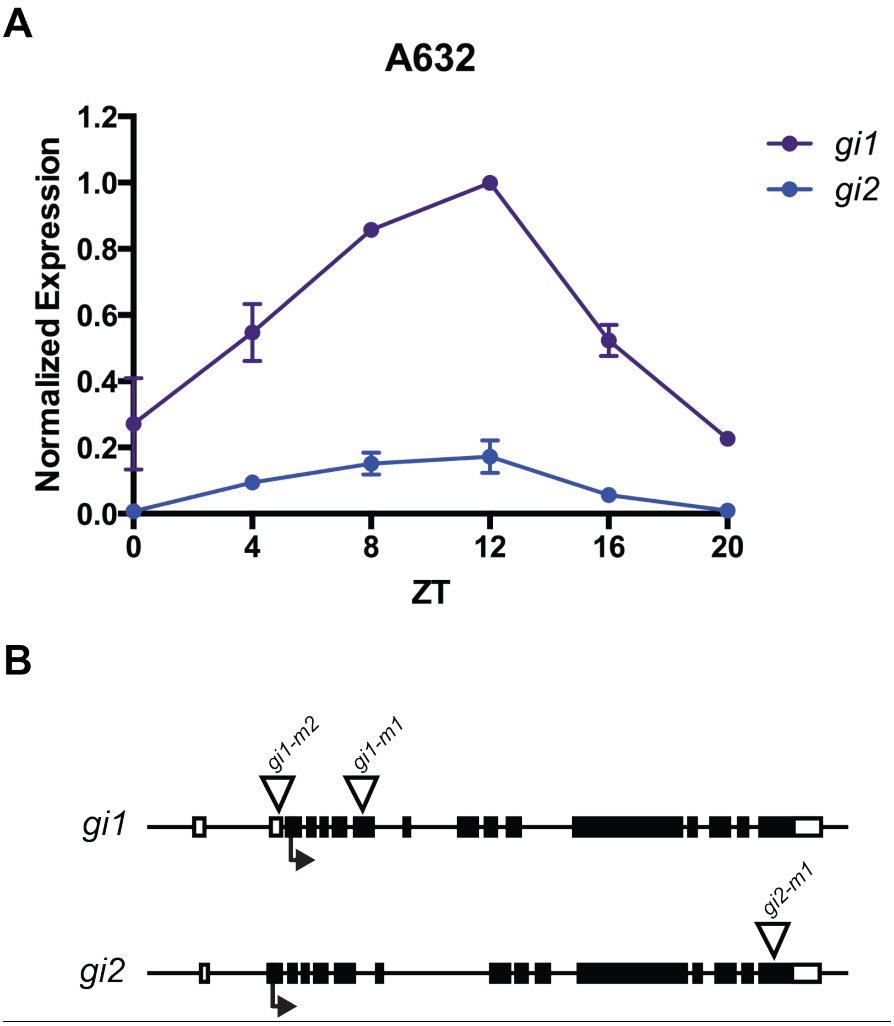

Figure 2.1. A) *gi1* (purple) and *gi2* (blue) expression peaks in the evening, at ZT12. Representative RT-qPCR of *gi1* and *gi2* expression patterns in A632 normalized against IPP2 expression levels. **B)** Schematics of the *gi1* and *gi2* genes. Open boxes represent untranslated regions (UTRs), closed boxes represent exons, and arrows below the genes indicate transcription start sites. Unfilled triangles above the gene schematic indicate the locations of *Mu* transposon insertions.

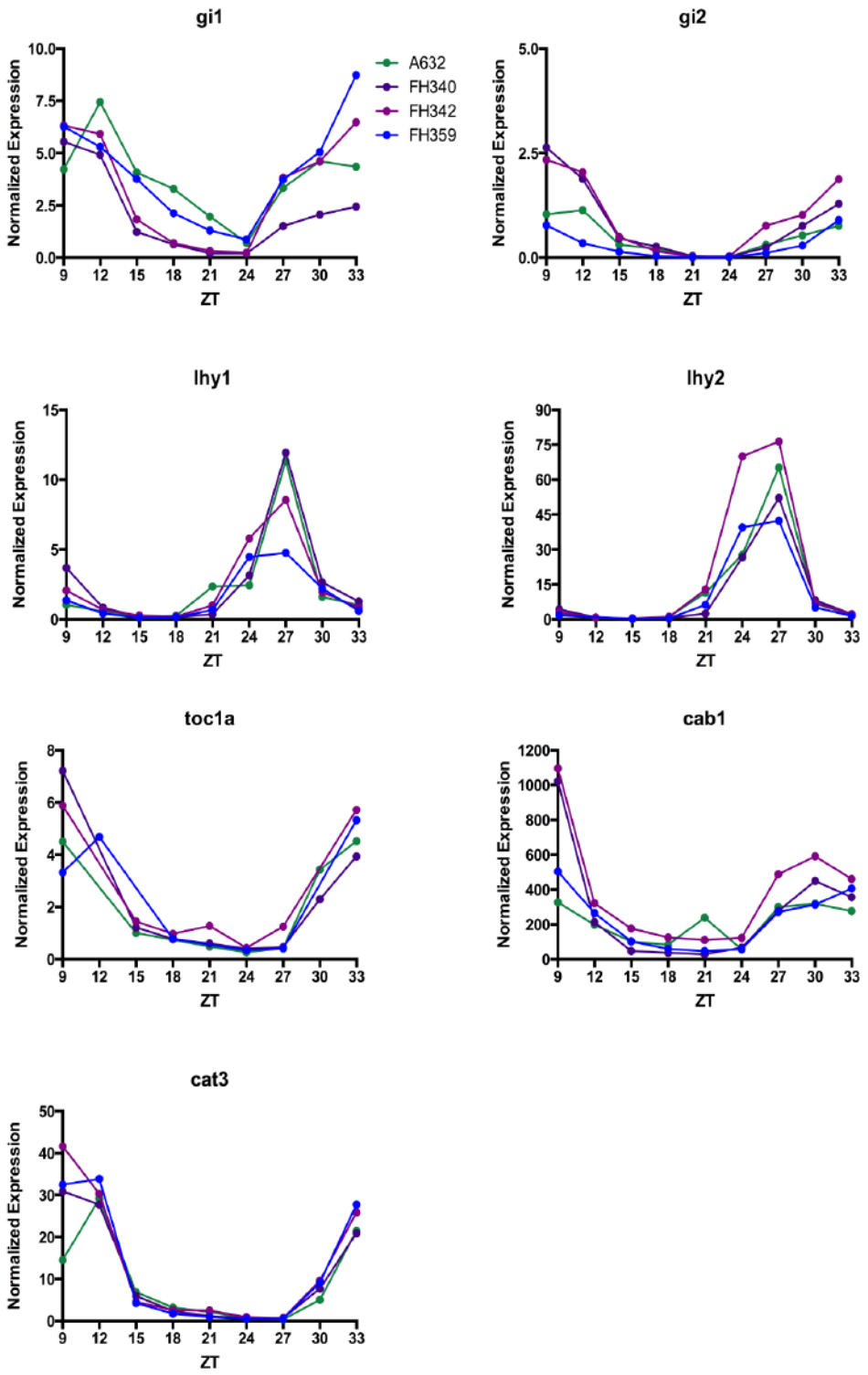

Figure 2.2. RT-qPCRs of maize circadian clock genes in A632 (green), GI1-M1 (FH340) (purple), GI1-M2 (FH342) (fuchsia), and FH359 (blue) lines grown under LD conditions. Timecourse spans from 9 hours after dawn (ZT9) of one day to 9 hours after dawn the next (ZT33), and graphs represent one biological replicate.

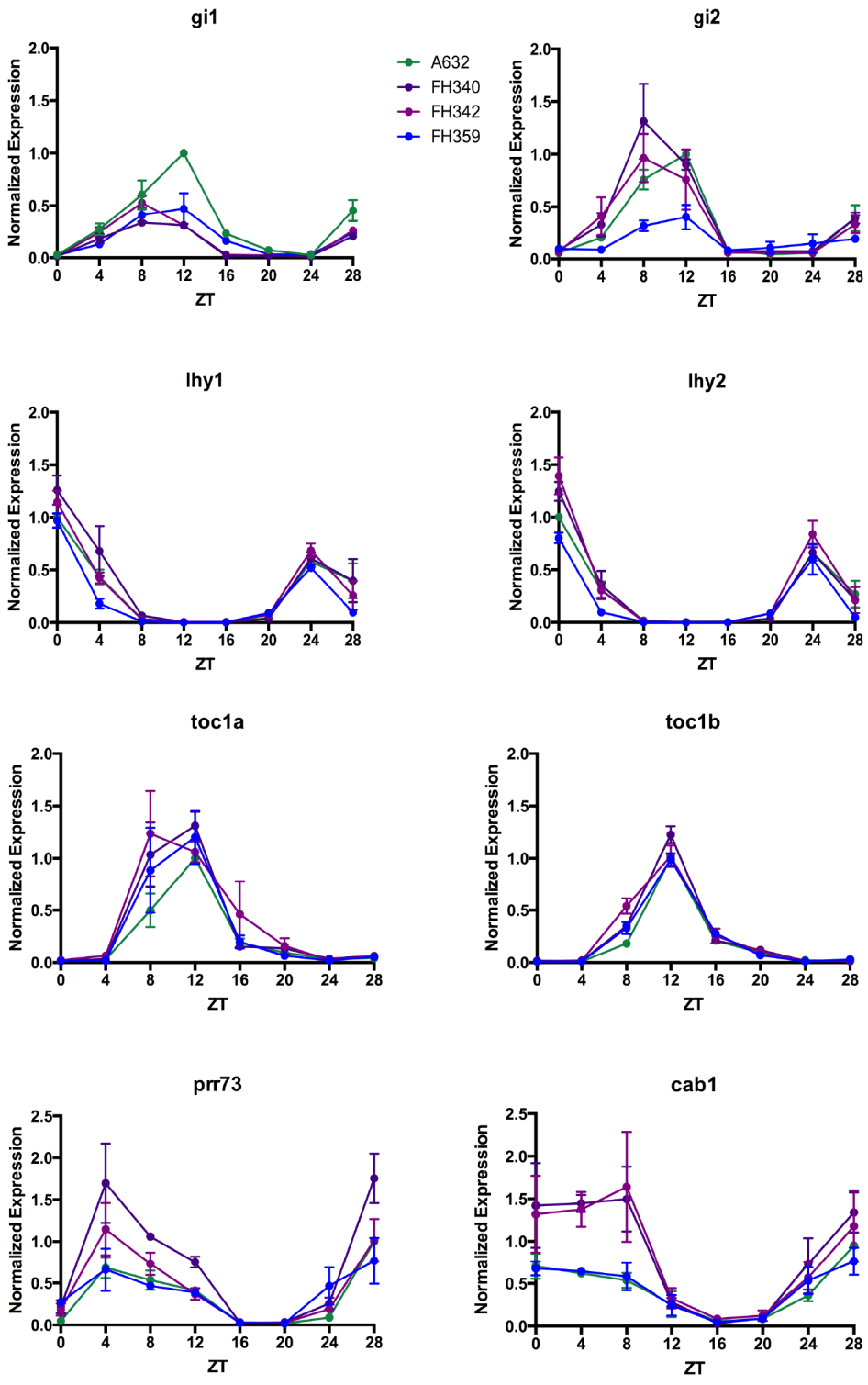
gi1
gi2
lhy1
lhy2
toc1a
toc1b
prr73
cab1
A632
FH340
FH342
FH359
Normalized Expression
ZT

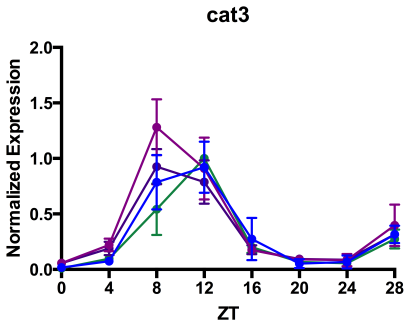

Figure 2.3 (this page and previous page). RT-qPCRs of maize circadian clock genes in A632 (green), GI1-M1 (FH340) (purple), GI1-M2 (FH342) (fuchsia), and FH359 (blue) lines grown under SD conditions. Timecourse spans dawn (ZT0) of one day to 4 hours after dawn (ZT28) the next. Graphs represent three biological replicates, and bars are SEMs.

A

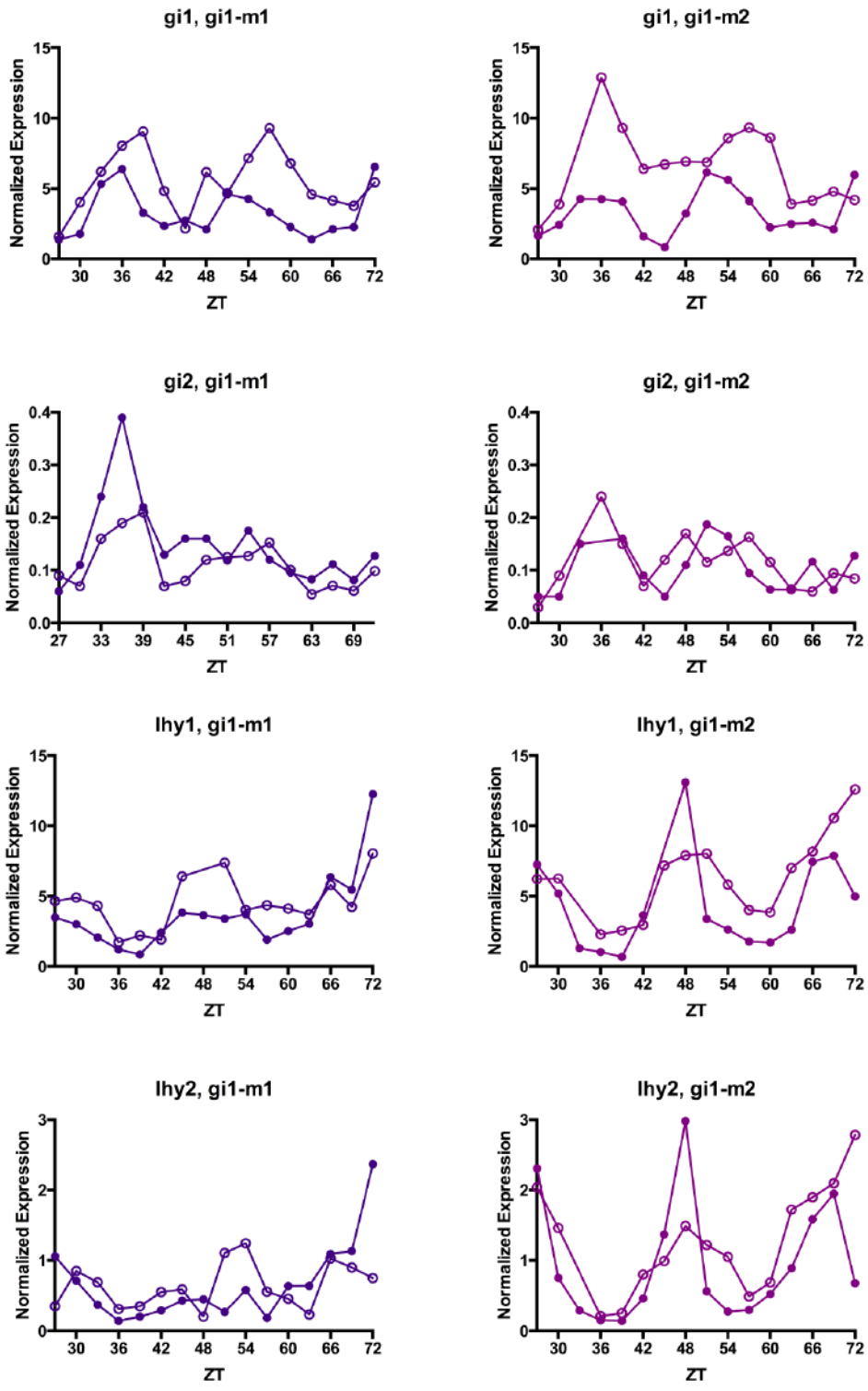
gi1, gi1-m1
gi1, gi1-m2
gi2, gi1-m1
gi2, gi1-m2
lhy1, gi1-m1
lhy1, gi1-m2
lhy2, gi1-m1
lhy2, gi1-m2
Normalized Expression
ZT

B

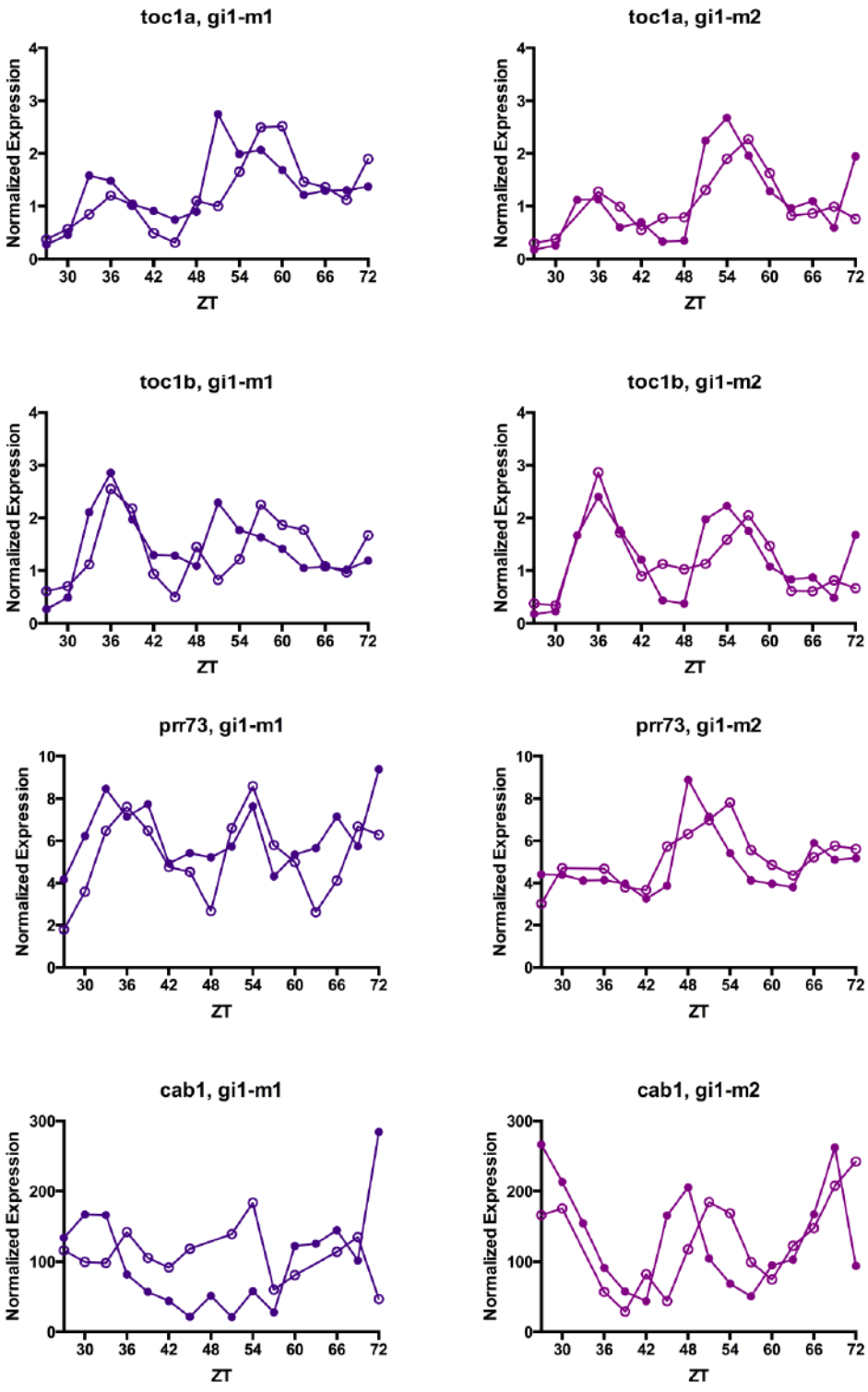
toc1a, gi1-m1
toc1a, gi1-m2
toc1b, gi1-m1
toc1b, gi1-m2
prr73, gi1-m1
prr73, gi1-m2
cab1, gi1-m1
cab1, gi1-m2
Normalized Expression
ZT
30 36 42 48 54 60 66 72

C

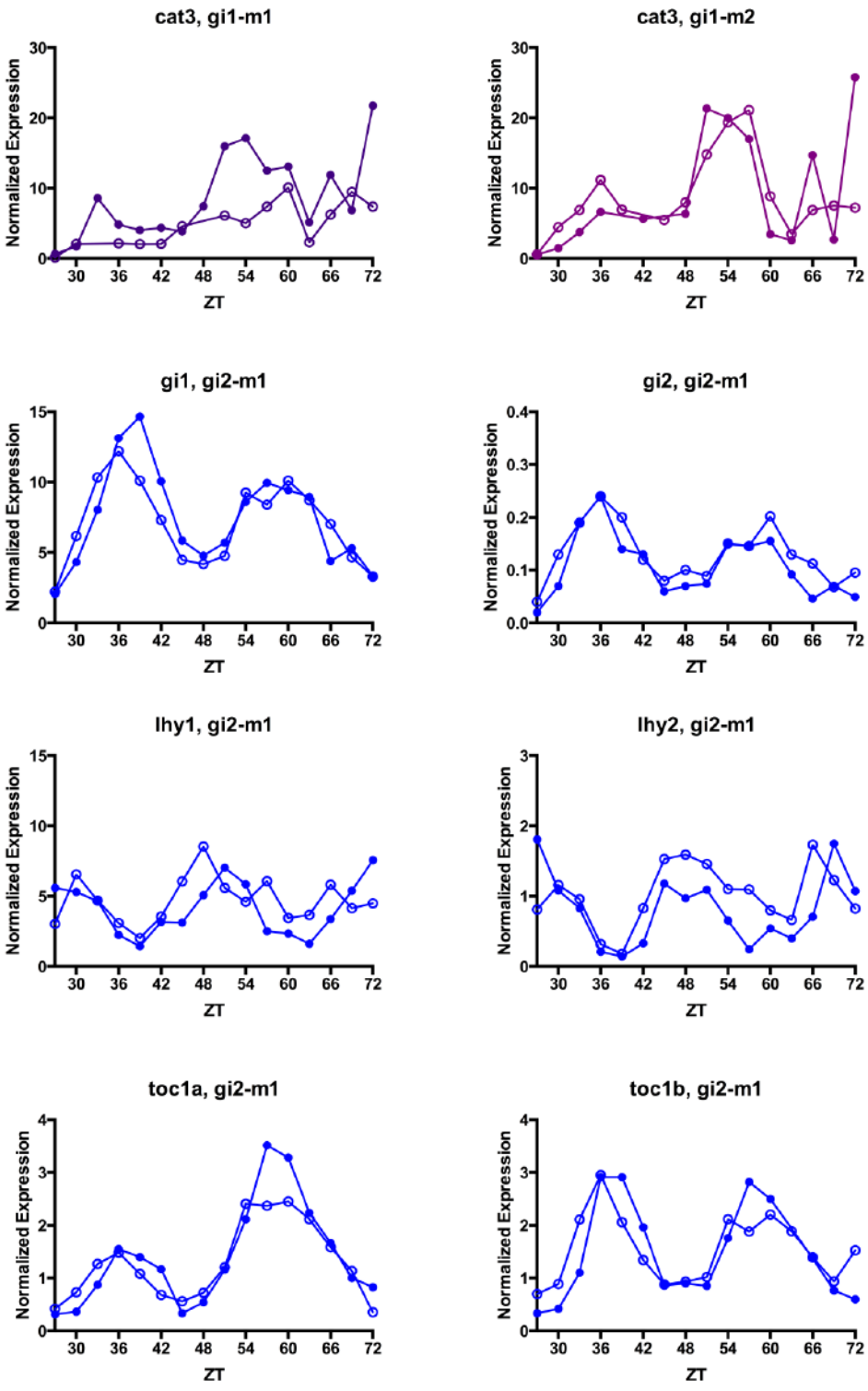
cat3, gi1-m1
cat3, gi1-m2
gi1, gi2-m1
gi2, gi2-m1
lhy1, gi2-m1
lhy2, gi2-m1
toc1a, gi2-m1
toc1b, gi2-m1
Normalized Expression
ZT

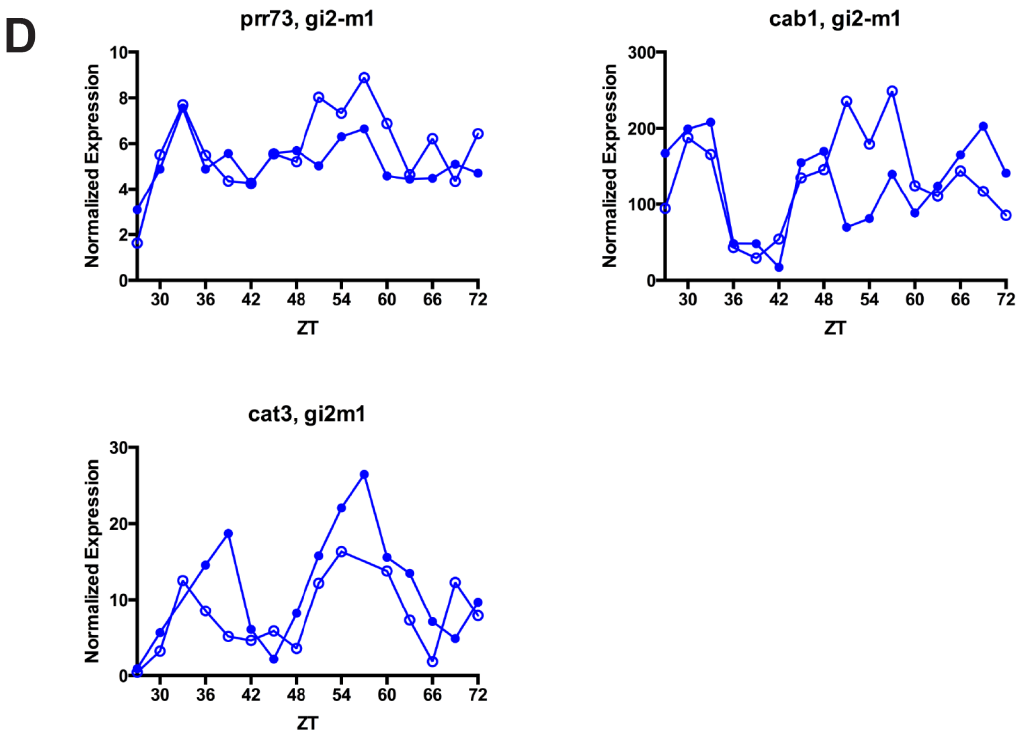

Figure 2.4 (this page and three previous pages). RT-qPCRs of maize circadian clock genes grown under LL conditions. Empty circles represent homozygous non-mutant sib lines, filled circles represent homozygous mutant lines. **A), B), C)** Expression of circadian clock genes in a *gi1-m1* non-mutant line (CB38, purple, empty circles), a *gi1-m1* mutant line (CB51, purple, filled circles), a *gi1-m2* non-mutant line (CB54, fuchsia, empty circles), and a *gi1-m2* mutant line (CB42, fuchsia, filled circles). **C)**, **D)** Expression of circadian clock genes in a *gi2-m1* non-mutant line (CB43, blue, empty circles), and a *gi2-m1* mutant line (CB44, blue, filled circles). Timecourse spans 3 hours after dawn after one full day in LL (ZT27) until dawn two days later (ZT72). Graphs represent one biological replicate.

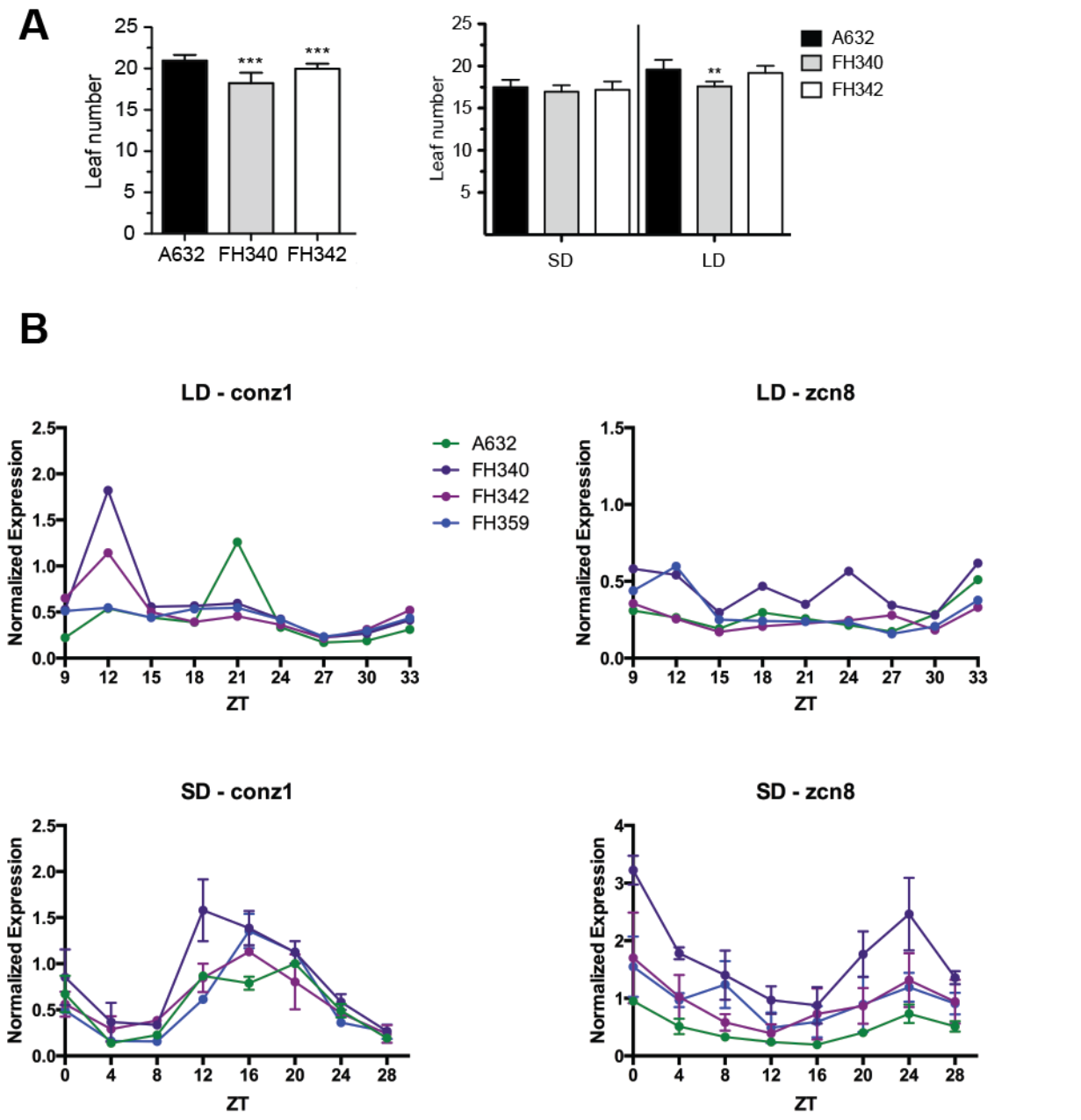

Figure 2.5.A) On left, Leaf number produced by field-grown A632 (black bar, n=122 individuals), GI1-M1 (FH340) (*gi1-m1*, grey bar, n=108), and GI1-M2 (FH342) (*gi1-m2*, white bar, n=91) plants. Leaf number is the average count, error bars are standard deviation, and asterisks over bars indicate p-values of <0.001 (***) or <0.01 (**) when compared to A632 with an unpaired two-tailed t-test. On right, leaf number produced by same lines in SD or LD conditions when grown in the greenhouse. **B)** RT-qPCRs of *conz1* and *zcn8* expression in A632 (green), GI1-M1 (FH340) (purple), GI1-M2 (FH342) (fuchsia), and FH359 (blue) plants grown in SD and LD conditions. Timecourses presented are those from Figures 2.2 and 2.3, and plants are not those used in **A)**.

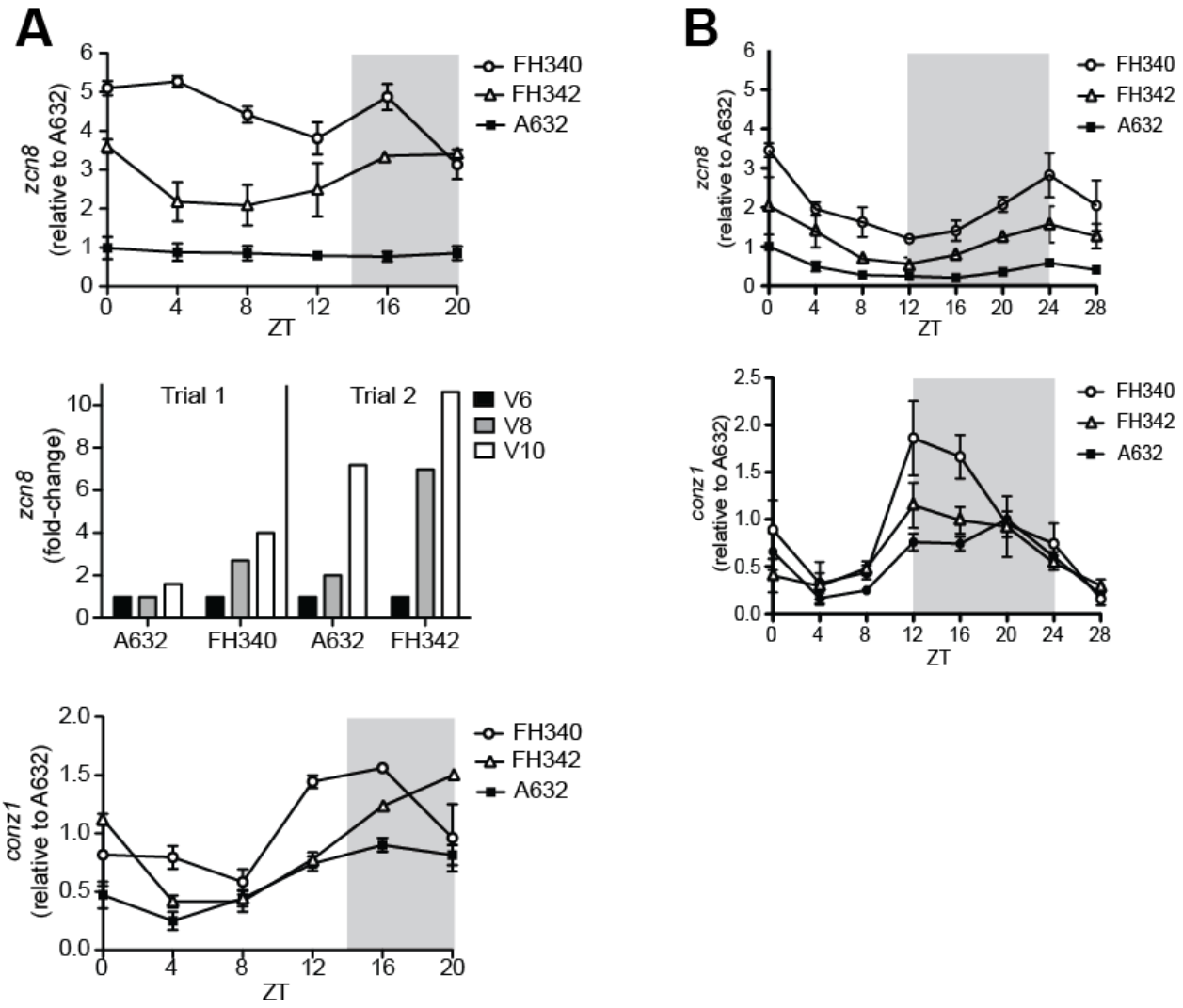

Figure 2.6. A) On top, Expression of *zcn8* in *gi1-m1* (FH340) (open circles), *gi1-m2* (FH342) (open triangles), and A632 (filled squares) beginning at dawn (ZT0) under LD field conditions at the V7 stage. The grey region denotes the dark period of the photoperiod. In middle, *zcn8* expression at ZT16 at stages V6 (black bars), V8 (grey bars), and V10 (white bars) for two independent trials in the field, and the fraction of the expression of the level observed in V6 plants of that genotype is shown. On bottom, expression of *conz1* in the same plants and same timepoints as on top. *zcn8* and *conz1* expression was determined with RT-qPCR in pooled samples of 10-15 plants. Relative expression for each time point is the average of at least two biological replicates and is presented as the fraction of the highest expression value for A632. Error bars are SEM. **B)** Expression of *zcn8* and *conz1* in stage 7 SD-grown plants, and normalization was done in the same way as described in **B).** These are the same plants as used in **2.5.A)**, and five individuals were used in two independent experimental replicates.

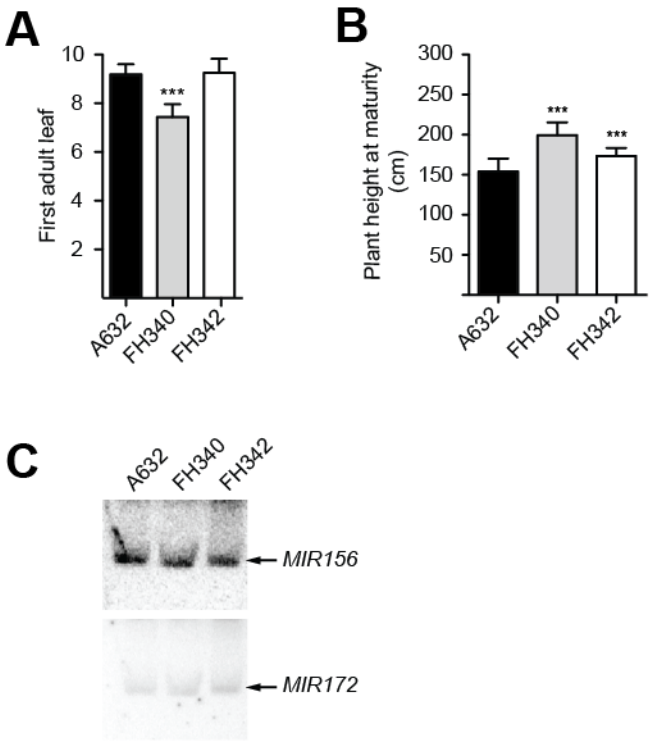

Figure 2.7. A) Timing of vegetative phase change in A632 (black bar), *gi1-m1* (FH340) (grey bar), and *gi1-m2* (FH342) (white bar) according to the appearance of the first adult leaf. **B)** Height of A632 (black bar, n=53), *gi1-m1* (FH340) (grey bar, n=52), *gi1-m2* (FH342) (white bar, n=53) plants from prop roots to flag leaf at anthesis/silking. For **A)** and **B)**, plants were a subset of those scored for flowering time in Figure 2.5. Error bars are standard deviation, and asterisks over bars indicate p-values of <0.001 (***) when compared to A632 with an unpaired two-tailed t-test. **C)** miR172 and miR156 levels were determined for A632, *gi1-m1* (FH340), and *gi1-m2* (FH342) in whole seedlings at the V3 stage by northern blot with ^{32}P-labeled oligonucleotide probes complementary to either zma-MIR156 or zma-MIR172c. The same blot was probed separately for each microRNA. Blots were performed as described previously (Chuck et al., 2007; Park et al., 2002). Labeled arrows indicate the position of the band corresponding to either miR172 or miR156.

A

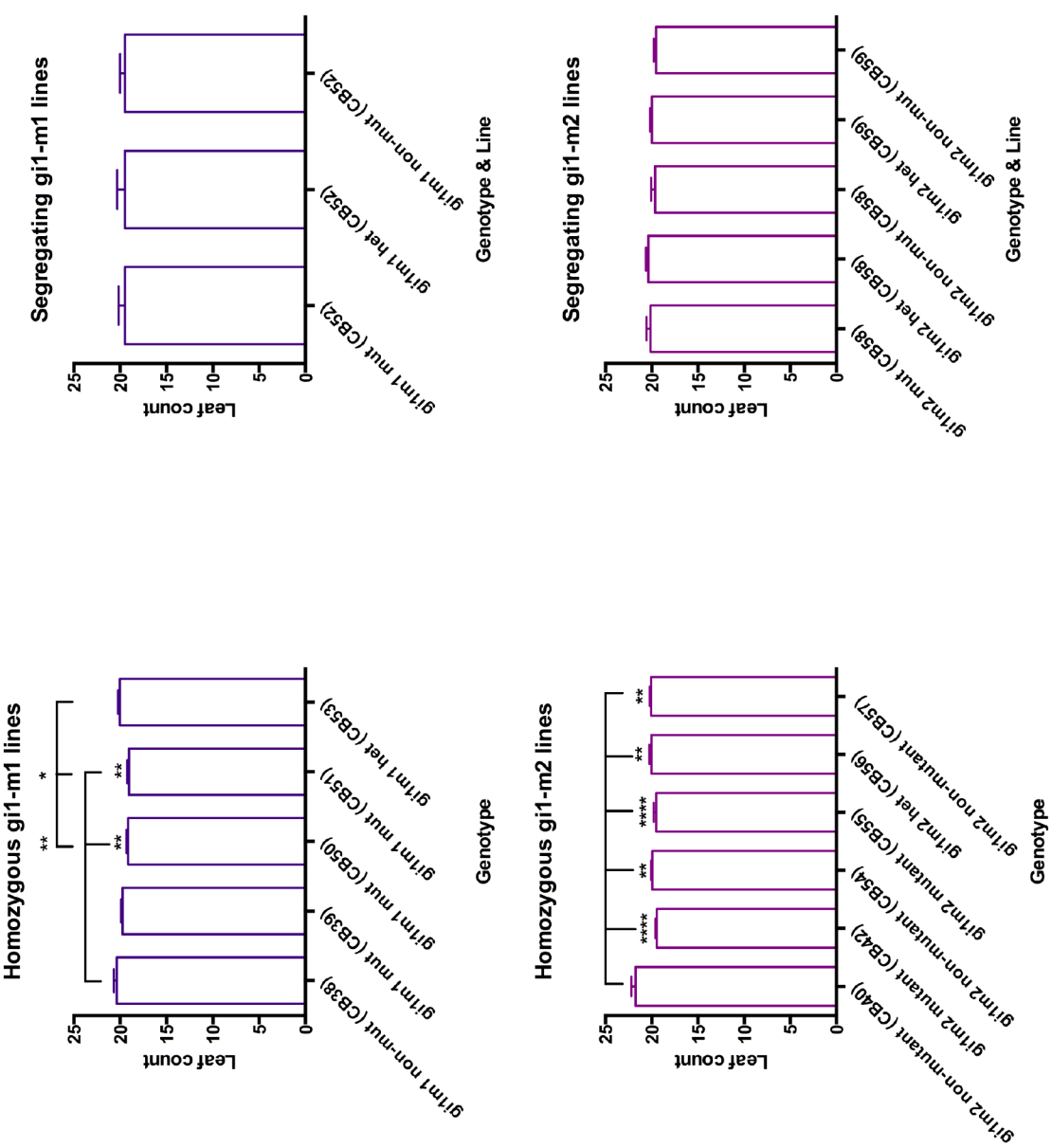
Segregating gi1-m1 lines
Leaf count
0
5
10
15
20
25
gi1m1 mut (CB52)
gi1m1 het (CB52)
gi1m1 non-mut (CB52)
Genotype & Line
Segregating gi1-m2 lines
gi1m2 mut (CB58)
gi1m2 het (CB58)
gi1m2 non-mut (CB58)
gi1m2 het (CB59)
gi1m2 non-mut (CB59)
Homozygous gi1-m1 lines
**
*
**
**
gi1m1 non-mut (CB38)
gi1m1 mut (CB39)
gi1m1 mut (CB50)
gi1m1 mut (CB51)
gi1m1 het (CB53)
Genotype
Homozygous gi1-m2 lines
****
**
****
**
**
gi1m2 non-mutant (CB40)
gi1m2 mutant (CB42)
gi1m2 non-mutant (CB54)
gi1m2 mutant (CB55)
gi1m2 het (CB56)
gi1m2 non-mutant (CB57)

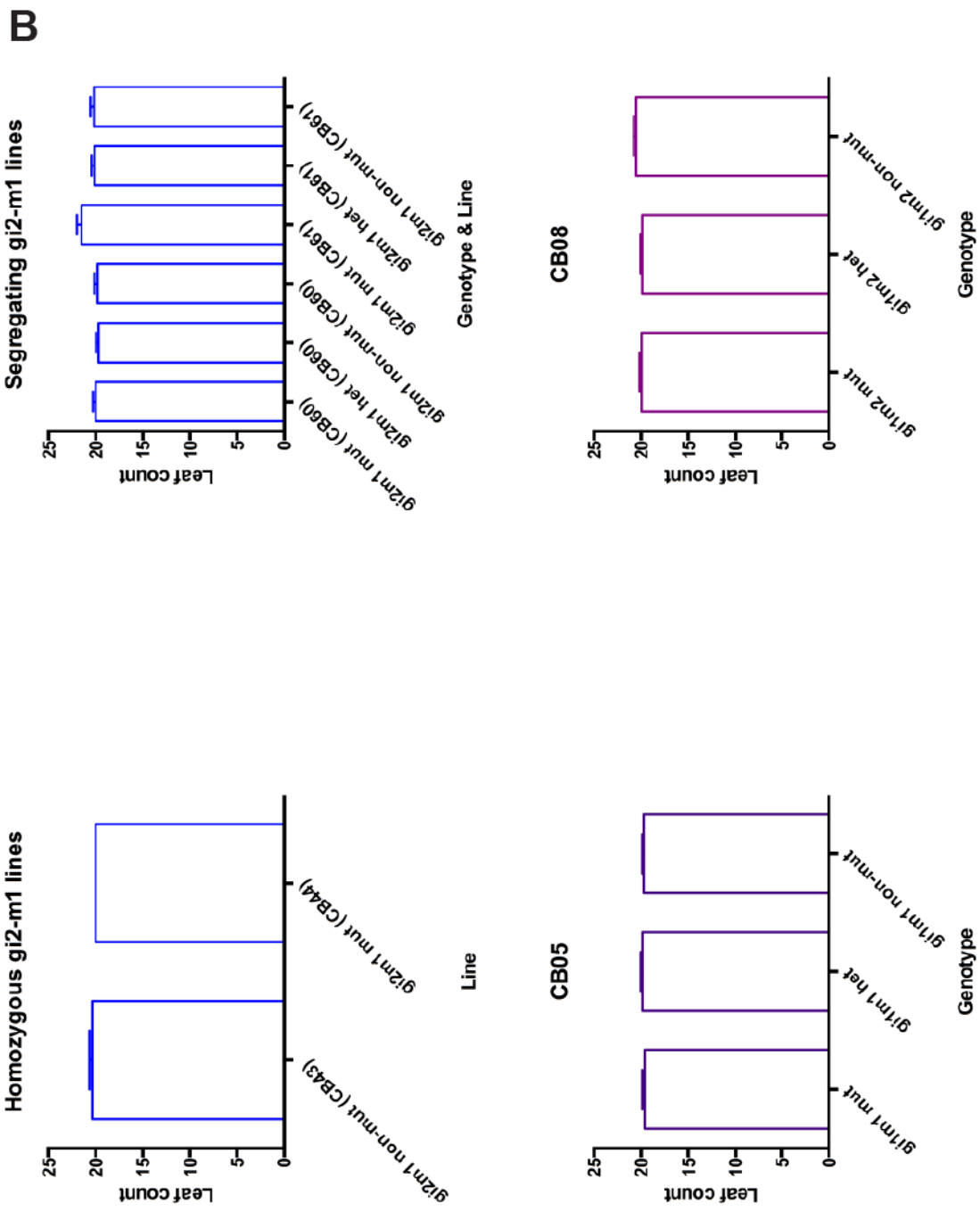
B
Segregating gi2-m1 lines
Leaf count
0
5
10
15
20
25
gi2m1 mut (CB60)
gi2m1 het (CB60)
gi2m1 non-mut (CB60)
gi2m1 mut (CB61)
gi2m1 het (CB61)
gi2m1 non-mut (CB61)
Genotype & Line
Homozygous gi2-m1 lines
gi2m1 non-mut (CB43)
gi2m1 mut (CB44)
Line
CB08
gi1m2 mut
gi1m2 het
gi1m2 non-mut
Genotype
CB05
gi1m1 mut
gi1m1 het
gi1m1 non-mut
Genotype

C

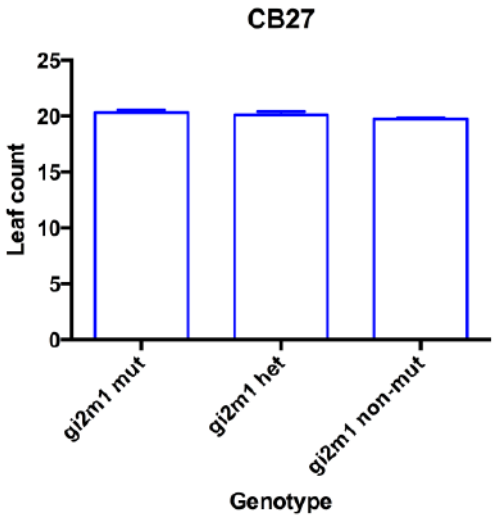

Figure 2.8 (this page and two previous pages). Final leaf counts of **A)** homozygous (n=12 to 23) and segregating (n=2-8) *gi1-m1* (purple) and homozygous (n=4 to 23 individuals) and segregating (n=6 to 9) *gi1-m2* (fuchsia) lines, **B)** homozygous (n=3 to 13) and segregating (n=2 to 13) *gi2-m1* (blue) lines, CB05 (purple, segregating *gi1-m1* line, n=84), and CB08 (fuchsia, segregating *gi1-m2* line, n=66), and **C)** CB27 (blue, segregating *gi2-m1* line, n=39). All plants grown in LD conditions in the field, and analyzed using ordinary one-way ANOVA and Tukey's multiple comparisons test. Error bars are SEM.

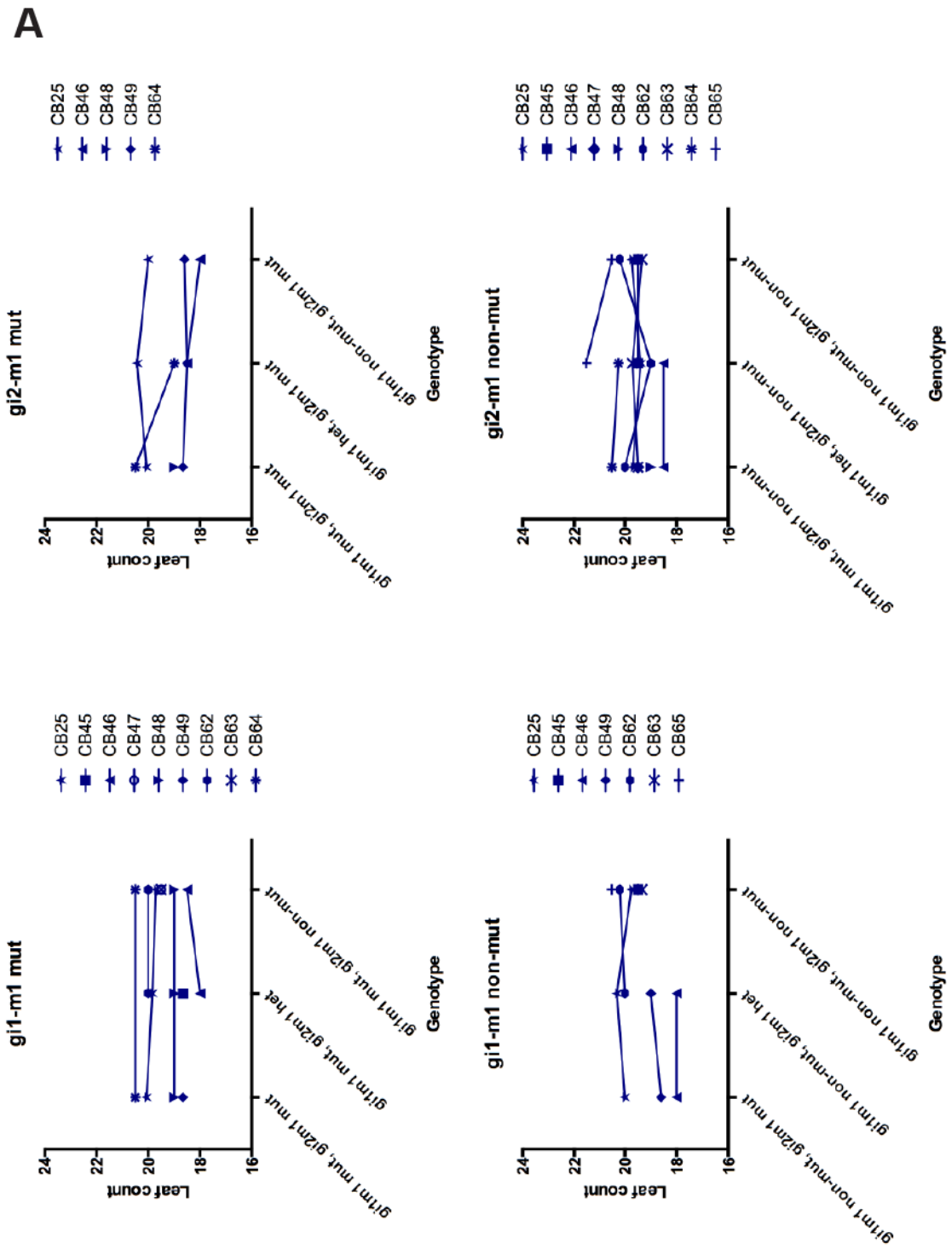
A
gi2-m1 mut
CB25
CB46
CB48
CB49
CB64
Leaf count
24
22
20
18
16
gi1m1 mut; gi2m1 mut
gi1m1 het; gi2m1 mut
gi1m1 non-mut; gi2m1 mut
Genotype
gi2-m1 non-mut
CB25
CB45
CB46
CB47
CB48
CB62
CB63
CB64
CB65
Leaf count
24
22
20
18
16
gi1m1 mut; gi2m1 non-mut
gi1m1 het; gi2m1 non-mut
gi1m1 non-mut; gi2m1 non-mut
Genotype
gi1-m1 mut
CB25
CB45
CB46
CB47
CB48
CB49
CB62
CB63
CB64
Leaf count
24
22
20
18
16
gi1m1 mut; gi2m1 mut
gi1m1 het; gi2m1 mut
gi1m1 non-mut; gi2m1 mut
Genotype
gi1-m1 non-mut
CB25
CB45
CB46
CB49
CB62
CB63
CB65
Leaf count
24
22
20
18
16
gi1m1 mut; gi2m1 non-mut
gi1m1 het; gi2m1 non-mut
gi1m1 non-mut; gi2m1 non-mut
Genotype

B

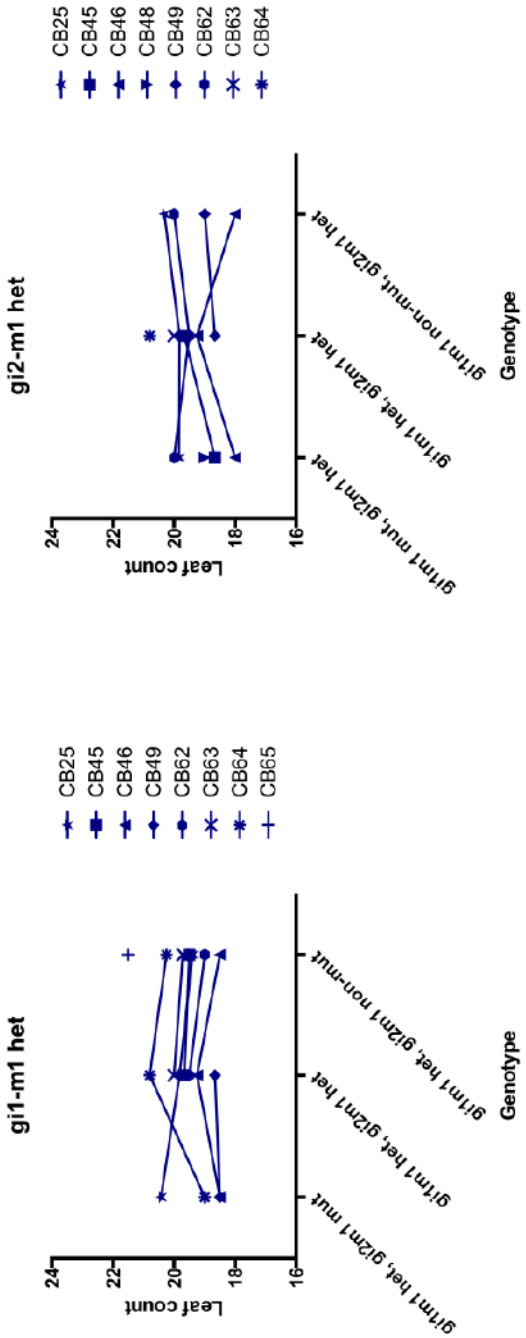

Figure 2.9 (this page and previous). Final leaf counts of double mutant lines carrying *gi1-m1* and *gi1-m2* insertions arranged by genotype. **A)** Homozygous mutant and homozygous non-mutant individuals for either insertion, and **B)** heterozygous individuals. Connecting lines were drawn between individuals belonging to the same line. CB25 is a segregating line (n=114), CB47 is a homozygous line (*gi1-m1* mut, *gi2-m1* non-mut, n=10), all other lines are segregating (n=6 to 16). Means plotted without error bars for clarity.

A

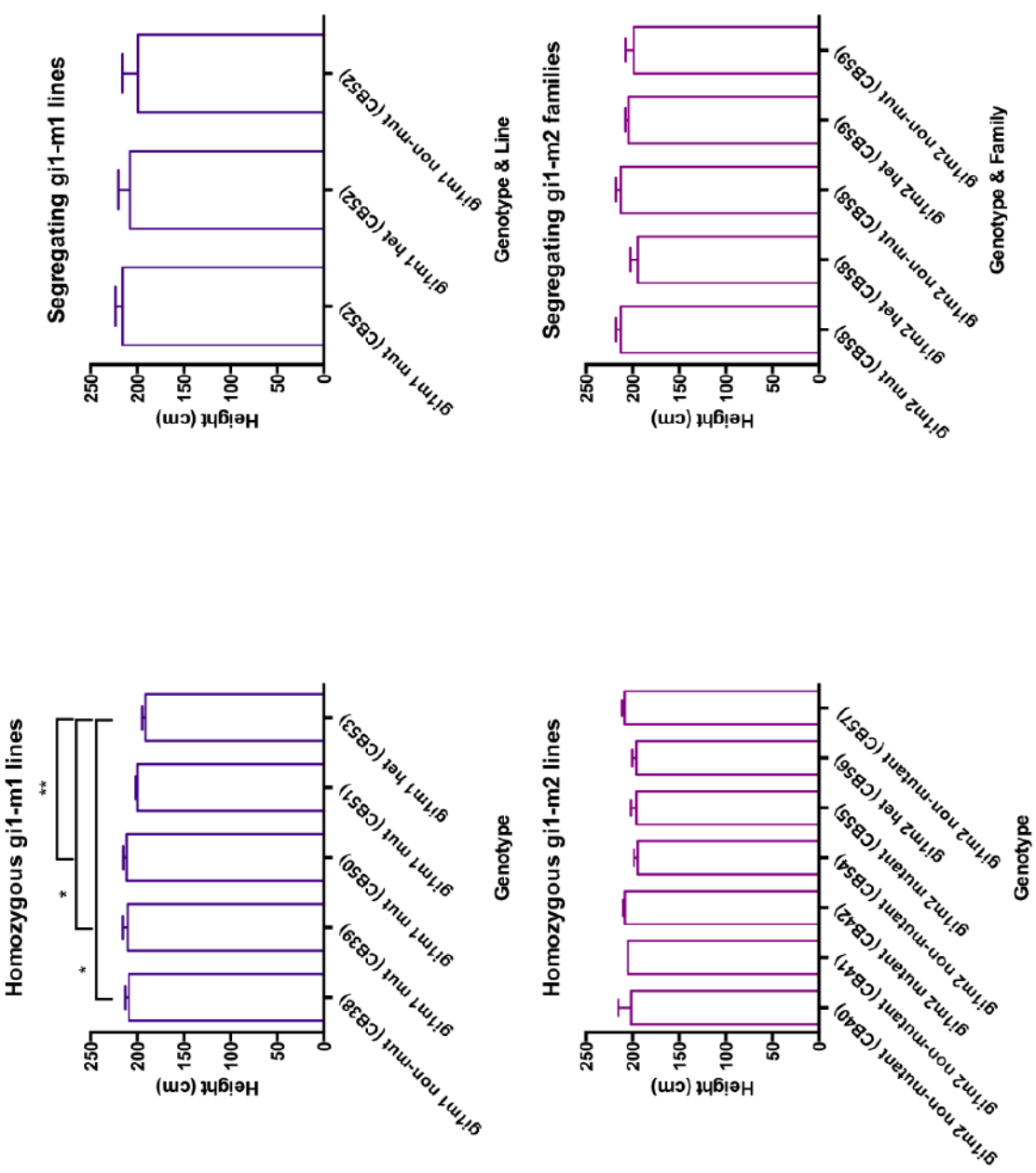
Homozygous gi1-m1 lines
Height (cm)
0
50
100
150
200
250
*
*
**
gi1m1 non-mut (CB38)
gi1m1 mut (CB39)
gi1m1 mut (CB50)
gi1m1 mut (CB51)
gi1m1 het (CB53)
Genotype
Homozygous gi1-m2 lines
Height (cm)
gi1m2 non-mutant (CB40)
gi1m2 mutant (CB41)
gi1m2 mutant (CB42)
gi1m2 non-mutant (CB54)
gi1m2 mutant (CB55)
gi1m2 het (CB56)
gi1m2 non-mutant (CB57)
Genotype
Segregating gi1-m1 lines
Height (cm)
gi1m1 mut (CB52)
gi1m1 het (CB52)
gi1m1 non-mut (CB52)
Genotype & Line
Segregating gi1-m2 families
Height (cm)
gi1m2 mut (CB58)
gi1m2 het (CB58)
gi1m2 non-mut (CB58)
gi1m2 het (CB59)
gi1m2 non-mut (CB59)
Genotype & Family

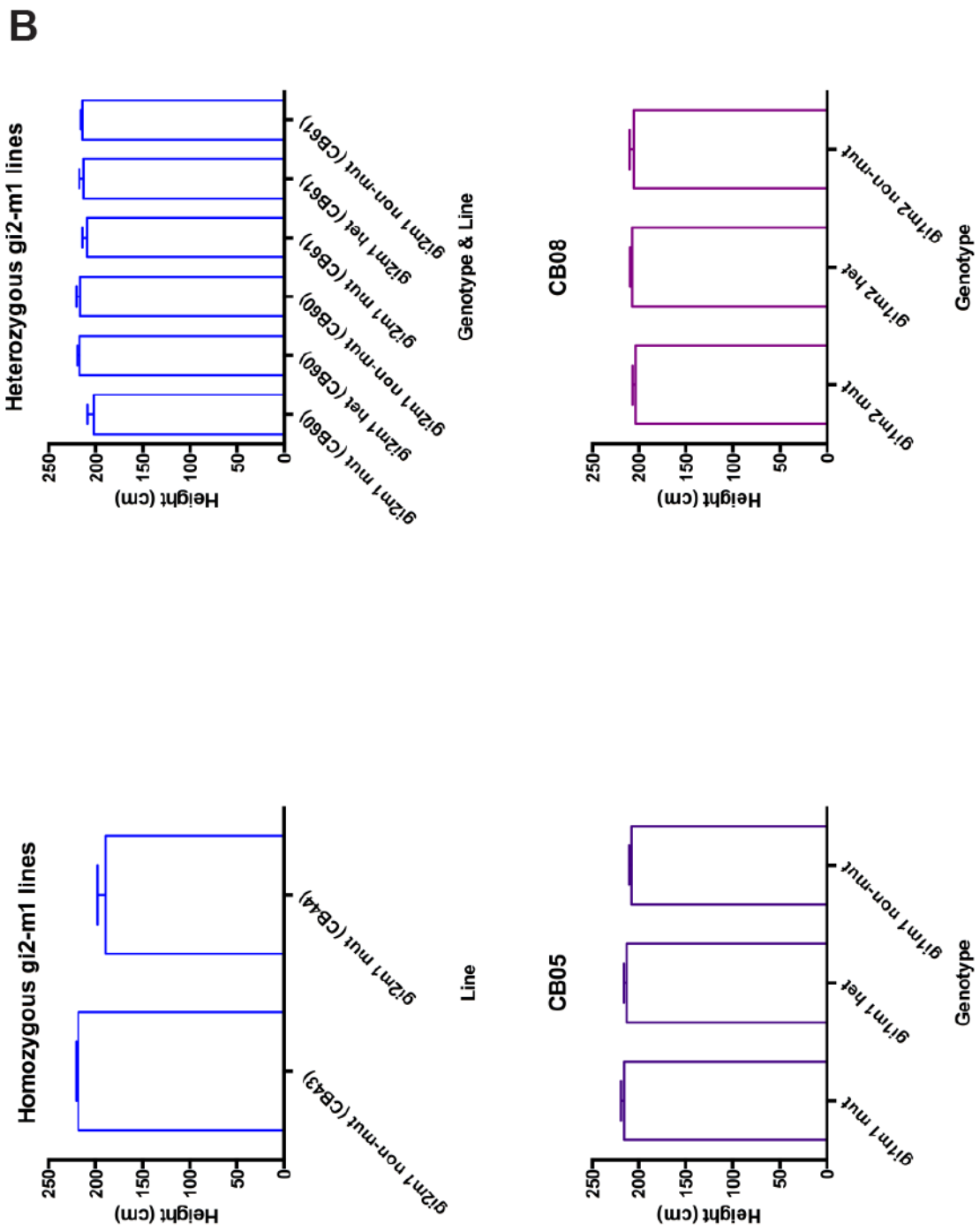
B
Heterozygous gi2-m1 lines
Height (cm)
250
200
150
100
50
0
gi2m1 mut (CB60)
gi2m1 het (CB60)
gi2m1 non-mut (CB60)
gi2m1 mut (CB61)
gi2m1 het (CB61)
gi2m1 non-mut (CB61)
Genotype & Line
CB08
gi1m2 mut
gi1m2 het
gi1m2 non-mut
Genotype
Homozygous gi2-m1 lines
gi2m1 non-mut (CB43)
gi2m1 mut (CB44)
Line
CB05
gi1m1 mut
gi1m1 het
gi1m1 non-mut
Genotype

C

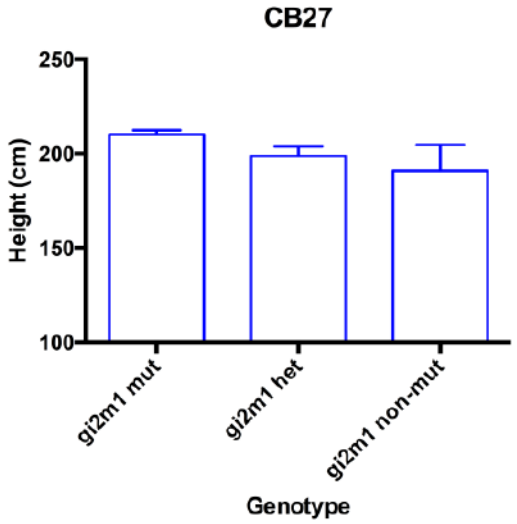

Figure 2.10. Final height measurements of **A)** homozygous (n=12 to 23) and segregating (n=2-8) *gi1-m1* (purple) and homozygous (n=4 to 23 individuals) and segregating (n=6 to 9) *gi1-m2* (fuchsia) lines, **B)** homozygous (n=3 to 13) and segregating (n=2 to 13) *gi2-m1* (blue) lines, CB05 (purple, segregating *gi1-m1* line, n=84), and CB08 (fuchsia, segregating *gi1-m2* line, n=66), and **C)** CB27 (blue, segregating *gi2-m1* line, n=39). All plants grown in LD conditions in the field, and analyzed using ordinary one-way ANOVA and Tukey's multiple comparisons test. Error bars are SEM.

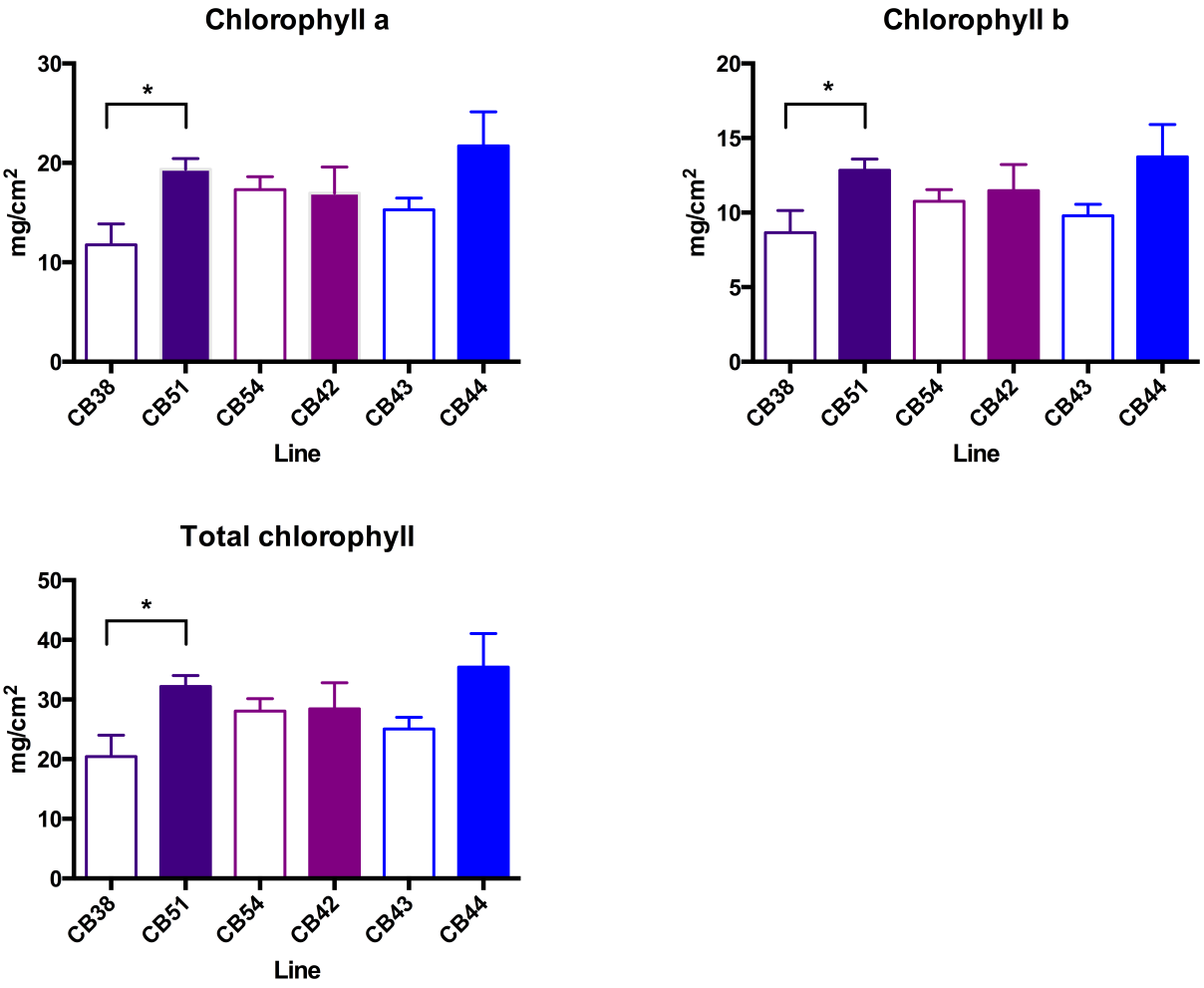

Figure 2.11. Measurement of leaf chlorophyll content in the lines CB38 (non-mutant, purple, empty bars), CB51 (*gi1-m1* mutant, purple, filled bars), CB54 (non-mutant, fuchsia, empty bars), CB42 (*gi1-m2* mutant, fuchsia, filled bars), CB43 (non-mutant, blue, empty bars), and CB44 (*gi2-m1* mutant, blue, filled bars). Means and SEMs of four pools of three plants each are depicted. Unpaired t-tests were done to compare each mutant with its non-mutant sib, and * = $p < 0.05$.

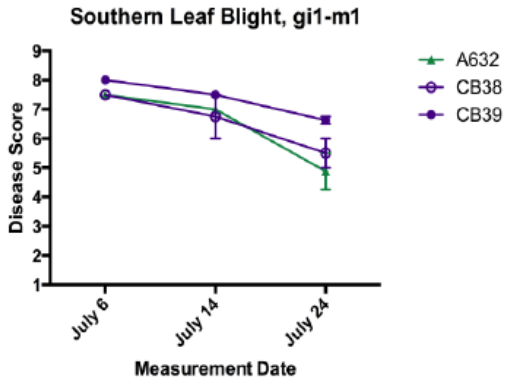
Southern Leaf Blight, gi1-m1
Disease Score
Measurement Date
July 6
July 14
July 24
A632
CB38
CB39

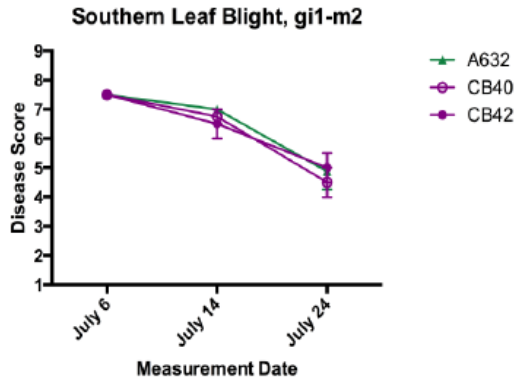
Southern Leaf Blight, gi1-m2
Disease Score
Measurement Date
July 6
July 14
July 24
A632
CB40
CB42

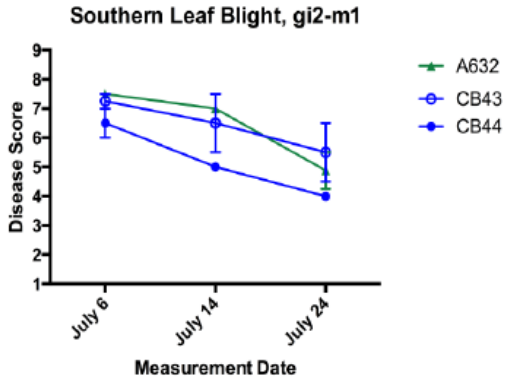
Southern Leaf Blight, gi2-m1
Disease Score
Measurement Date
July 6
July 14
July 24
A632
CB43
CB44

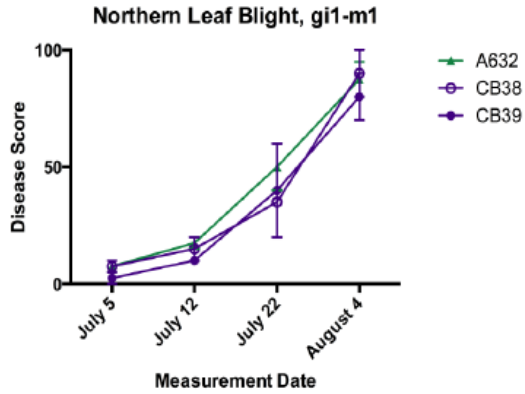
Northern Leaf Blight, gi1-m1
Disease Score
Measurement Date
July 5
July 12
July 22
August 4
A632
CB38
CB39

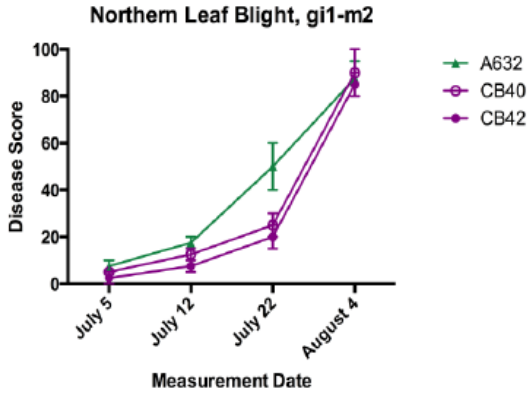
Northern Leaf Blight, gi1-m2
Disease Score
Measurement Date
July 5
July 12
July 22
August 4
A632
CB40
CB42

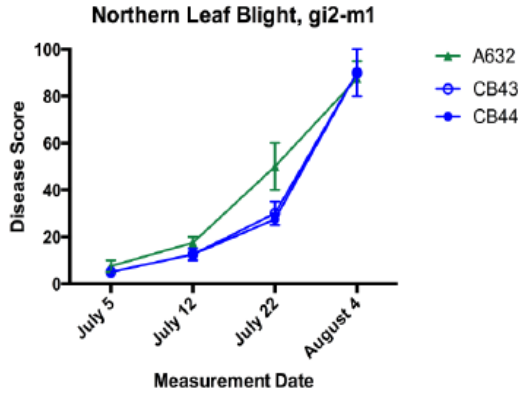
Northern Leaf Blight, gi2-m1
Disease Score
Measurement Date
July 5
July 12
July 22
August 4
A632
CB43
CB44

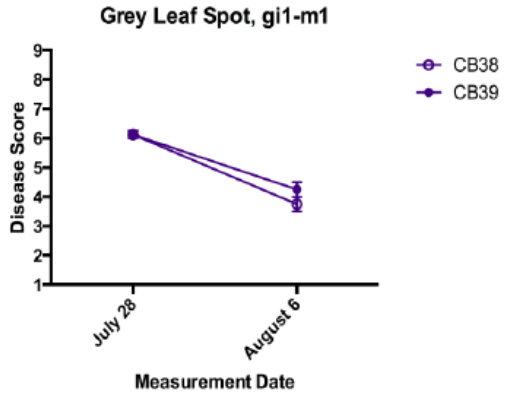
Grey Leaf Spot, gi1-m1
Disease Score
Measurement Date
July 28
August 6
CB38
CB39

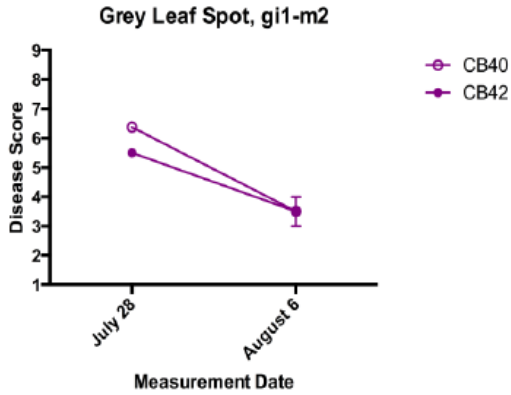
Grey Leaf Spot, gi1-m2
Disease Score
Measurement Date
July 28
August 6
CB40
CB42

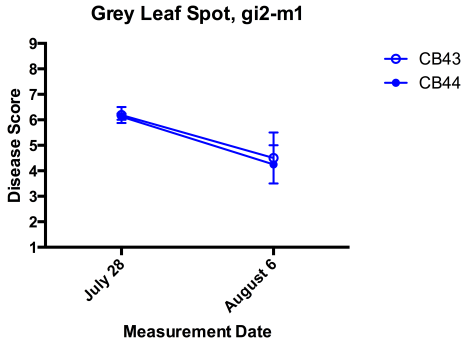

Figure 2.12 (this page and previous page). Measurement of disease responses in the lines A632, CB38 (non-mutant, purple, empty circles), CB39 (*gi1-m1* mutant, purple, filled circles), CB40 (non-mutant, fuchsia, empty circles), CB42 (*gi1-m2* mutant, fuchsia, filled circles), CB43 (non-mutant, blue, empty circles), and CB44 (*gi2-m1* mutant, blue, filled circles). The response to three separate diseases was tested: Southern Leaf Blight (SLB), Northern Leaf Blight (NLB), and Grey Leaf Spot (GLS). Measurements represent two biological replicates planted and inoculated at different times, and in some cases different fields. Error bars are SEM. Scoring was done on a scale of 1-9 for SLB and GLS with 9 being resistant, and on a scale of 0-100 for NLB with 0 being resistant.

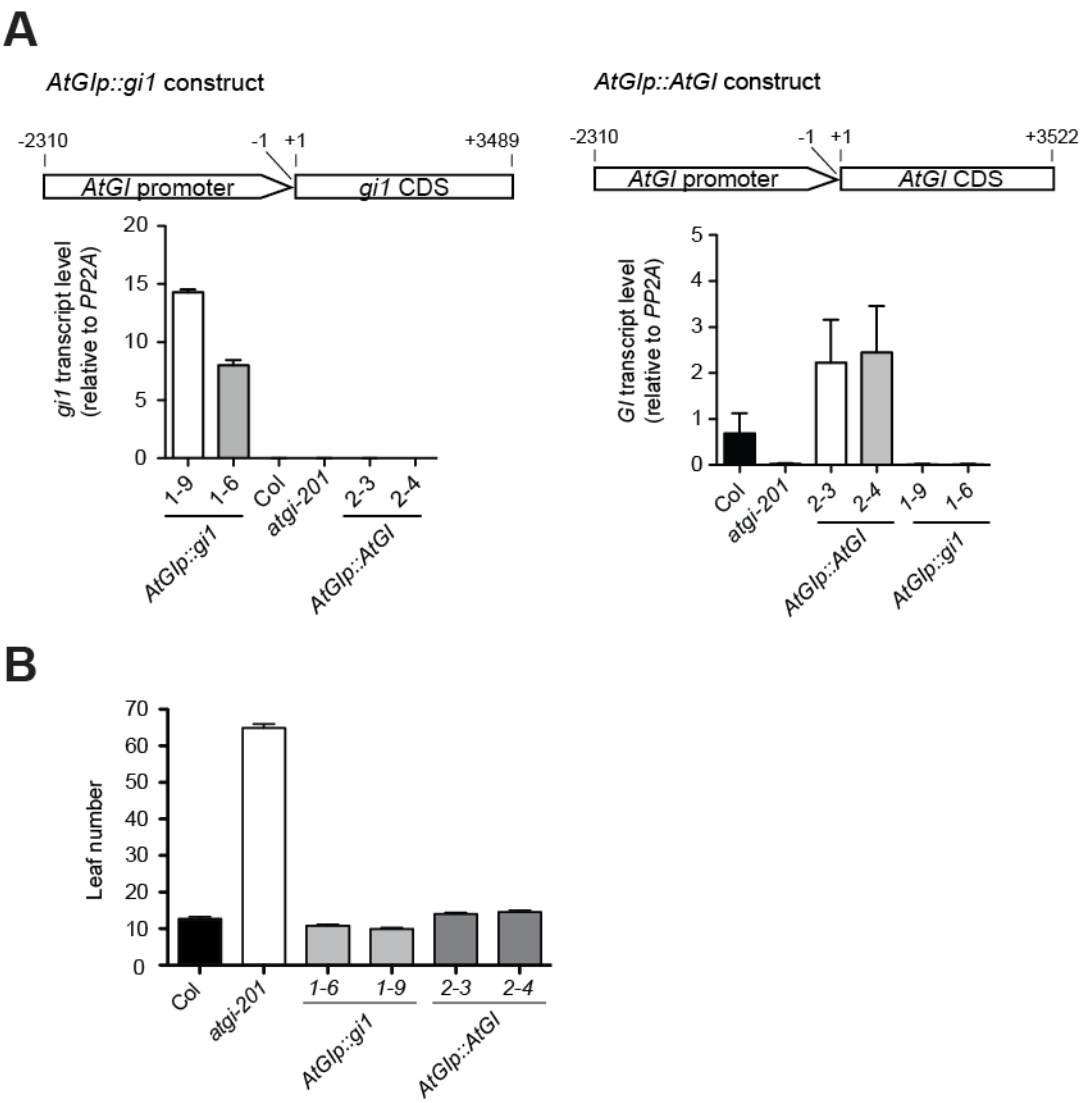

Figure 2.13. A) Above each graph is a schematic of the corresponding transcriptional fusion. Plants were grown in LD photoperiods for 1 week before harvest, and then RT-qPCR was used to quantify expression of *gi1* and *AtGI*. To account for technical variation, *gi1* and *AtGI* expression is presented as the ratio of their transcript number to that of *AtPP2A*. The number of transcript molecules in samples was calculated from a standard curve based on Ct value from RT-qPCR reactions. Data are the mean of three experimental replicates and error bars are standard deviation. **B)** Mean rosette leaf number at flowering of Arabidopsis WT (black bar, n = 15), *atgi-201* (white bar, n = 17) grown, *AtGIp::gi1* lines (grey bar; *1-6* (n = 28), *1-9* (n = 26)) and *AtGIp::AtGI* lines (dark grey bar; *2-3* (n = 30), *2-4* (n = 32)) in LD photoperiods. Data shown are from one representative experiment out of three independent experimental replicates, and error bars are standard deviation.

Supplemental Figures

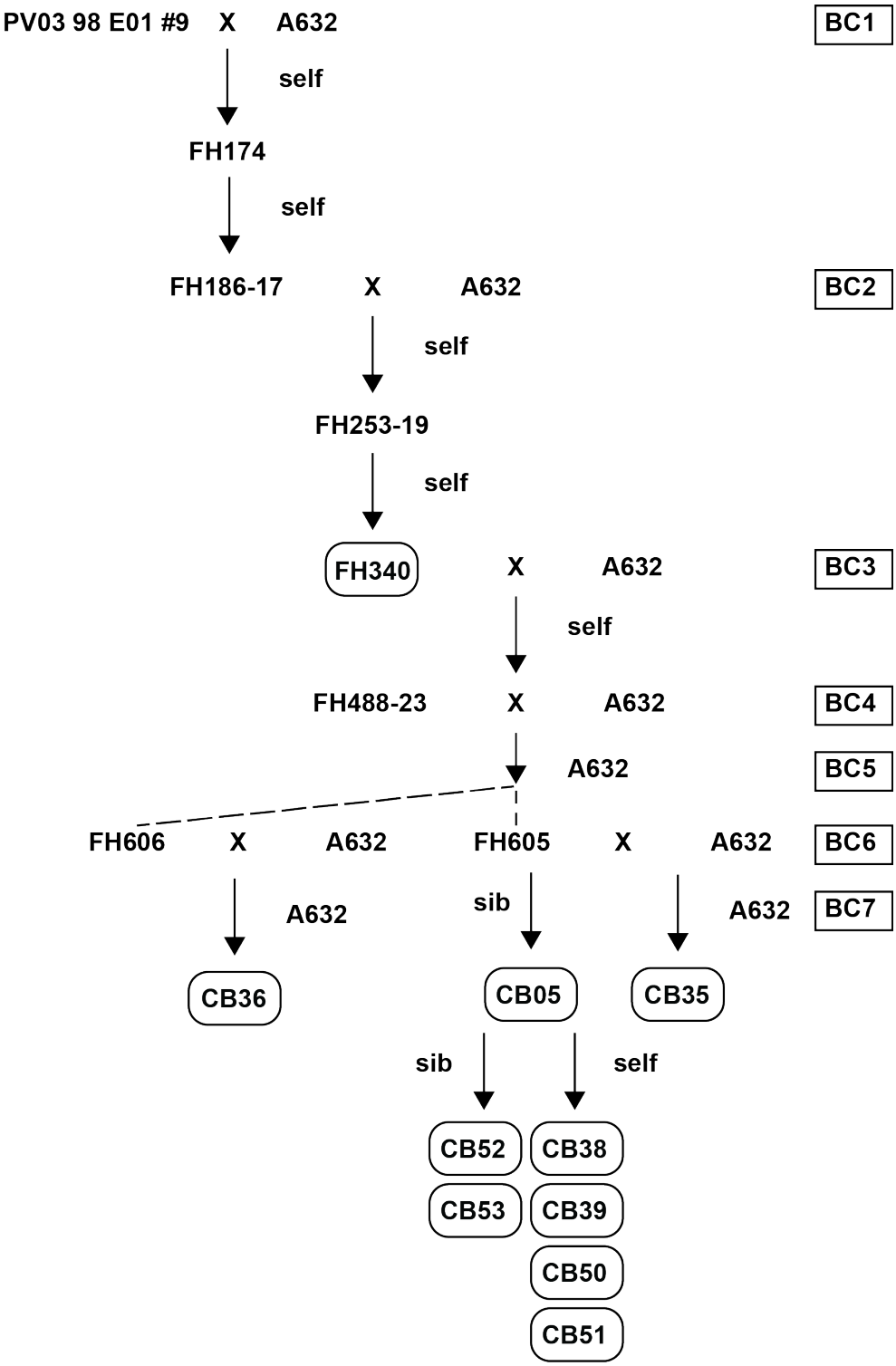

Supplemental Figure 2.1.1. Genealogy of *gi1-m1* lines. BC = Backcross, and only applies if cross is to A632. Round-cornered boxes denote lines used in experiments.

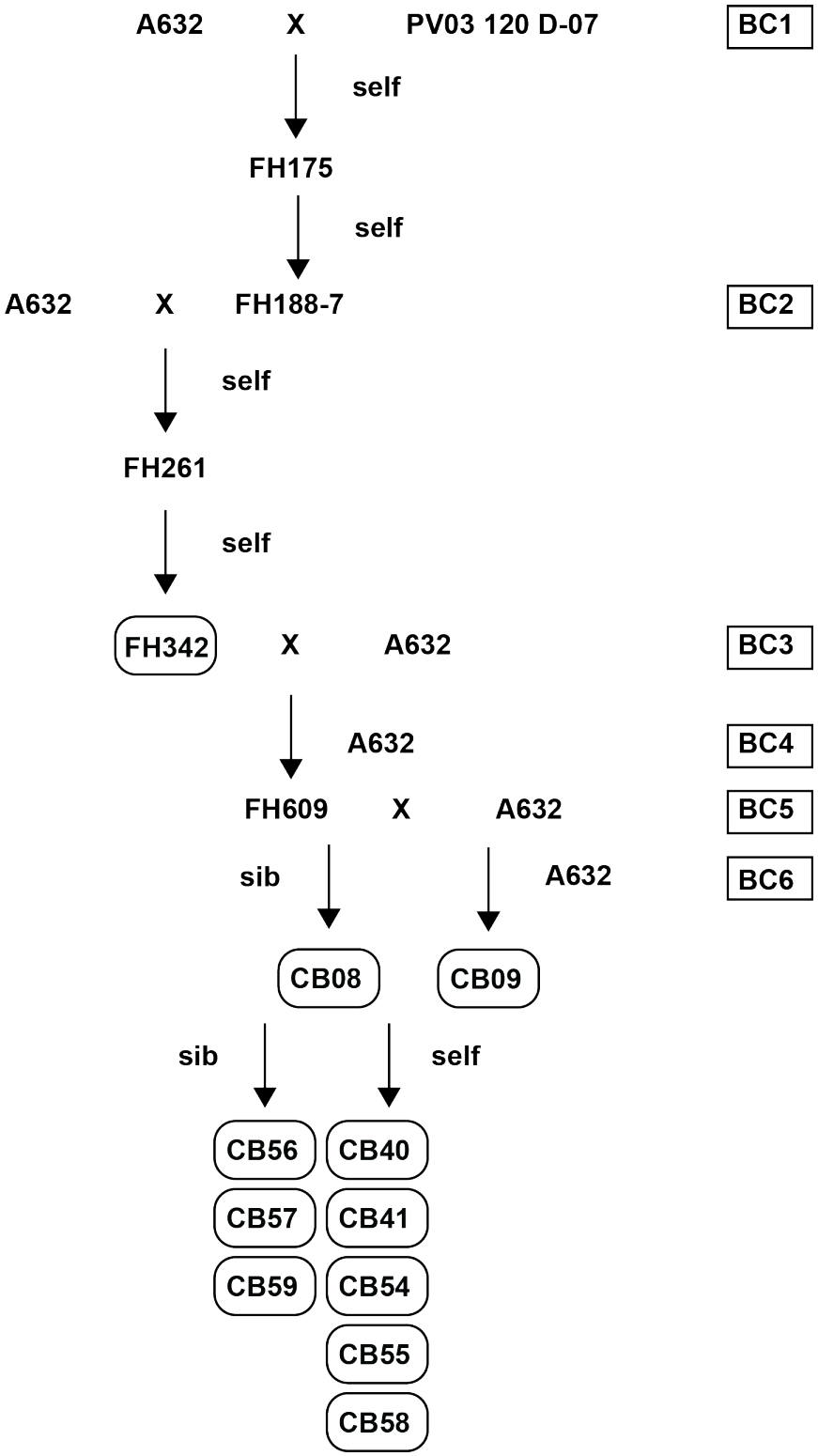

Supplemental Figure 2.1.2. Genealogy of *gi1-m2* lines. BC = Backcross, and only applies if cross is to A632. Round-cornered boxes denote lines used in experiments.

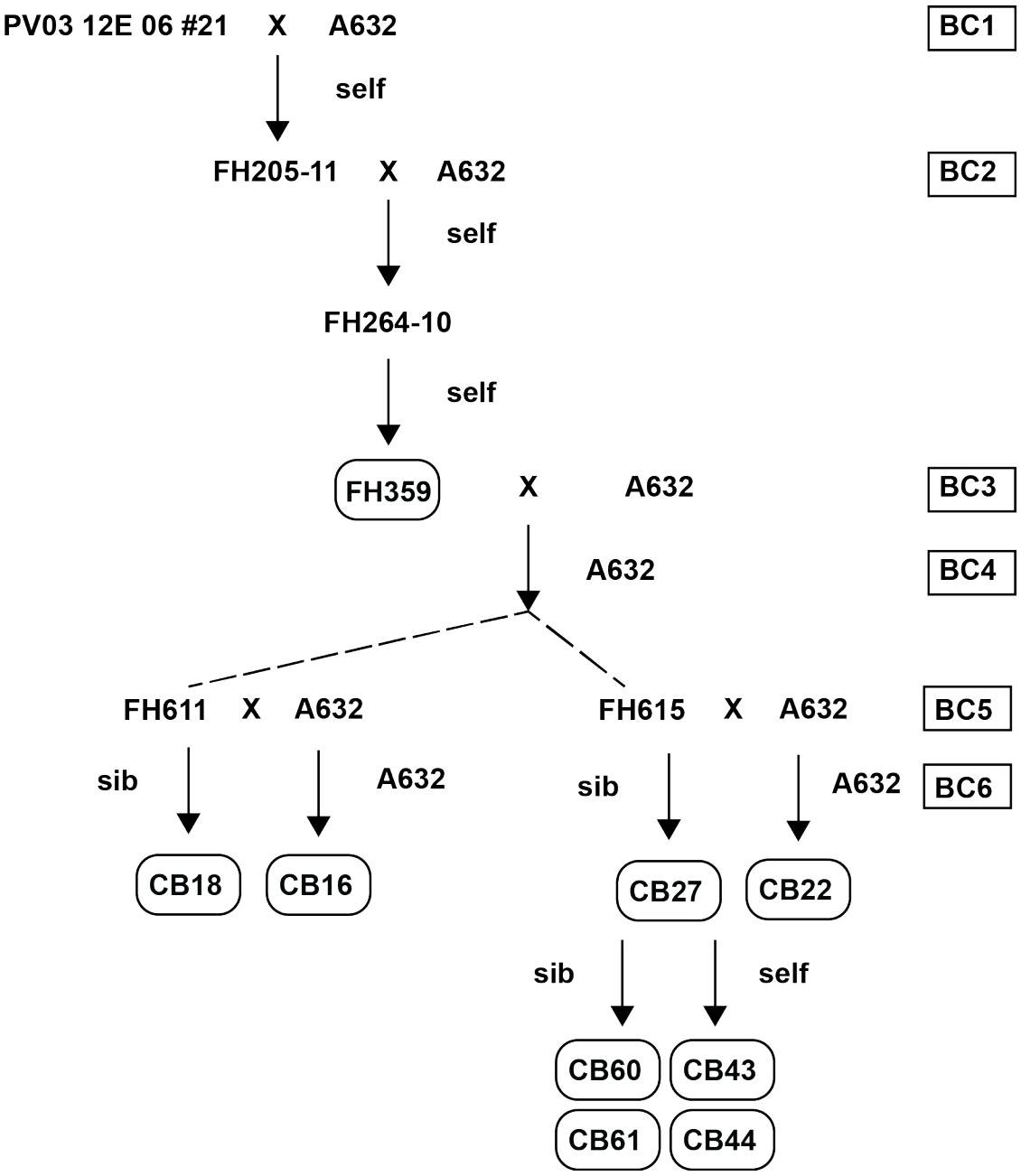

Supplemental Figure 2.1.3. Genealogy of *gi2-m1* lines. BC = Backcross, and only applies if cross is to A632. Round-cornered boxes denote lines used in experiments.

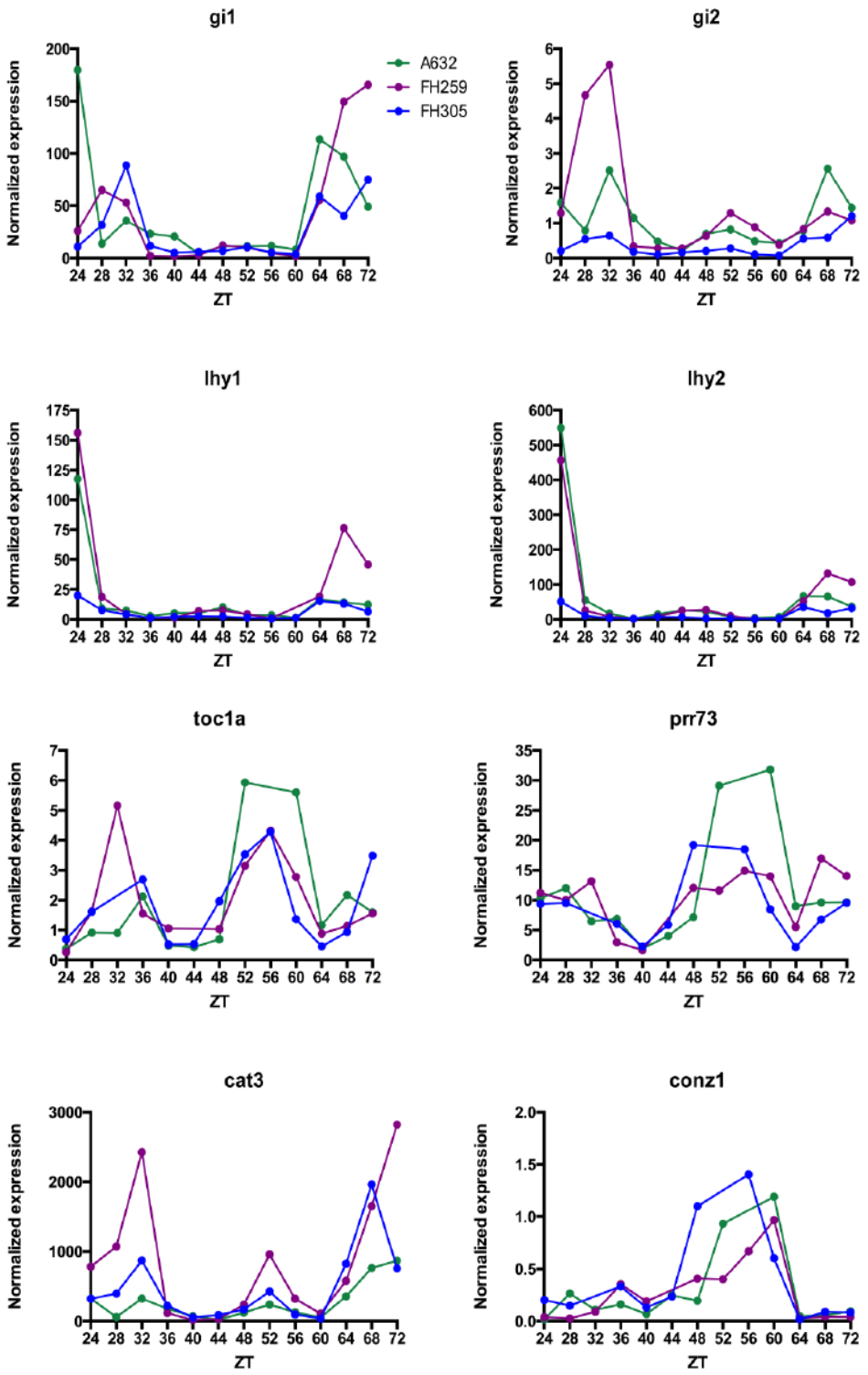

Supplemental Figure 2.2. RT-qPCRs of maize circadian clock genes and conz1 in A632 (green), FH259 (*gi1-m2*, fuchsia), and FH305 (*gi2-m1*, blue) lines grown under LL conditions. Lines used were not the main lines later developed into BC5/BC6, but were genotyped as being homozygous mutants. Timecourse spans dawn after one full day in LL (ZT24) until dawn two days later (ZT72). Graphs represent one biological replicate.

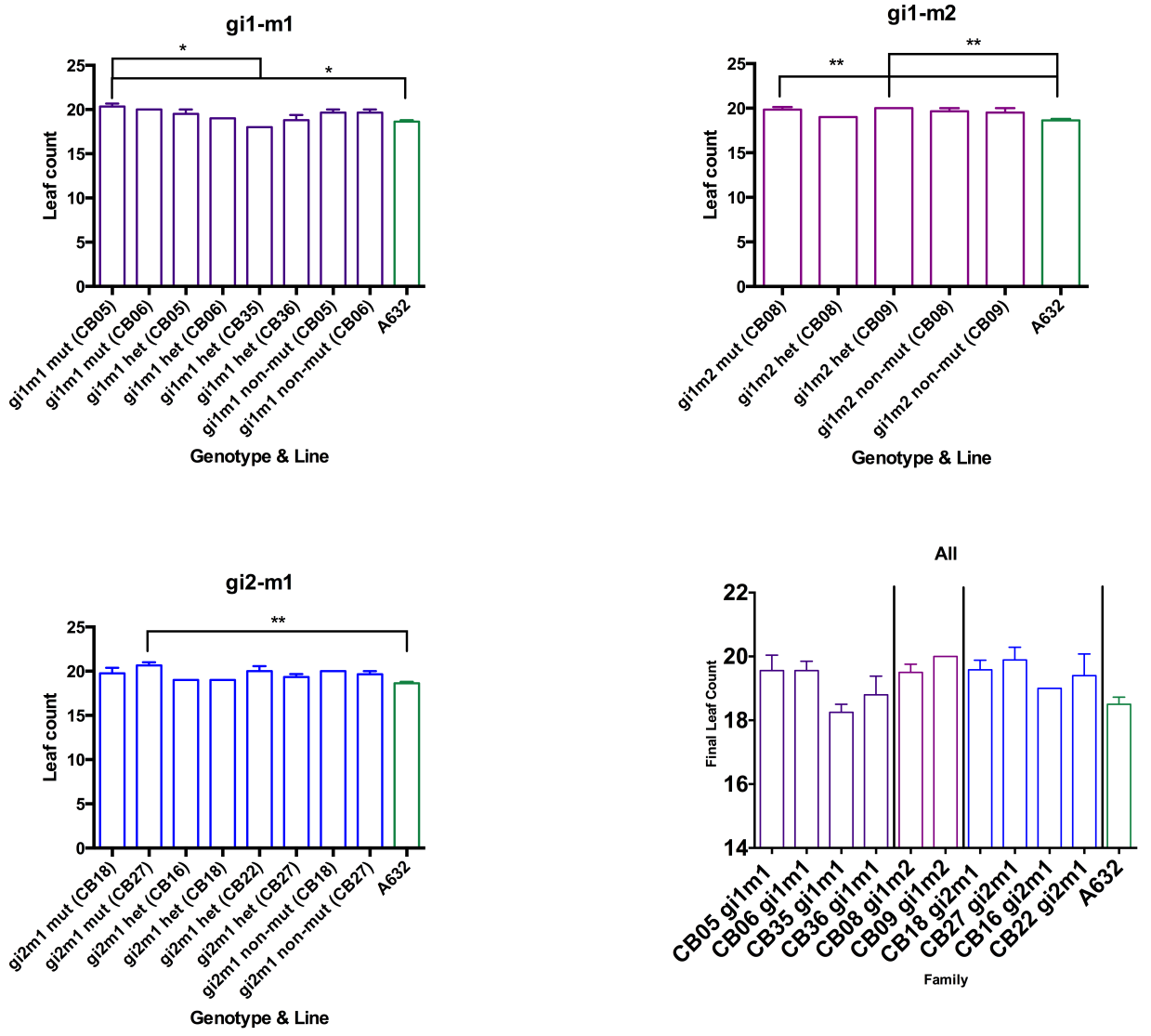

Supplemental Figure 2.3. Final leaf counts of BC5/BC6 plants grown over the winter in the greenhouse in artificial-light LD conditions. Analyzed using ordinary one-way ANOVA and Tukey's multiple comparisons test to determine which differences among means were statistically significant (P value < 0.05 = * and P value < 0.005 = **). Error bars are SEMs.

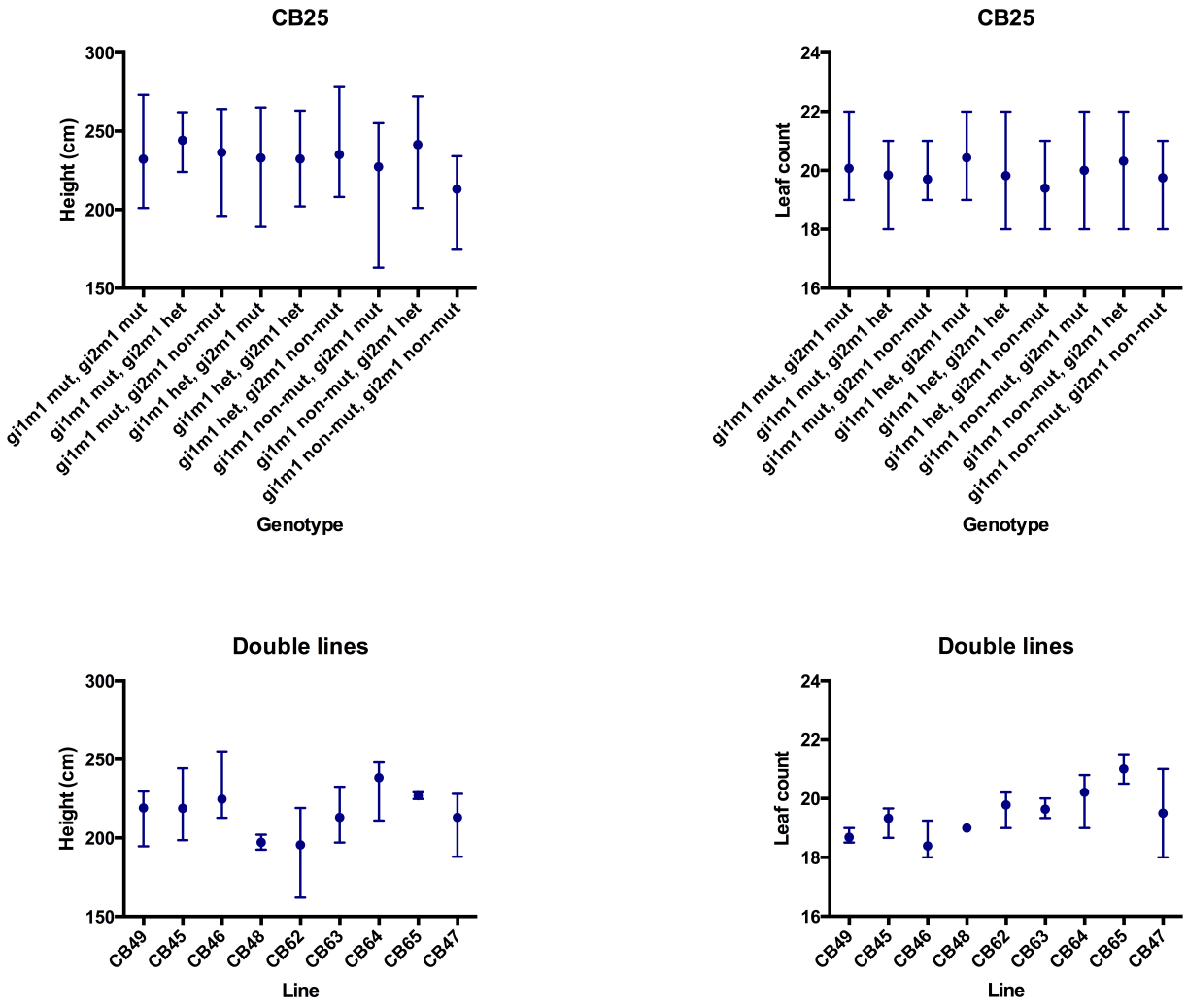

Supplemental Figure 2.4. Final measurements of the double mutant lines used in Figure 2.9. CB25 measurements are divided by genotype, while measurements of segregating and homozygous lines are grouped by line so that differences between lines become apparent. Bars are ranges.

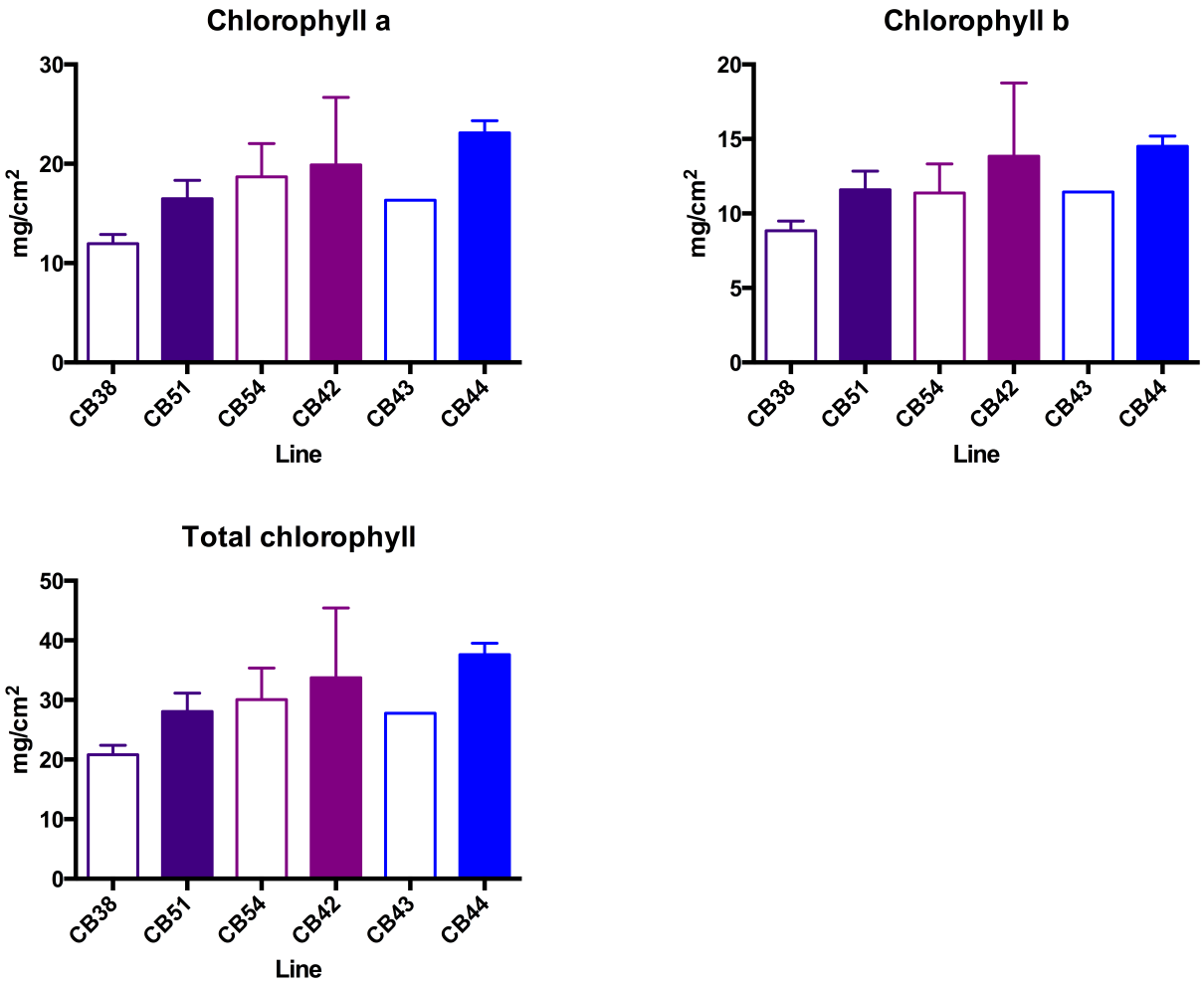

Supplemental Figure 2.5. Measurement of leaf chlorophyll content in the lines CB38 (non-mutant, purple, empty bars), CB51 (*gi1-m1* mutant, purple, filled bars), CB54 (non-mutant, fuchsia, empty bars), CB42 (*gi1-m2* mutant, fuchsia, filled bars), CB43 (non-mutant, blue, empty bars), and CB44 (*gi2-m1* mutant, blue, filled bars). Means and SEMs of three individuals per line are depicted.

Supplemental Figure 2.6. Photos from disease trials. **A)** *gi2-m1* mutant (CB44) line, and **B)** *gi2-m1* non-mutant (CB43) line inoculated with Southern Leaf Blight.

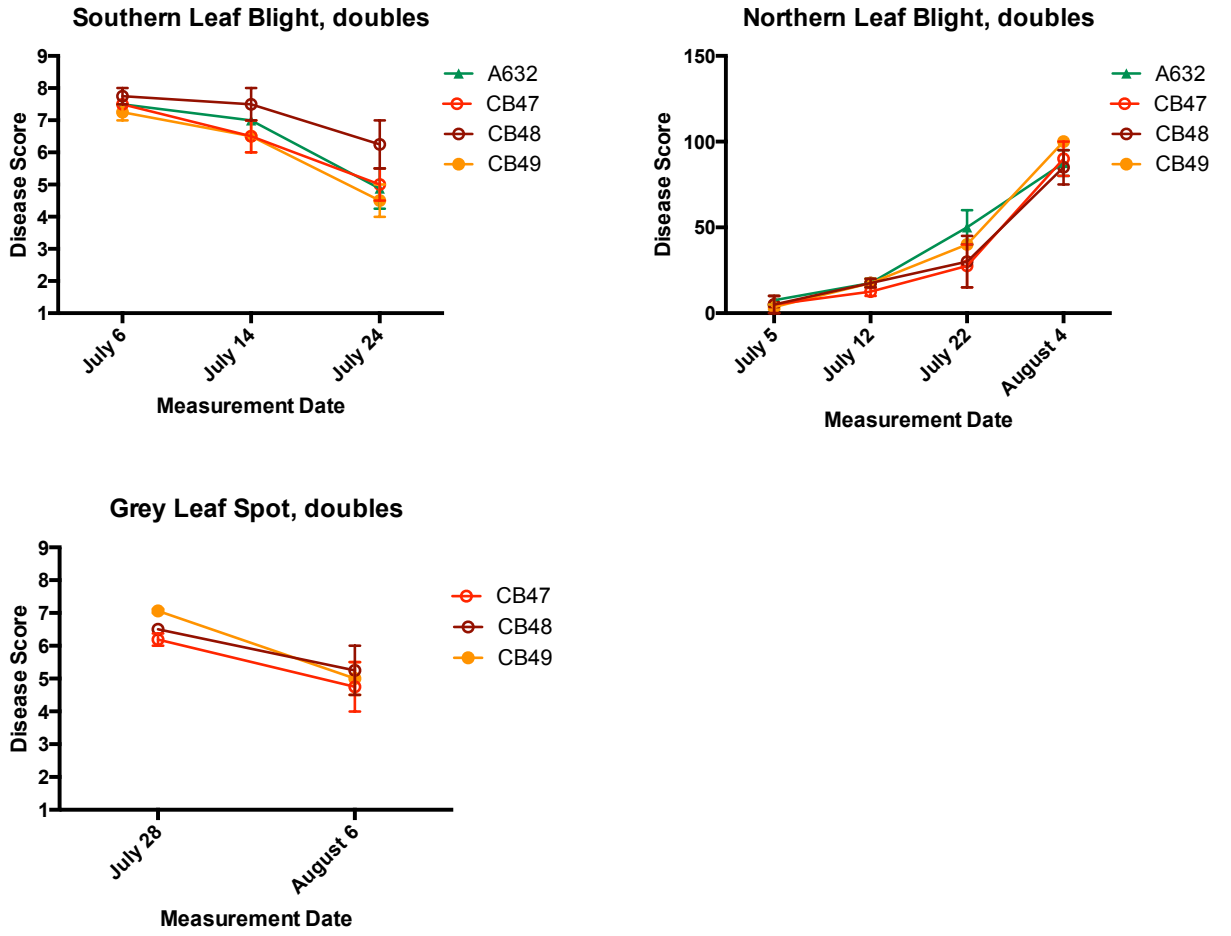

Supplemental Figure 2.7. Measurement of disease responses in the lines A632, CB47 (*gi1-m1* mutant, *gi2-m1* non-mutant), CB48 (*gi1-m1* mutant, *gi2-m1* segregating), and CB49 (*gi1-m1* segregating, *gi2-m1* mutant). The response to three separate diseases was tested: Southern Leaf Blight (SLB), Northern Leaf Blight (NLB), and Grey Leaf Spot (GLS). Measurements represent two biological replicates planted and inoculated at different times, and in some cases different fields. Scoring was done on a scale of 1-9 for SLB and GLS with 9 being resistant, and on a scale of 0-100 for NLB with 0 being resistant. Error bars are SEMs.

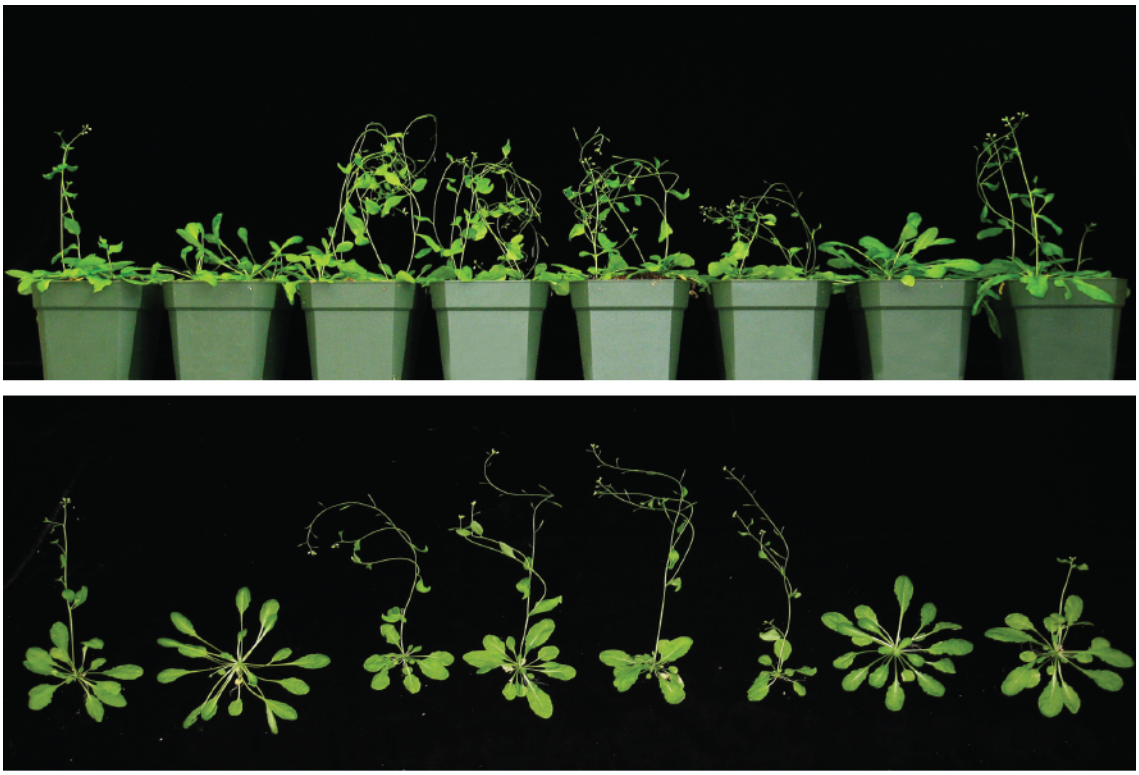
2 (4)
2 (3)
1 (6)
1 (9)
3 (10)
3 (14)
Col
atgi-201
AtGIp::AtGI
AtGIp::gi1
AtGIp::gi2

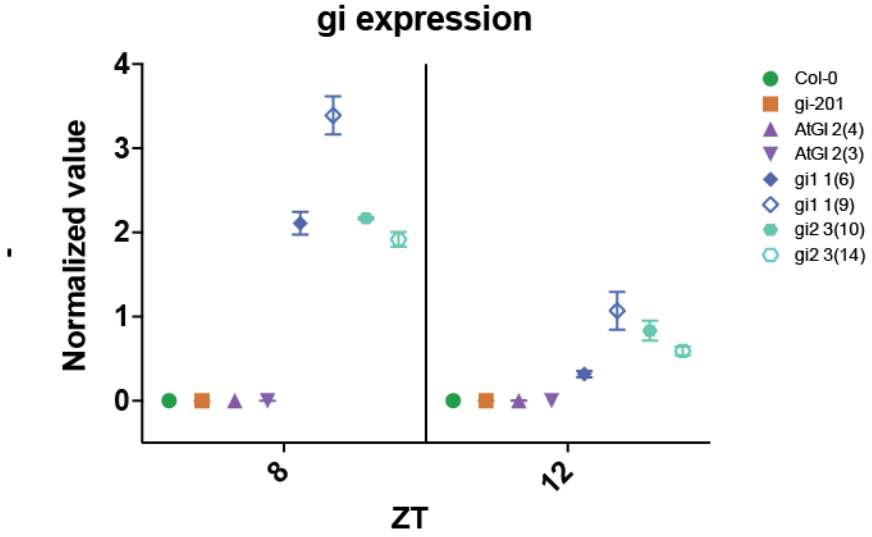
gi expression
Normalized value
4
3
2
1
0
8
12
ZT
Col-0
gi-201
AtGI 2(4)
AtGI 2(3)
gi1 1(6)
gi1 1(9)
gi2 3(10)
gi2 3(14)

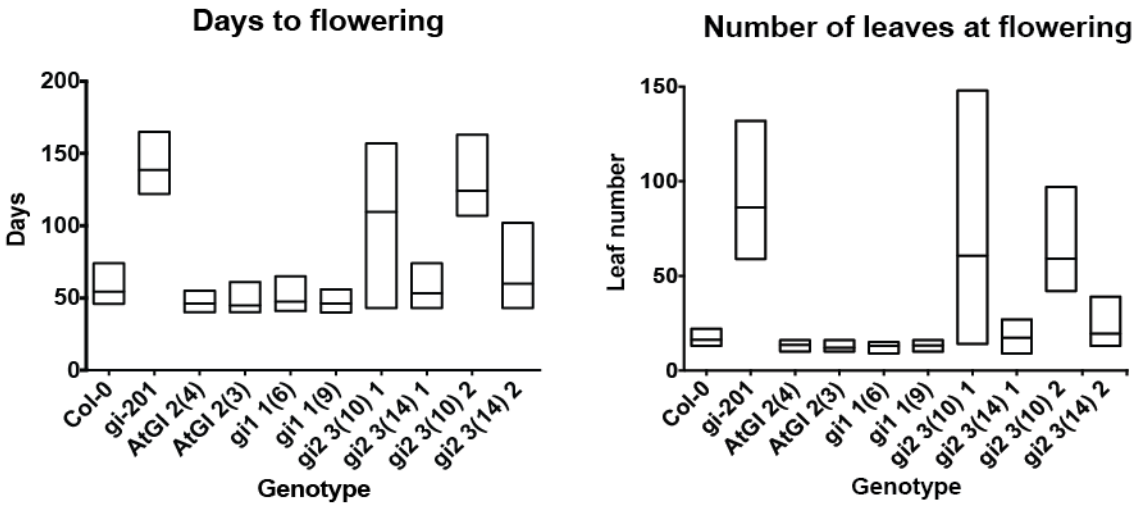

Supplemental Figure 2.8 (this page and previous page). Phenotypes of Arabidopsis transgenic lines and gene expression levels of maize transgenes. On this page, the boxes represent range, while the lines in the middle indicate the mean (n <= 36 plants). On the previous page, the top photo shows full pots containing four plants per pot, while the bottom photo shows individual plants. Gene expression levels were obtained as described in Materials and Methods using primers that did not distinguish between *gi1* and *gi2.*

Supplemental Tables

Sequence (5' to 3')	Gene/Purpose
RT-qPCR Primers	
CGAGACCAGGAGAACCAAAAG	GRMZM5G816228 (normalizer)
TGAGGAGTTTGTCCATAACCAC	GRMZM5G816228
CGCGTTCACTGTGGTTTGTT	GRMZM2G064954 (normalizer)
CAGTGACCCAAGTAGCAGCA	GRMZM2G064954 (normalizer)
CCATTCCTGGATCTGACATCG	*gi1*
ATTAGAGCCGTCCTACTCGC	*gi1*
CGGCGAGTAGGACGCTAATC	*gi2*
AACACCATCTAATATCAGTTTGATCAC	*gi2*
GGTGGGCAACACAAGGTCTT	*lhy1*
AGCTGGCACAAATGAAAAAGC	*lhy1*
AGCCGTACACAATAACGAAGCA	*lhy2*
AAGGCTTCAAGGAACCGTTTG	*lhy2*
CCCTTTTTGCTCACACACAG	*toc1a*
AACCAGGGTAACAGCCACAT	*toc1a*
GACGAAGATGACGATCCAAC	*toc1b*
CAAGAGGACCTCTCCACTAC	*toc1b*
GCGCATCTTCGTCGACAGAT	*prr73*
GTTGGGAATCAGTGGGCTACTAT	*prr73*
TCGCTCGGACACCCAAAG	*cat3*
TTGGCGAGGAGGTCTATCCA	*cat3*
TCTCCATGTTCGGATTCTTCGT	*cab1*
CAATGTGGTCAGCGAGGTTCT	*cab1*
GGTCAGTGCTTACACAGATTC	*conz1*
GAGCTTGGCATGTCTGTC	*conz1*
TGTCACTGCCACCGATATCG	*zcn8*
TACTTCTGCCAAGTGCTGAGCTA	*zcn8*
Primers used for and with Arabidopsis transgenic lines	
CACCACCAGCATATCTCTAATCAG	*AtGI* promoter cloning
GATGCGGCCGCACCGAAACTAAACCCCAAC	*AtGI* promoter cloning
CACCATGTCAGATTCAAATGTGAAGTGGATTGATGGG	*gi1* CDS cloning
TCATGACGGGAGAGGGCAG	*gi1* CDS cloning
CACCATGGCTAGTTCATCTTCATCTGAGAGATG	*AtGI* CDS cloning
TTATTGGGACAAGGATATAGTACAGCCG	*AtGI* CDS cloning
TATCGGATGACGATTCTTCGTGCAG	qPCR of *AtPP2A* (normalizer)

Sequence (5’ to 3’)	Gene/Purpose
GCTTGGTCGACTATCGGAATGAGAG	qPCR of *AtPP2A*
GGGTAAATATGCTGCTGGAGA	qPCR of *AtGlp::AtGl* lines
CAGTATGACACCAGCTCCATT	qPCR of *AtGlp::AtGl*
TGATGTCGTTTCAGCCTCAC	qPCR of *AtGlp::gi1* lines
CAAGGCTGCAAGTCCTTCTC	qPCR of *AtGlp::gi1*

Supplemental Table 2.1. Primers used for RT-qPCR, to construct Arabidopsis transgenic lines, and to measure transgene expression.

Chapter Three: GI1 and GI2 protein interaction partners

Abstract

GIGANTEA (GI) is a plant-specific protein with no characterized protein domains. It is known to have many protein interaction partners, and has also been shown to bind DNA. These interactions allow GI to participate in many different processes, including circadian clock regulation, flowering time regulation, and stress responses. To characterize the protein interaction partners of the maize proteins GI1 and GI2, two approaches were taken. The candidate approach confirmed some of the interactions known from Arabidopsis, and showed that others are likely altered in maize. The library screen, instead of confirming these results, opened up multiple new avenues for research.

Introduction

GIGANTEA (GI) is a large protein (~130kDa) unique to plants with no characterized protein domains. Through protein interaction assays such as yeast two hybrid (Y2H) and co-immunoprecipitation (co-IP), AtGI has been shown to have multiple protein interaction partners. At present, it is thought that GI primarily acts as a molecular scaffold that assembles protein complexes (Fowler et al., 1999; Huq et al., 2000; Park et al., 1999), and is involved in regulating protein activity and stability. GI also has DNA-binding ability, and may therefore regulate gene expression (Sawa and Kay, 2011; Sawa et al., 2007; Song et al., 2014).

Heterologously expressed AtGI in *E. coli* has been shown to associate into homotetramers, suggesting endogenous GI may be present in this form and potentially stabilized via interactors (Black et al., 2011). Trypsin digestion of AtGI indicates that the amino-terminal domain of GI is independently folded, and has an exceptionally stable alpha-helix domain at the amino-terminal (N-terminal) spanning amino acids 1-398 (Black et al., 2011). Some GI interaction partners preferentially interact with the N-terminal domain in Y2H assays (Sawa et al., 2007; Yu et al., 2008), which could indicate that this is the primary protein-protein interaction domain. A recent study in *Brassica rapa* found a single amino acid substitution (S264A) in GI to be the basis of a major quantitative trait locus that controls circadian period (Xie et al., 2015). This again indicates that the N-terminal domain is of primary importance to GI function.

The effects of GI protein interaction can be divided into four main categories: circadian clock function, photoperiodic flowering time regulation, growth regulation, and stress response. In the circadian clock, GI primarily interacts with two proteins, namely ZTL and ELF3. The interaction with the blue light receptor ZTL is reciprocal co-stabilization that protects both proteins from degradation by the 26S proteasome, and also acts to regulate GI localization (Demarsy and Fankhauser, 2009; Ito et al., 2012; Kim et al., 2013a, 2007b). HSP90 has also been implicated as stabilizing ZTL, perhaps in conjunction with GI (Kim et al., 2011). The GI-LOV domain interaction has successfully been used as an optogenetic tool despite there being no known protein interaction domains in GI (Polstein and Gersbach, 2014).

The ZTL-GI complex interacts with the PRR proteins TOC1 or PRR5 and leads to their degradation by the 26S proteasome (Fujiwara et al., 2008; Kiba et al., 2007; Kim et al., 2007b; Más et al., 2003). Alternatively, the GI-ZTL-HSP90 interaction may just

stabilize ZTL and GI, while the ZTL-PRR5 and ZTL-TOC1 complexes lead to PRR protein degradation (Zoltowski and Imaizumi, 2014) Either way, ZTL acts to remove the repression exerted by TOC1 and PRR5, which allows the next cycle of the clock to commence.

The second clock protein interaction is with the evening complex protein ELF3 and the E3 ubiquitin ligase CONSTITUTIVE PHOTOMORPHOGENIC 1 (COP1). This interaction leads to GI degradation by the 26S proteasome (Yu et al., 2008), and so temporally restricts the activity of the GI protein. Both of these interactions assist in correctly timing the activities of other clock proteins.

The role of GI within flowering time regulation is complex, and studies have shown that GI acts at multiple levels within known flowering time pathways. Perhaps most importantly, GI forms a complex with FLAVIN-BINDING, KELCH-REPEAT, F-BOX 1 (FKF1), the main regulator of photoperiodic flowering (Song et al., 2014; Zoltowski and Imaizumi, 2014). This complex degrades CYCLING DOF FACTOR 1 (CDF1), which releases CO repression; the GI-FKF1 complex also directly interacts with CO protein, as does GI alone (Song et al., 2014). In addition, the GI-CDF interaction has also been shown to affect growth (Fornara et al., 2015).

CO protein then promotes flowering by activating the mobile florigen FT. In another pathway, GI forms a complex with SVP, TEM1, TEM2, and maybe FLC (Sawa and Kay, 2011). This complex interacts with the FT promoter and may promote flowering by removing FT repression. GI also directly binds to the *FT* promoter, which promotes flowering independently of CO (Sawa and Kay, 2011). Interestingly, GI interaction with a clock protein, ELF4, may also affect flowering time. ELF4 stabilizes GI and sequesters it in subnuclear bodies, which appears to result in the negative regulation of *CO* expression by preventing GI from binding the *CO* promoter (Kim et al., 2013c).

A further layer of complexity is added to the role of GI in flowering time by the involvement of COP1. For one, COP1 acts to transfer the light input signals from CRYPTOCHROME 2 (CRY2) to the circadian clock by interacting with ELF3 to promote the degradation of GI (Yu et al., 2008). COP1 also promotes the degradation of CO at night (Jang et al., 2008; Liu et al., 2008). Recent work showed that COP1 degrades GI at low temperatures, thus delaying flowering by another mechanism (Jang et al., 2015).

Another way in which GI may affect flowering time is by interacting with SPINDLY (SPY), an O-linked *N*-acetylglucosamine transferase (Tseng et al., 2004). The SPY-GI complex is involved in hypocotyl length regulation (Tseng et al., 2004) as well as transpiration (Sothern et al., 2002). SPY negatively regulates flowering time and growth by somehow stabilizing DELLA proteins, which are themselves negative regulators of GA signaling (Schwechheimer, 2008). GA has been shown to promote flowering via a GI- and CO-independent pathway that promotes FT and TSF expression (Galvão et al., 2012). The exact mechanisms whereby GI interacting with SPY would affect the GA pathway remain unclear.

The effect of GI on growth seems to primarily be due to its multiple protein interaction partners, and its involvement in light, hormone, and flowering time pathways (see Chapter Two). In its DNA-binding capacity, GI protein may directly regulate the expression of growth-related genes, but no research has been done on this yet.

Finally, the role of GI in stress response processes is a relatively new discovery. Although it was long known that *atgi* mutants were tolerant to paraquat treatment, protein-level interactions that could explain the role of GI in stress tolerance have only been discovered recently. One of these is the complex formation between GI and SALT OVERLY SENSITIVE 2 (SOS2), which keeps the SOS system inactive under normal growing conditions. Under salt stress, GI releases SOS2, which forms a complex with SOS3 that activates SOS1, a Na^+/H^+ antiporter that confers salt tolerance (Kim et al., 2013b; Park et al., 2013). GI protein is expressed in response to heat shock and then modified with Small Ubiquitin-like Modifiers (SUMOs) at amino acids 226 and 975 (López-Torrejón et al., 2013). SUMOylation is thought to block ubiquitin attachment, and so these modifications could prevent GI degradation in heat stress conditions.

We chose to take a two-pronged approach to elucidate GI1 and GI2 protein interactors in maize. The first approach involved pairwise Y2H assays, for which putative interactors were identified, cloned, and mated with the two gis. For this approach, we used N-terminal, C-terminal, and full length constructs to test for specificity of protein interaction domains. The second approach was a Y2H library screen, for which we constructed a maize cDNA library against which we screened full-length GI1 and full-length GI2. This approach allowed us to expand the scope of interaction testing, and provided the possibility of identifying maize-specific protein interactors.

Results

Conservation between maize gi1 and gi2 and AtGI

The GI1 and GI2 protein sequences are 95% identical, and the differences between the two are primarily single amino acid (aa) changes (Jalview results - not shown). For the most part, these aa changes result in chemically similar aas, making it unlikely that overall protein structure is substantially different between GI1 and GI2 (Figure 3.1). If these alterations are located in interaction domains, however, they could potentially result in functional changes.

Although there are many highly conserved regions, GI1 and GI2 are only 68% identical to AtGI. The differences are spread across the length of the proteins and involve numerous substantial changes to aa properties (Figure 3.1). Again, many alterations appear to be at single unconserved aas, although there are multiple stretches with larger alterations. Most of the highly conserved regions fall in the second two thirds of the N-terminal half of the protein (Figure 3.2). The first third, which is the start of the protein coding domain, is not well conserved. The C-terminal half of the protein has a few short conserved regions (Figure 3.3). There appears to be a higher level of non-conserved aas throughout the C-terminal region, indicating that this half of the protein is the one in which more evolutionary divergence has occurred. The AKDD SUMOylated motif in the C-terminal region of AtGI (López-Torrejón et al., 2013) is minimally changed in maize to ARDD. Overall, the N-terminal region, which appears more functionally important, is more conserved between dicots and monocots.

Predictions of protein secondary structure indicate there are many helix domains in both the N- and C-terminal halves of all GIs (Supplemental Figure 3.1). There are, however, many residues for which no structural predictions could be inferred from characterized protein structures. Color-coding aas by their hydrophobicity does not

reveal any larger patterns, although there are some hydrophilic regions toward the beginning of the N-terminal half and the middle of the C-terminal half (Supplemental Figure 3.2). While neither of these approaches provides clear structural information, they do indicate that GI is a globular protein that does not have larger hydrophobic regions.

Pairwise yeast two hybrid assays: dilution series

Plating dilution series showed that GI1 and GI2 have similar interaction partners, in particular themselves, each other, and ZTL1 (Figure 3.4). The ability of GI to interact with itself is one of the clearest results of this assay, with GI1-GI1 and GI2-GI2 interactions as some of the strongest measured. Heterodimers of GI1-GI2 were equally strong. AtGI did not interact especially strongly with itself or GI2, whereas the AtGI-GI1 interaction was stronger.

The other strong interaction was seen between all GIs and ZTL1. This was apparent regardless of which interactor was in the bait plasmid: all GI-ZTL1 matings resulted in the strongest interaction level measured. In addition, when ZTL1 was the bait, exceptionally strong interactions with all N-terminal GI constructs were seen.

The other interactors tested provided less clear results. When in bait plasmids, GI1 and GI2 interacted strongly with ELF3B and less strongly with ELF3A. On the other hand, when ELF3A and ELF3B were in bait plasmids, no growth was recorded. These matings grew well on DDO plates, but not well on TDO plates, indicating issues with more stringent nutritional selection. AtGI showed a similar pattern of stronger interaction with ELF3B than ELF3A, but both interactions were considerably weaker than seen with the GI1 and GI2 baits.

The interactions with COP1A and SPY both showed a similar pattern: weak or no interaction with the full length protein, and moderate interaction with the N-terminal construct. This was borne out by the results seen from matings with the COP1A bait construct, where the only interactions were with the GI1 and GI2 N-terminal constructs. The SPY bait protein provided results much like the ELF3A and ELF3B baits: growth on DDO plates, poor growth on TDO plates, and no measurable interactions on QDO plates. The ELF4B prey also showed weak to moderate interaction with the N-terminal constructs, but no bait was constructed to test this reciprocally.

Finally, the Arabidopsis proteins provided a confirmation of the interaction patterns observed. Preys of AtZTL and AtELF3 interacted with both GI1 and GI2 full length baits, AtCOP1 only interacted with their N-terminal domains. The AtGI full length bait also interacted with AtZTL and AtELF3, but only weakly with AtCOP1. The AtGI N-terminal bait showed little to no interaction with any prey, unlike the GI1 and GI2 N-terminal constructs.

Pairwise yeast two hybrid assays: liquid culture assay using ONPG

The liquid culture assay confirmed the results of the dilution series, and showed GI1 and GI2 primarily interact with themselves, each other, and ZTL1 (Figure 3.5.A). Although some of the other interactions may be above baseline, these are far and away the strongest. AtGI shows the same pattern of interactors, although at a lower level (Figure 3.5.B). This could either indicate conserved functionality between the three GIs, or strong activating ability in GI1, GI2, and ZTL1 proteins, with the baseline level of activity shown in the AtGI graph.

N- and C-terminal GI baits were also tested in this assay (Supplemental Figure 3.3). Similar interaction patterns to the full length GI baits were seen with the N-terminal constructs, while the C-terminal constructs did not appear to interact at all. Interestingly, none of the N-terminal interactions had a strength over 2.5 Beta-gal units, indicating the interaction strengths seen in the full length constructs were additive effects of having the full length protein.

The results for the COP1A and SPY baits show increased interaction with N-terminal constructs, which was previously only seen when COP1A and SPY were preys (Figure 3.6.A). The results for ZTL1 bait show the same strengths of interactions as seen in the plate assays, but a preference for full length GI1 and GI2 over N- or C-terminal fragments becomes apparent (Figure 3.6.B). As baits, both ELF3A and ELF3B have the strongest interaction with GI2, especially ELF3B (Supplemental Figure 3.4). Both, however, do not have very high interaction levels overall and ELF3B's strongest interaction is with pGADT7.

Yeast two hybrid library screen

The GI1 and GI2 library screens each resulted in a large amount of putative interacting partners, indicating these proteins are promiscuous. This made looking through the screen to saturation prohibitive, and so a subset of interactors was chosen to sequence. This approach provided a good sense of the type of proteins with which GIs interact, although it meant that a specific subset of strong and functional interactors could not be identified.

The protein interaction partners obtained from the library screen did not include those demonstrated in pairwise assays, and were largely uncharacterized proteins in maize. They also showed the risks inherent to doing this type of screen in plants, as many protein interaction partners were involved in photosynthesis or located in organelles. Those in organelles are less likely to have biologically relevant interactions in plant cells, but some of those involved in photosynthesis might.

At first glance, most of the GI1 interaction partners appear to be false positives (Table 3.1). Many of the proteins identified are involved in photosynthesis, as well as glucose and starch-related processes. A closer look at the GO categories, however, reveals a few themes to the identified proteins. One theme is protein stabilization, modification, and proteolysis, which is consistent with the protein scaffold function of AtGI. Another theme is biosynthesis, and chlorophyll as well as jasmonic acid are explicitly listed. The third theme is response to stress, primarily of the abiotic kind. The methyltransferase is the most promising of the most frequently recovered interaction partners.

The GI2 interaction partners had some similar categories, but also represented a shift relative to GI1 (Table 3.2). The themes of starch, glucose, and glycogen processes are much more prevalent in the GI2 interaction partners. There is again a stress response theme, but this time the stress is pathogen-based. As well as multiple genes with GO annotations related to pathogen stress response, a LRR protein and a pathogenesis-related protein were identified as interactors. Finally, there are a couple GI2 interactors similar to known clock proteins in Arabidopsis. The most convincing of these is *GRMZM2G049549*, which is a cryptochrome. Other potentially interesting proteins include one that responds to cadmium ions, one involved in protein ubiquitination, and a PIN protein involved in auxin transport.

Discussion

The multiple approaches taken to quantify protein interactions resulted in a number of interesting results. From the candidate approach, two clear results were obtained: GI1 and GI2 interact with each other and with ZTL1. Moreover, GI1 and GI2 interacted with AtGI and AtZTL, indicating that the protein domains necessary for these interactions are conserved in flowering plants. Pairwise tests with other possible interaction partners from maize provided much less clear results, with interaction strength and sometimes presence being dependent on the form of the assay. Although the candidate approach provided some interesting insights, and confirmed that some of the interactions known from Arabidopsis are present in maize, it was limited by the amount of interactors cloned.

The yeast two hybrid library screen had entirely unexpected results. Multiple uncharacterized proteins were recovered, as were many photosynthesis-related proteins. GO term analysis of the identified interaction partners, however, found that many of them are likely involved in processes to which GI has been linked. These include protein modification, starch regulation, and stress response. None of the cloned candidates were recovered when using either bait.

The dilution series on plates also indicated that GI1 and GI2 interact with the ELF3s. The interaction with ELF3B was stronger for both GIs, perhaps indicating that this is the ELF3 that acts within the clock. These interactions were, however, only seen when the GIs were the bait construct. Both GI1 and GI2 also interact with AtELF3.

On plates, GI1 and GI2 also appear to interact with COP1A and SPY. Again, this interaction was only seen when the GIs were the bait construct. Unlike the other interactors, COP1A and SPY preferentially interacted with the N-terminal half over the full length protein. AtCOP1 also preferentially interacted with N-terminal halves, and AtSPY was not tested.

A few general conclusions can also be drawn from the plate assays. For one, the pGBKT7 empty vector functions well as a negative control, while in some cases, the pGADT7 empty vector does not. It can be seen that LAM also resulted in interactions in these cases (where LAM-pGAD was tested). It is possible that in the bait vector, GIs (and ZTL1) are able to autoactivate the cassettes necessary for growth on QDO. This would indicate that GI protein (and ZTL1) contains a domain sufficient for transcriptional activation, which given its DNA-binding ability is quite possible. This effect is, however, not seen when these proteins are in prey vectors. Another conclusion that can be drawn is that the C-terminal domain is not sufficient to establish protein-protein interactions, nor does it demonstrate any form of autoactivation. It does, however, contribute to interaction strength.

The results from the liquid assays with ONPG as a substrate generally overlap with those from the dilution series assay, and provide another line of evidence supporting the strongest interactions seen there. These interactions were many times stronger than those that have previously been reported using this assay and ZTL bait constructs (Yon et al., 2012). The less clear interactions, with the ELF3s, COP1A, and SPY, remain difficult to quantify. Depending on test conditions, they either appear to be present and moderately strong, or not present at all. This variability in outcome could indicate less strong interactions or that complex formation requires multiple partners.

The library screen identified a number of photosynthesis-related proteins as interaction partners. While some of this may be due to an overrepresentation of these proteins in the library, or their ability to activate reporters in yeast, a few are annotated as being involved in chlorophyll biogenesis. Altered chlorophyll content is consistently seen in plants with mutant *GI* genes (Mishra and Panigrahi, 2015), including maize *gi1-m1* and *gi2-m1* plants (Chapter Two), indicating these proteins may be true GI interaction partners. Both GIs also have multiple interaction partners that link them to glucose, glycogen, and starch, which is consistent with the role that AtGI plays in starch regulation (Dalchau et al., 2011; Eimert et al., 1995).

The stress response proteins pulled out by the screen are also likely true interactors. AtGI is directly and indirectly involved in multiple stress response pathways, some of which have been characterized at the protein level. The GI2 protein interactors are primarily involved in pathogen response, which may indicate that GI2 is directly involved in these pathways. In disease tests, *gi2-m1* mutants had an increased susceptibility phenotype not seen in *gi1* mutants (Chapter Two), providing a further line of evidence that gi2 is directly involved in pathogen response. Like AtGI, GI1 appears to primarily interact with proteins involved in abiotic stress response (Cao et al., 2005; Park et al., 2013; Riboni et al., 2013; Rodrigues et al., 2015).

One of the interaction partners of GI1 that was present multiple times in the sequencing is a methyltransferase. In Arabidopsis, methylation has been shown to link the clock to alternative splicing processes, as well as to more fundamentally regulate clock gene expression (Ng et al., 2014; Ni et al., 2009; Sanchez et al., 2010). AtGI has not been linked to methylation in these studies, yet these results indicate there may be a role for GI at the protein level.

Cryptochromes are blue light receptors, and an important light input component in the Arabidopsis circadian clock (Chaves et al., 2011; Wang et al., 2014). Within the context of the circadian clock, cryptochromes are essential for temperature compensation, and regulate flowering time (Gould et al., 2013; Nefissi et al., 2011). A recent study showed that including Cryptochrome 1, Phytochrome A, and Phytochrome B in a mathematical model of the circadian clock was sufficient to reproduce experimental results (Ohara et al., 2015). Previous work has established a relationship between CRY2 and GI, which is thought to be indirect: CRY2 negatively controls COP1, which together with ELF3 degrades GI (Yu et al., 2008). Finding a cryptochrome as a direct interaction partner of GI2 indicates that this interaction could be direct. This putative interaction is an ideal subject for further investigation.

The library screen provided multiple new paths of inquiry into GI protein function. It indicated there is direct interaction in multiple cases that were previously thought to be indirect or circadian-clock regulated. These include pathogen-response proteins, cryptochromes, and maybe even chlorophyll biosynthesis proteins. Further experiments will need to be done to confirm all of the results presented here, especially *in planta*.

Materials and Methods

Protein alignments and visualization

The default option of MAFFT (mafft.cbrc.jp/alignment/software) was used to align proteins, and then protein similarities were calculated using Jalview (jalview.org). Protein alignment for all visualizations was done using the default settings of PRALINE (www.ibi.vu.nl/programs/pralinewww/) (Simossis and Heringa, 2005).

Pairwise yeast two hybrid assays

Putative maize interactors were computationally identified on the basis of known *Arabidopsis* GI interactors. Genes likely to be functional were chosen after protein domain analysis and expression analysis. Putative interactors were amplified using a processive polymerase such as Phusion or Q5. Where there were multiple paralogs present in maize, only one or two were chosen. The N- and C-terminal GI constructs were made by dividing each GI coding sequence in half, and so each is between 581 and 586 amino acids long. Official gene designations are listed in Supplemental Table 3.1.

The PCR products were then gel extracted, and cloned into pENTR. Once in pENTR, the genes were moved into the bait plasmid pGBKT7 or the prey plasmid pGADT7 via Gateway cloning. The constructs LAM pGBKT7 and LAM pGAD424 were made by Bryan Thines, and the constructs ELF3A pGADT7 and ELF3B pGADT7 were made by Desirée Stanley, via restriction site cloning.

Once cloned, the bait plasmids were transformed into Y187 strain yeast cells, while the prey plasmids were transformed into AH109 strain yeast cells. Transformation was done according to the 'Lazy Bones' yeast transformation protocol (from the Gottschling lab website: http://research.fhcrc.org/gottschling/en/protocols/yeast-protocols/transformation.html). To check proteins were expressed in yeast, protein extractions of transformed yeast were done using the TCA Method described in the Clontech Yeast Protocols Handbook. Protein extracts were analyzed using a standard Western blot protocol. All pGBKT7 constructs expressed proteins at similar levels, while pGADT7 construct expression level differed (not shown).

To test protein interactions, transformed Y187 and AH109 strains were mated according to the standard yeast mating procedure described in the Clontech Yeast Protocols Handbook. Matings were then streaked out on plates containing appropriate selective media.

Protein interaction strength was assayed using two experimental procedures. In the first procedure, overnight cultures of matings were set up in 1ml SD-T-L (DDO) media. In the morning, 100ul of culture was mixed with 900ul TE and then the OD600 was measured. This measurement was used to dilute all matings to a uniform OD600 = 3, and then matings were loaded into a 96-well plate. Using a multichannel pipette, these standardized matings were then serially diluted in the series 1:5, 1:10, 1:50, 1:100, 1:500, 1:1000. The entire dilution series for each mating was then plated on DDO, TDO (SD-A-L-T and SD-H-L-T), and QDO (AD-A-H-L-T) plates, the plates were sealed with micropore tape, and placed in the 30°C incubator. Plates were scanned after 5 days, 7 days, and 10 days to monitor growth and development. Each mating done was plated in this manner at least once, and most were plated two to four times.

The second procedure was the 'Liquid Culture Assay Using ONPG as Substrate' outlined in the Clontech Yeast Protocols Handbook. Each mating was tested using at least three separate overnight cultures (three biological replicates), and each culture had three separate technical replicates (as described in protocol). Many matings were tested with more than three overnight cultures, meaning measurements represent four, five, or six, and in some cases up to ten biological replicates.

Yeast two hybrid library screen

B73 maize inbred line seedlings were grown under LD conditions in a growth chamber. Once the seedlings had grown to V4 stage, they were sampled at timepoints spanning the peak expression time of GI, namely ZT8, ZT10, ZT12, and ZT14. Two leaf punches were taken per seedling using the lid of an Eppendorff tube, and five different plants were sampled at each timepoint. RNA was extracted using a modified version of the Trizol protocol, and then ethanol precipitated to improve purity. RNA concentration of each sample was calculated as the average of three NanoDrop measurements, and then a pooled sample was made containing equal amounts of each sample. The cDNA library was constructed and transformed into yeast using Clontech's Make Your Own "Mate & Plate" Library System.

The bait plasmids used were the same GI1 fl pGBKT7 and GI2 fl pGBKT7 used in the pairwise assays. They were transformed into the Matchmaker® Gold yeast strain from Clontech, and passed the mating efficiency tests. In autoactivation tests, both GI1 and GI2 were found to autoactivate the X-alpha-gal reporter (colonies were blue instead of white). When also grown with Aureobasidin A (AbA), this effect disappeared. As a result of this, it was decided to use QDO (SD-L-T-H-A) plates with AbA to select interaction partners from the library matings.

Baits were then mated with the library according to the protocols in Clontech's Matchmaker® Gold Yeast Two-Hybrid System User Manual. Plating 100nl of the mated library resulted in 77 colonies for the GI1-library mating, and 218 colonies for the GI2 mating. This meant that plating 10ml of each was equivalent to plating ~7.7 million matings for GI1 and ~21.8 million matings for GI2. Plates were checked for colonies after three days of growth, and colonies were counted. Mating efficiency was calculated, and then 48 candidates of each were chosen. This number of candidates represents a screen of approximately 10^6 matings for GI1 and 7.5×10^5 matings for GI2, and these amounts are comparable to other yeast two hybrid library screens reported in the literature.

Candidates were selected, re-streaked, and amplified using colony PCR. PCR cleanup and sequencing was done by the campus sequencing facility. Sequencing results were then BLASTed using the default settings of NCBI's nucleotide BLAST against the *Zea mays* refseq RNA collection. GO annotations were obtained from both Uniprot (www.uniprot.org) and Gramene (tools.gramene.org), and where necessary from orthologous genes.

Figures

Figure 3.1 (pages 86-87). N- and C-terminal halves of all GI proteins color-coded by amino acid similarity. Polar and neutral amino acids are orange, polar and positive amino acids are red, non-polar and aromatic amino acids are blue, and non-polar and aliphatic amino acids are green.

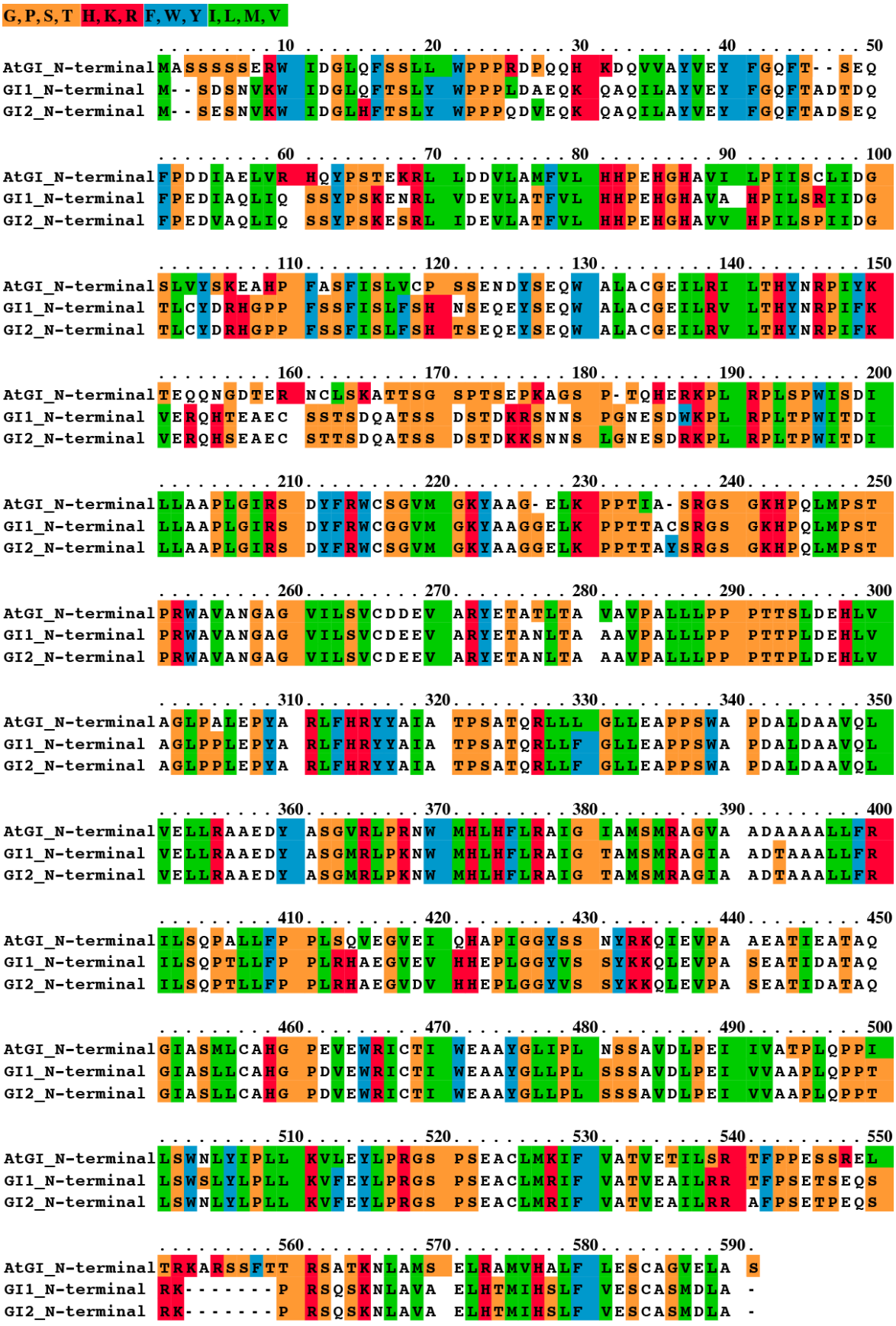
G, P, S, T
H, K, R
F, W, Y
I, L, M, V
AtGI_N-terminal
GI1_N-terminal
GI2_N-terminal

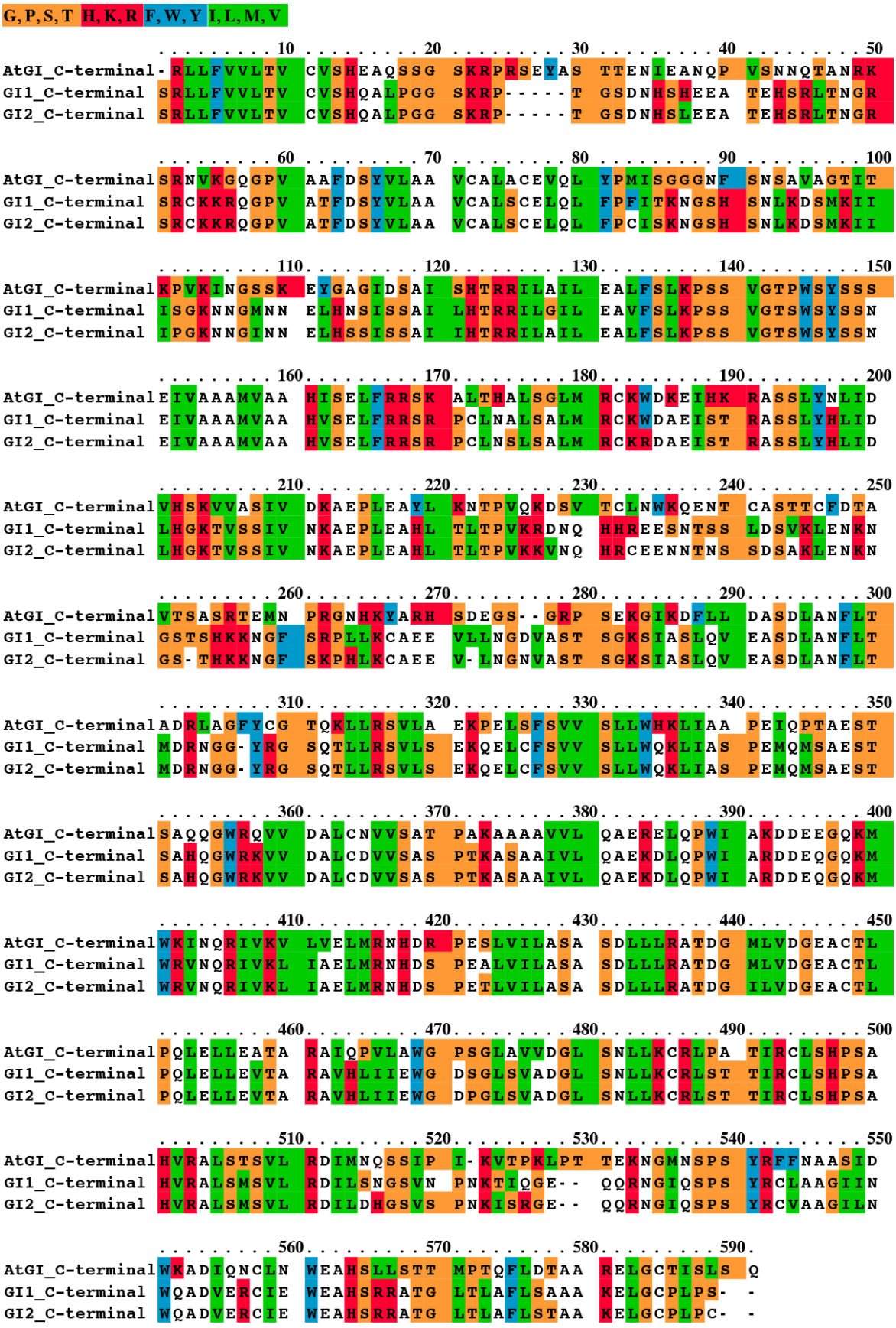
G, P, S, T
H, K, R
F, W, Y
I, L, M, V
AtGI_C-terminal
GI1_C-terminal
GI2_C-terminal

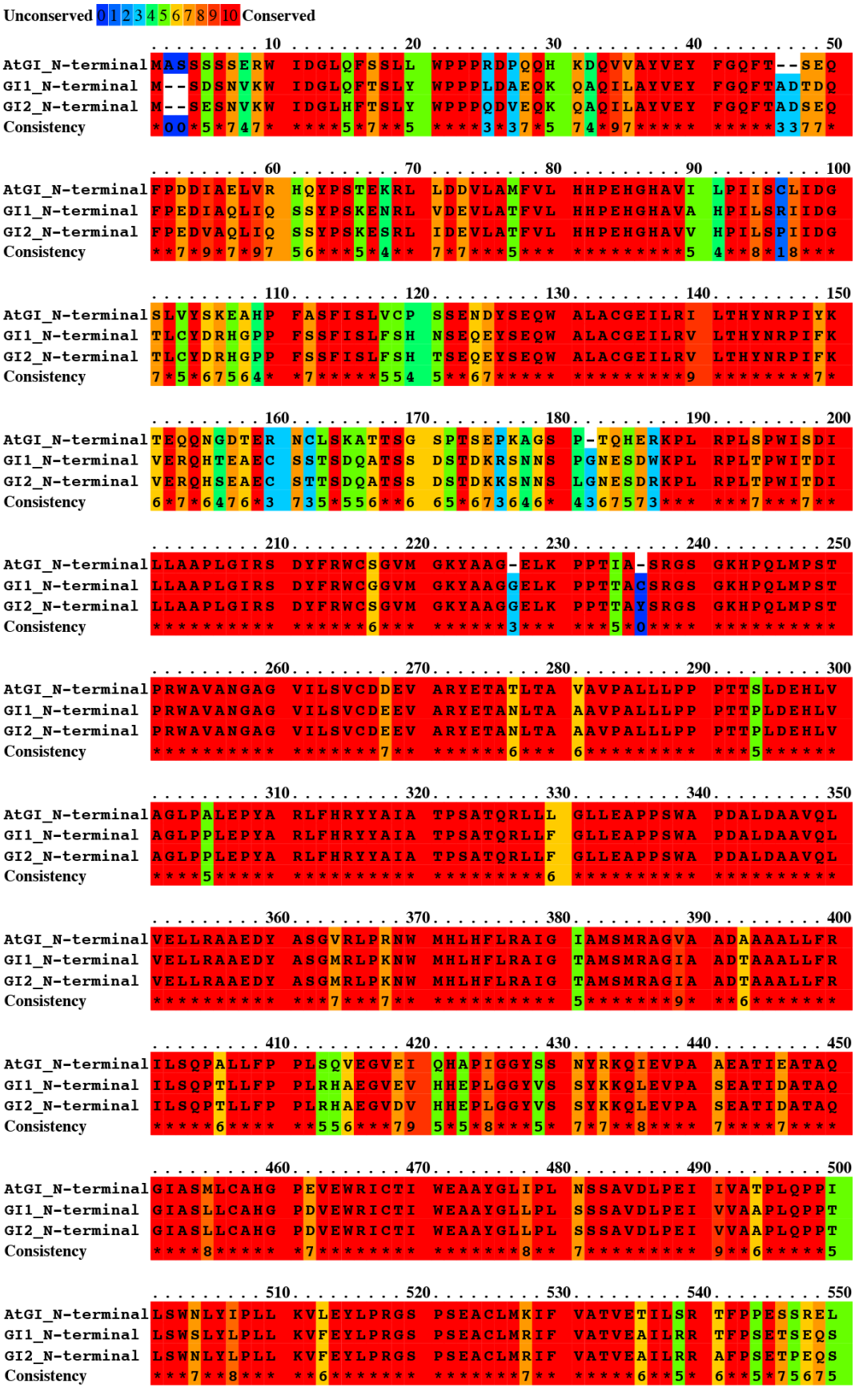
Unconserved 0 1 2 3 4 5 6 7 8 9 10 Conserved
AtGI_N-terminal
GI1_N-terminal
GI2_N-terminal
Consistency

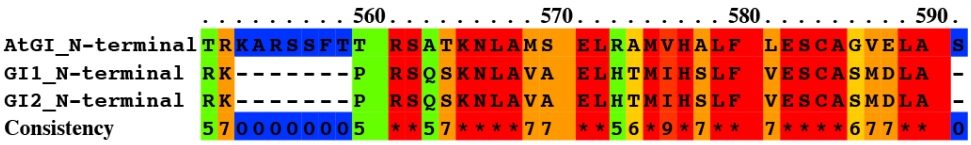

Figure 3.2 (this page and previous page). Alignment of N-terminal GI constructs color-coded by degree of conservation. Unconserved residues are colored blue, while conserved residues are colored red.

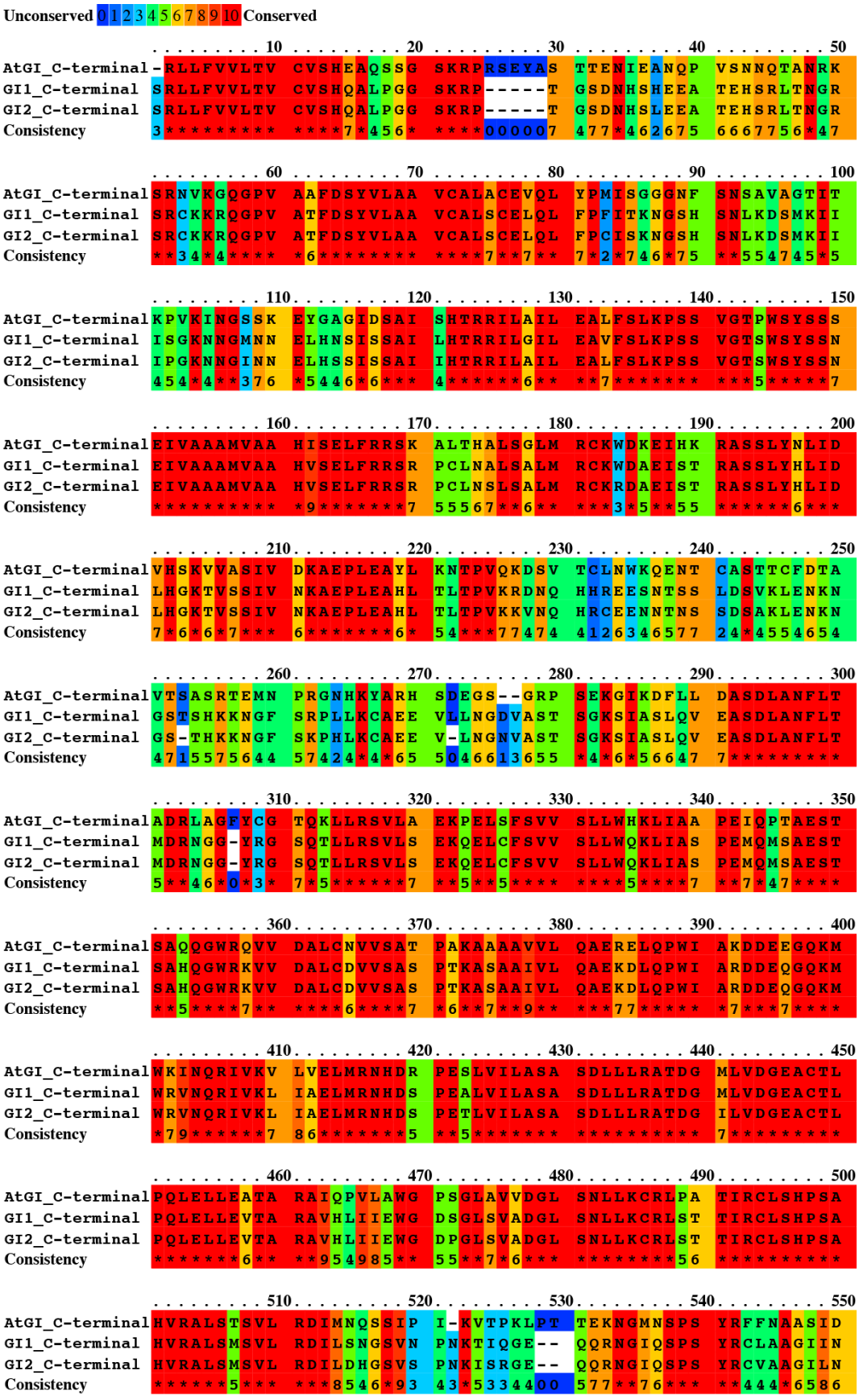
Unconserved 0 1 2 3 4 5 6 7 8 9 10 Conserved
AtGI_C-terminal
GI1_C-terminal
GI2_C-terminal
Consistency

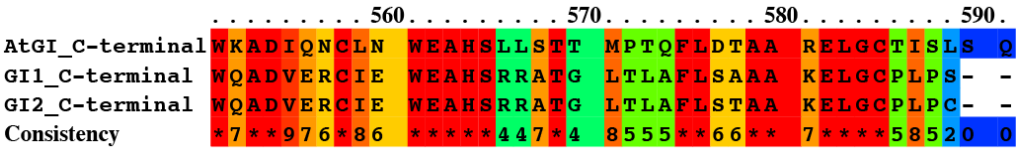

Figure 3.3 (this page and previous page). Alignment of C-terminal GI constructs color-coded by degree of conservation. Unconserved residues are colored blue, while conserved residues are colored red.

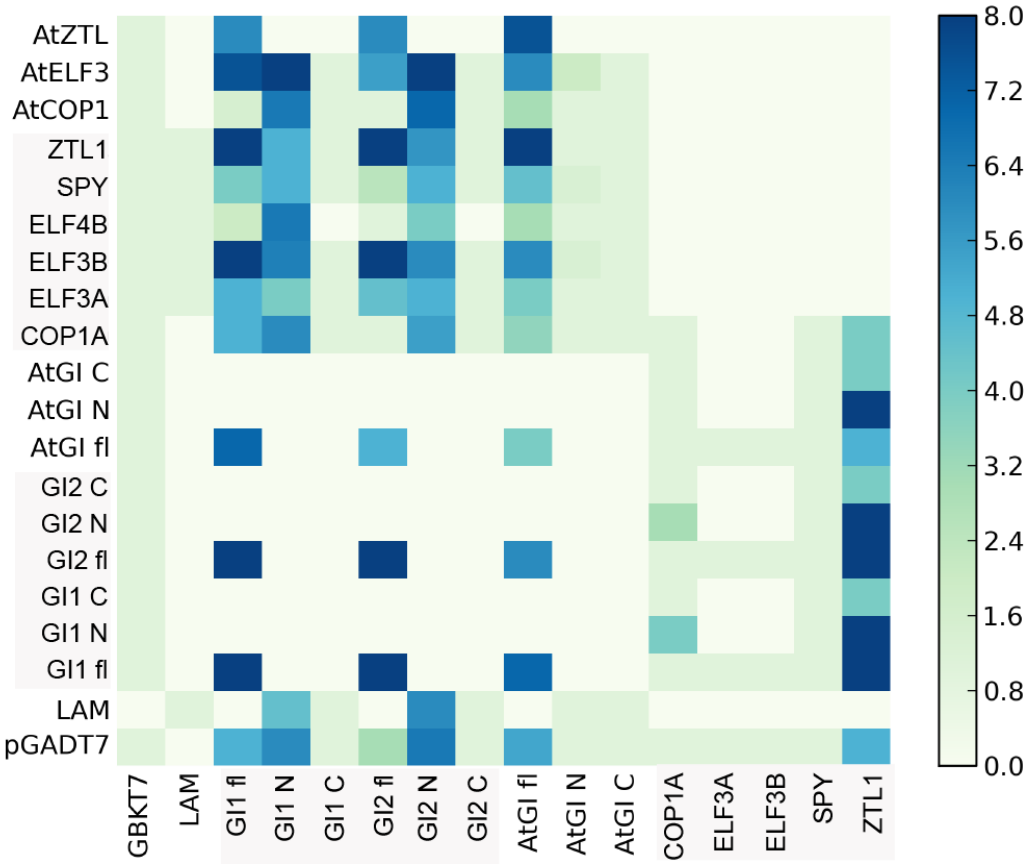

Figure 3.4. Serial dilution results from 7 days' growth on QDO (SD-L-T-H-A) plates represented as an interaction matrix. Bait plasmids (in pGBKT7) are on the x-axis, and prey plasmids (in pGADT7/pGAD424) are on the y-axis. A score of 0 indicates the mating was not tested, while a score of 1 indicates the mating was tested, but there was no interaction. Interactions scored with 2 grew only in the most concentrated spot (samples diluted to a uniform OD=3). Scores 3 through 8 represent the last dilution in which growth was still seen, with 3 indicating 1:5 and 8 indicating 1:1000 (see Materials & Methods for full list). Growth at 1:1000 dilution indicates a strong interaction. Scores are averages from two or more separate platings.

A

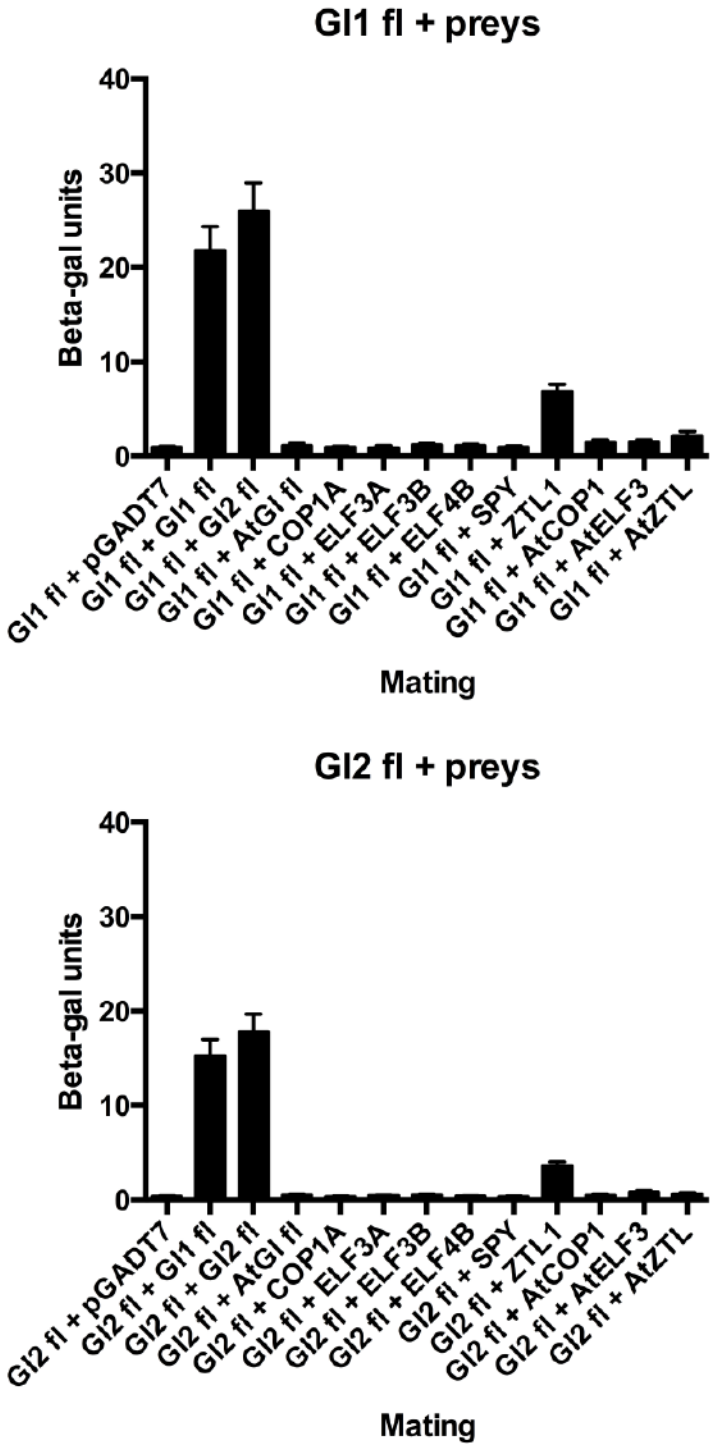
Gl1 fl + preys
Beta-gal units
40
30
20
10
0
Gl1 fl + pGADT7
Gl1 fl + Gl1 fl
Gl1 fl + Gl2 fl
Gl1 fl + AtGI fl
Gl1 fl + COP1A
Gl1 fl + ELF3A
Gl1 fl + ELF3B
Gl1 fl + ELF4B
Gl1 fl + SPY
Gl1 fl + ZTL1
Gl1 fl + AtCOP1
Gl1 fl + AtELF3
Gl1 fl + AtZTL
Mating
Gl2 fl + preys
Beta-gal units
40
30
20
10
0
Gl2 fl + pGADT7
Gl2 fl + Gl1 fl
Gl2 fl + Gl2 fl
Gl2 fl + AtGI fl
Gl2 fl + COP1A
Gl2 fl + ELF3A
Gl2 fl + ELF3B
Gl2 fl + ELF4B
Gl2 fl + SPY
Gl2 fl + ZTL1
Gl2 fl + AtCOP1
Gl2 fl + AtELF3
Gl2 fl + AtZTL
Mating

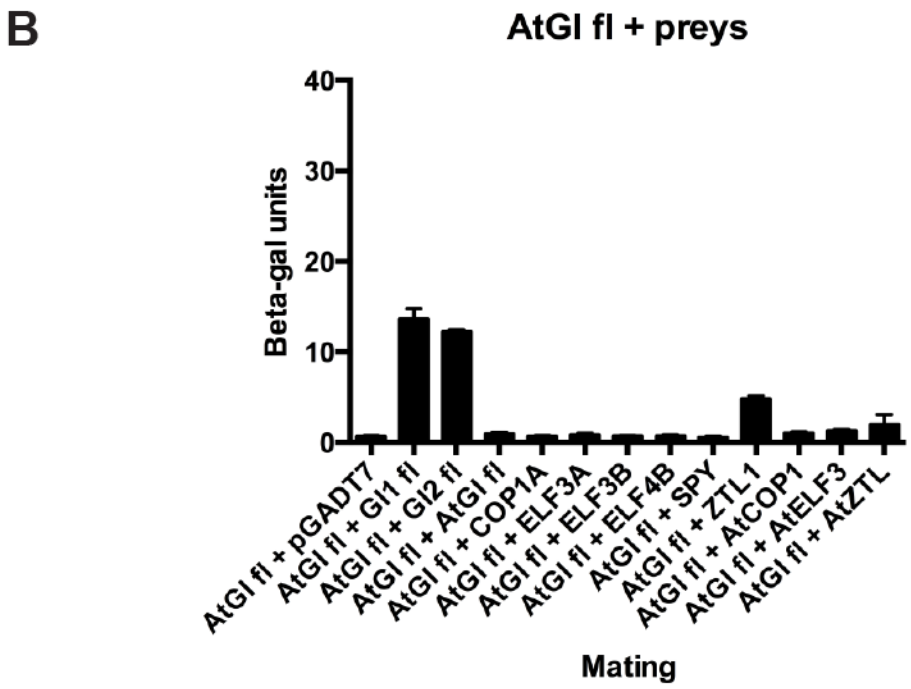

Figure 3.5 (this page and previous page). Full length (fl) GI bait constructs (in pGBKT7) tested against preys in liquid culture assays using ONPG as a substrate. **A)** GI1 and GI2 baits, and **B)** AtGI bait.

A

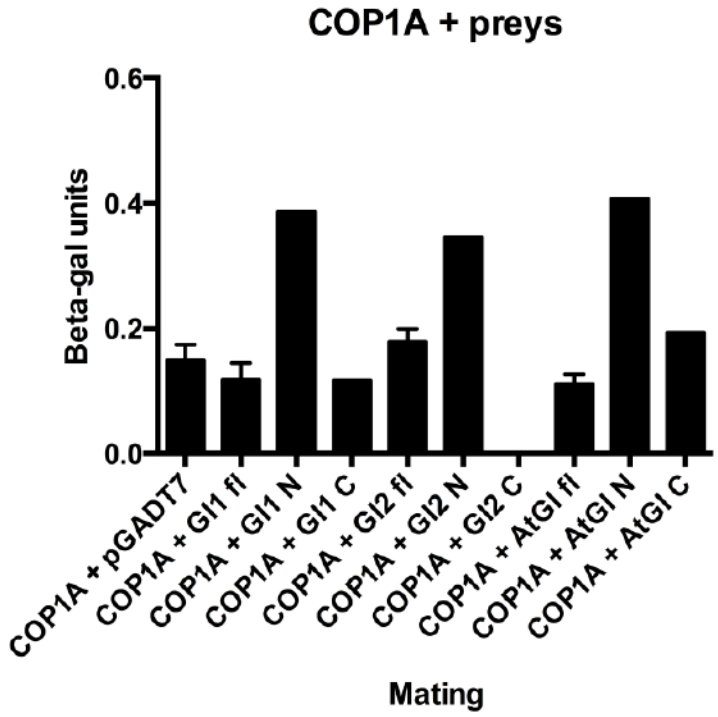
COP1A + preys
Beta-gal units
0.6
0.4
0.2
0.0
COP1A + pGADT7
COP1A + Gl1 fl
COP1A + Gl1 N
COP1A + Gl1 C
COP1A + Gl2 fl
COP1A + Gl2 N
COP1A + Gl2 C
COP1A + AtGl fl
COP1A + AtGl N
COP1A + AtGl C
Mating

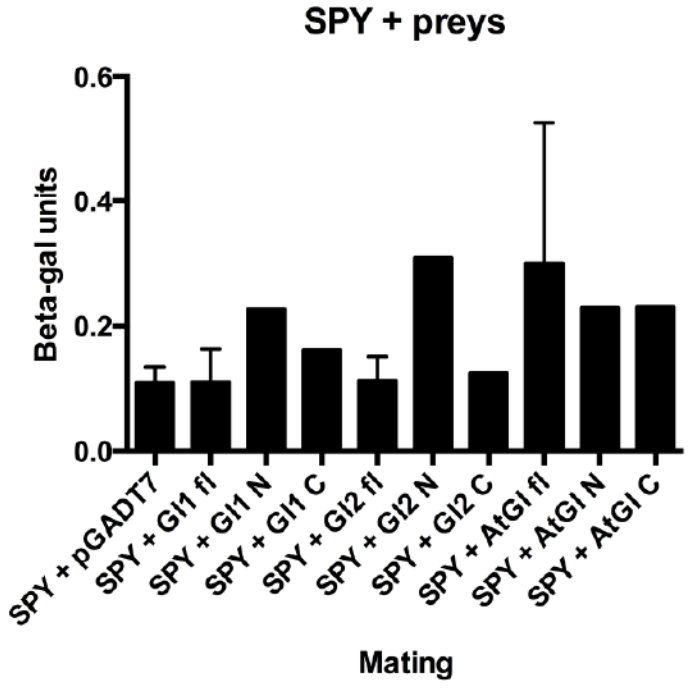
SPY + preys
Beta-gal units
0.6
0.4
0.2
0.0
SPY + pGADT7
SPY + Gl1 fl
SPY + Gl1 N
SPY + Gl1 C
SPY + Gl2 fl
SPY + Gl2 N
SPY + Gl2 C
SPY + AtGl fl
SPY + AtGl N
SPY + AtGl C
Mating

B

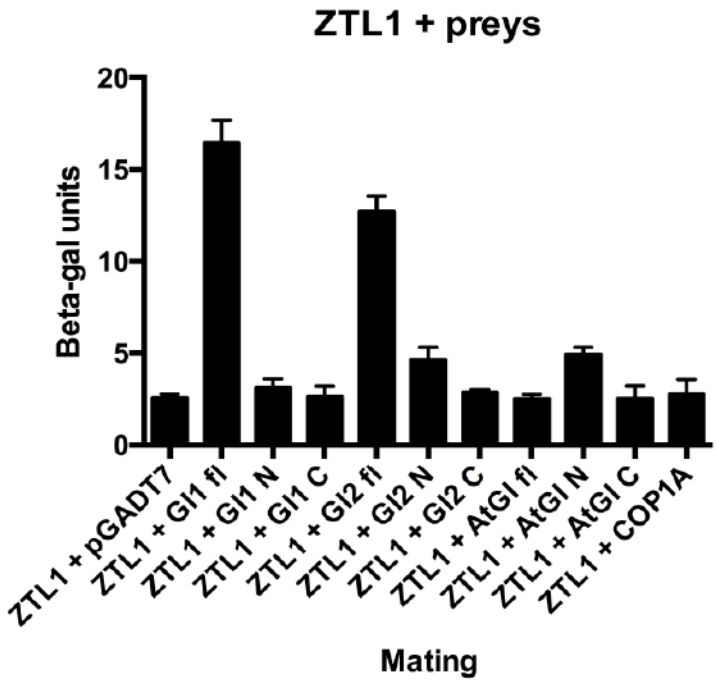

Figure 3.6 (this page and previous page). Bait constructs (in pGBKT7) of putative interactors tested against GI preys in liquid culture assays using ONPG as a substrate. **A)** COP1A and SPY baits, and **B)** ZTL1 bait.

Tables

GI1 interactors	Name/Protein type	GO - biological process	Uniprot
GRMZM2G345493	fructose-bisphosphate aldolase	glycolytic process	B6SSU6
GRMZM2G050307	S-adenosyl-L-methionine-dependent methyltransferase	methylation	B4FVQ7
GRMZM2G377855	photosystem I reaction center subunit V	photosynthetic electron transport in photosystem I; photosynthetic NADP+ reduction; photosystem I stabilization; protein stabilization	B4G1K9
GRMZM2G059083	ferredoxin/L-FNRII	photosynthetic electron transport chain; defense response to fungus, incompatible interaction; defense response to bacterium; oxidation-reduction process	Q9SLP5
GRMZM2G396553	arginine decarboxylase 1	arginine catabolic process; spermidine biosynthetic process	K7W734
GRMZM2G092311	Chlorophyll a-b binding protein 6A	photosynthesis, light harvesting; protein-chromophore linkage	B6SSN3
GRMZM2G041060	FKBP-like peptidyl-prolyl cis-trans isomerase family protein, chloroplast; FK506 binding protein	protein peptidyl-prolyl isomerization; protein folding	C0P3F1/ K7UBG1 /C0HHL 0/B6T5Z 4
GRMZM2G038636	CCP2; cysteine protease 2; SEE1	proteolysis; aging; response to ethylene	Q10717/ Q43705
GRMZM2G119249	shikimate kinase family protein	cellular amino acid metabolic process; jasmonic acid biosynthesis process; chlorophyll biosynthetic process; phosphorylation; positive regulation of transcription, DNA-templated	B6TNV8

GI1 interactors	Name/Protein type	GO - biological process	Uniprot
GRMZM2G163671	TRAF transcription factor; Maternal effect lethal family member; BTB/POZ domain-containing protein	fatty acid beta-oxidation; intra-Golgi mediated vesicle transport; proximal/distal pattern formation; floral organ abscission; protein import into peroxisome matrix; flower morphogenesis	K7UBS0 /B4FLP5 /B6TM0 3
GRMZM2G120652	PDXS; subunit of pyridoxal 5'-phosphate synthase; pyridoxin biosynthesis protein ER1	cellular amino acid metabolic process; response to stress; response to oxidative stress; response to lipid hydroperoxide; pyridoxine biosynthetic process; response to salt stress; response to UV-B; response to non-ionic osmotic stress; chlorophyll metabolic process; hyperosmotic salinity response; vitamin B6 biosynthetic process; pyridoxal phosphate biosynthetic process	B4FQA2 /B4FRZ2
GRMZM2G066496	terpenoid synthase superfamily protein, mitochondrial	protein folding; protein targeting to mitochondrion; biosynthetic process; response to heat; response to high light intensity; response to hydrogen peroxide*	B6TWB6
GRMZM2G337113	CPA1; glyceraldehyde 3-phosphate dehydrogenase 1, chloroplastic	glucose metabolic process; oxidation reduction process	P09315
GRMZM2G083841	PEP1; phosphoenolpyruvate carboxylase 1	tricarboxylic acid cycle; carbon fixation	Q43267
GRMZM2G351259	putative cytochrome P450 superfamily protein	oxidation-reduction process	B4FS98
GRMZM2G081462	magnesium-protoporphyrin IX monomethyl ester [oxidative] cyclase, chloroplastic	chlorophyll biosynthetic process; photosynthesis; protein peptidyl-prolyl isomerization; protein folding; root development	K7USR3

GI1 interactors	Name/Protein type	GO - biological process	Uniprot
GRMZM2G084521	peptidyl-prolyl cis-trans isomerase CYP19-4; cyclophilin ABH-like	protein peptidyl-prolyl isomerization; protein folding; root development*	B6TIP7
GRMZM2G115273	GST1; glutathione S-transferase	toxin catabolic process; response to toxic substance	P12653
GRMZM2G176519	CBL-interacting serine/threonine-protein kinase 11	protein phosphorylation; signal transduction	B6SK56
GRMZM2G094928	Vacuolar (H+)-ATPase G subunit	proton transport	B4FPE4
GRMZM2G058450	RING/U-box superfamily protein	response to chitin*	B4FCS7
GRMZM2G096546	plant-specific domain TIGR01627 family protein	plant-type secondary cell wall biogenesis; xylan biosynthetic process*	B6UI35
GRMZM2G003762	glutamine aminotransferases class-II	glutamine metabolic process; response to aluminum ion; response to auxin*	C4J9Y2
GRMZM2G005887	cysteine synthase 2	L-cysteine biosynthetic process from L-serine; cellular amino acid biosynthetic process; cysteine biosynthetic process	B8A377/ P80608
GRMZM2G126190	actin-7		B4FRH8
GRMZM2G030203	50S ribosomal protein L10	Ribosome biogenesis	B6SUJ0
LOC100275739	26S ribosomal RNA gene		
GRMZM2G087918	DUF1997		A0A096 RCC6
GRMZM2G157522	DUF3741		K7UJR0
GRMZM2G142093	DUF1517		B4FV42
GRMZM2G157296	unknown	cellular cation homeostasis; divalent metal ion transport*	B6TMU3
GRMZM2G030240	unknown		K7U311/ B6U3W9

Table 3.1 (this page and two previous pages). GI1 interaction partners from the yeast two hybrid library screen. GO terms are from both Uniprot (www.uniprot.org) and Gramene (tools.gramene.org). The first four genes (separated from the rest by a bold line) were each present in the sequencing two times. GO terms marked with a * are taken from Arabidopsis orthologs.

GI2 interactors	Name/Protein type	GO - biological process	Uniprot
GRMZM2G059083	ferredoxin/L-FNRII	photosynthetic electron transport chain; defense response to fungus, incompatible interaction; defense response to bacterium; oxidation-reduction process	Q9SLP5
GRMZM2G126079	ARF GTPase-activating domain family protein	nucleocytoplasmic transport; response to virus*	B4FY47
GRMZM2G001696	Phosphoenolpyruvate carboxykinase (PEPCK)	gluconeogenesis; defense response to fungus, incompatible interaction; cellular response to phosphate starvation; response to cadmium ion	C0P3W9
GRMZM2G330635	glutathione S-transferase GSTU6	de-etiolation; response to cadmium ion; lateral root development; response to growth hormone; response to karrikin^	B6TL20
GRMZM2G019267	cyclin-dependent protein kinase C family protein	mRNA processing; protein phosphorylation; response to virus; flower development; phosphorylation; leaf development; carpel development; regulation of viral process	B4F9F3
GRMZM5G814314	ubiquitin-conjugating enzyme E2	protein ubiquitination*	B6SIU1
GRMZM2G303044	Grx_A2 - glutaredoxin subgroup III	cell redox homeostasis	B6UGY1
GRMZM2G065928	cytochrome p450	response to red or far red light; abscisic acid metabolic process; release of seed from dormancy; defense response to fungus; oxidation-reduction process	B4F9T8
GRMZM2G436986	oxygen evolving enhancer protein 3 containing protein; PSII-Q subunit	maltose metabolic process; photosynthesis; starch biosynthetic process; positive regulation of catalytic activity	B4FT19
AC217401.3_FG003	serine/threonine protein kinase; leucine-rich repeats; transmembrane	protein phosphorylation	C4J1V0

GI2 interactors	Name/Protein type	GO - biological process	Uniprot
GRMZM5G850966	60S ribosomal protein L36-like	translation	B4FW07
GRMZM2G064302	PGH1; ENO1; enolase 1	glycolytic process	P26301
GRMZM2G052812	auxin-induced protein PCNT115; aldo-keto reductase	response to cadmium ion	B6TD84
GRMZM2G180625	cytosolic glyceraldehyde-3-phosphate dehydrogenase GAPC2	glucose metabolic process; glycolytic process	B4FS87/ Q09054
GRMZM2G160496	PIN10b; putative auxin efflux carrier component	auxin-activated signaling pathway; auxin polar transport; auxin homeostasis; auxin efflux; transmembrane transport*	I3RWW1
GRMZM2G169005	oxidoreductase activity; NAS(P)-binding domain; Rossmann-fold NAD(P)(+)-binding proteins	oxidation-reduction process	B4FBT1
GRMZM2G351259	putative cytochrome P450 superfamily protein	oxidation-reduction process	B4FS98
GRMZM2G017654	serine/threonine kinase sepA-like	protein phosphorylation; plasma membrane organization; pollen development	A0A0B4 J2Y9
GRMZM2G122337	FDX1; chloroplast ferredoxin 1	response to light stimulus; photosynthetic electron transport chain; response to karrikin	B1P759
GRMZM2G027955	AGP2; ADP-glucose pyrophosphorylase; chloroplast	starch biosynthesis; glycogen biosynthesis	B6TCZ8
GRMZM2G048907	ATPC2; ATP synthase gamma subunit2 (organellar)	ATP synthesis coupled proton transport	B6TUD4 /P0C1M 0
GRMZM2G049549	cryptochrome; FAD binding domain of DNA photolyase	DNA repair; response to water deprivation; detection of light stimulus; response to blue light; photomorphogenesis; blue light signaling pathway; regulation of meristem growth; stomatal	B4FHJ0/ B8A2L5

GI2 interactors	Name/Protein type	GO - biological process	Uniprot
		movement; singlet oxygen-mediated programmed cell death; circadian regulation of calcium ion oscillation; anthocyanin-containing compound metabolic process; protein autophosphorylation; regulation of unidimensional cell growth; oxidation-reduction process	
GRMZM5G870932	PCK2; phosphoenolpyruvate carboxykinase homolog2	gluconeogenesis; defense response to fungus, incompatible interaction; cellular response to phosphate starvation; response to cadmium ion	K7VNE2
GRMZM2G115049	VDAC2; voltage-dependent anion channel protein 2; mitochondrial	anion transport; response to bacterium; defense response to bacterium; regulation of anion transport; transmembrane transport	Q9SPD7
GRMZM2G046804	GAPC1; glyceraldehyde-3-phosphate dehydrogenase	glucose metabolic process; oxidation-reduction process	K7U1H6
GRMZM2G133428	TPR repeat; MYND finger; F-box-like; SLR repeat	protein binding	A0A096S7C0
GRMZM2G402631	PR-5; pathogenesis-related protein	thaumatin-like protein; defense activity; antifungal activity; antifreeze activity[1]	B4FV91
GRMZM2G125072	3Fe-4S ferredoxin		B6TSX7
GRMZM2G126190	Actin-7		B4FRH8
GRMZM2G017654	serine/threonine kinase sepA-like		A0A0B4J2Y9
LOC100275482	DUF1997		B6SU04

Table 3.2 (this page and two previous pages). GI2 interaction partners from the yeast two hybrid library screen. GO terms are from both Uniprot (www.uniprot.org) and Gramene (tools.gramene.org). The first gene was present six times in the sequencing, the second gene three times, and the third gene two times (separated from the rest by a bold line). GO terms marked with a * are taken from Arabidopsis orthologs, while those marked with a ^ are taken either from rice or *Sorghum*. [1] (Liu et al., 2010)

Supplemental Figures

Supplemental Figure 3.1 (pages 104-105). Predictions of protein secondary structure in the N- and C-terminal halves of GI proteins according to DSSP (Kabsch and Sander, 1983) and PSIPRED (Jones, 1999). Red indicates a helix domain, while blue indicates a strand domain.

Supplemental Figure 3.2. (pages 106-107). N- and C-terminal halves of GI proteins color-coded according to the hydrophobicity of their amino acids (Eisenberg et al., 1984). Blues indicate hydrophobic amino acids, reds indicate hydrophilic amino acids, and purples indicate intermediate amino acids.

HELIX (H) STRAND (E)

```
                        .........10 .........20 .........30 .........40 .........50
(PRED) AtGI_N-terminal MASSSSSERW IDGLQFSSLL WPPPRDPQQH KDQVVAYVEY FGQFT--SEQ
(PRED) GI1_N-terminal  M--SDSNVKW IDGLQFTSLY WPPPLDAEQK QAQILAYVEY FGQFTADTDQ
(PRED) GI2_N-terminal  M--SESNVKW IDGLHFTSLY WPPPQDVEQK QAQILAYVEY FGQFTADSEQ

                        .........60 .........70 .........80 .........90 .........100
(PRED) AtGI_N-terminal FPDDIAELVR HQYPSTEKRL LDDVLAMFVL HHPEHGHAVI LPIISCLIDG
(PRED) GI1_N-terminal  FPEDIAQLIQ SSYPSKENRL VDEVLATFVL HHPEHGHAVA HPILSRIIDG
(PRED) GI2_N-terminal  FPEDVAQLIQ SSYPSKESRL IDEVLATFVL HHPEHGHAVV HPILSPIIDG

                        .........110.........120.........130.........140.........150
(PRED) AtGI_N-terminal SLVYSKEAHP FASFISLVCP SSENDYSEQW ALACGEILRI LTHYNRPIYK
(PRED) GI1_N-terminal  TLCYDRHGPP FSSFISLFSH NSEQEYSEQW ALACGEILRV LTHYNRPIFK
(PRED) GI2_N-terminal  TLCYDRHGPP FSSFISLFSH TSEQEYSEQW ALACGEILRV LTHYNRPIFK

                        .........160.........170.........180.........190.........200
(PRED) AtGI_N-terminal TEQQNGDTER NCLSKATTSG SPTSEPKAGS P-TQHERKPL RPLSPWISDI
(PRED) GI1_N-terminal  VERQHTEAEC SSTSDQATSS DSTDKRSNNS PGNESDWKPL RPLTPWITDI
(PRED) GI2_N-terminal  VERQHSEAEC STTSDQATSS DSTDKKSNNS LGNESDRKPL RPLTPWITDI

                        .........210.........220.........230.........240.........250
(PRED) AtGI_N-terminal LLAAPLGIRS DYFRWCSGVM GKYAAG-ELK PPTIA-SRGS GKHPQLMPST
(PRED) GI1_N-terminal  LLAAPLGIRS DYFRWCGGVM GKYAAGGELK PPTTACSRGS GKHPQLMPST
(PRED) GI2_N-terminal  LLAAPLGIRS DYFRWCSGVM GKYAAGGELK PPTTAYSRGS GKHPQLMPST

                        .........260.........270.........280.........290.........300
(PRED) AtGI_N-terminal PRWAVANGAG VILSVCDDEV ARYETATLTA VAVPALLLPP PTTSLDEHLV
(PRED) GI1_N-terminal  PRWAVANGAG VILSVCDEEV ARYETANLTA AAVPALLLPP PTTPLDEHLV
(PRED) GI2_N-terminal  PRWAVANGAG VILSVCDEEV ARYETANLTA AAVPALLLPP PTTPLDEHLV

                        .........310.........320.........330.........340.........350
(PRED) AtGI_N-terminal AGLPALEPYA RLFHRYYAIA TPSATQRLLL GLLEAPPSWA PDALDAAVQL
(PRED) GI1_N-terminal  AGLPPLEPYA RLFHRYYAIA TPSATQRLLF GLLEAPPSWA PDALDAAVQL
(PRED) GI2_N-terminal  AGLPPLEPYA RLFHRYYAIA TPSATQRLLF GLLEAPPSWA PDALDAAVQL

                        .........360.........370.........380.........390.........400
(PRED) AtGI_N-terminal VELLRAAEDY ASGVRLPRNW MHLHFLRAIG IAMSMRAGVA ADAAAALLFR
(PRED) GI1_N-terminal  VELLRAAEDY ASGMRLPKNW MHLHFLRAIG TAMSMRAGIA ADTAAALLFR
(PRED) GI2_N-terminal  VELLRAAEDY ASGMRLPKNW MHLHFLRAIG TAMSMRAGIA ADTAAALLFR

                        .........410.........420.........430.........440.........450
(PRED) AtGI_N-terminal ILSQPALLFP PLSQVEGVEI QHAPIGGYSS NYRKQIEVPA AEATIEATAQ
(PRED) GI1_N-terminal  ILSQPTLLFP PLRHAEGVEV HHEPLGGYVS SYKKQLEVPA SEATIDATAQ
(PRED) GI2_N-terminal  ILSQPTLLFP PLRHAEGVDV HHEPLGGYVS SYKKQLEVPA SEATIDATAQ

                        .........460.........470.........480.........490.........500
(PRED) AtGI_N-terminal GIASMLCAHG PEVEWRICTI WEAAYGLIPL NSSAVDLPEI IVATPLQPPI
(PRED) GI1_N-terminal  GIASLLCAHG PDVEWRICTI WEAAYGLLPL SSSAVDLPEI VVAAPLQPPT
(PRED) GI2_N-terminal  GIASLLCAHG PDVEWRICTI WEAAYGLLPL SSSAVDLPEI VVAAPLQPPT

                        .........510.........520.........530.........540.........550
(PRED) AtGI_N-terminal LSWNLYIPLL KVLEYLPRGS PSEACLMKIF VATVETILSR TFPPESSREL
(PRED) GI1_N-terminal  LSWSLYLPLL KVFEYLPRGS PSEACLMRIF VATVEAILRR TFPSETSEQS
(PRED) GI2_N-terminal  LSWNLYLPLL KVFEYLPRGS PSEACLMRIF VATVEAILRR AFPSETPEQS

                        .........560.........570.........580.........590.
(PRED) AtGI_N-terminal TRKARSSFTT RSATKNLAMS ELRAMVHALF LESCAGVELA S
(PRED) GI1_N-terminal  RK-------P RSQSKNLAVA ELHTMIHSLF VESCASMDLA -
(PRED) GI2_N-terminal  RK-------P RSQSKNLAVA ELHTMIHSLF VESCASMDLA -
```

HELIX (H) STRAND (E)

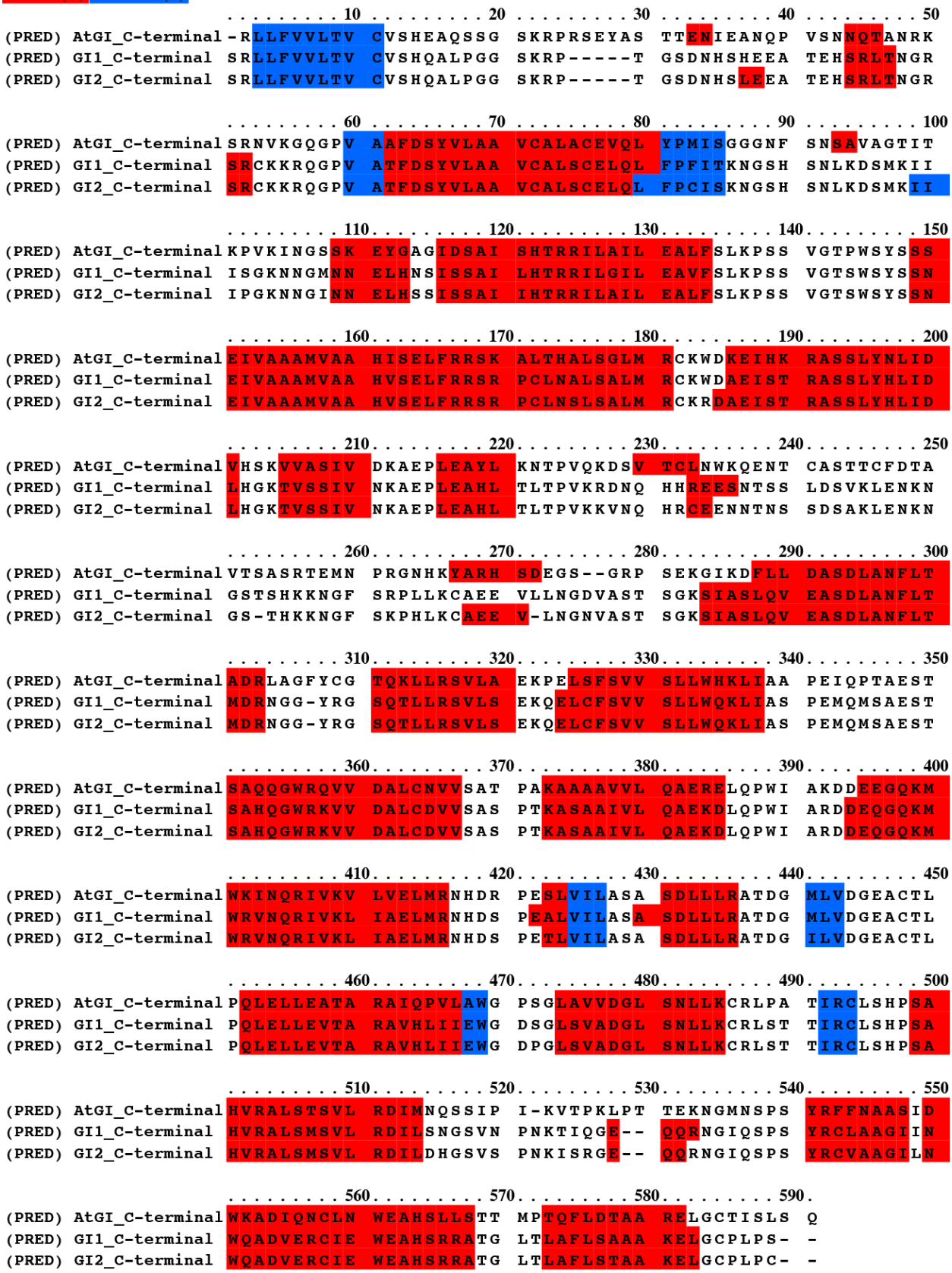

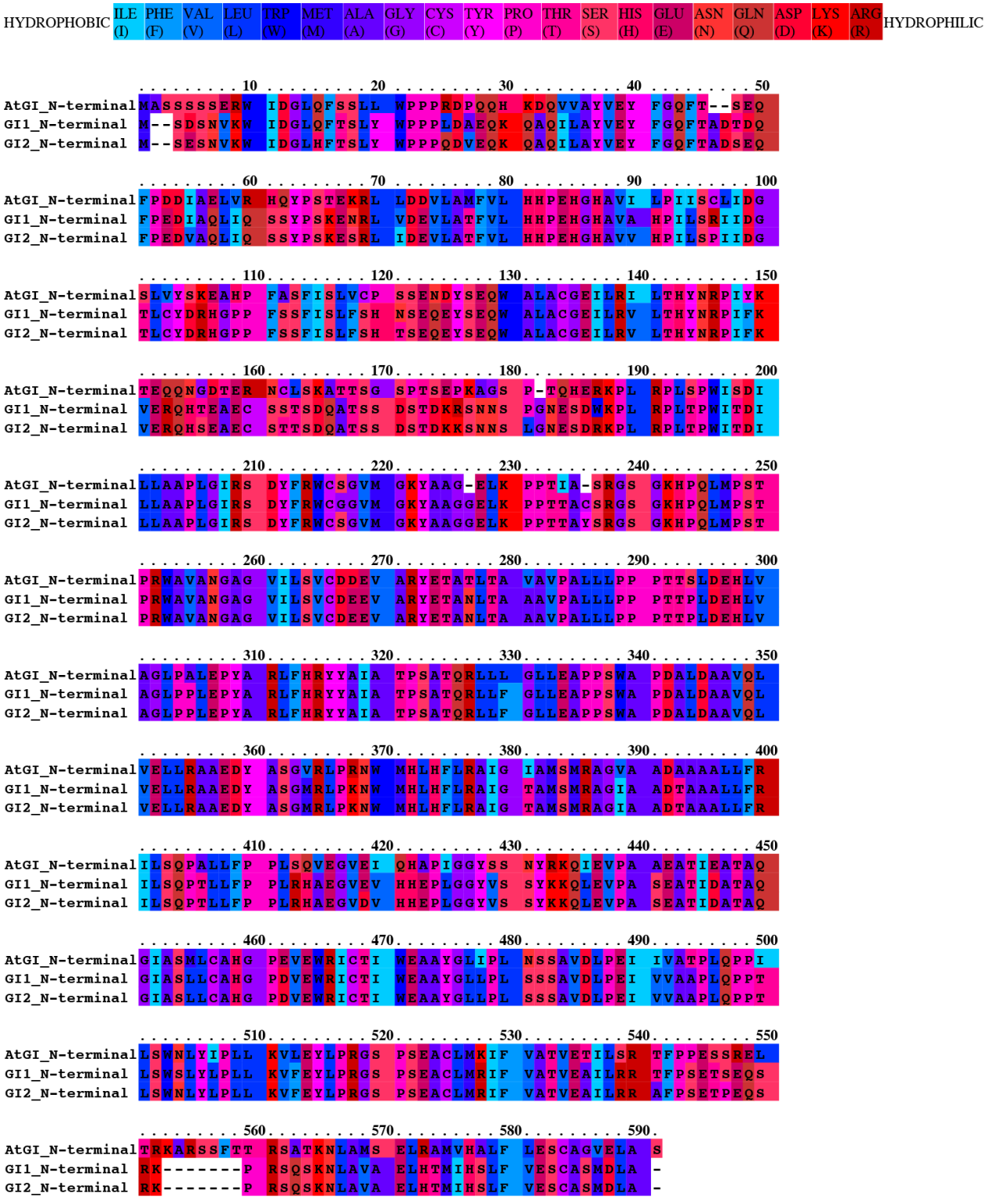
HYDROPHOBIC
ILE (I)
PHE (F)
VAL (V)
LEU (L)
TRP (W)
MET (M)
ALA (A)
GLY (G)
CYS (C)
TYR (Y)
PRO (P)
THR (T)
SER (S)
HIS (H)
GLU (E)
ASN (N)
GLN (Q)
ASP (D)
LYS (K)
ARG (R)
HYDROPHILIC
AtGI_N-terminal
GI1_N-terminal
GI2_N-terminal

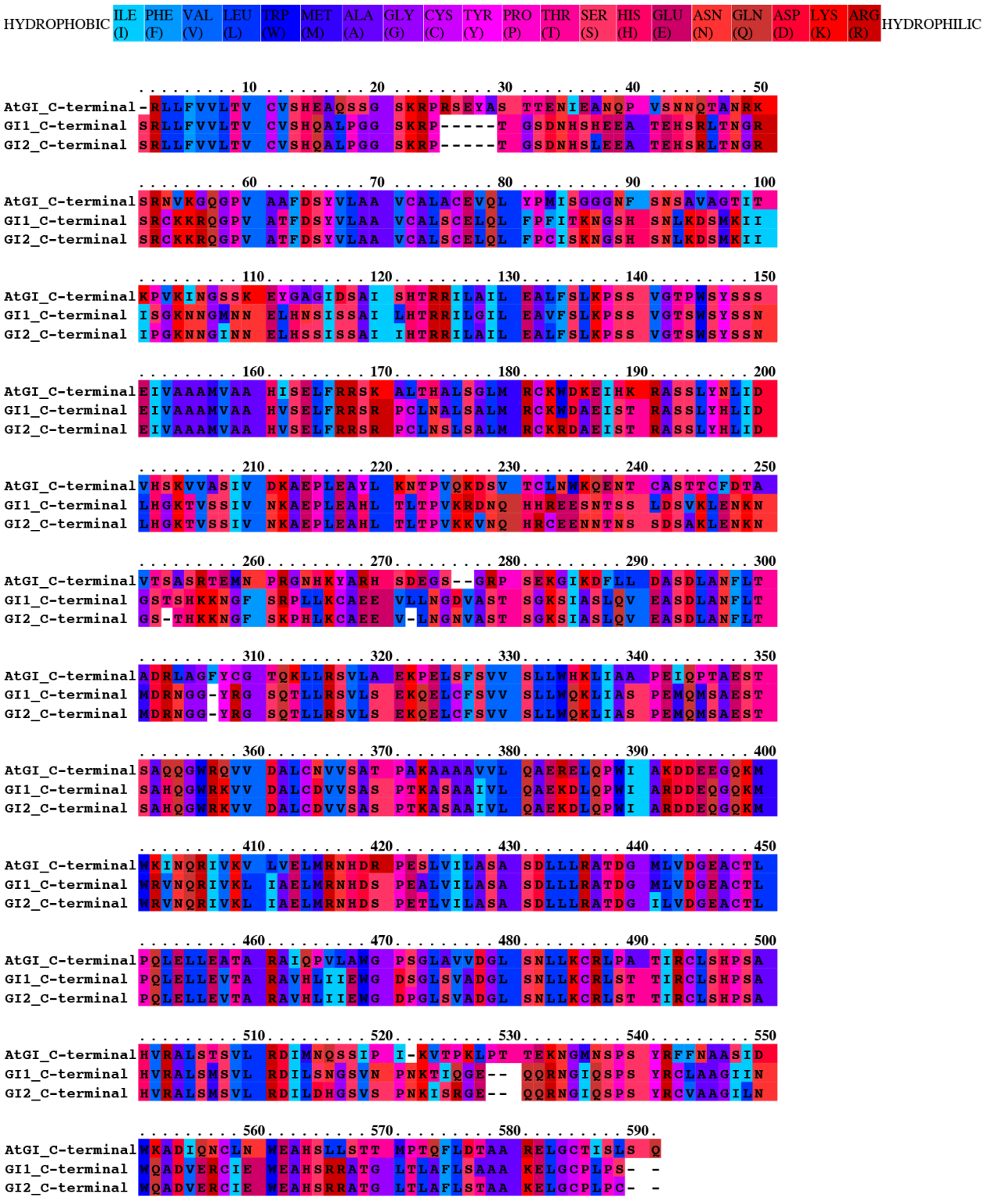
HYDROPHOBIC
ILE (I)
PHE (F)
VAL (V)
LEU (L)
TRP (W)
MET (M)
ALA (A)
GLY (G)
CYS (C)
TYR (Y)
PRO (P)
THR (T)
SER (S)
HIS (H)
GLU (E)
ASN (N)
GLN (Q)
ASP (D)
LYS (K)
ARG (R)
HYDROPHILIC
AtGI_C-terminal
GI1_C-terminal
GI2_C-terminal

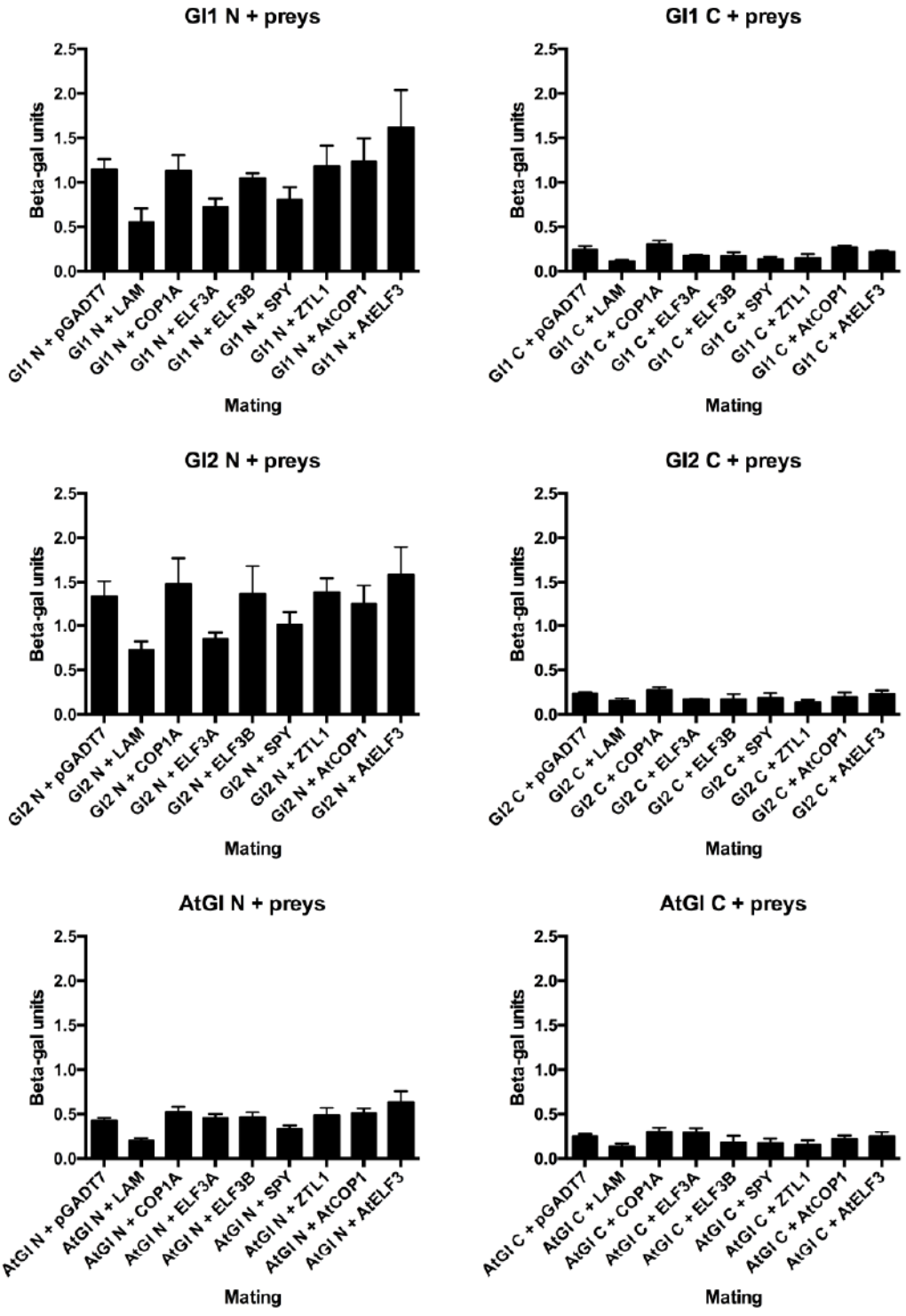

Supplemental Figure 3.3. N- and C-terminal GI bait constructs (in pGBKT7) tested against preys in liquid culture assays using ONPG as a substrate.

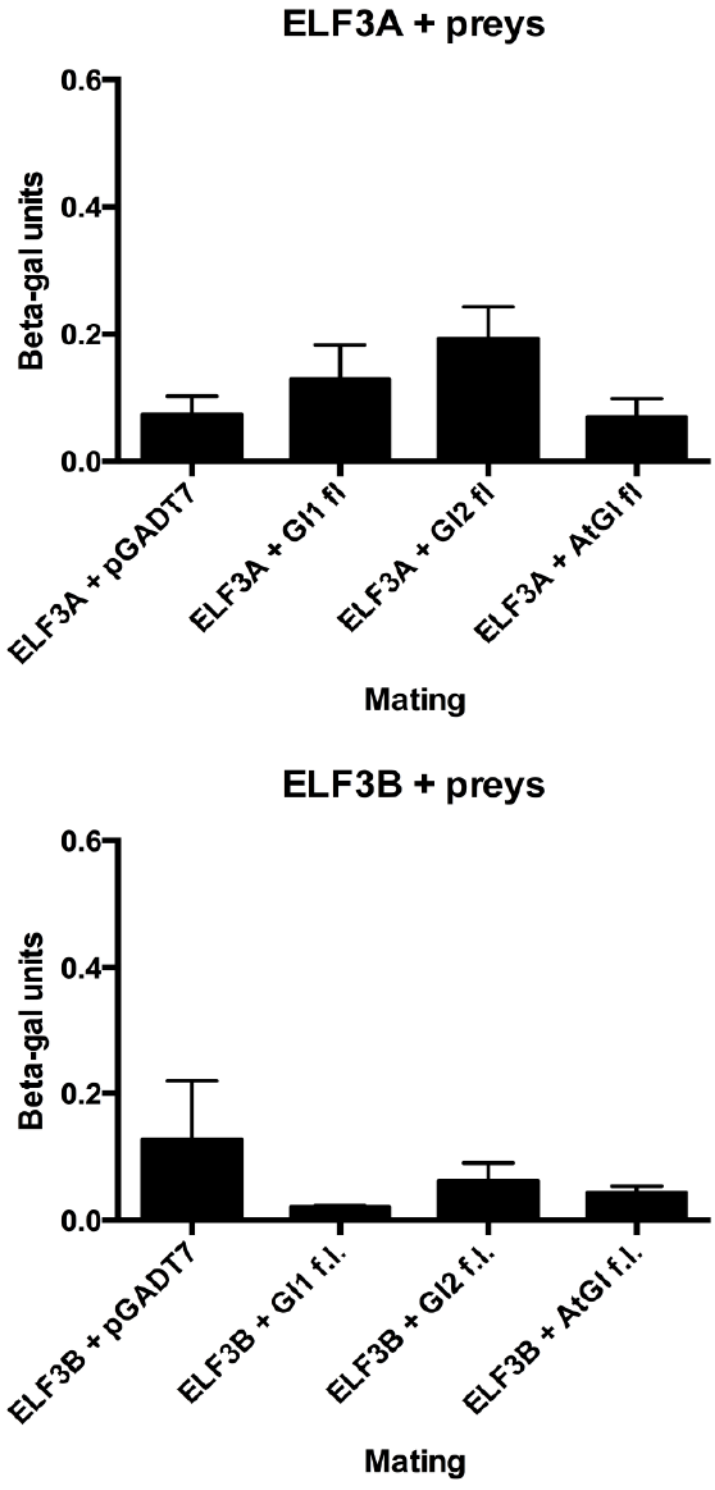

Supplemental Figure 3.4. ELF3A and ELF3B bait constructs (in pGBKT7) tested against preys in liquid culture assays using ONPG as a substrate.

Supplemental Tables

Official designation	Working name
GRMZM2G107101	*gi1*
GRMZM5G844173	*gi2*
GRMZM2G175265 + GRMZM2G474769	*lhy1*
GRMZM2G014902	*lhy2*
GRMZM2G020081	*toc1a*
GRMZM2G148453	*toc1b*
GRMZM2G104920	*cop1a*
GRMZM2G045275	*elf3a*
AC233870.1_FG003	*elf3b*
GRMZM2G382774	*elf4b*
GRMZM2G357804	*spy*
GRMZM2G147800	*ztl1*
AT1G22770	*AtGI*
AT2G32950	*AtCOP1*
AT2G25930	*AtELF3*
AT5G57360	*AtZTL*

Supplemental Table 3.1. Genes used in this chapter and their working names. Note that maize gene names are lower case, and their protein names are upper case, while Arabidopsis gene and protein names are upper case. In both cases, gene names are italicized while protein names are not.

Chapter Four: Bioinformatic identification and characterization of maize circadian clock genes and grass circadian gene expression

Abstract

The current understanding of the plant circadian clock is primarily based on research done in the model plant *Arabidopsis thaliana.* Using the Arabidopsis network as a basis for characterizing circadian clocks in other species has provided a useful starting point, but has also shown that some assumptions are incorrect. As circadian research is done across more plant species, it is becoming increasingly clear that other plant clock systems are divergent from that of Arabidopsis. Phylogenetic analysis shows that most grass species have more copies of clock components than Arabidopsis, and that some Arabidopsis clock components do not have orthologs in grass species. The analysis presented in this chapter identifies likely maize circadian clock components, and shows that less essential clock components are more likely to diverge in expression pattern. This research provides the basis for future in-depth characterization of the maize circadian clock.

Introduction

Circadian clocks are found across plant species, and are defined by three consistent molecular characteristics, namely an endogenous rhythm of approximately 24 hours, the capacity to be entrained by external cues, and the ability to maintain consistent timekeeping in a wide range of temperatures (Harmer, 2009; Hsu and Harmer, 2014; Nagel and Kay, 2012). The rhythmic waveforms of gene expression produced by the circadian clock have multiple terms to describe the timing of peak expression and waveform characteristics (described in detail in Figure 4.1). In Arabidopsis*,* over twenty clock or clock-associated components have been identified and characterized (Table 4.1) (Hsu and Harmer, 2014). Many phenotypic effects and regulatory interactions are known, and the important gene families have been characterized. Depictions of the clock, however, vary between papers, and it is difficult to comprehensively evaluate circadian clock studies (Flis et al., 2015; Hsu and Harmer, 2014; Nagel and Kay, 2012). Research in other species has therefore often focused on specific gene families deemed particularly important.

Arabidopsis clock system characteristics are used as a basis to characterize clock systems in other plants. One metric often cited is the percentage of the transcriptome regulated by the clock, i.e. the proportion of genes that are rhythmically expressed. Studies in Arabidopsis*,* however, have shown that this percentage varies according to the entraining conditions, plant genotypes, experimental protocol, and analysis methods. If divided by conditional effects, an estimated 15-30% of transcripts cycle under constant conditions (LL or DD), while under diurnal conditions 30-50% cycle (Bläsing et al., 2005; Covington et al., 2008; Michael and McClung, 2003). Thus, rhythmic gene expression arises from both circadian clock control and direct responses to environmental cues in diurnal conditions. The percentage of genes under true circadian control is lower than the total number of rhythmic genes. Similar percentages have been seen in studies of other species (Table 4.2). It should be noted that circadian control is only one component of diurnal oscillations, and that the regulation of transcriptome dynamics is complex (Nagano et al., 2012).

Arabidopsis clock component characteristics are also used as a basis to characterize clock components in other plants (see Chapter One). *Brassica rapa,* another species from the *Brassicaceae* family, appears to have similar clock components and clock component behavior to Arabidopsis*,* although some genes are present in multiple copies (Lou et al., 2012; Xie et al., 2015). In grapevine cultivars (*Vitis vinifera* L.), multiple circadian gene homologs were identified, and *VvRVE1* was shown to oscillate in berry tissues with a pattern similar to *AtLHY* (Carbonell-Bejerano et al., 2014). Studies on barley have identified *HvCCA1* (Kusakina et al., 2015), *HvLUX1* (Campoli et al., 2013), and *HvPHYc* (Pankin et al., 2014) as core clock components, while *HvPRR37* (Kusakina et al., 2015) is primarily involved in flowering time, and *HvELF3* (Deng et al., 2015) and *HvGI* (Dunford et al., 2005; Pasam et al., 2012; Wang et al., 2010) have no clearly identifiable role. Similar studies have been done in the eudicots tomato (Facella et al., 2008), wild tobacco (Yon et al., 2012), and legumes (Liu et al., 2009; Weller and Ortega, 2015), as well as the monocots *Lemna gibba* (Miwa et al., 2006; Serikawa et al., 2008), wheat (Gawroński et al., 2014), and rice (Izawa et al., 2011; Murakami et al., 2007; Yang et al., 2013; Zhao et al., 2012).

Variations in clock function are seen in plants with growth habits that differ from that of Arabidopsis*.* In chestnut trees, oscillation of circadian genes disappears during the winter, indicating that winter dormancy is linked to clock dormancy (Ibañez et al., 2008; Ramos et al., 2005). Studies in poplar have also linked the circadian clock to other seasonal processes. During winter dormancy, circadian genes no longer oscillate, but their constant expression levels appear important both for freezing tolerance and bud burst in the spring (Ibáñez et al., 2010). These studies show that the environment can prevent oscillations, and that circadian clock genes can continue to play important regulatory roles without their hallmark oscillations.

Some clock research has been done in species quite evolutionarily distant from Arabidopsis (Supplemental Figure 4.1). Putative circadian clock genes from the gymnosperm Norway spruce (*Picea abies* L. Karst) were partially able to complement Arabidopsis circadian mutant phenotypes, indicating conserved clock component function (Karlgren et al., 2013). The spruce clock appears to have a similar regulation of seasonal processes as the poplar clock does, and population-level studies of spruce find clinal variation in circadian genes (Chen et al., 2012). A transcriptome study in the gymnosperm Japanese cedar (*Cryptomeria japonica* (L.f.) D.Don) was able to identify a network of circadian-clock associated genes, as well as likely core clock genes (Nose and Watanabe, 2014). During the diurnal cycles, some genes that cycle diurnally in angiosperms did not in cedar, and a number of cycling genes had no identifiable angiosperm orthologs. Diurnal rhythms were lost during winter dormancy, similar to the chestnut and poplar clocks. The two cedar *LHY* orthologs had different expression patterns and were also associated with regulating different genes, while the *CjZTL* transcripts were found to oscillate.

The moss *Physcomitrella patens* also has a number of circadian clock gene orthologs, but lacks *TOC1*, *GI*, and *ZTL* genes (Holm et al., 2010). Because of this, it has been proposed that the moss clock is simpler than that of angiosperms or gymnosperms, and potentially represents an ancestral clock form (Holm et al., 2010). There have, however, been few direct investigations of the moss circadian clock, which could therefore have evolved other complexities lacking in angiosperms. Green algae

also lack these three clock gene groups. Cyanobacteria, which are photosynthetic and share common ancestors with chloroplasts, but are otherwise unrelated to plants, encode a circadian clock that is regulated entirely at the protein level, which is composed of three core proteins; KaiA, KaiB, and KaiC (Egli, 2014).

A common theme emerging from these studies is that clock network structure and clock component function varies the more evolutionarily distant the plants are from Arabidopsis (Supplemental Figure 4.1). Dicots tend to have conserved clock component functions, and when these are perturbed, dicots have similar phenotypes to those seen in Arabidopsis. Monocots may have similar clock components, but the function of these often differs, and mutant phenotypes vary in strength and directionality. Non-angiosperm plants have some similar clock components, but the network structure of the clock likely differs.

Additionally, recent research has shown that domestication also plays an important role in modifying the clock (see Chapter One). Tomato domestication selectively fixed an allelic variant of *SlEID1,* which slows down the clock and allows tomatoes to thrive under LD conditions (Müller et al., 2015). Breeding barley to grow in high-latitude short growing seasons selected alleles of evening complex genes that cause clock arrhythmia (Faure et al., 2012). Domestication has also complicated clock research at the genomic level, as many crop species are polyploid and therefore carry multiple copies of clock genes.

The fact that our current understanding of the clock is based on an undomesticated annual plant has skewed clock research in perennial and crop plants. The above-mentioned studies and many more indicate that Arabidopsis is the outlier in more ways than one. This chapter presents evidence from maize supporting this conclusion by demonstrating that the maize circadian clock has evolved significant differences compared to the model genetic system, Arabidopsis. Maize circadian clock genes were identified with phylogenetic and bioinformatic analysis. The genes were then named according to maize nomenclature rules and paralogy. To obtain expression data as well as a global overview of diurnal expression in grasses, a RNA-Seq timecourse experiment in diurnal conditions comparing maize, *Sorghum*, and *Setaria* was performed. This data set will provide a basis for further characterization of the maize circadian clock and may allow for predictive network modeling.

Results

Diversity and evolution of circadian clock genes in grasses

We used publicly available databases to identify putative homologs of the clock genes described in Arabidopsis. Multiple well-sequenced dicot and monocot species were chosen, and protein lists were constructed using NCBI protein BLAST and Gramene. Protein sequences were used over nucleotide sequences due to the evolutionary distances between the species used. MAFFT was used to align the sequences, and RAxML was used to build the trees (for more detail, see Materials and Methods). Five major clock gene groups were chosen, and the following results are divided according to group.

***LHY* and *RVE* genes**

LHY (LATE ELONGATED HYPOCOTYL) is a Myb transcription factor that is a core component of all models of the plant circadian clock. Maize has two *LHY-like* (*lyl*) genes, making it unique among the grasses with sequenced genomes (Figure 4.2), although two or more *LHY*s are common in the non-grass species. Both maize and *Setaria* had incorrectly annotated gene models that separated their *LHY*s into two separate genes. Poplar also has a split gene annotated, and so may only have two LHYs, and in banana there are three full-length and one short *LHY*. As with maize and *Setaria,* this may be a case of misannotation, or it may be evidence of gene fragmentation. Soybean has four *LHY*s, while most other species featured have one or two. The duplication that resulted in the *LHY* named *CCA1* appears to be unique to the *Brassicaceae*, and both Arabidopsis and *Brassica rapa* have one copy of *LHY* and one copy of *CCA1*.

Both of the maize *lyl* genes have clear rhythmic expression patterns with peak expression beginning around dawn and continuing until three hours after (Figure 4.3.A). *lyl1* has been annotated as two separate genes due to the presence of a large transposon-introduced intron, so fpkm values from each of these gene models are presented here. Peak expression of the orthologs seems to be earlier, closer to dawn (Figure 4.4.A).

The *LHY* genes are nestled within the larger *RVE* gene family (Supplemental Figure 4.2.A), of which *RVE4, RVE6,* and *RVE8* are principal clock activators. *RVE1, RVE2,* and *RVE7* form the next most closely related groupings to the *LHY* genes (Figure 4.5). These groups have low bootstrap support, and so the names of these genes may be incorrect. *RVE1* appears to only be found in the *Brassicaceae*. All grasses have retained two duplicates of the *RVE7-like* (*RE7L*) gene after the basal monocot duplication event, and maize has two further copies from its later duplication event. Banana has at least three *RE7L* genes, as well as two identical ones annotated on different chromosomes. Finally, the *RVE2* group consists of Arabidopsis and *Brassica rapa,* and there is a monocot group of *RVE2-like* (*RE2L*) genes. These are all single-copy, including the one maize *re2l.*

The single *re2l* gene has strong rhythmicity, and peak expression at dawn (Figure 4.3.A). The expression of the *re2l* orthologs is consistent in that peak times appear to be the same, but both orthologs have wider peaks than maize *re2l* (Figure 4.4.A). All four *re7l* genes are also rhythmically expressed, with *re7l3* and *re7l4* having three- to five-fold higher peak expression than *re7l1* and *re7l2* (Figure 4.3.B). The peak expression time of *re7l1*, *re7l3*, and *re7l4* is three hours before dawn, and falls off sharply at dawn. *re7l2* peak expression is shifted a little later: it peaks at dawn and only decreases about three hours after dawn. The orthologs of *re7l1* and *re7l2* in *Sorghum* and *Setaria* have exactly the same expression pattern as *re7l1*, but over six-fold higher expression at peak expression times (Figure 4.4.C). Apart from these high and clearly defined peaks, expression in the orthologs is as low as in maize. The *re7l3* and *re7l4 Sorghum* ortholog is expressed at a lower level than either of the maize copies, and appears to have a slightly earlier peak (Figure 4.4.D). The *Setaria* ortholog, on the other hand, has a distinctly earlier peak, by about six hours, which lasts longer than the peaks of the other genes.

One of the other major *RVE* groups is the *RVE6* group. *RVE3* and *RVE5* are nested within *RVE6*, and again are only in the *Brassicaceae* (Figure 4.6). An ancestral duplication of *RVE6* before the divergence of monocots led to the evolution of two distinct lineages within angiosperms. This means that in all the species chosen there are anywhere from two to eight *RVE6* or *RVE6-like* (*RE6L*) genes. Maize has five *re6l* genes, of which three are on one branch of the monocot *RE6L*s, and two on another. There are two shorter *RE6L* genes on very long branches, one each from banana and *Selaginella,* which apart from perhaps being incorrectly annotated may or may not actually belong within this grouping.

Of the *re6l* genes in maize, only *re6l5* shows strong rhythmic expression that peaks at dawn (Figure 4.3.B). *re6l1* has similarly rhythmic expression, but at a much lower level. *re6l4* appears to be expressed rhythmically as well, yet it lacks the distinct peaks seen in the other two. The last two, *re6l2* and *re6l3* are expressed also, and much less clearly rhythmic than *re6l5* and *re6l1.* The expression patterns of *re6l* orthologs correspond quite closely to *re6l* genes. The *re6l1* orthologs have the same peak timing as *re6l1*, and similar expression levels to each other, which are both higher than *re6l1* expression levels throughout (Figure 4.4.B). The *Sorghum* ortholog of *re6l2* and *re6l3* is expressed at a similar level and also arrhythmic (Figure 4.4.B). The *Setaria* ortholog, on the other hand, has increased expression levels throughout the night. Finally, the *re6l4* and *re6l5 Sorghum* ortholog has identical timing and phase as *re6l5,* while the *Setaria* ortholog is similarly expressed, but at a higher level and with broader peaks (Figure 4.4.C).

The final group is the *RVE8* group, which consists of one dicot branch and one monocot branch (Figure 4.7). *RVE4* is again *Brassicaceae*-specific. Within the monocot *RVE8-like* (*RE8L*) gene group, there was either a basal duplication with subsequent gene loss, or specific lineages had later duplications. Rice, *Brachypodium*, and *Setaria* each have two genes with one on each branch, while maize has two genes in one branch. These genes are local duplicates recently moved via transposons. Neither of the *re8l* genes are expressed (Figure 4.3.C), and this also holds true for both *re8l* orthologs (Figure 4.4.D).

At the protein level, all of the maize LHY-like and RVE-like proteins have similar domains to their Arabidopsis counterparts (Tables 4.1 and 4.3). While this provides some indication of their functional similarity, there are likely more domains to these proteins that have not been identified. This is especially problematic in cases like the RE8L proteins, which are shorter than their counterparts and apparently not expressed, but their main protein motifs are intact. This makes it difficult to determine whether the gene models are in fact accurate or not.

PRR genes

In Arabidopsis, five *PSEUDO-RESPONSE REGULATOR (PRR)* genes act within the clock and are sequentially expressed over the course of the day. The *PRR* genes fall into three main clades, namely the *TOC1* clade, the *PRR3/7* clade, and the *PRR5/9* clade (Supplemental Figure 4.2.B). In order to be consistent with maize nomenclature rules, all of these genes are named with the suffix '*-like'* to allow numbering. In other monocot species, the *PRR* names are used with prefixes denoting species names (e.g. *OsPRR37*), and so these names have been used in the trees.

Many dicot species have multiple *TOC1* genes, whereas the grasses more often have one copy (Figure 4.8). Maize is the exception to the rule with six *TOC1-like* (*t1l*) genes, and the basal monocot banana has three *TOC1*s. The six maize *t1l*s form two distinct groups. The first group consists of *t1l1* and *t1l2*, which are similar to dicot *TOC1*s. The second group consists of the other *t1l*s; *t1l3*, which is quite short, and *t1l4, t1l5,* and *t1l6,* all of which are long with many exons. The T1L5 and T1L6 proteins are identical to one another and appear to have recently duplicated via transposons.

t1l1 and *t1l2* are both rhythmically expressed, with *t1l1* expressed over two-fold higher at the peak (Figure 4.3.C). Peak expression for both is at dusk, although *t1l1* has a broad peak that spans the six hours before and nine hours after dusk, while *t1l2* expression begins to increase at the same time but falls off more sharply after. The three long *t1l*s (4,5, and 6) have rhythmic expression that is almost identical: there are no sharp peaks, but instead an undulation that increases and declines when *t1l1* does. *t1l3* appears to have a similar expression pattern, but is expressed at very low levels. The *t1l* ortholog in *Sorghum* is both no longer rhythmic and barely expressed (Figure 4.4.E). The *Setaria* ortholog on the other hand, is clearly rhythmic and more highly expressed than either maize gene.

The first two maize TOC1-like proteins are similar to the Arabidopsis TOC1 protein (Tables 4.1 and 4.3), as both have response regulator receiver domains and CCT motifs. The T1L3 protein may have a response regulator receiver domain, but also does not have a CCT motif, possibly due to its short length. The T1L5 protein does not have any recognizably TOC1-like motifs, but instead has an IQ motif. Both T1L5 and T1L6, being identical, either have a response regulator receiver domain, a myosin motor domain, and an IQ domain or both of the latter without the former. These domain identifications are likely due to the lack of well-studied plant-specific protein domains. The results do, however, indicate that *t1l4-6* differ fundamentally from the other *t1l* genes.

In the *PRR3/7/37/73* clade, many dicots have duplicate *PRR7* and *PRR3* genes, and the split between *PRR3* and *PRR7* appears to be basal within the dicots (Figure 4.9). Arabidopsis and tomato have only one of each, while poplar appears to have lost its *PRR7* genes. In monocots, the genes from the basal monocot duplication have also been given different names, with one duplicate branch called *PRR37* and one called *PRR73*. This was done on the basis of protein similarities to either *PRR3* or *PRR7* (Murakami et al., 2005), but given that the dicot and monocot divisions were independent, the distinction is somewhat misleading. There are three maize genes that fall within this group, two within the *PRR37*s, and one within the *PRR73*s. *Selaginella* has retained two *PRR7* genes, perhaps indicating two copies are necessary for functionality.

p37l1 is expressed more highly than *p37l2*, and both are rhythmic (Figure 4.3.D). Peak expression time is midday. The *p73l* gene is also rhythmically expressed, and peak expression is similarly timed (Figure 4.3.E). Expression levels remain higher for longer than those of either *p37l* gene. The *p37l* ortholog in *Sorghum* has a similar expression pattern to *p37l1,* while the *Setaria* ortholog is no longer expressed (Figure 4.4.E). Both *p73l* orthologs have very similar expression patterns to *p73l* (Figure 4.4.F). The *Setaria* ortholog is almost identical, while the *Sorghum* ortholog has slightly higher expression levels.

In the *PRR9/5/95* clade, it can be seen that the dicot *PRR5* group nests within the *PRR9* group, indicating this was a more recent evolutionary innovation (Figure 4.10). Arabidopsis is the only dicot to have one copy of *PRR5.* All of the monocot genes group outside both of the dicot groups, and have been named *PRR95*. There are two maize genes within this group, *GRMZM2G179024* (*p95l1*) and *GRMZM2G367834* (*p95l2*), which are paralogs of each other. This appears to be a recent duplication, as none of the other grasses have more than one copy.

The two *prr95l* genes are rhythmically expressed, and have more similar expression levels than many other paralogs shown here (Figure 4.3.F). At the peak expression time, around mid-afternoon, *p95l1* expression is approximately twice that of *p95l2*. Both orthologs have similar expression patterns and higher levels at the peak than either maize gene (Figure 4.4.G).

There are two further groupings within the *PRR*s (Figure 4.11). One consists of the *PRR2* and *PRR4* genes, which are generally not considered circadian genes. The important rice flowering time regulator *Ehd1* (*Os10g0463400*), however, is a *PRR4* and falls within this clade. There is a single maize counterpart to this gene, *GRMZM2G379656* (*p4l*). The other group is entirely composed of monocots, and these genes are named *PRR59*s. This group is evolutionarily distinct from the *PRR9/5/95* group, making this name somewhat misleading, however the two maize genes within the group are accordingly named *prr59-like1* (*p59l1*) and *p59l2*.

The *p4l* gene is not expressed, and given its similarity to *Ehd1,* may only be induced at certain developmental times (Figure 4.3.D). Both *p4l* orthologs also were not expressed during the timecourse (Figure 4.4.G). *p59l* expression is timed the same as *p95l*, and the two paralogs have similar expression patterns to those seen with the *p37l* genes (Figure 4.3.E). Unlike those genes, however, *p59l2* remains expressed during trough times when *p59l1* expression approaches zero, meaning that which *p59l* is more highly expressed fluctuates over the course of the day. The *Sorghum* ortholog has the same peak expression time, but differently shaped troughs than either maize gene (Figure 4.4.F). The *Setaria* ortholog has the same peaks as *p59l1*, as well as troughs in which expression continues at a consistent level, as it does in *p59l2.*

For the most part, the maize PRR-like proteins contain all the same motifs as the Arabidopsis PRRs (Tables 4.1 and 4.3). This indicates the gene models are complete, and may indicate that the proteins function similarly. The one notable exception to this is P4L, the ortholog of rice *Ehd1.* As the Ehd1 protein does contain the normal PRR domains, this either means that the *p4l* gene model is incomplete or that the gene is in the process of being lost.

GI genes

GIGANTEA (GI) genes are conserved throughout vascular plants, and maize has two *gi* genes, namely *gi1* and *gi2*. As can be seen from the tree, both are quite similar to their *Sorghum* counterpart (Figure 4.12). Apart from maize, all of the grasses have one *GI* copy, while many of the dicots have two or three. At least in the species chosen here, Arabidopsis again appears to be an exceptional case, being one of the few species with a single *GI* gene.

Banana likely also has three *GI*s: the two labeled “split” are directly adjacent to each other on chromosome 10. They may in fact be one recently split GI that is no longer functional, or they may be misannotated. Without expression-level support for

these gene models these two cases are difficult to distinguish. In constructing the gene list, other species also were listed as having more *GI* paralogs than present on this gene tree. These paralogs, however, were approximately 100 amino acids long and clearly not full-length GI proteins. In the case of soybean, this paralog (*GLYMA02G08680*) sits within a domain in which about fifty other equally short genes are annotated. There is EST support for many of them, and for this one that support extends to maize and Arabidopsis*,* but larger exons do not appear to be present. There are multiple possible explanations for this, including that this *GI* is in the process of fragmentation or that this represents one small functional domain that remains expressed and active.

The expression patterns and levels seen for the two *gi* genes confirm previous findings that the gene on maize subgenome 2 is more highly expressed than that on subgenome 1 (Figure 4.3.F). At the peak times of expression, *gi1* levels are four-fold higher than those of *gi2.* In comparison to the other circadian genes presented here, the *gi*s have very broad peaks, especially *gi1*. Although the maximum expression level is in the late afternoon, relatively high expression levels are seen throughout the day, with *gi1* having a trough that only seems to span a couple hours before and after dawn. Both *gi* orthologs have higher expression levels than *gi1,* and similar slightly broader expression peaks to each other (Figure 4.4.H).

There are no protein motifs or domains that can be identified in GI (Tables 4.1 and 4.3). From the alignments, however, GI1 and GI2 appear to be complete relative to Arabidopsis GI (Chapter Three).

Evening complex genes: *ELF3, ELF4,* and *LUX*

In Arabidopsis, the evening complex is a trimeric protein assembly composed of the EARLY FLOWERING 3 (ELF3), ELF4, and LUX ARRHYTHMO (LUX) proteins that represses circadian gene expression in the evening. Maize has two *ELF3* genes, *GRMZM2G045275* (*ef3l1*) and AC233870_1_FG003 (*ef3l2*)*.* Both genes are on maize subgenome 1, and neither has a direct paralog. From the tree, it can be seen that this is the result of a duplication of *ELF3-like* (*EF3L*) genes in the monocots (Figure 4.13). *Sorghum* and *Setaria* each have two *EF3L*s, with one grouping with each maize copy while *Brachypodium* only has one *EF3L* that groups with *ef3l2.* Rice has two *EF3L*s that are closely related, and have been characterized as *OsELF3-1 (Os06g0142600, Hd17, Ef7)* and *OsELF3-2* (*Os01g0566100*) (Fu et al., 2009; Matsubara et al., 2012; Saito et al., 2012; Yang et al., 2013; Zhao et al., 2012). Both are more closely related to maize *ef3l1,* indicating that this may be the maize *ef3l* active within the clock, light signaling, and flowering time.

The expression of the *ef3l* genes is rhythmic, although the peaks are quite irregular (Figure 4.3.G). Interestingly, *ef3l1* has peak expression around dawn, while *ef3l2* peaks in the early night. The *Setaria* ortholog of *ef3l1* has both similar expression pattern and expression level, while the *Sorghum* ortholog has narrower peaks and deeper troughs (Figure 4.4.H). The orthologs of *ef3l2* are somewhat different: the *Setaria* ortholog has higher expression throughout, but narrower peaks, while the *Sorghum* ortholog seems to have broader and somewhat later peaks (Figure 4.4.I).

The *ELF4* gene tree is somewhat more complicated than the *ELF3* gene tree, as Arabidopsis *ELF4* belongs to a gene family also containing *ELF4-like 1 (EF4L1), EF4L2, EF4L3,* and *EF4L4* (Supplemental Figure 4.2.C)*. ELF4* and *EF4L1* are members of one

clade (*ELF4/EF4L1* clade), while *EF4L2, EF4L3,* and *EF4L4* belong to another (*EF4L2/EF4L3/EF4L4* clade). To distinguish non-dicot *ELF4-like* genes, the nomenclature *ELF4-related* (*EF4R*) is used. As well as distinguishing them, this nomenclature also indicates the evolutionary relationships more clearly, as none of the monocot, *Amborella,* or *Selaginella* genes have clear dicot counterparts, and naming them *ELF4-like* would lead to confusion.

The *ELF4/EF4L1* clade contains only dicots, indicating this clade is unique to the dicots (Figure 4.14). Although there is also an *Amborella* gene that groups with this clade, it sits on a very long branch. Most grass genes fall within the *EF4L2/EF4L3/EF4L4* clade, including two maize genes (Figure 4.15). *GRMZM5G877647* (*ef4r3)* and *GRMZM2G025646* (*ef4r4*) are both members of this clade, but each has lost their paralog (Table 4.3). *ef4r3* appears more similar to the dicot *EF4L* genes, while *ef4r4* sits out on a long branch with other single-copy grass *EF4R* genes.

A further clade basal to both others was seen in constructing this tree (Figure 4.15). This clade appears to be monocot-specific, and contains two maize genes, *GRMZM2G382774* (*ef4r1*) and *GRMZM2G359322* (*ef4r2*), which are paralogs of each other (Table 4.3). While these genes are commonly annotated as *ELF4* in other monocots, this tree clearly shows that they are most closely related to dicot *EF4L* genes 2-4. It appears that monocots do not possess “true” *ELF4*s.

Of the *ef4r* genes, *ef4r1* is the most clearly rhythmic (Figure 4.3.G). *ef4r3* also shows some rhythmicity*,* which is echoed by *ef4r4* at a much lower level*.* The *ef4r2* gene was not expressed throughout the timecourse, and may be in the process of being lost from the genome. The *Sorghum* ortholog of *ef4r1* has similar expression levels with slightly more pronounced peaks, while the *Setaria* ortholog has higher peaks than all the other genes, but matching troughs (Figure 4.4.I). *ef4r3* only has a *Sorghum* ortholog, which has somewhat higher arrhythmic expression. There is also only a *Sorghum* ortholog of *ef4r4,* yet interestingly it shows clear rhythmicity with a sharp peak at dusk (Figure 4.4.J).

LUX/PCL1 is again a simpler story, with only one gene present in maize (Figure 4.16). Many non-dicot genes are currently annotated as *PCL-like*, but given that this is an alternative name for the Arabidopsis *BOA* gene, here all non-dicot genes are renamed *LUX-like* (*LXL*) to avoid confusion. *GRMZM2G067702* (*lxl*) has single orthologs in all other grass species included in the tree. Only soybean, banana, poplar, and tomato have two copies of *LUX.* The *BOA/PCLL* gene duplication appears to be Arabidopsis-specific, with even *Brassica rapa* not having a copy (Lou et al., 2012). This could mean that the role of *BOA* within the clock is not essential, or that Arabidopsis has subfunctionalized *LUX* function over two genes.

The expression of *lxl* is rhythmic, and has clearly defined peaks at dusk (Figure 4.3.H). Both orthologs have similar waveforms, although the *Sorghum* ortholog is expressed at the same levels as maize and has a slightly broader peak (Figure 4.4.K).

Both EF3L proteins appear to be complete, although ELF3 proteins have no identifiable protein domains (Tables 4.1 and 4.3). The EF4R proteins also seem to be correctly annotated, and all four contain the DUF1313 domain that is the hallmark of ELF4 and ELF4-like proteins. The LXL protein contains the correct domain, yet is substantially shorter than that found in Arabidopsis*.*

ZTL, FKF1, and LKP2 genes

The three closely related genes *ZEITLUPE (ZTL)/ADAGIO 1 (ADO1), LOV KELCH PROTEIN 2 (LKP2)/ADAGIO 2 (ADO2),* and *FLAVIN-BINDING, KELCH REPEAT, F-BOX 1 (FKF1)/ADAGIO 3 (ADO3)* are essential to clock protein turnover and also involved in flowering time processes. Of the three gene groups, the *ZTL* group of genes has undergone the most expansion. Some species, such as soybean, carry up to four copies. In the grasses, a similar early duplication of genes as that seen in *ELF3* is visible, and many of the genes have been retained (Figure 4.17). Throughout the tree, the '*-like*' suffix is used for monocot, *Amborella,* and *Selaginella* genes, and the *ZTL, LKP2,* and *FKF1* names are preferentially used over the *ADAGIO* names.

Brachypodium and rice each have two *ZTL-Like (ZLL)* genes, one each from the early duplication. *Sorghum* and *Setaria* also have two evenly divided among the branches, while maize has four, two copies per branch. Each of the maize pairs represents both paralogs, meaning that this is one of the few maize gene groups in which all duplicates are present. One of the maize genes, *zll4,* is quite short. It appears to be a part of a larger gene from expression data, but as with the short *GI* paralog in soybean, it is in a region where many small genes are annotated. This makes it difficult to determine what exactly is happening, but it is on the fractionating maize subgenome 2. *The LKP2* gene group only consists of Arabidopsis and *Brassica rapa,* making this another gene group in which Arabidopsis is an outlier.

The two pairs of *zll* paralogs each have one gene that no longer appears to be expressed, namely *zll1* and *zll4* (Figure 4.3.H). *zll3* is the most highly expressed of all of them, and is expressed throughout the day, with peak expression soon after dawn. *zll2* is also expressed throughout the day, but peaks at dusk. The *Sorghum* ortholog of *zll3* peaks at the same time and is expressed at approximately the same level (Figure 4.4.L). The *Setaria* ortholog, on the other hand, has lower peaks that are shifted six hours earlier, and longer trough times. The orthologs of *zll1* and *zll2* are more similar to each other than to the maize genes, although they are also expressed throughout the day (Figure 4.4.K). Both peak around midnight rather than at dusk. The *Sorghum* ortholog of *zll3* peaks at the same time and is expressed at approximately the same level. The *Setaria* ortholog, on the other hand, has lower peaks that are shifted six hours earlier, and longer trough times.

Maize has two *FFL* genes, *GRMZM2G107945* (*ffl1*) and *GRMZM2G10636* (*ffl2*), which are paralogs of each other. This seems to be unique among the grasses, as none of the others have more than one *FFL* gene. Dicot species also have two or less, and *Brassica rapa* has none. Both *ffl1* and *ffl2* peak in the mid-afternoon, and otherwise have very similar expression patterns (Figure 4.3.I). *ffl2* is more highly expressed at peak times even though it is located on maize subgenome 2. The *Sorghum ffl* ortholog has identical expression patterns and levels to *fll1,* while the *Setaria ffl* peak is slightly higher than all the rest (Figure 4.4.L).

All of the ZLL proteins contain some of the domains found in Arabidopsis ZTL (Tables 4.1 and 4.3). ZLL2 appears the most similar, as it has the same number and order of Kelch repeats. Of the others, ZLL3 also appears similar, yet has an extra Kelch repeat. The ZLL1 protein is both shorter than the other two, has a different Kelch repeat, and seems to lack the PAS domain, perhaps indicating an incomplete gene model. Finally, ZLL4 appears to consist of a single Kelch repeat and therefore either is a

misannotated or fragmented gene. Both FFL proteins contain all the domains of FKF1 and appear complete.

RNA-Seq reveals the diel expression patterns of grass genes

In order to characterize the expression patterns of grass genes under diurnal conditions, we did a RNA-Seq timecourse experiment. This experiment was done to figure out multiple questions, including whether the types of genes under maize circadian control are different from those under circadian control in close relatives of maize. The data allows comparison of rhythmic behavior between orthologs, and could provide the basis for predicting circadian regulatory networks. Reference lines for each grass species were chosen; B73 for *Zea mays,* BTx623 for *Sorghum bicolor,* and Yugu1 for *Setaria italica.* We chose day-neutral LD conditions (12 hour light, 12 hours dark) with warm-cool cycles, because all three species grow well under these conditions.

RNA-Seq rhythmic analysis

As well as being used to obtain expression information for all of the maize genes of interest, the RNA-Seq dataset was used to analyze phase, period, and amplitude. Period estimates for genes in each of the filtered datasets were quite similar, with most genes having an estimated period of 24 hours. The next largest bin for each was 27 hours, and this was similar across all three species (Figure 4.18).

After all periods were adjusted to 24 hours, the phase bins for each species were graphed. Of genes with diel rhythmic expression, most showed peak expression in the evening for all three species. *Setaria* had no clearly predominant phase bins, while *Sorghum* had a few, and maize had about five (Figure 4.19). It is unclear whether this indicates differences in circadian system organization between the species or is an effect of the analysis method.

Overall, maize had 38.7% rhythmic genes, *Sorghum* had 60.25%, and *Setaria* had 52.8%. These percentages are all within the ranges of those reported in other species. The somewhat higher percentages seen in *Sorghum* and *Setaria* may indicate that these species are more responsive to diurnal cues than maize.

When the phase information is grouped by orthology, it can be seen that there are only a few cases in which the same phase is estimated across all genes in all species (Table 4.4). Most of the phase difference estimates are, however, quite small. Comparison to the expression graphs shows many cases in which peaks are apparently uniform between species, but phase differences are called. This is likely in part due to differences in peak shape, as can be seen clearly in the *t1l1/2* graph (Figure 4.3.C), but may also indicate the algorithm is problematic. Nevertheless, those graphs that showed clear visual differences between peak timing are called as having different phases, such as *re7l3/4* and *zll3/4*.

The *lyl* genes illustrate one of the issues that misannotated genes can cause: one half of *lyl1* (*GRMZM2G474769*) was called as having a phase of 1.5, while the other half (*GRMZM2G175265*) has a phase of 0 despite appearing to have the same peak timing on the expression graph. Depending on which gene is used, the orthologs therefore either appear to have the same phase or to be shifted. The two *Setaria* orthologs (*Si013398m* and *Si014685m*) both have a phase of 0, perhaps because their expression patterns are almost identical where the *t1l1* expression patterns differ slightly.

Discussion

As demonstrated here, the *lyl* genes, the *re6l* genes, most *prr-like* genes, the *gi* genes, the *ef3l* genes, the *lxl* gene, and some *zll* genes are likely to be active in the maize circadian clock. While some of the other gene groups may also play roles within the clock, they are either expressed differently than their Arabidopsis orthologs or evolutionarily distant from them. Of the gene groups with multiple copies, often more than one have rhythmic expression over a 24 hour period, as well as having the same protein domains as the Arabidopsis protein. It is likely that the characteristics and regulatory relationships of maize core clock genes and proteins are similar to those seen in Arabidopsis, and where multiple copies are present, that they all have similar roles. The genes with less essential roles likely differ between species. These findings illustrate the utility inherent to characterizing the clock in more than one species: multiple functional copies could allow more accurate differentiation of input signals or specialized regulation of output control. Moreover, those genes with limited function in the clock of one species are unlikely to have conserved functions across species boundaries.

The *LHY* tree shows that duplicates of this gene are present in many species, but the duplicate lineage named *CCA1* is unique to the *Brassicaceae.* Many core oscillator studies in Arabidopsis have focused on *CCA1* over its partially redundant homolog *LHY,* and so *LHY* function remains under-characterized. *CCA1* is, however, a *LHY* duplicate, which could mean that the partial redundancy seen in Arabidopsis is present in other species when multiple *LHY*s are present. The expression of the *lyl* genes is similar to the Arabidopsis *LHY* expression pattern, which provides one line of evidence indicating that these genes have comparable functions within the circadian clock. Arabidopsis *LHY*, however, peaks at dawn like the *Setaria* and *Sorghum* orthologs (Flis et al., 2015). This could indicate a difference in regulation has evolved in maize, or be linked to the differential response to day length or light signals likely present across the grasses. Another line of evidence linking the *lyl* genes to the maize circadian clock is seen when *gi1* mutants are grown in constant light conditions: both *lyl1* and *lyl2* have altered expression patterns (Chapter Two).

Of the many *RVE*s, only *RVE8, RVE6,* and *RVE4* are considered principal clock activators in Arabidopsis (Chaudhury et al., 1999; Kuno et al., 2003; Rawat et al., 2009, 2011; Zhang et al., 2007). They appear to act partially redundantly, with only the triple mutant having a significantly longer phase than wild type plants (Hsu et al., 2013). In maize, only one of these groups is a viable component of the circadian clock, namely the *re6l* genes. *RVE4* is specific to *Brassicaceae,* and both maize *re8l* genes are not rhythmic. The *re6l* genes have expression patterns similar to those described for *AtRVE8,* with peaks at dawn. In addition, *re6l5* represents one of only a few cases found here where the gene on maize subgenome 2 is more highly expressed than its paralog on maize subgenome 1: the other two cases are *gi1* and *zll2*. Two other gene groups, *re2l* and *re7l,* have multiple rhythmic genes. This could indicate that these genes are involved in the clock in monocots.

In terms of tree building, the larger RVE/LHY protein tree has the least bootstrap support. Multiple branches have values under 50 associated with their nodes, indicating they are likely wrong. This explains the appearance of the overall tree too, with each group diverging from the next, and few clearly related groups (Supplemental Figure

4.2.A). There are only three nodes with reasonable bootstrap support: the node between the RE8L group and the RVE1 group (70%), the node between the RVE2 group and the LHY/LYL group (67%), and the split between the dicots and monocots within the LHY/LYL group (97%). Many of the branches at the ends of the groups are well supported, but the otherwise low values indicate the uncertainty of the overall topology of this gene tree.

The *PRR* tree shows the early divergence of the *TOC1* genes, and the subsequent split between the *PRR3/7* clade and the *PRR5/9* clade (Supplemental Figure 4.2.B). Maize appears to be unique in having not only two *TOC1-like* genes similar to other *TOC1*s, but also four more divergent genes. The *t1l1* and *t1l2* genes may be active within the circadian clock, but the function of the more divergent genes will need to be determined experimentally because there are no orthologs of these genes in other species. Both *t1l1* and *til2* have altered expression patterns in *gi1* mutants grown in constant light, which may indicate they are involved in the maize circadian clock (Chapter Two). The T1L1 and T1L2 proteins have the same domains as Arabidopsis TOC1.

As well as these genes, maize also has many other *PRR* genes, almost all of which are rhythmically expressed and appear to be functional. Those *prr-like* genes that correspond to the ones active within the Arabidopsis and rice clocks show similar sequential expression peaks. Expression of the *p73l* gene is altered in *gi* mutants grown under constant light conditions, indicating this gene may play a role in the maize circadian clock (Chapter Two). The expression patterns of the *prr59l* genes and their orthologs suggest the intriguing possibility that peak and trough expression phases are under separate control. Perhaps the maize gene duplication allowed these forms of control to be applied to two separate genes.

The *GOLDEN2-LIKE1* (*GLK1)* and *GOLDEN2-LIKE2* (*GLK2*) clade is nestled within the clade containing *PRR4* and *PRR2* (Supplemental Figure 4.2.B). It was omitted from the *PRR* tree to improve clarity, but provides a further indicator of the importance of this clade that is often overlooked in circadian contexts. *GLK1* and *GLK2* are highly conserved transcription factors that regulate chloroplast development and chlorophyll (Yasumura et al., 2005). The two genes act partially redundantly in C3 plants, spatially distinctly in C4 plants, and integrate external and internal signals (Wang et al., 2013). Previous phylogenies have shown their close relation to *RR* genes (Yasumura et al., 2005), but the relationship with clock components has not been further investigated. A recent study characterizing transcriptome dynamics in developing maize leaves showed that expression levels of both maize *GLK1* and *GLK2* are modulated by light and dark (Yu et al., 2015), while a tomato study showed that *GLK*s played a role in fruit ripening (Nguyen et al., 2014). While neither of these studies directly links *GLK*s to the circadian clock, they suggest that members of this gene family act to regulate development in response to environmental conditions.

The *ELF3* tree shows that duplication is a common theme throughout evolution, and two, three, or even five copies can be retained. In fact, only Arabidopsis (Hicks et al., 2001), poplar (Keller et al., 2012), *Amborella,* and *Brachypodium* have a single *ELF3* copy. Three out of these four species have been chosen as models for biological study, and at least this small sample would suggest that their lone *ELF3*s are the exception rather than the rule.

There are two *elf3-like* genes in maize, both of which have lost their paralogs. The expression patterns of these genes are quite irregular in comparison to other circadian genes, but actually *AtELF3* has a similarly odd pattern (Flis et al., 2015). The different peak times of *ef3l1* and *ef3l2* may indicate that after the early duplication of the *ef3l* genes in grasses the regulatory control of the genes evolved in different directions. On the basis of expression pattern and evolutionary relationship, *ef3l1* appears to be the more likely candidate for a circadian gene. On the basis of protein interactions, however, EF3L2 is the more likely candidate, because it had a clearer interaction with GI1 and GI2 (Chapter Three).

The *ELF4* tree indicates there are no true *ELF4* genes in grasses. It is unclear to what extent other genes within the clade are involved in the Arabidopsis clock, so making predictions about what this would mean for evening complex formation is difficult. None of the maize *ef4r* genes display expression patterns similar to Arabidopsis *ELF4,* although a couple of the orthologs in *Sorghum* and *Setaria* have the same well-defined peaks (Flis et al., 2015). The *ef4r3* and *ef4r4* genes are the two most closely related to Arabidopsis *ELF4*, and show some rhythmicity, so perhaps these are the two most similar in function. The EF4R2 protein was tested for interaction with the GI1 and GI2 proteins, and showed moderate interaction with the N-terminal domain of GI1 (Chapter Three). In the EF4R and EF4L2/3/4 protein subtree (Figure 4.15), there are branches with low bootstrap support, indicating these relationships are unresolved.

All of the *LUX* genes are considered members of the larger *RR-PRR* gene family by the Gramene Plant Compara function. This is interesting for two reasons: firstly, because this link is not one that is often discussed, and secondly, because there are many similar looking genes that are not actually members of the smaller *LUX* clade. Previously published papers on *LUX* in other species have stated there are many more copies of *LUX* in maize (Campoli et al., 2013) in part for this reason. In terms of expression, all of the *lxl* genes show quite similar patterns to Arabidopsis *LUX* (Flis et al., 2015).

There appear to be two functional *zll* genes in maize, as well as two functional *ffl* genes. All of these genes have rhythmic expression patterns, which is unlike Arabidopsis *ZTL,* but similar to *ZTL* genes studied in cedar. In protein interaction tests, ZLL3 was shown to be a strong interaction partner with GI1 and GI2 (Chapter Three). It is tempting to speculate that this strength might be due to the additional Kelch repeat, as interactions with AtZTL were less strong. The *zll3* gene is also the most highly expressed of the *zll* genes.

The tree was trimmed of the most closely related clade of genes for greater clarity, much as the *PRR* tree was trimmed. This clade consists of F-box genes, in dicots called *FBK21* and in non-dicots here designated *F21L* (Figure 4.20). The split between this clade and the clade containing *ZTL*, *LKP2*, and *FKF1* is an ancient one, as *Selaginalla* contains one of each gene type. There is one *f21l* gene in maize, *GRMZM2G121096*.

Early analysis of phase differences among maize, *Setaria,* and *Sorghum* indicates that, in many cases, the rhythmic expression of orthologous clock genes are similarly phased. When there are differences, the shifts in phase are minor (shifted by less than two hours towards dawn or dusk. Larger phase differences among orthologs

were often seen in genes that are less well studied and characterized, such as the *re7l* genes.

One possibility is that these less studied genes play ancillary roles in the circadian clock, allowing them to evolve different expression patterns without causing disruption to circadian clock function. Another possibility is that the phase shifts observed for some of these genes are adaptive, and reflect the different growth habits and domestication history of each species. Whereas many functional studies have focused on the highly conserved clock components across species, investigations of these genes that have evolved different expression patterns could yield exciting new discoveries about the role of the circadian clock in plant environmental adaptation and domestication.

Materials and Methods

Creation of protein lists and tree building

Protein lists were created using NCBI protein BLAST (BLASTp) default settings and the Gramene (ensemble.gramene.org) Plant Compara function. The *Arabidopsis* clock proteins were used as starting points for BLASTp (Table 4.1), and non-redundant protein sequences of the target species were chosen as the search set. The top BLASTp results by coverage and e-value were chosen, and the protein sequence was obtained from UniProt. Where there was no UniProt listing, the gene was identified in Gramene using the chromosomal location provided by the GeneID listing.

As well as further BLASTp searches, the Gramene Plant Compara function was used to find within-species paralogs and between species orthologs. Although the ortholog search was not always thorough between monocots and dicots, it provided a starting point and means to verify BLASTp results. The paralog function was used to find other members of the family within species, and often identified genes BLASTp did not. This was especially helpful for the two larger trees (Supplemental Figure 4.2.A, B). Throughout, the Gramene gene name was used to identify sequences for consistency.

For maize genes that were already known to be misannotated from previous studies, a more complete sequence was used to build the tree. Where possible, this sequence was constructed from translated mRNA.

Once a protein list was made, it was aligned using the MAFFT online tool (mafft.cbrc.jp/alignment/server) set to G-INS-1 (progressive method with an accurate guide tree) with an Unalignlevel = 0.4. These settings were chosen because of the evolutionary distance between the protein sequences, although the Auto method produced similar results.

The MAFFT online tool was then used to build an average linkage (UPGMA) tree, which was viewed using Archaeopteryx. On the basis of this tree, the protein list was iteratively refined. For example, the PRR protein list originally also contained RR proteins, as the PRR clades fall within the larger RR protein family. Using the UPGMA tree as a guide, proteins that fell within RR clades could be removed. As many of the proteins were either unannotated or only annotated with their protein motifs, this procedure allowed accurate selection, which would otherwise not have been possible. Then another alignment was made and another tree built to check where the remaining proteins dell, and this was done repeatedly until the protein list only contained the proteins of interest.

In order to build a tree, the FASTA-formatted alignment from the MAFFT online tool was then analyzed using the CIPRES server to run RAxML-HPC BlackBox (embnet.vital-it.ch/raxml-bb/). The options chosen were protein sequence type, no estimate of proportion of invariable sites, JTT protein substitution matrix, no use of empirical base frequencies, fund best tree using maximum likelihood search, and let RAxML halt bootstrapping automatically. The first tree shown is from the output 'Best Tree' file, which was edited using Mesquite to display branches proportional to their length, and to list branch lengths on the tree. All branch lengths were scaled by multiplying by 100. Note that these branch lengths represent amino acid changes rather than evolutionary distance. The second tree shown is from the output 'Bipartitions' file, and bootstrap values shown are percentage support from 1000 rapid bootstrap inferences.

Despite best efforts to obtain a complete list of unique genes, it is possible that some gene copies have been missed or that duplicate genes may still be present. The methods used were not exhaustive, and more importantly, genome assembly is continually evolving. The species represented on trees were chosen for the quality of their genome sequencing and annotation, but with every new genome release come alterations. In some cases, the RAxML tree revealed highly similar copies (short branch length, polytomous branching), which were compared by protein BLAST, and if alignment scores were >=200 and identity was over 95%, were removed. In these cases, the tree was edited to remove that branch in Mesquite, and the other gene annotation was added to the remaining gene left on the tree. This was particularly the case with the *Selaginella* genes, as often two copies were found when the literature stated one was present (Satbhai et al., 2011). It is unclear whether these two copies are protein isoforms, mis-assembled, or in fact true extra copies, but in any case the extra copies were removed for greater visual clarity.

Naming maize genes and finding protein domains

Genes were named according to maize nomenclature rules, which specify that maize genes have lower-case names and paralogs are denoted with numbers (see http://www.maizegdb.org/nomenclature). Genes located on maize subgenome 1 were numbered as 1, and genes located on subgenome 2 were numbered as 2. The *gi* genes are an exception to this, as they had already been published. Where direct paralogs were not present, genes were numbered sequentially. In addition to this, previous naming conventions were upheld. For example, monocot *PRR*s are named *PRR37* or *PRR73* instead of *PRR3* and *PRR7* (Murakami et al., 2003). Previous working names of genes as well as their subgenome are listed in Table 4.5. Protein domains were checked using the Prosite (prosite.expasy.org) and Pfam (pfam.xfam.org) websites.

RNA-Seq Experiment

For the RNA-Seq experiment, reference lines for each grass species were chosen; B73 for *Zea mays,* BTx623 for *Sorghum bicolor,* and Yugu1 for *Setaria italica.* Plants were grown in day neutral LD conditions, with 12 hours of light and 12 hours of dark. A walk-in growth chamber was used that provided white light at about 440 µmol photosynthetically active radiation (PAR) m^{-1} s^{-1} at shelf level and about 698 µmol PAR m^{-1} s^{-1} at top height of B73 plants. As B73 plants were 2-3 times the height of BTx623

and Yugu1, they received greater light intensity. Daytime temperatures were between 26°C and 28°C (depending on shelf) and nighttime temperatures were 22 °C.

Samples were taken every 3 hours over 72 hours. Each sample consisted of a pool of 4 (B73, Yugu1) or 2 (BTx623) entire fully expanded third leaves. The difference in number was due to different germination efficiencies of seed stocks. Leaves were cut off with fresh razor blades for every timepoint and genotype, and only those plants were used that had fully expanded third leaves – any plants developmentally behind were omitted. Different plants were used at every timepoint. Once leaves were harvested, they were wrapped in aluminum foil and immediately frozen in liquid nitrogen.

Frozen leaf samples were then hand-ground with a pre-chilled mortar and pestle. Ground samples were then quickly distributed into two separate 1.5ml microcentrifuge tubes, with approximately 500 µl of B73 tissue per tube and approximately 250 µl for both other genotypes. Tubes were immediately placed on dry ice. Total RNA was purified with TRIzol using a modified version of the manufacturer's recommendations.

Once purified, RNA was NanoDropped to determine concentration and purity. If samples were found to have A_{260nm}/A_{230nm} values under 1.9, they were precipitated using both 3M sodium acetate and ethanol. For those samples where both extractions had concentrations below 400 ng, the two separate extractions were pooled before precipitation. RT-qPCR was performed on putative maize circadian genes using the B73 samples as described in Chapter Two to test expression patterns and levels. RT-qPCR traces were rhythmic across all three days, with no uneven oscillations or outlier samples, and so RNA was packaged and sent to the Schnable lab.

RNA library preparation was done in the Schnable lab according to the published protocol from the Brutnell lab (Wang et al., 2011a). Libraries were multiplexed, and half were sent to Cornell for sequencing, half to UC Davis. Alignment of raw reads and FPKM calculation was done in the Schnable lab using GSNAP, SAMTOOLS, and CUFFLINKS (Li et al., 2009; Trapnell et al., 2010; Wu and Nacu, 2010). JTK-cycle analysis was done in the Harmon lab using the default settings(Hughes et al., 2010). Datasets were filtered and adjusted according to Hsu and Harmer (Hsu and Harmer, 2012). Genes with an amplitude of N/A were discarded, as they mostly had FPKM values of 0. Then, those genes were chosen that had estimated period values between 20-28 hours, and adjusted p-values that were less than 0.05. This rhythmic dataset was then adjusted to circadian time (CT) so that all period and phase values were within a 24-hour reference frame ((ZT phase/period)*24 = CT phase). This was done using the ratio of the estimated period to 24 hours.

Spreadsheets of paralogs generated by James Schnable and constructed trees were used to identify paralogs in *Sorghum* and *Setaria*, and then phase was identified from the rhythmic datasets described above. Where needed, Phytozome's tBLASTn tool was used to search the *Sorghum bicolor* v2.1 genome for the Sobic names of genes.

Figures

A

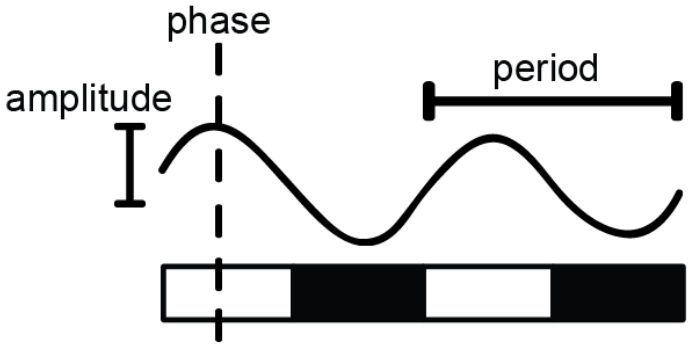

B

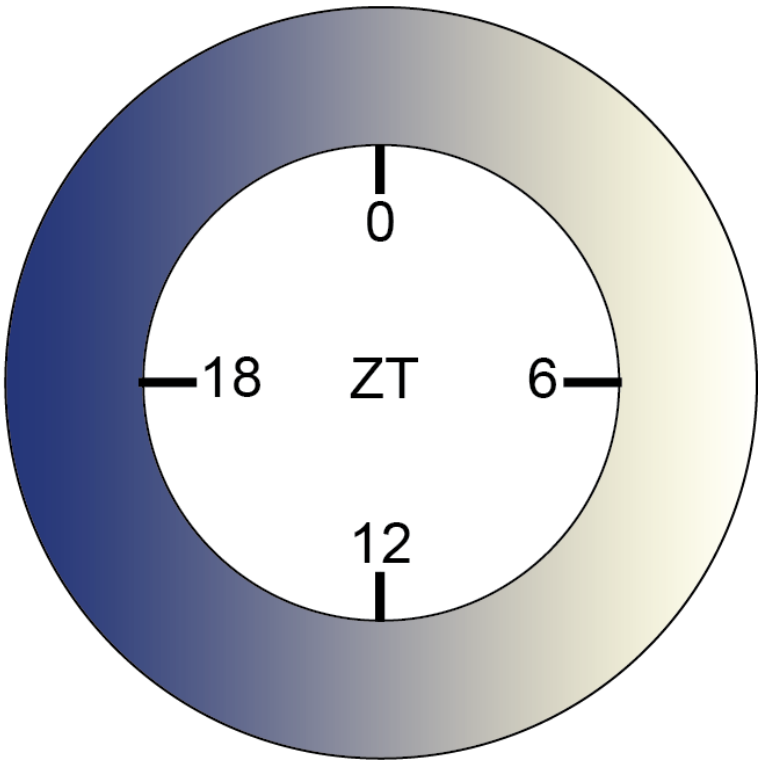

Figure 4.1. A) Period is the time in which one complete cycle occurs, phase is the time of day at which an event occurs, and amplitude is half the distance between the peak and the trough of the cycling output. **B)** Zeitgeber time (ZT) is used to denote the time at which an external stimulus provides the clock with information. Here, the entraining factor is light and a 12 hour day/12 hour night photoperiod is shown, so ZT0 = dawn and ZT12 = dusk. As the photoperiod changes, the ZT time referring to dusk also changes.

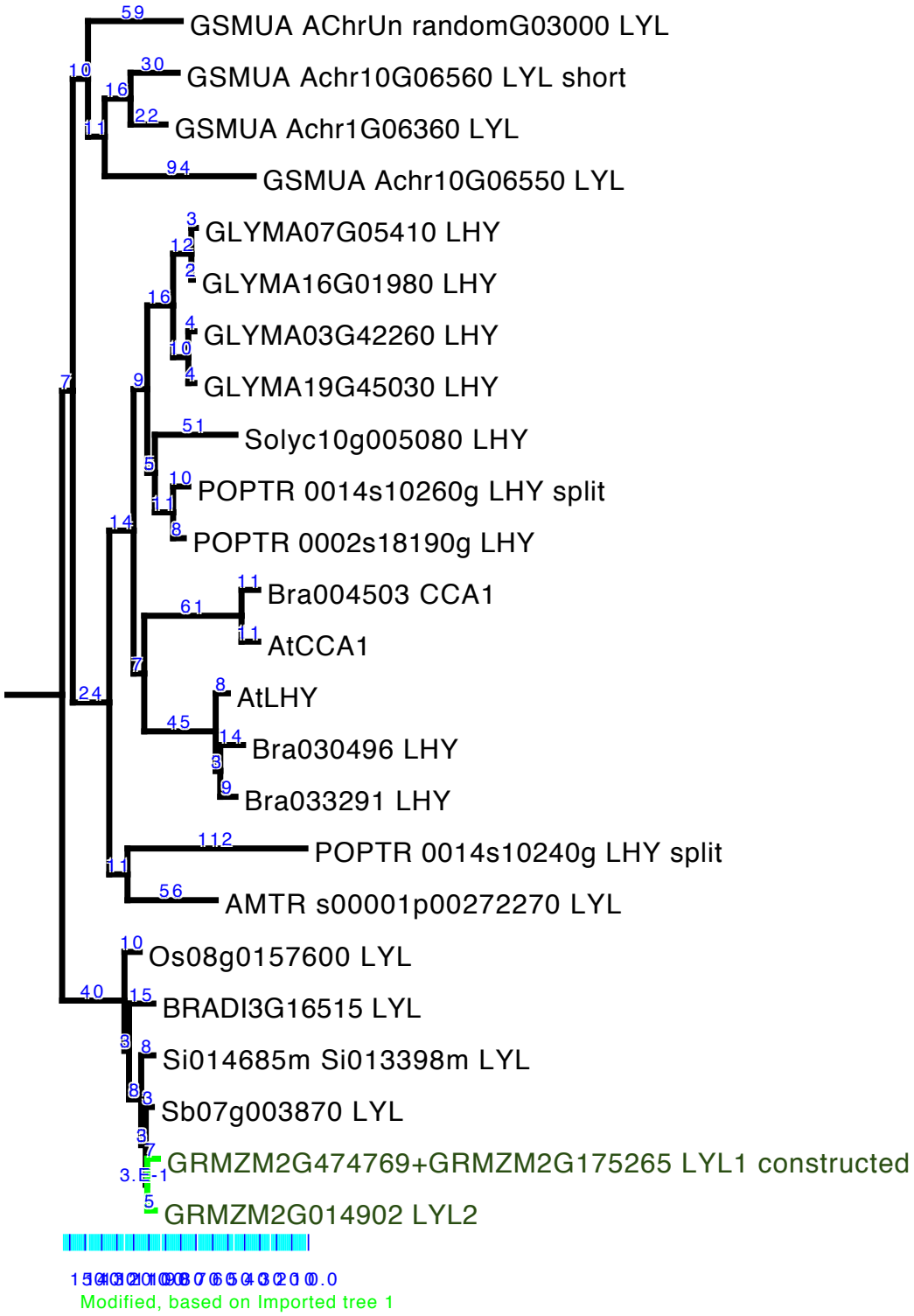
GSMUA AChrUn randomG03000 LYL
GSMUA Achr10G06560 LYL short
GSMUA Achr1G06360 LYL
GSMUA Achr10G06550 LYL
GLYMA07G05410 LHY
GLYMA16G01980 LHY
GLYMA03G42260 LHY
GLYMA19G45030 LHY
Solyc10g005080 LHY
POPTR 0014s10260g LHY split
POPTR 0002s18190g LHY
Bra004503 CCA1
AtCCA1
AtLHY
Bra030496 LHY
Bra033291 LHY
POPTR 0014s10240g LHY split
AMTR s00001p00272270 LYL
Os08g0157600 LYL
BRADI3G16515 LYL
Si014685m Si013398m LYL
Sb07g003870 LYL
GRMZM2G474769+GRMZM2G175265 LYL1 constructed
GRMZM2G014902 LYL2
Modified, based on Imported tree 1

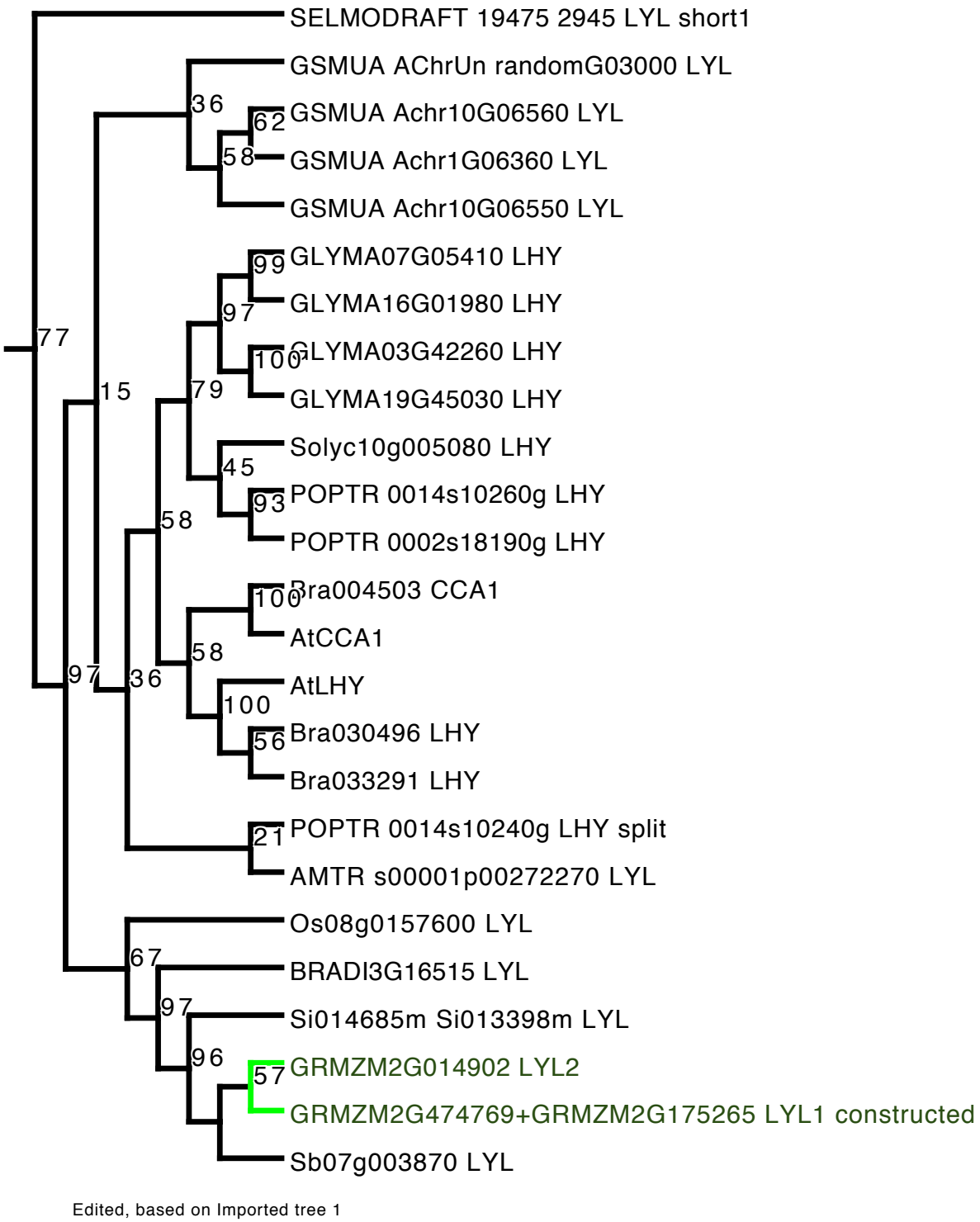

Figure 4.2 (this page and previous page). LHY protein subtree (see Supplemental Figure 4.2.A). Maize gene branches are highlighted in green, as are maize genes. On this page, numbers indicate percentage bootstrap values from 1000 rapid bootstrap inferences. On previous page, numbers indicate estimated branch lengths.

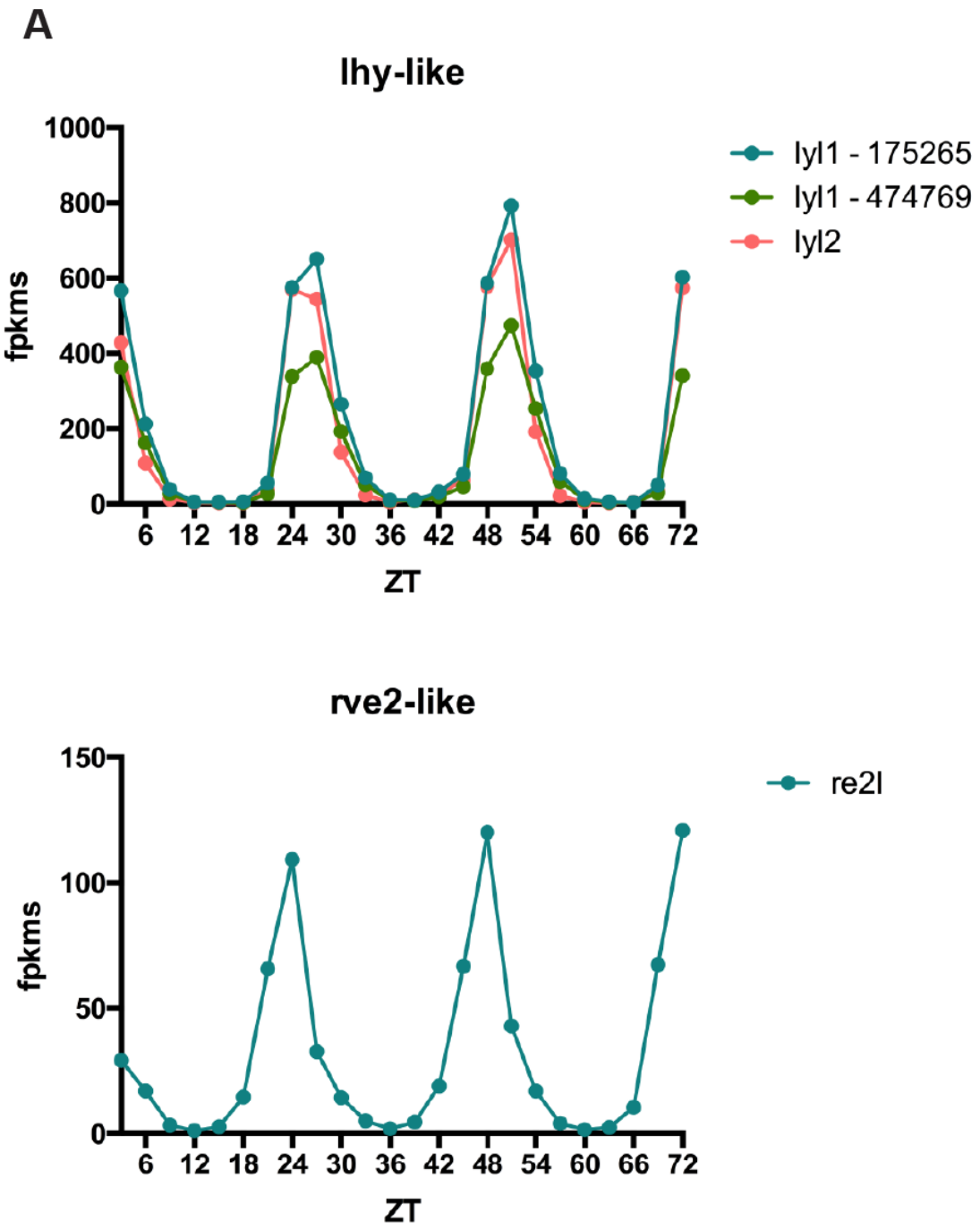

Figure 4.3. Expression levels of maize circadian clock and circadian-clock associated genes over the course of the RNA-Seq experiment. Coloring done sequentially rather than to denote paralogs, and in order of teal, fern, salmon, cayenne, ocean, and tangerine.

A) Expression levels of *lhy-like* (*lyl*) and *rve2-like* (*re2l*) genes.

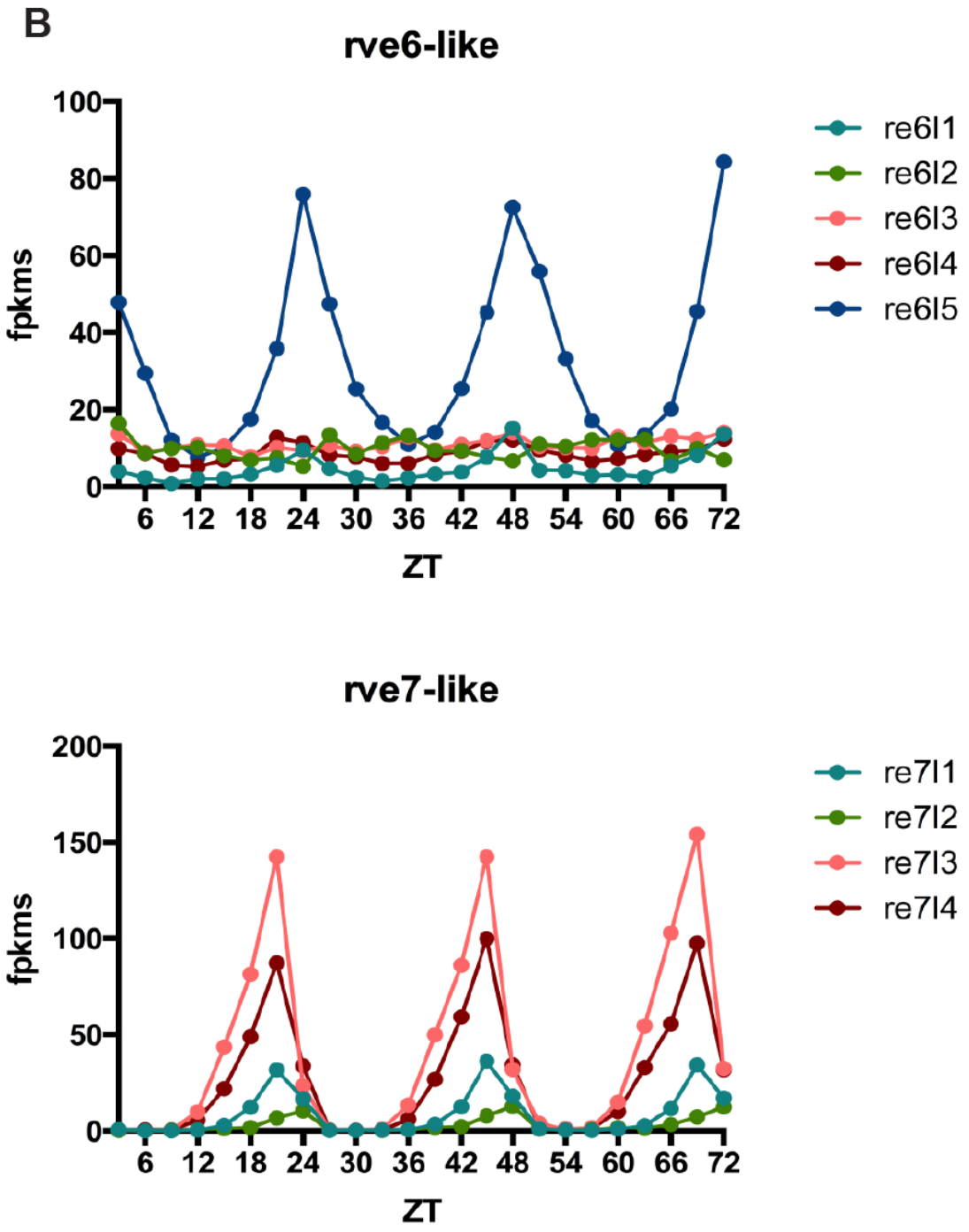

B) Expression levels of *rve6-like* (*re6l*) and *rve7-like* (*re7l*) genes.

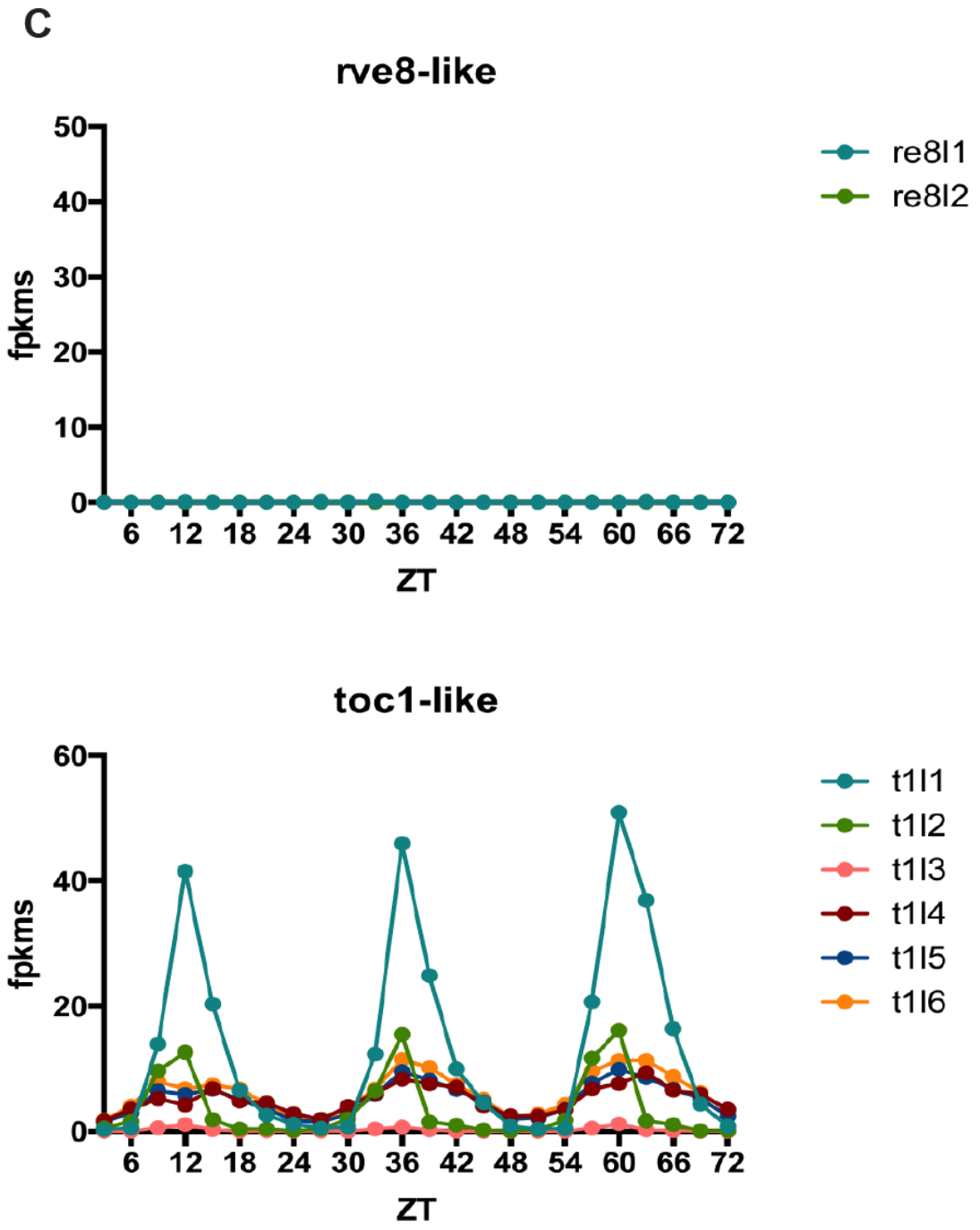

C) Expression levels of *rve8-like* (*re8l*) and *toc1-like* (*t1l*) genes.

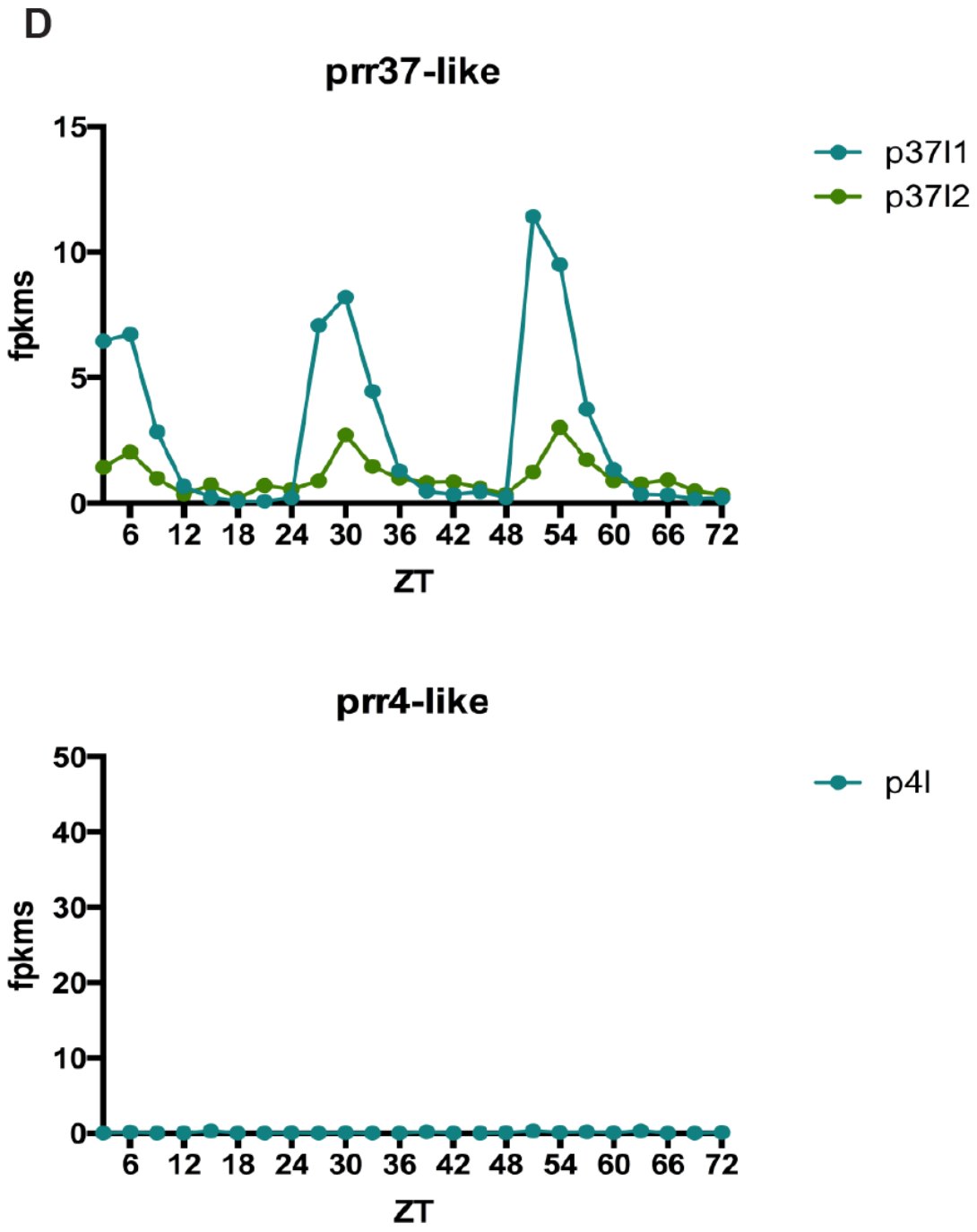

D) Expression levels of *prr37-like* (*p37l*) and *prr4-like* (*p4l*) genes.

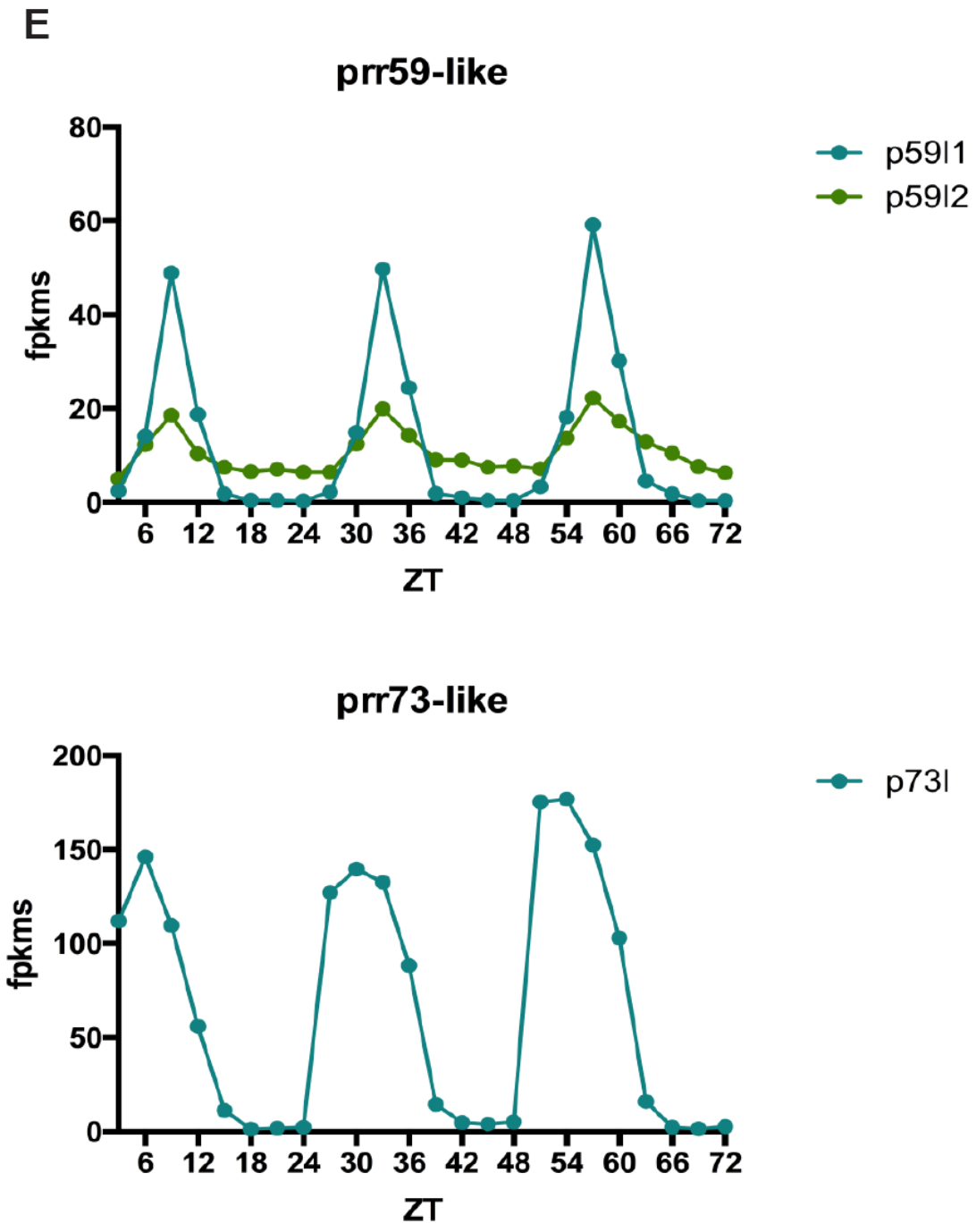

E) Expression levels of *prr59-like* (*p59l*) and *prr73-like* (*p73l*) genes.

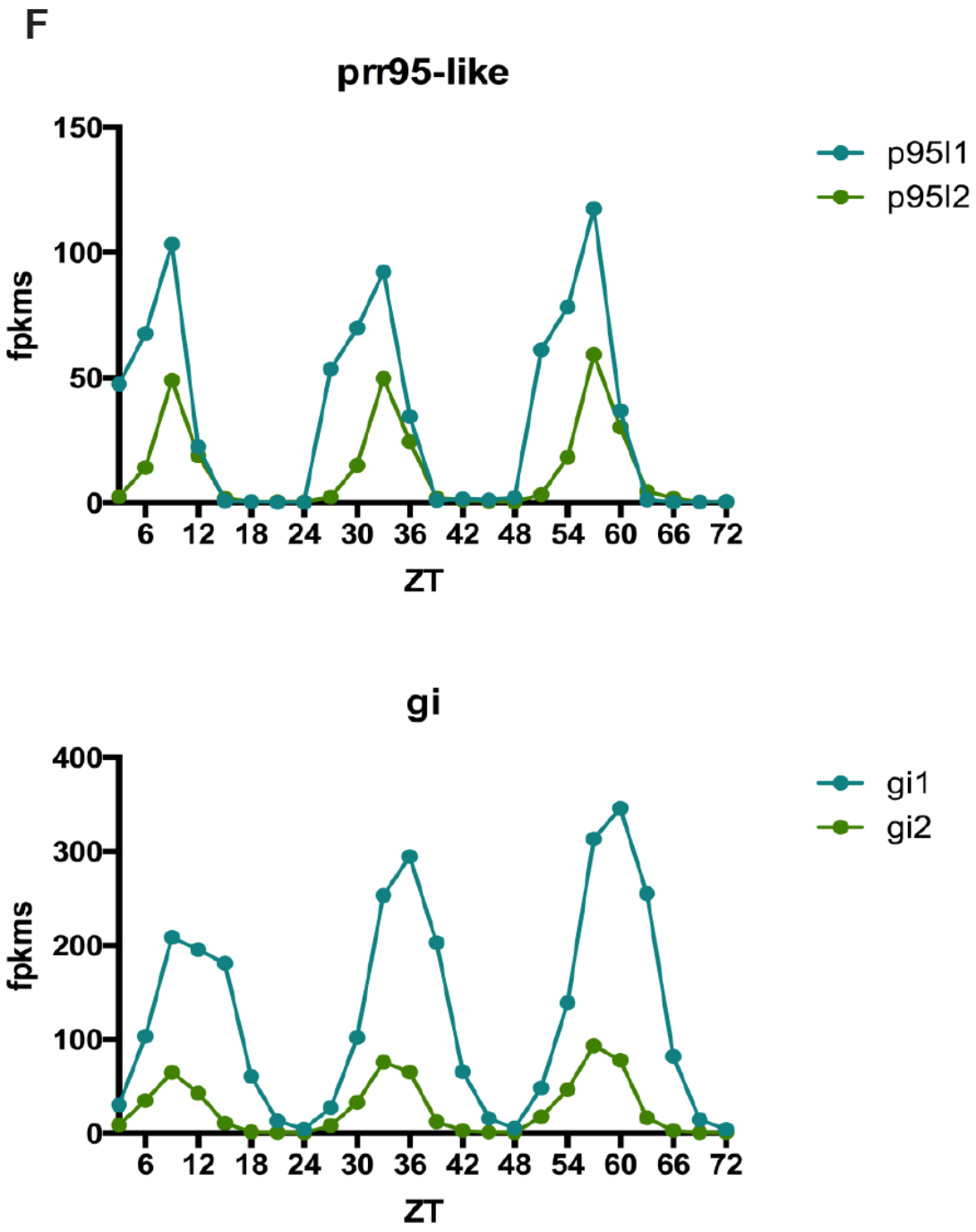

F) Expression levels of *prr95-like* (*p95l*) and *gigantea* (*gi*) genes.

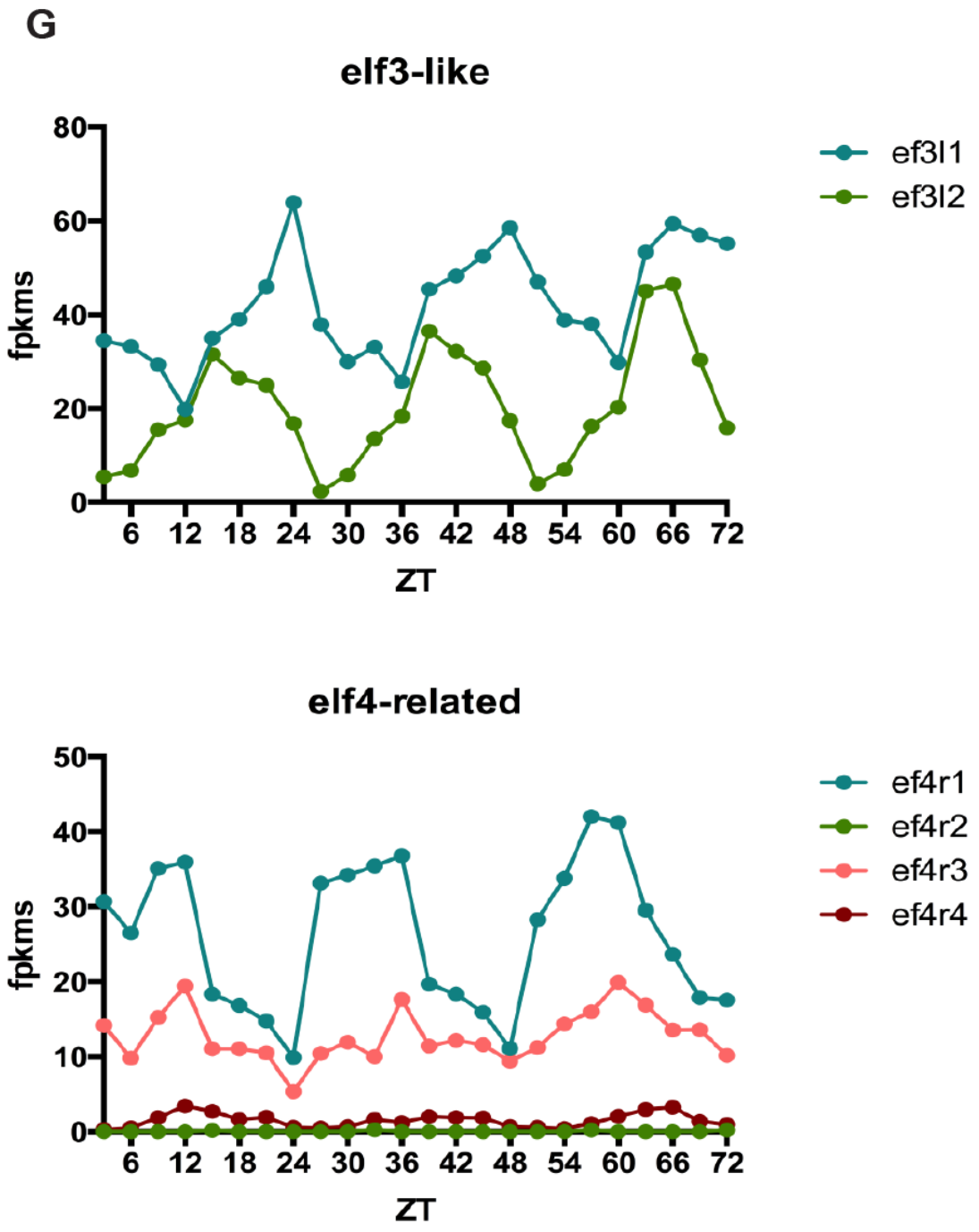

G) Expression levels of *elf3-like* (*ef3l*) and *elf4-related* (*ef4r*) genes.

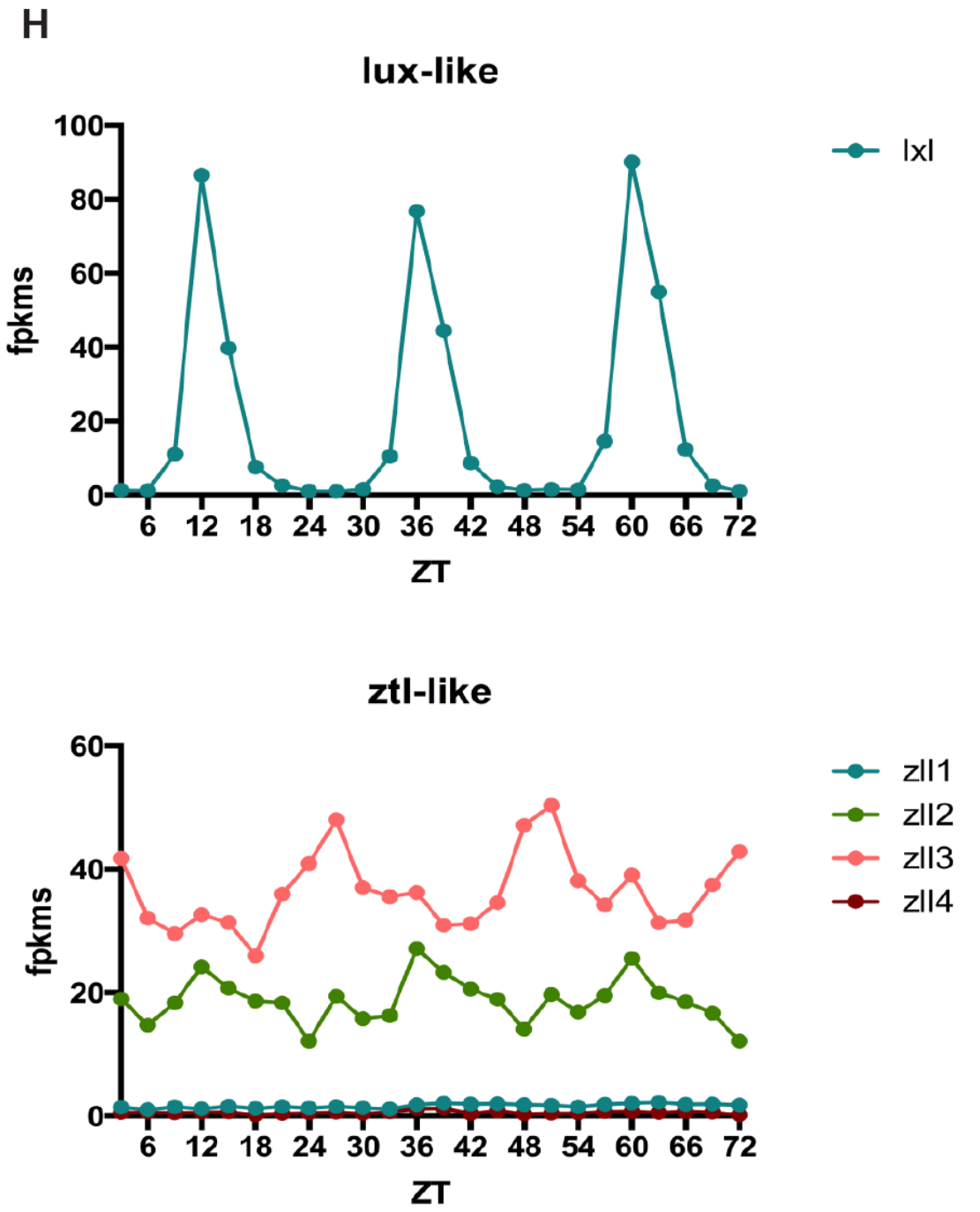

H) Expression levels of *lux-like* (*lxl*) and *ztl-like* (*zll*) genes.

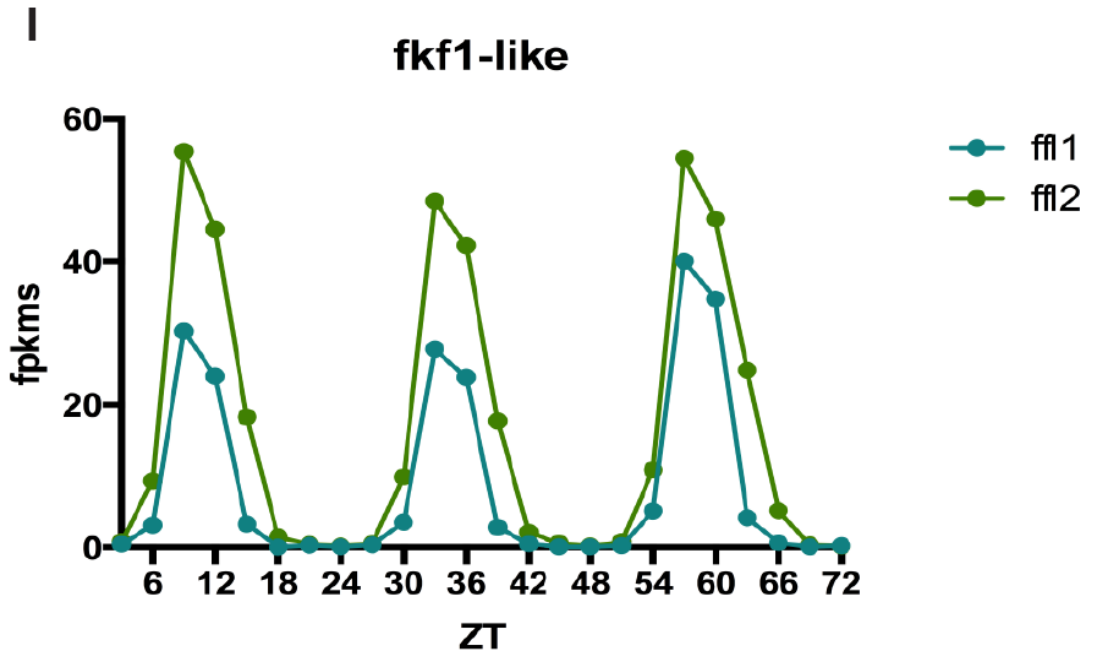

l) Expression levels of *fkf1-like* (*ffl*) genes.

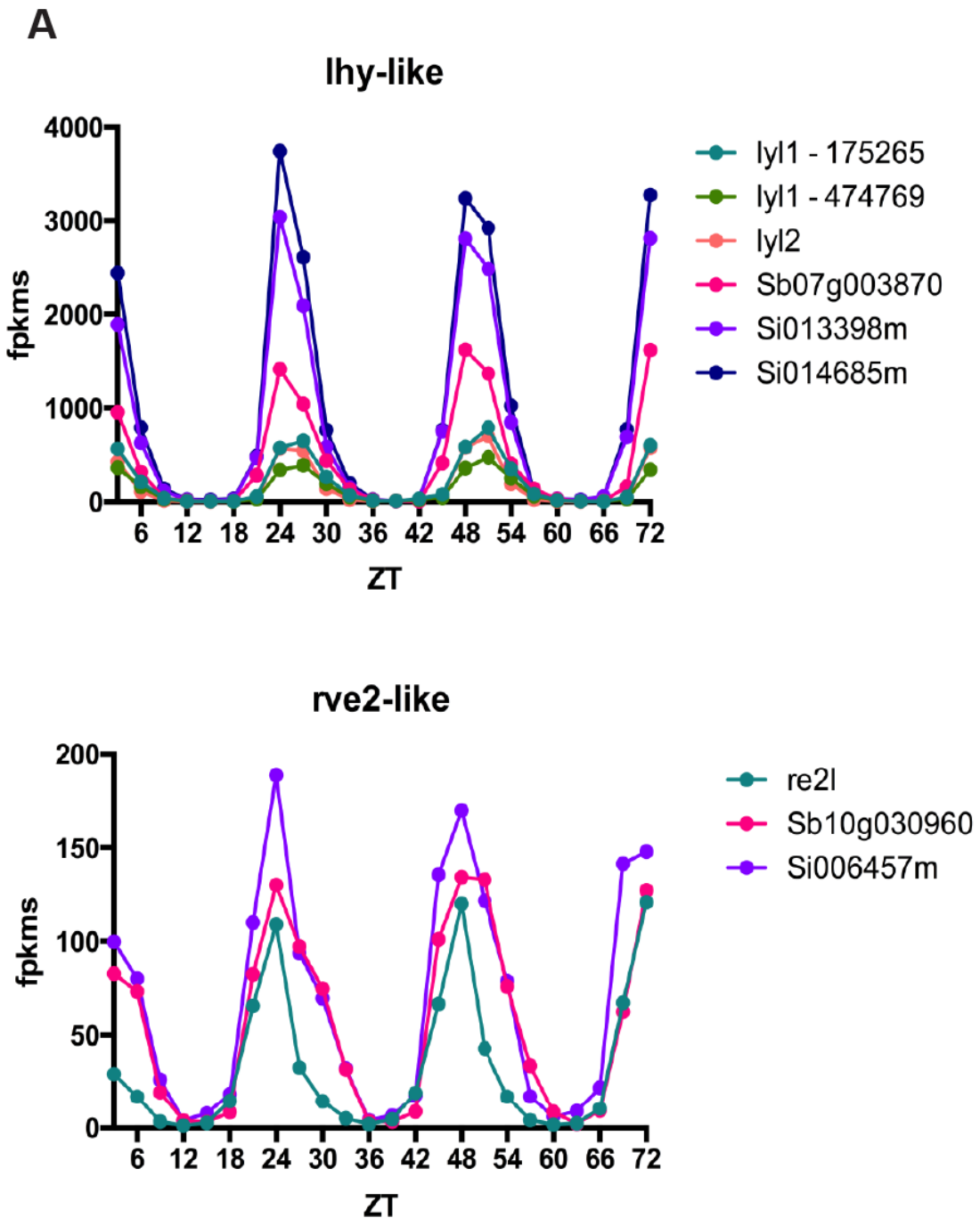

Figure 4.4. Expression levels of maize, *Sorghum,* and *Setaria* orthologs of circadian clock and circadian-clock associated genes over the course of the RNA-Seq experiment. Maize paralogs are colored teal, fern, and salmon, while *Sorghum* genes are strawberry, and *Setaria* genes are grape and midnight.

A) Expression levels of *lhy-like* (*lyl*) and *rve2-like* (*re2l*) genes.

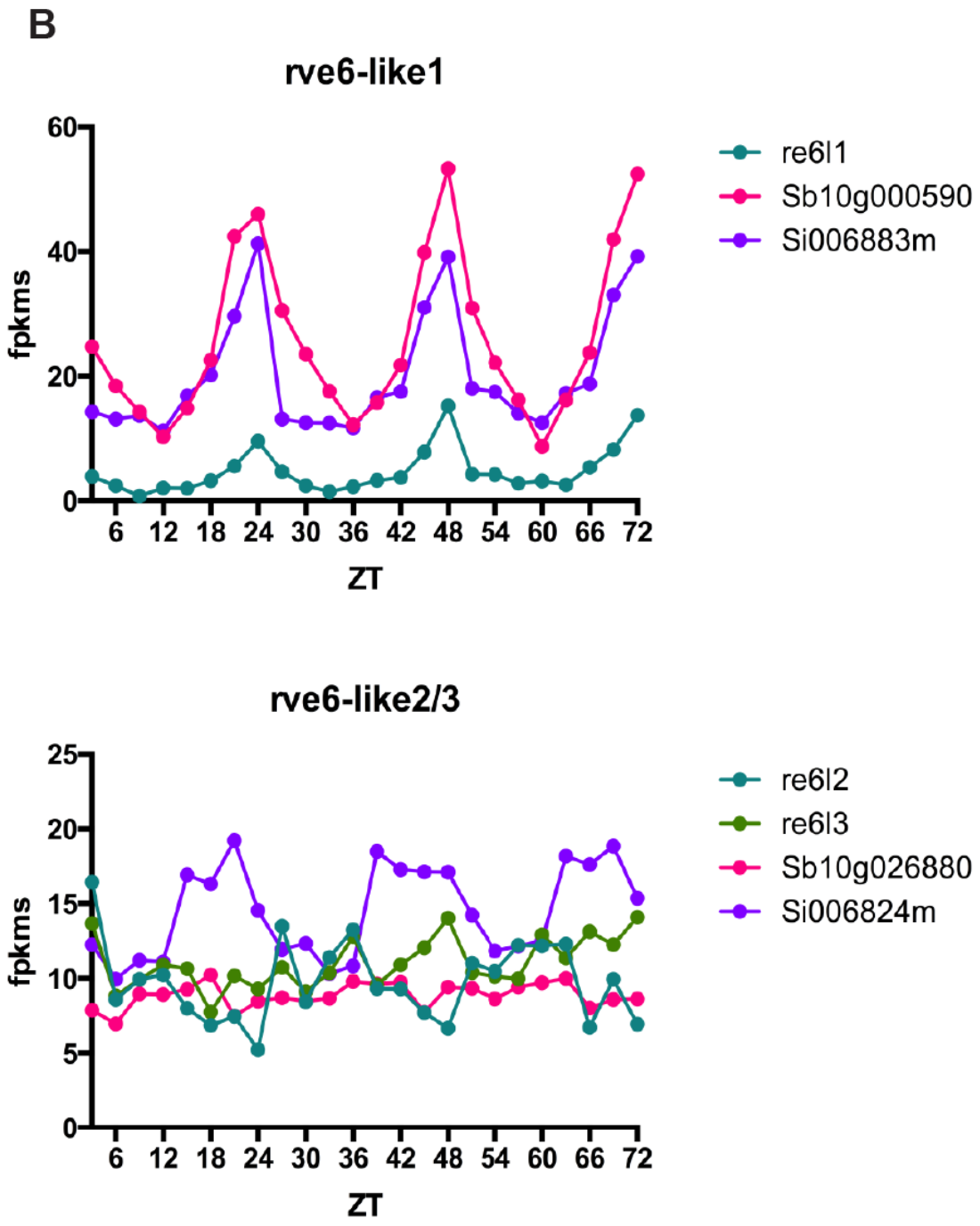

B) Expression levels of *rve6-like 1*(*re6l1*) and *rve6-like2/3* (*re6l2/3*) genes.

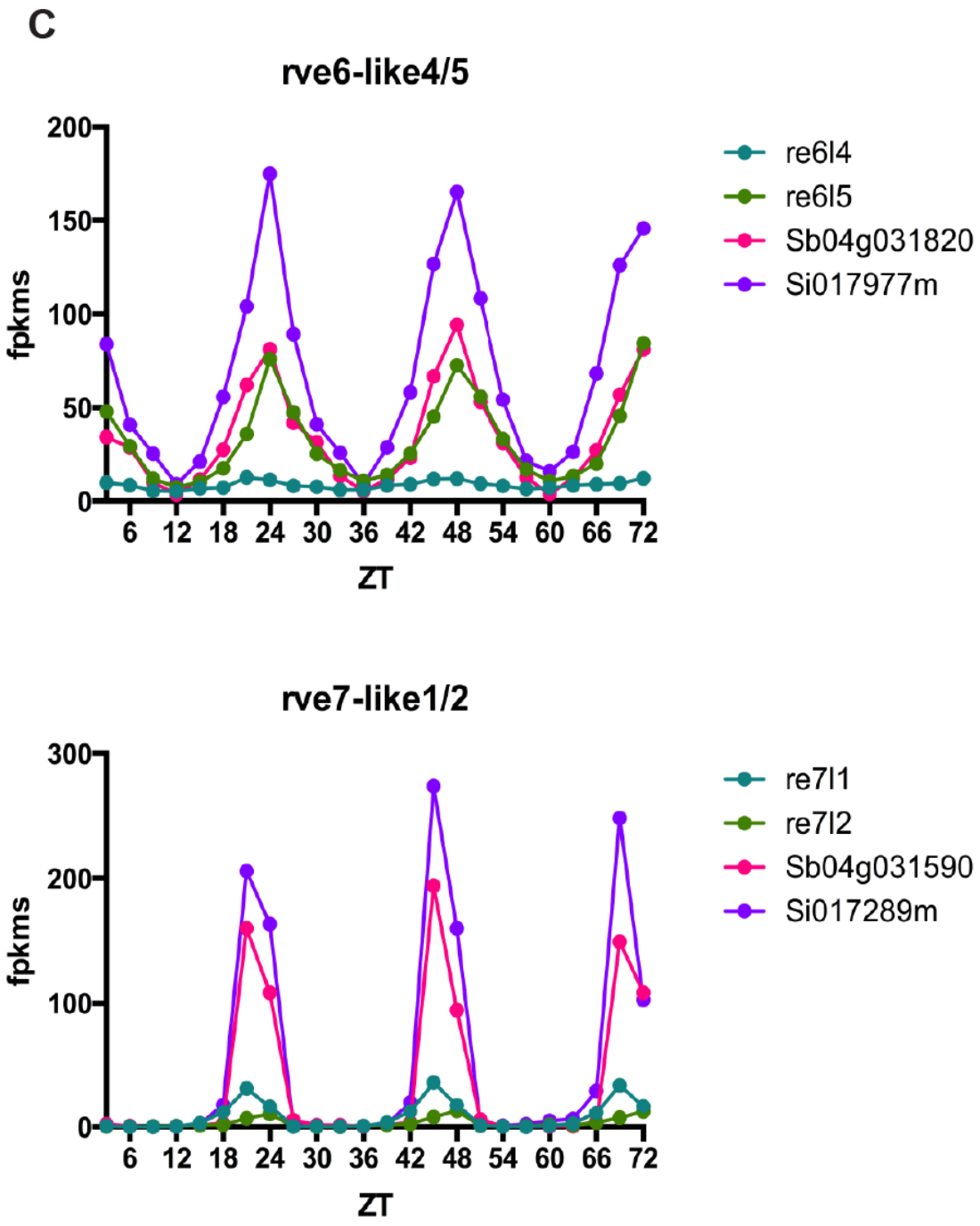

C) Expression levels of *rve6-like 4/5* (*re6l4/5*) and *rve7-like1/2* (*re7l1/2*) genes.

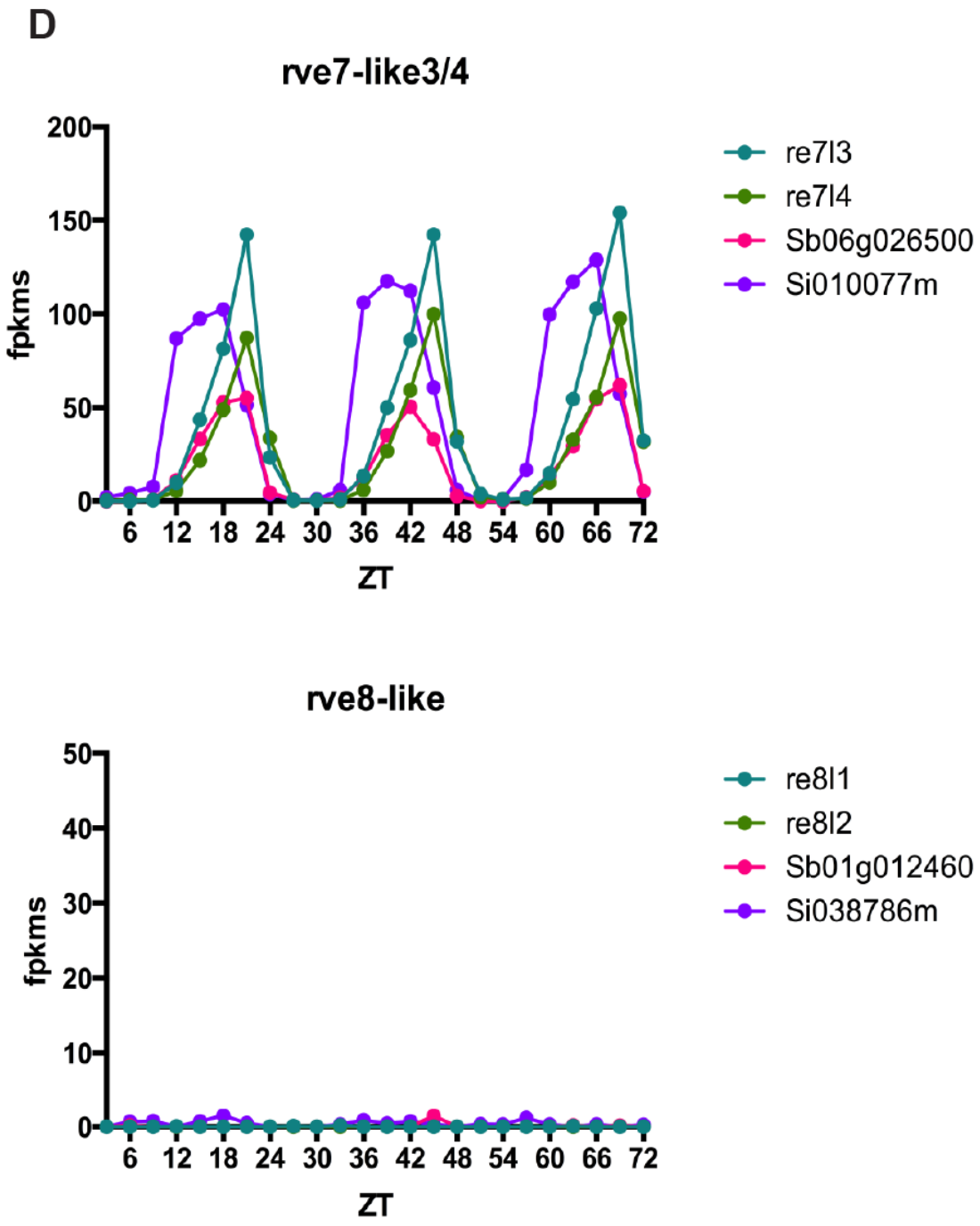

D) Expression levels of *rve7-like 2/3* (*re7l2/3*) and *rve8-like* (*re8l*) genes.

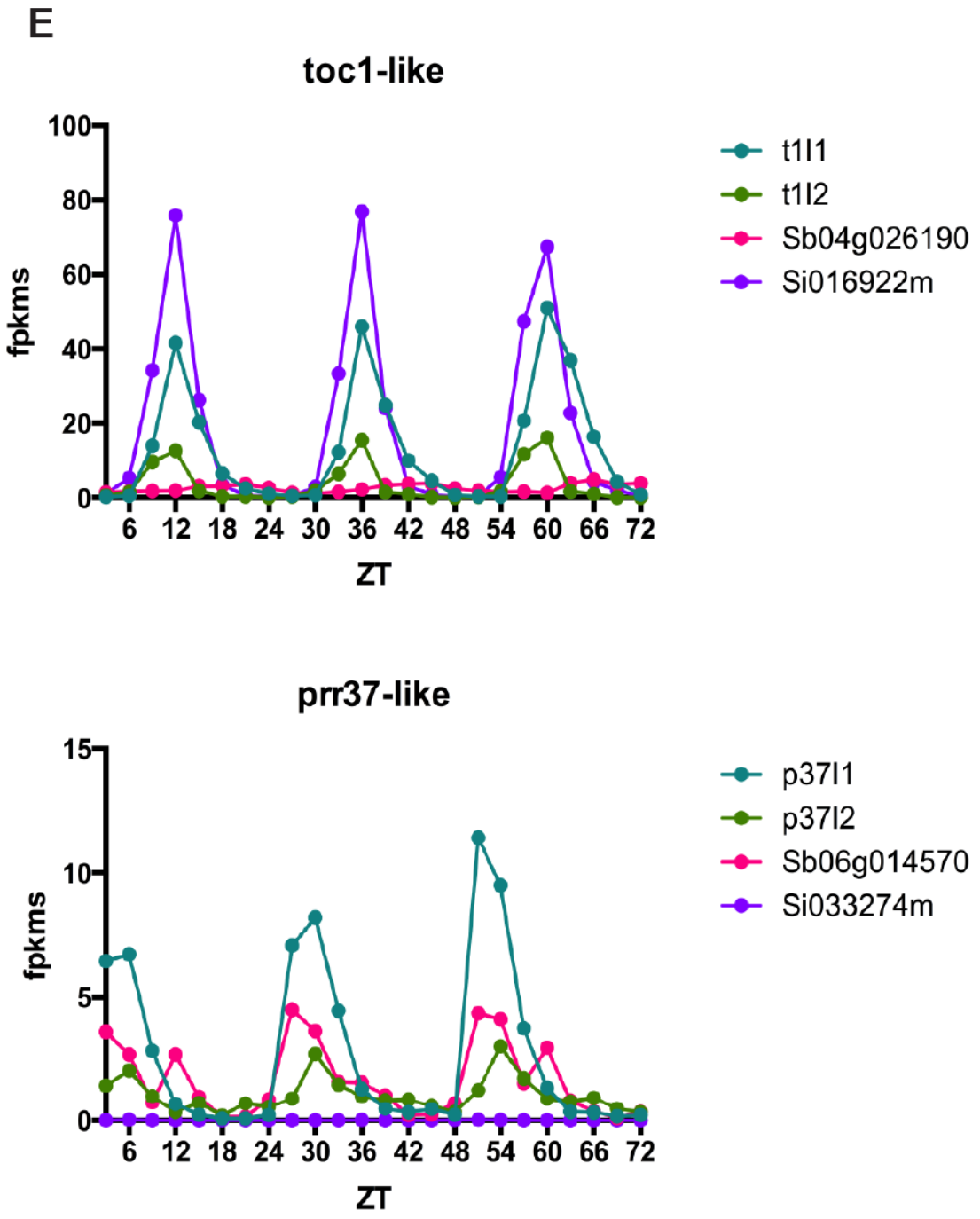

E) Expression levels of *toc1-like* (*t1l*) and *prr37-like* (*p37l*) genes.

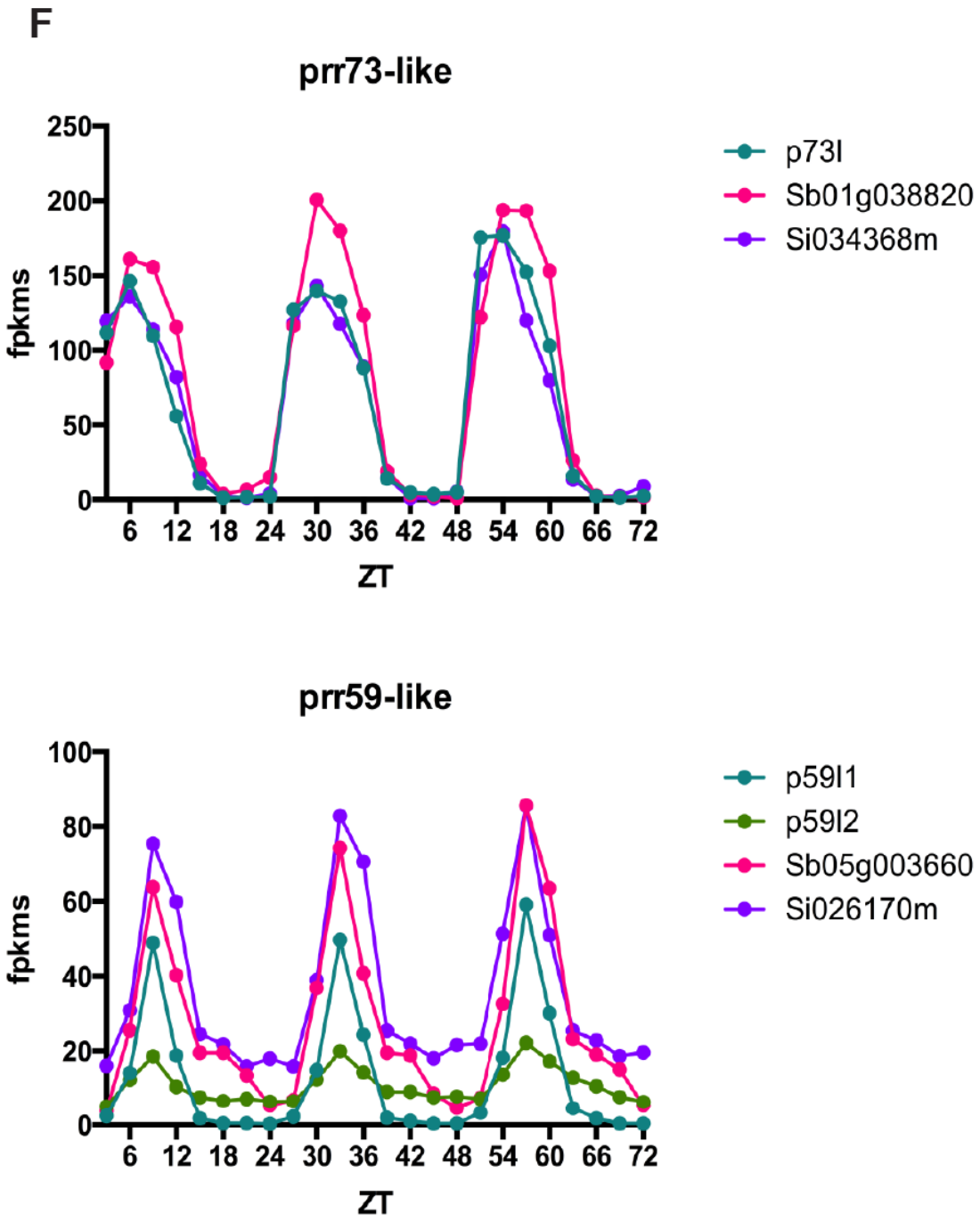

F) Expression levels of *prr73-like* (*p73l*) and *prr59-like* (*p59l*) genes.

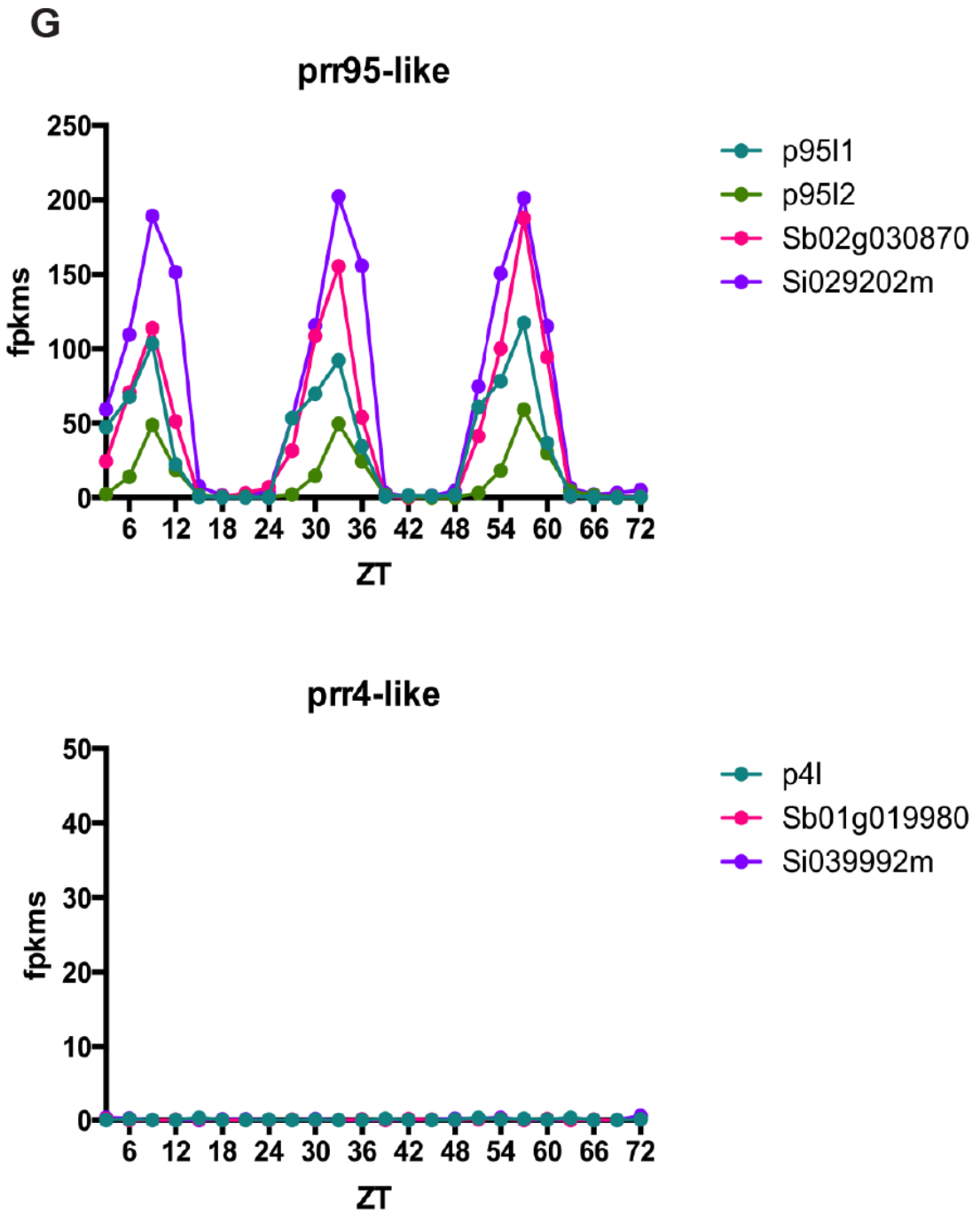

G) Expression levels of *prr95-like* (*p95l*) and *prr4-like* (*p4l*) genes.

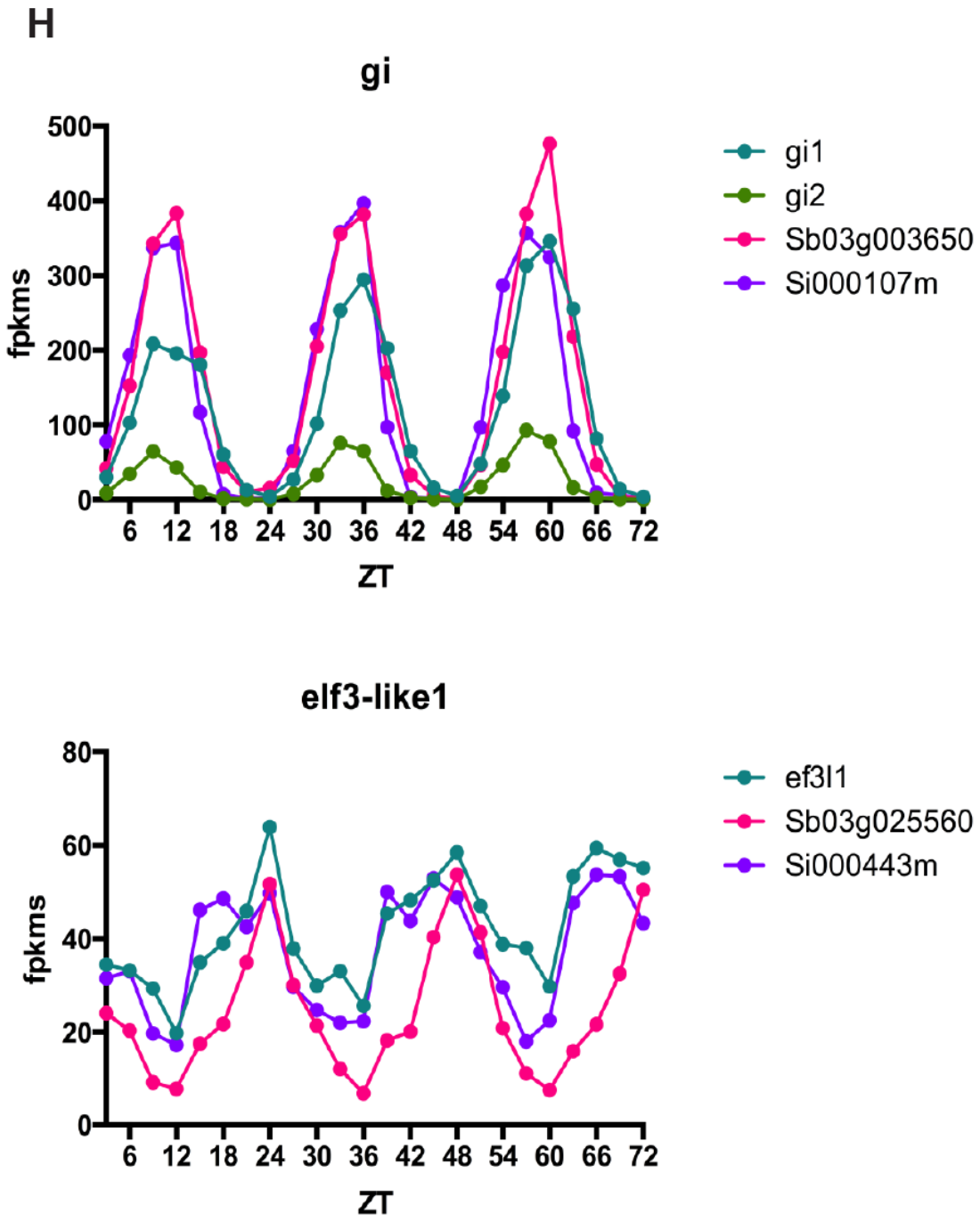

H) Expression levels of *gigantea* (*gi*) and *elf3-like 1* (*ef3l1*) genes.

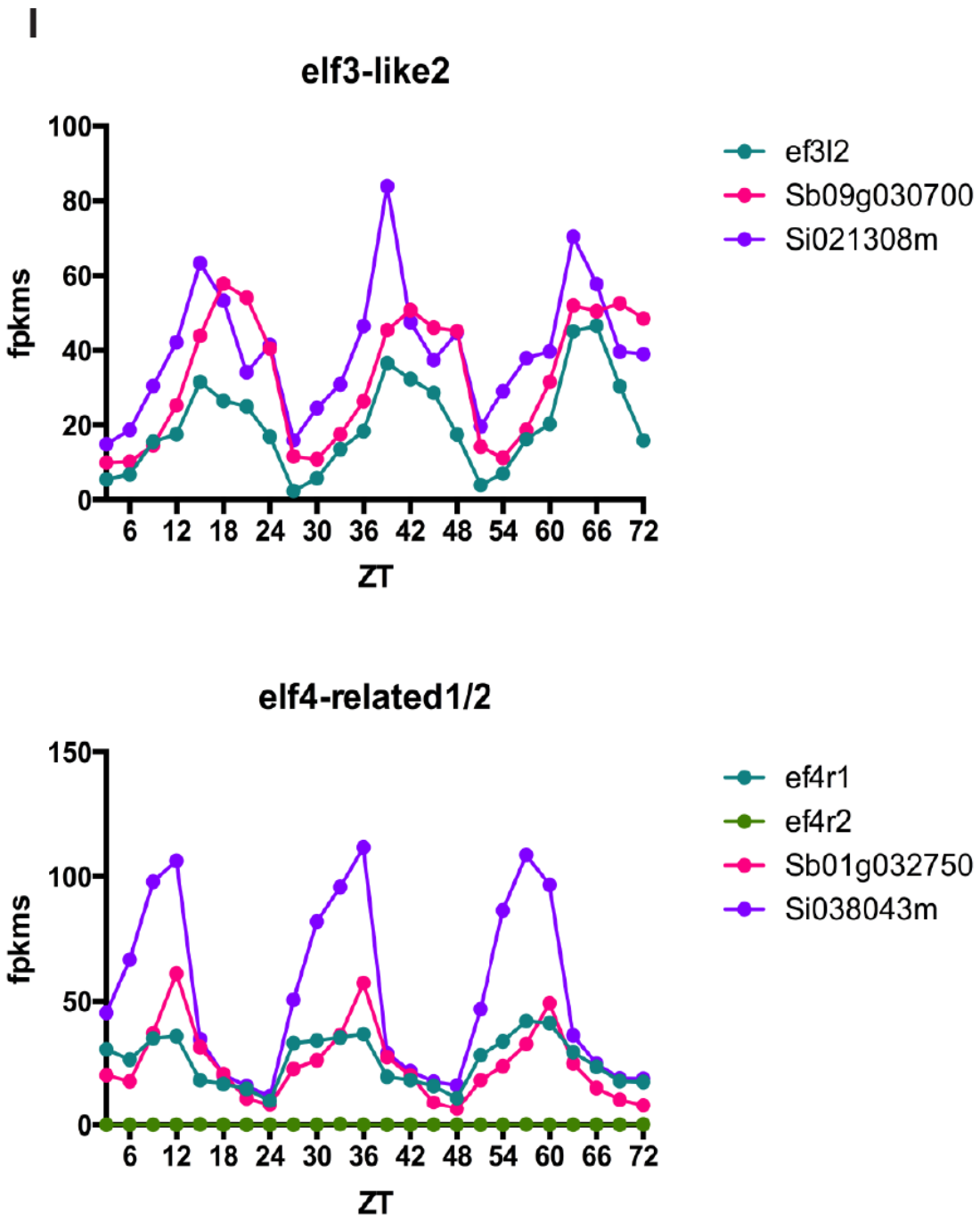

I) Expression levels of *elf3-like 2* (*ef3l2*) and *elf4-related 1/2* (*ef4r1/2*) genes.

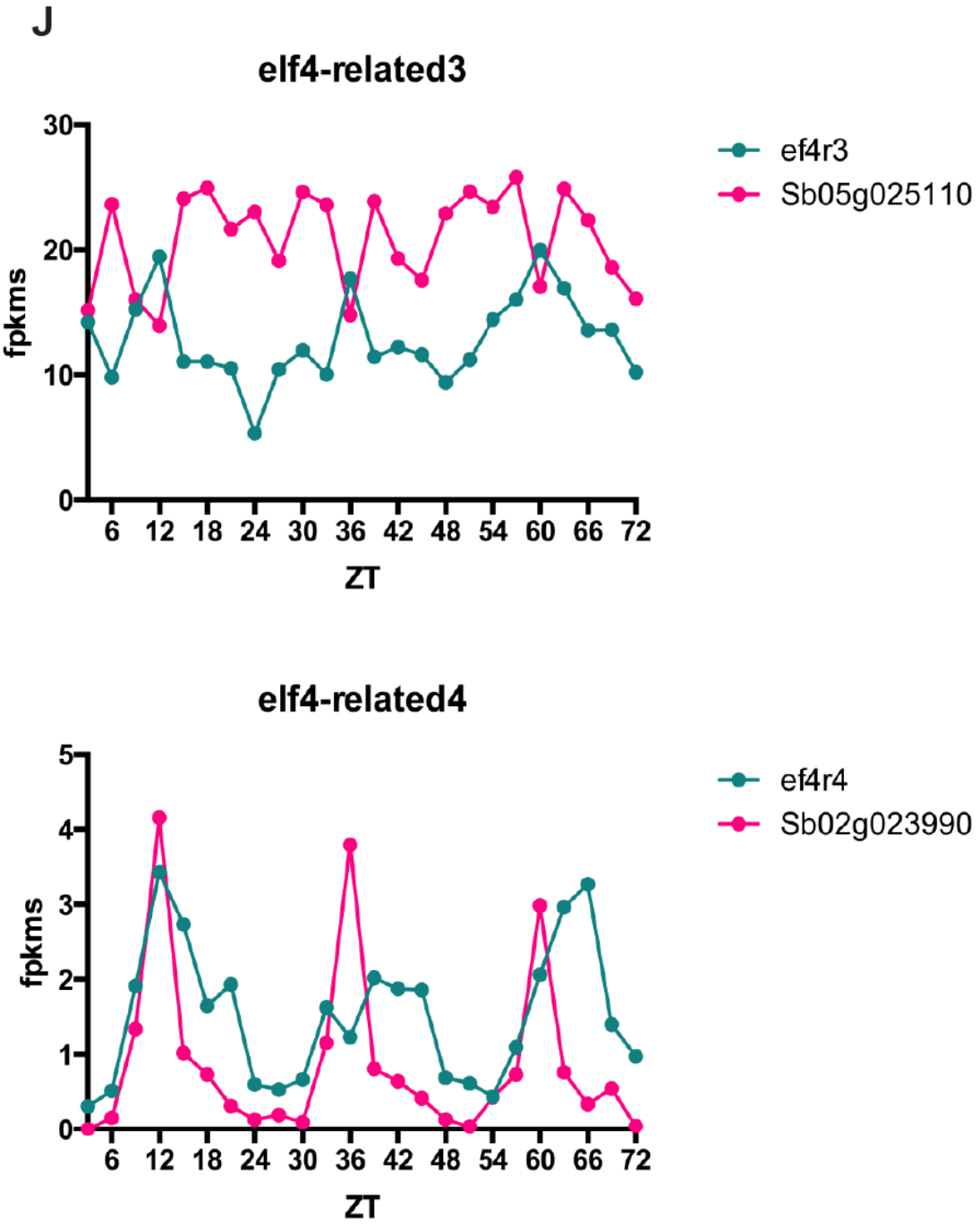

J) Expression levels of *elf4-related 3* (*efr3*) and *elf4-related 4* (*efr4*) genes.

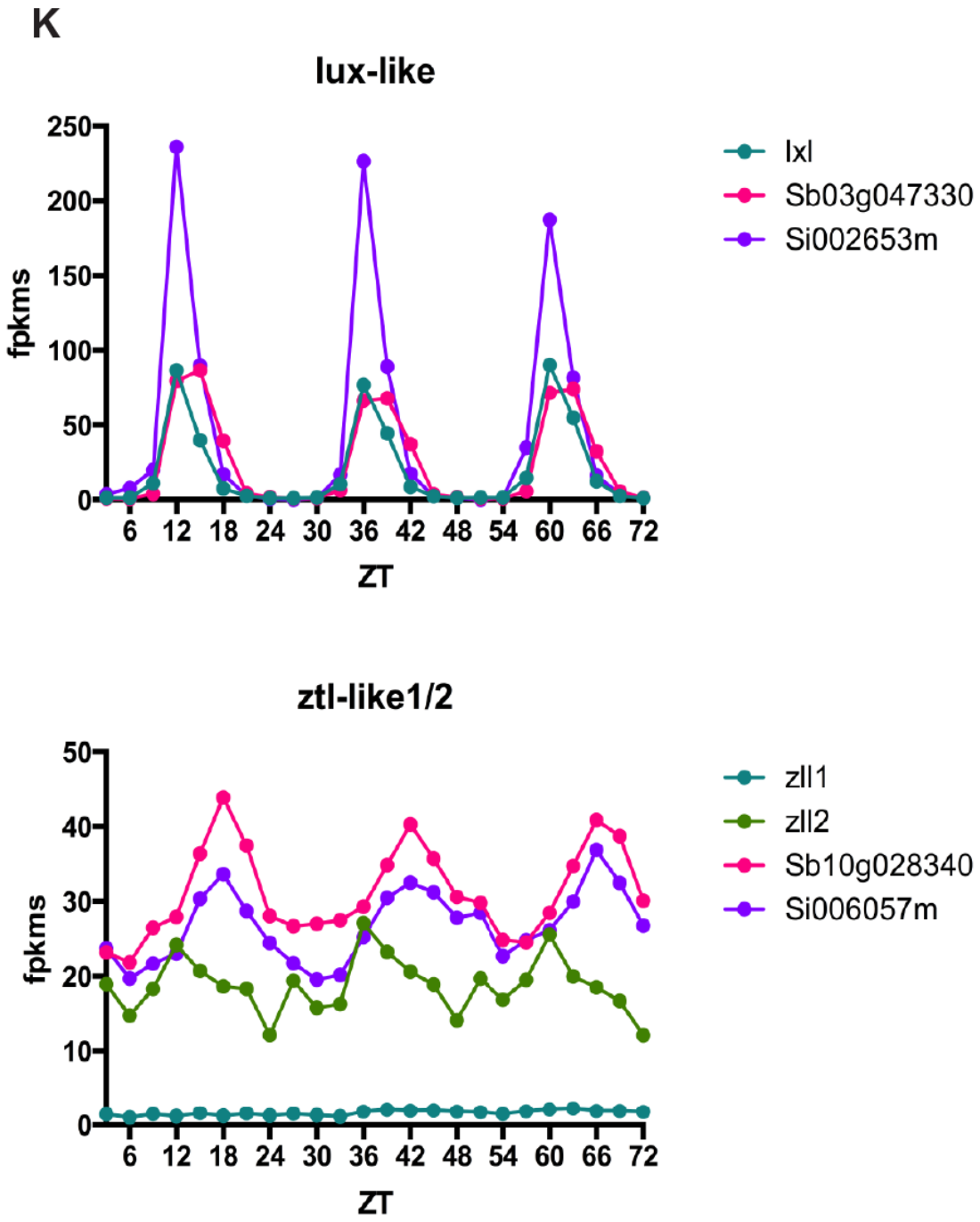

K) Expression levels of *lux-like* (*lxl*) and *ztl-like 1/2* (*zll1/2*) genes.

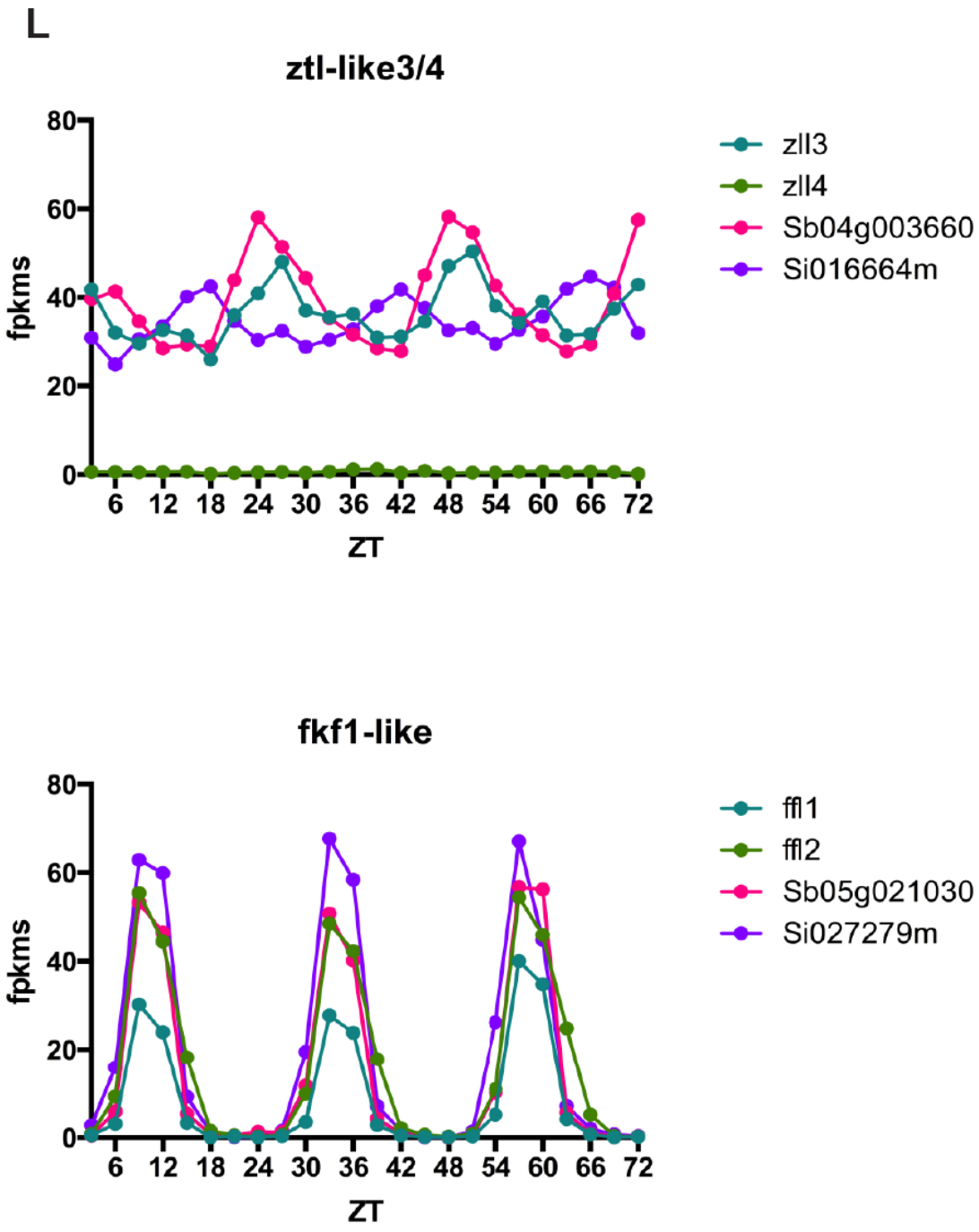

L) Expression levels of *ztl-like 3/4* (*zll3/4*) and *fkf1-like* (*ffl*) genes.

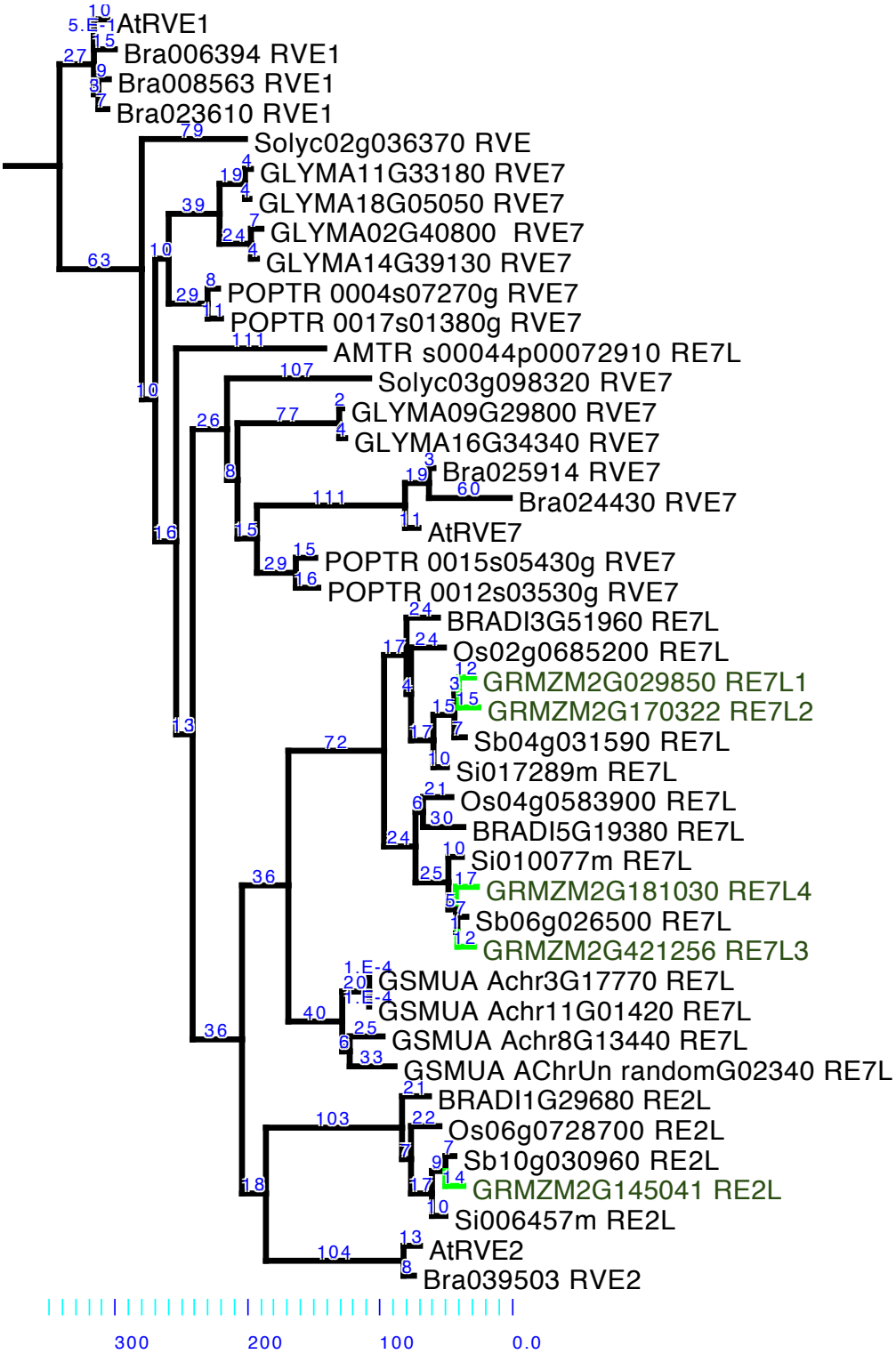

Modified, based on Imported tree 1

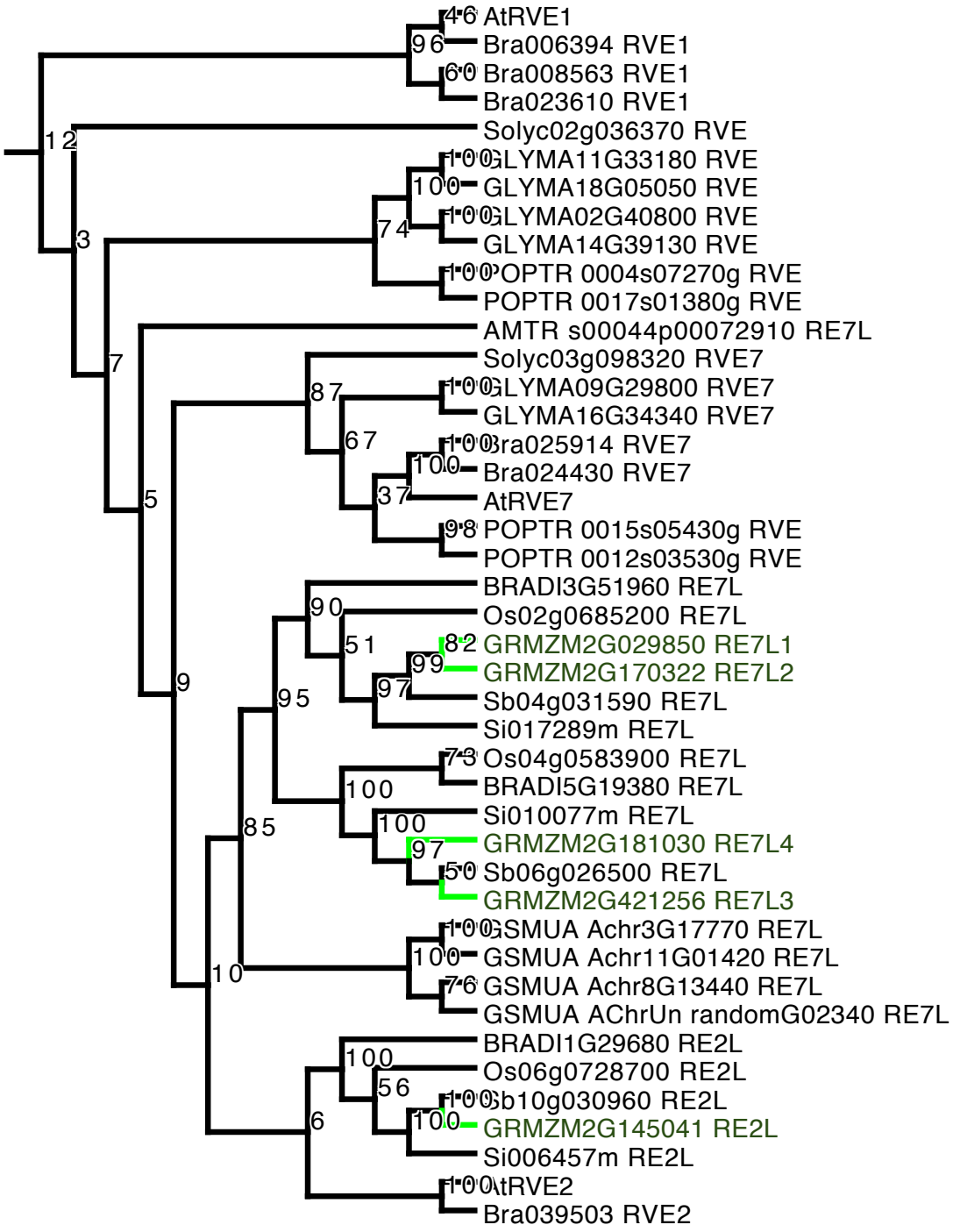

Figure 4.5 (this page and previous page). RVE1, RVE2, and RVE7 protein subtree (see Supplemental Figure 4.2.A). Maize gene branches are highlighted in green, as are maize genes. On this page, numbers indicate percentage bootstrap values from 1000 rapid bootstrap inferences. On previous page, numbers indicate estimated branch lengths.

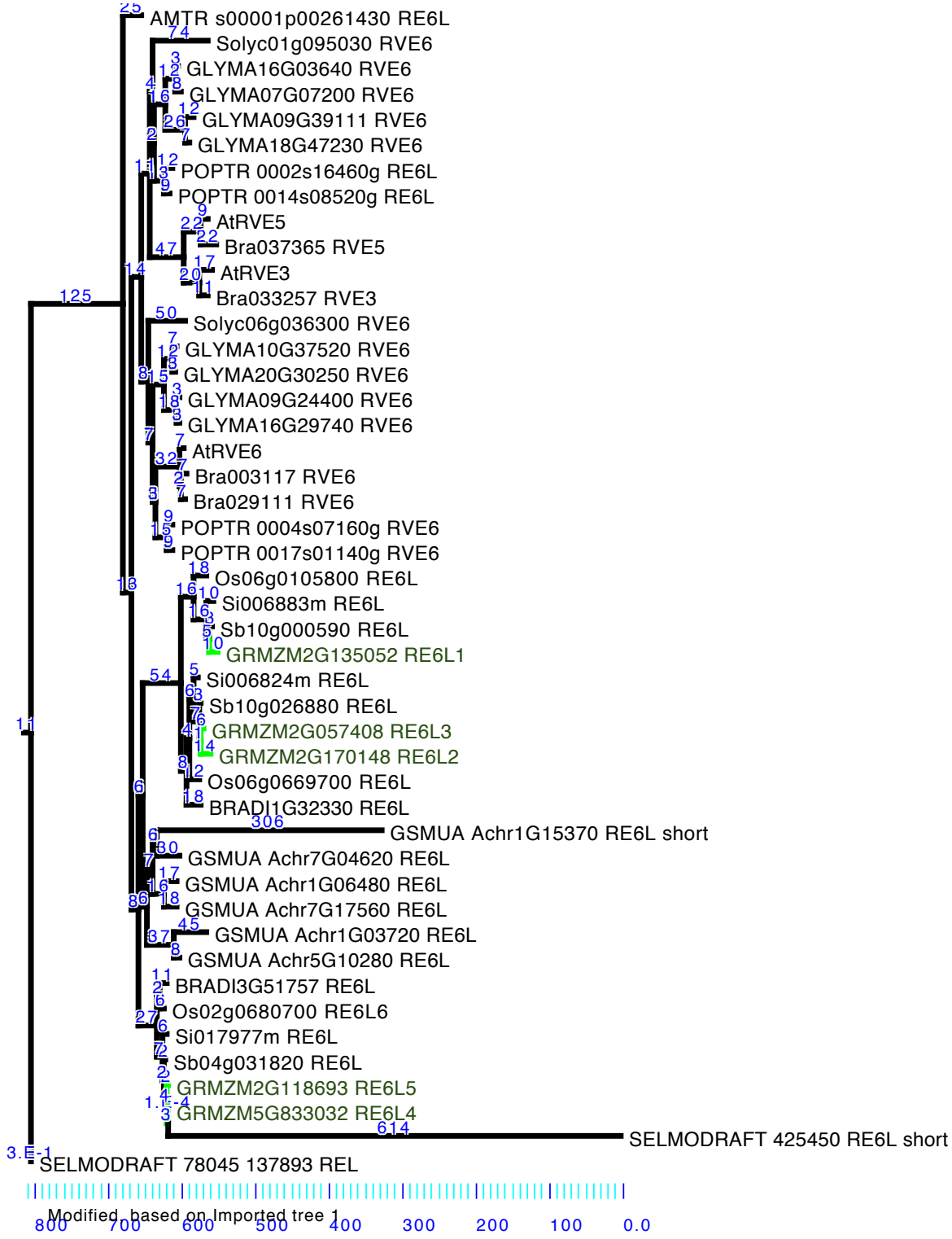
AMTR s00001p00261430 RE6L
Solyc01g095030 RVE6
GLYMA16G03640 RVE6
GLYMA07G07200 RVE6
GLYMA09G39111 RVE6
GLYMA18G47230 RVE6
POPTR 0002s16460g RE6L
POPTR 0014s08520g RE6L
AtRVE5
Bra037365 RVE5
AtRVE3
Bra033257 RVE3
Solyc06g036300 RVE6
GLYMA10G37520 RVE6
GLYMA20G30250 RVE6
GLYMA09G24400 RVE6
GLYMA16G29740 RVE6
AtRVE6
Bra003117 RVE6
Bra029111 RVE6
POPTR 0004s07160g RVE6
POPTR 0017s01140g RVE6
Os06g0105800 RE6L
Si006883m RE6L
Sb10g000590 RE6L
GRMZM2G135052 RE6L1
Si006824m RE6L
Sb10g026880 RE6L
GRMZM2G057408 RE6L3
GRMZM2G170148 RE6L2
Os06g0669700 RE6L
BRADI1G32330 RE6L
GSMUA Achr1G15370 RE6L short
GSMUA Achr7G04620 RE6L
GSMUA Achr1G06480 RE6L
GSMUA Achr7G17560 RE6L
GSMUA Achr1G03720 RE6L
GSMUA Achr5G10280 RE6L
BRADI3G51757 RE6L
Os02g0680700 RE6L6
Si017977m RE6L
Sb04g031820 RE6L
GRMZM2G118693 RE6L5
GRMZM5G833032 RE6L4
SELMODRAFT 425450 RE6L short
SELMODRAFT 78045 137893 REL
Modified based on Imported tree 1
800
700
600
500
400
300
200
100
0.0

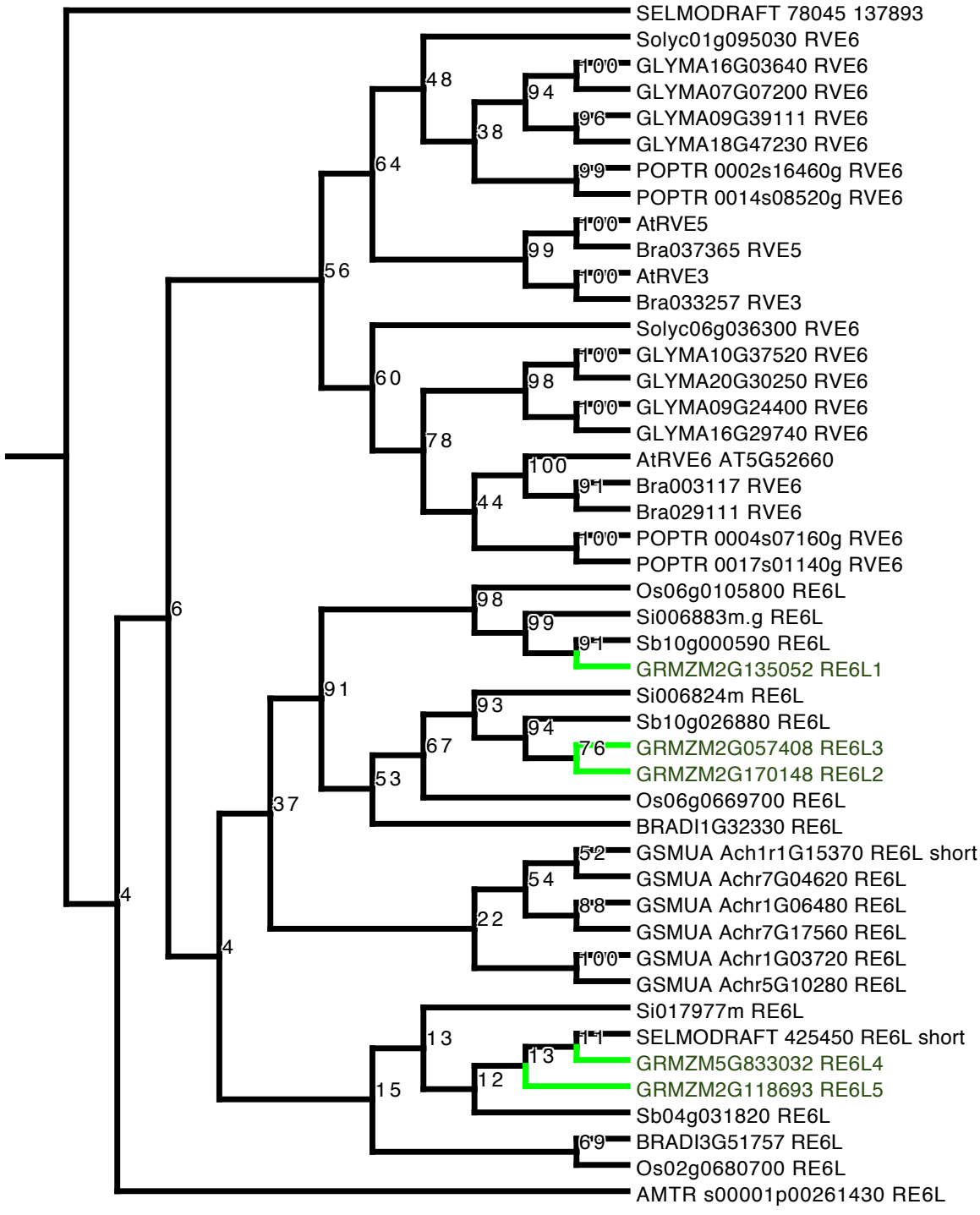

Figure 4.6 (this page and previous page). RVE6 protein subtree (see Supplemental Figure 4.2.A). Maize gene branches are highlighted in green, as are maize genes. On this page, numbers indicate percentage bootstrap values from 1000 rapid bootstrap inferences. On previous page, numbers indicate estimated branch lengths.

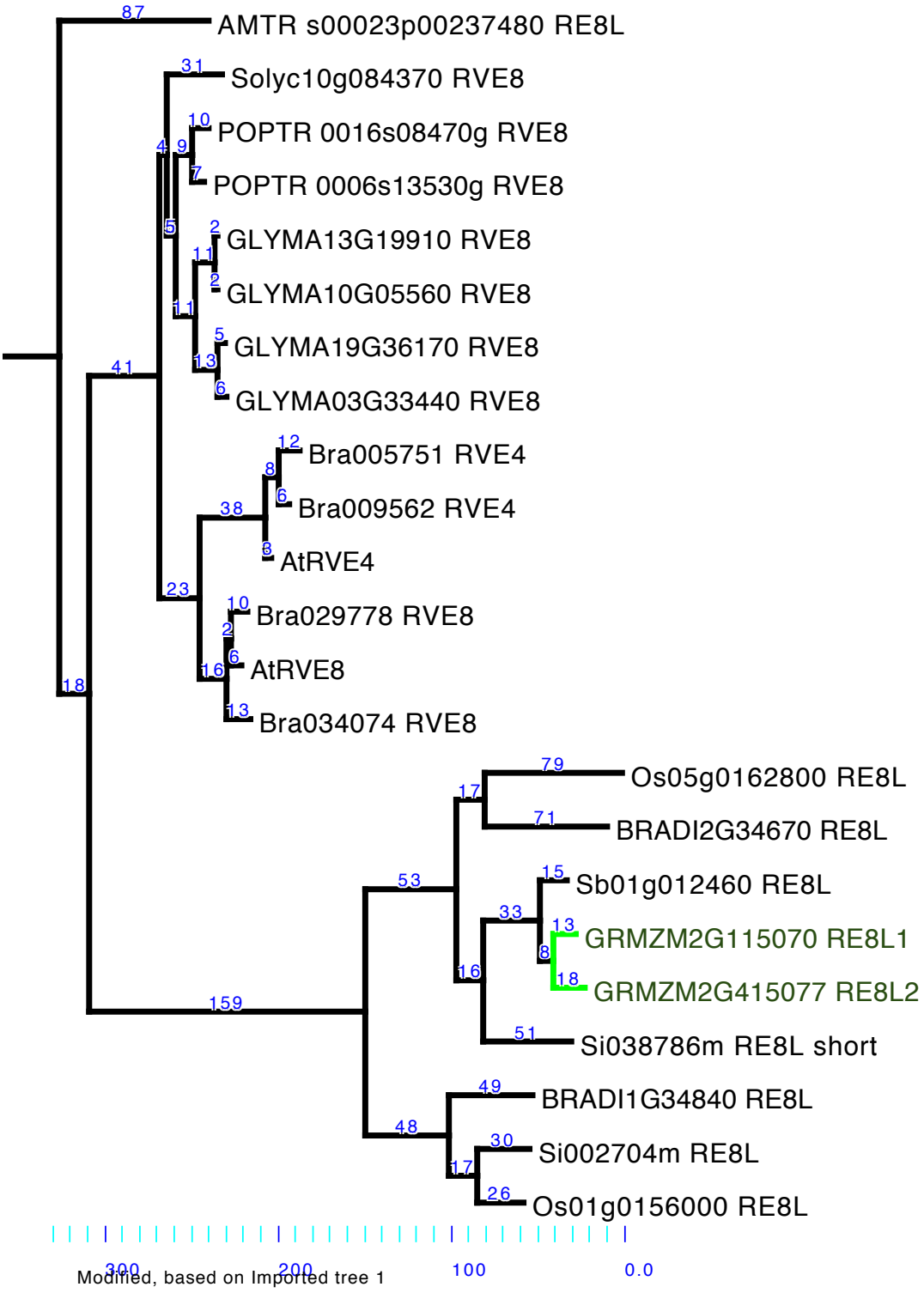
87
AMTR s00023p00237480 RE8L
31
Solyc10g084370 RVE8
10
POPTR 0016s08470g RVE8
4
9
7
POPTR 0006s13530g RVE8
5
2
GLYMA13G19910 RVE8
11
2
GLYMA10G05560 RVE8
11
5
GLYMA19G36170 RVE8
13
6
GLYMA03G33440 RVE8
41
12
Bra005751 RVE4
8
6
Bra009562 RVE4
38
6
AtRVE4
23
10
Bra029778 RVE8
2
6
AtRVE8
16
13
Bra034074 RVE8
18
79
Os05g0162800 RE8L
17
71
BRADI2G34670 RE8L
53
15
Sb01g012460 RE8L
33
13
GRMZM2G115070 RE8L1
8
18
GRMZM2G415077 RE8L2
16
159
51
Si038786m RE8L short
49
BRADI1G34840 RE8L
48
30
Si002704m RE8L
17
26
Os01g0156000 RE8L
300
200
100
0.0
Modified, based on Imported tree 1

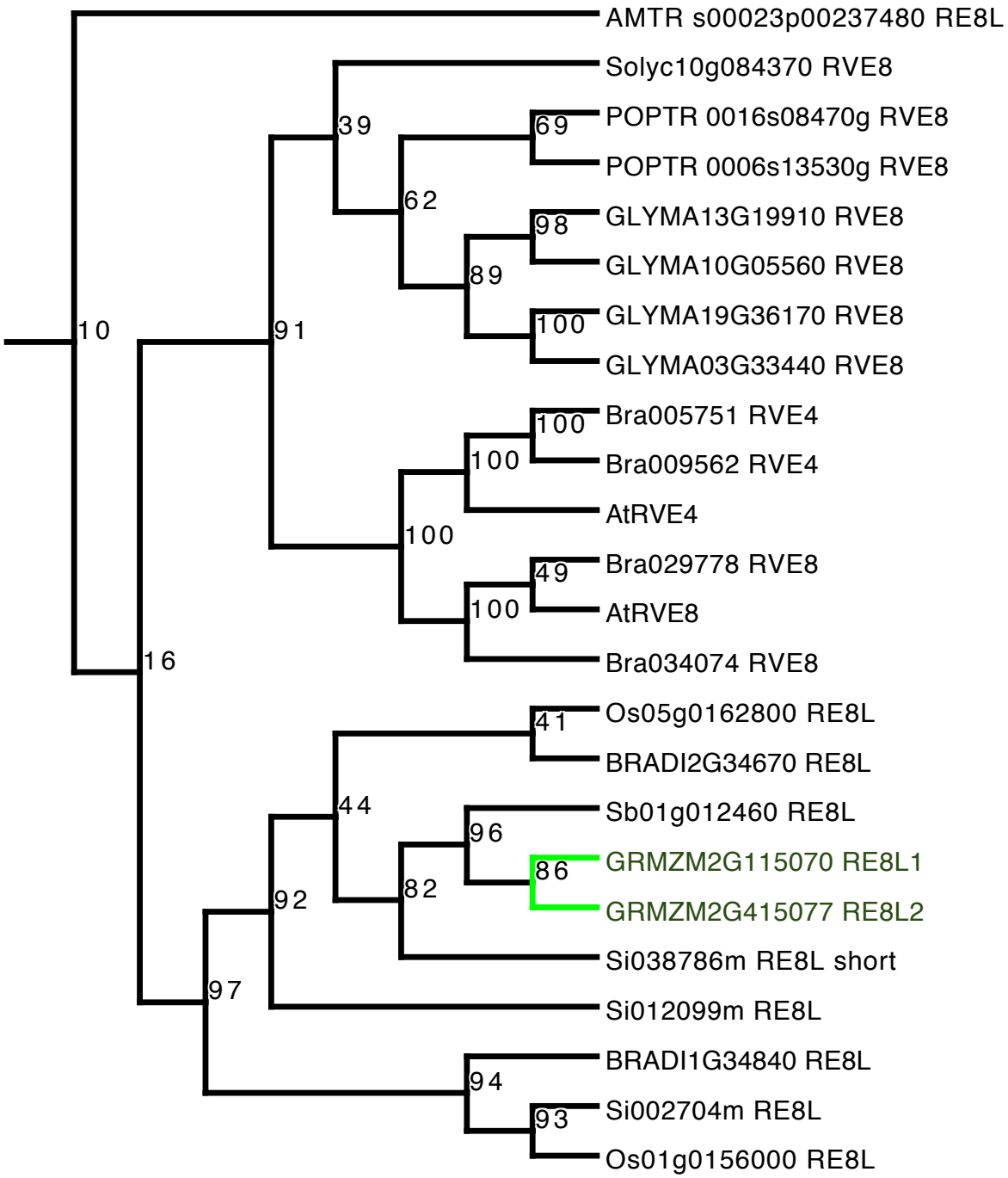

Figure 4.7 (this page and previous page). RVE8 protein subtree (see Supplemental Figure 4.2.A). Maize gene branches are highlighted in green, as are maize genes. On this page, numbers indicate percentage bootstrap values from 1000 rapid bootstrap inferences. On previous page, numbers indicate estimated branch lengths.

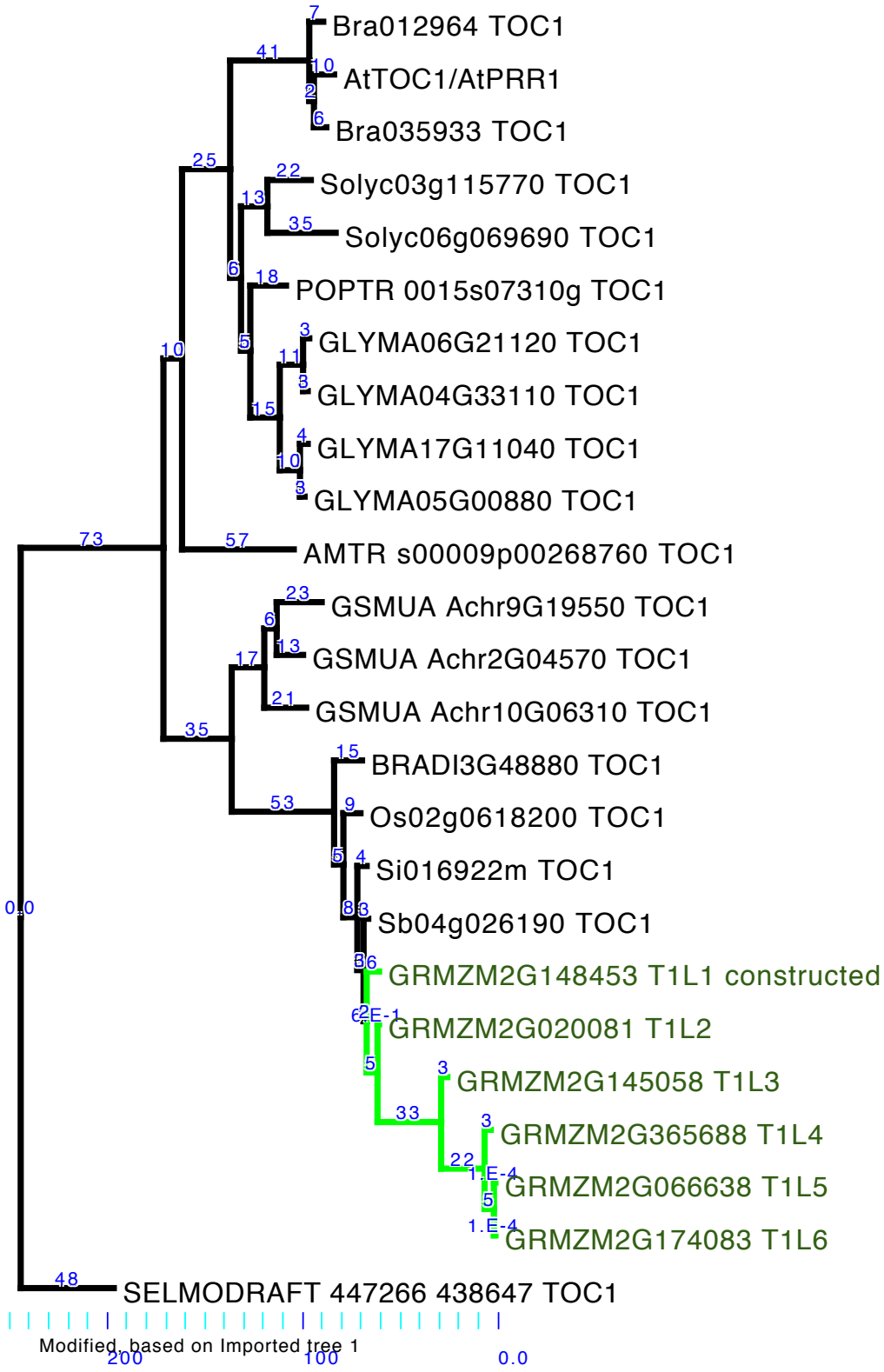
Bra012964 TOC1
AtTOC1/AtPRR1
Bra035933 TOC1
Solyc03g115770 TOC1
Solyc06g069690 TOC1
POPTR 0015s07310g TOC1
GLYMA06G21120 TOC1
GLYMA04G33110 TOC1
GLYMA17G11040 TOC1
GLYMA05G00880 TOC1
AMTR s00009p00268760 TOC1
GSMUA Achr9G19550 TOC1
GSMUA Achr2G04570 TOC1
GSMUA Achr10G06310 TOC1
BRADI3G48880 TOC1
Os02g0618200 TOC1
Si016922m TOC1
Sb04g026190 TOC1
GRMZM2G148453 T1L1 constructed
GRMZM2G020081 T1L2
GRMZM2G145058 T1L3
GRMZM2G365688 T1L4
GRMZM2G066638 T1L5
GRMZM2G174083 T1L6
SELMODRAFT 447266 438647 TOC1
Modified, based on Imported tree 1
200
100
0.0

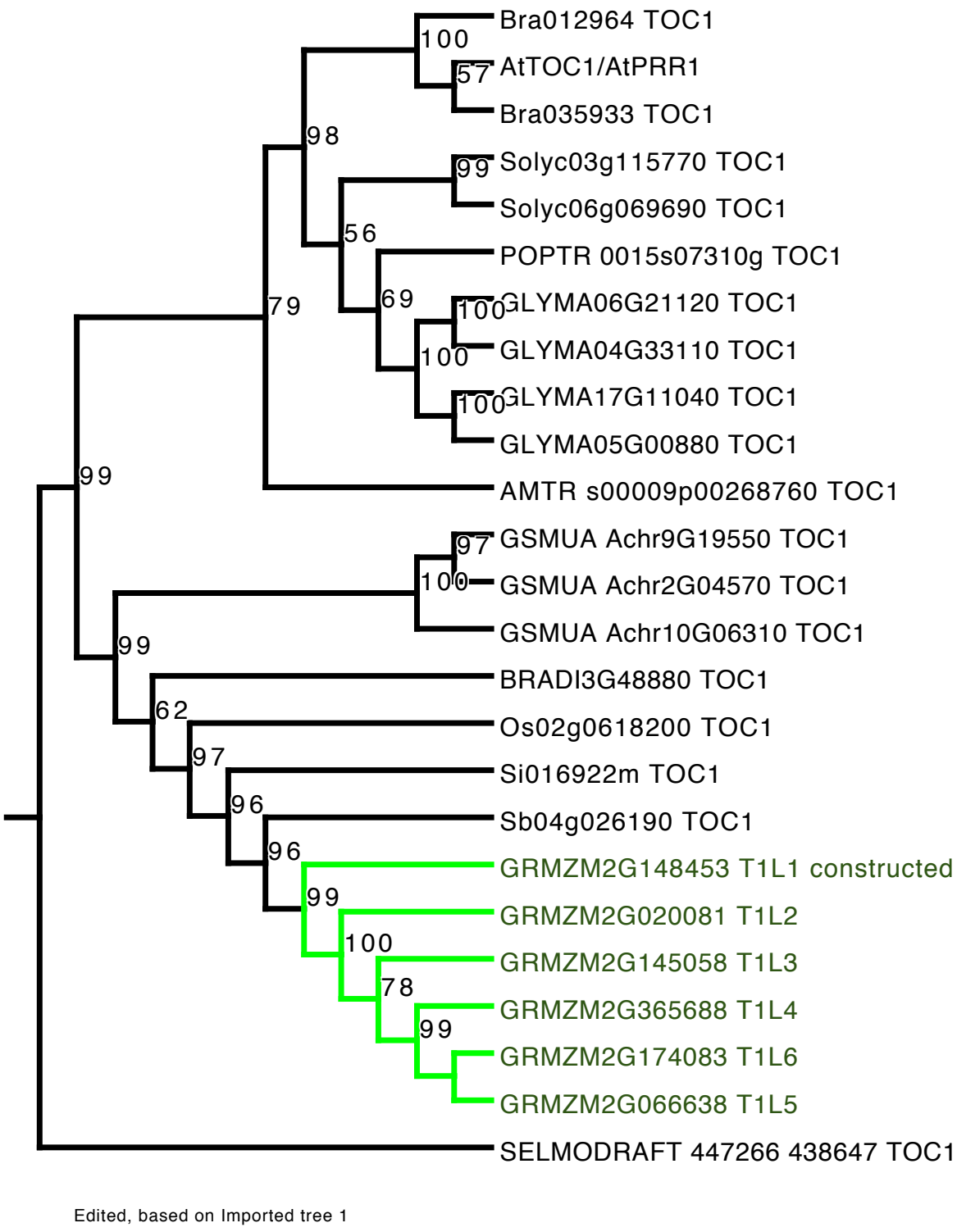

Figure 4.8 (this page and previous page). TOC1 protein subtree (see Supplemental Figure 4.2.B). Maize gene branches are highlighted in green, as are maize genes. On this page, numbers indicate percentage bootstrap values from 1000 rapid bootstrap inferences. On previous page, numbers indicate estimated branch lengths.

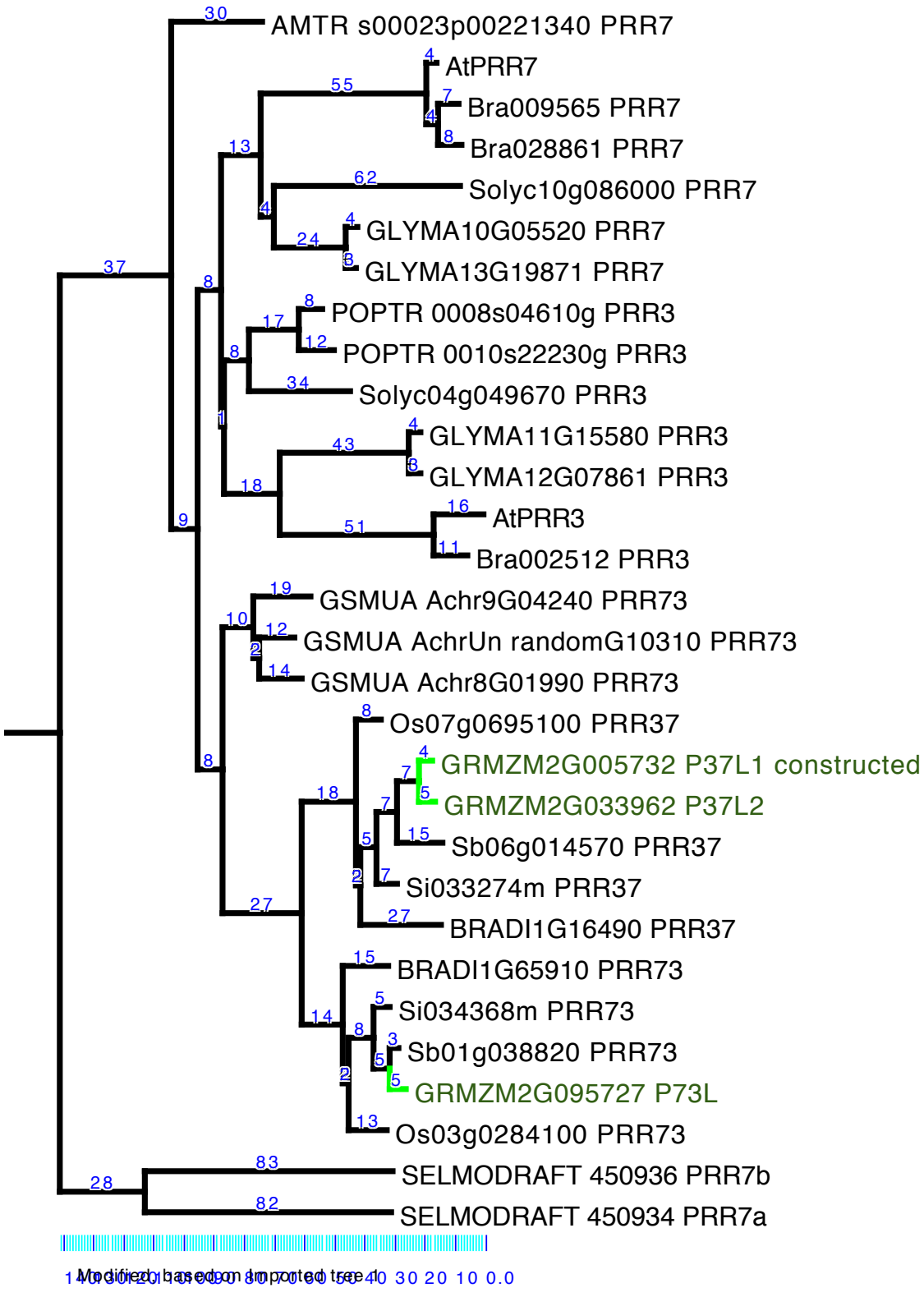
AMTR s00023p00221340 PRR7
AtPRR7
Bra009565 PRR7
Bra028861 PRR7
Solyc10g086000 PRR7
GLYMA10G05520 PRR7
GLYMA13G19871 PRR7
POPTR 0008s04610g PRR3
POPTR 0010s22230g PRR3
Solyc04g049670 PRR3
GLYMA11G15580 PRR3
GLYMA12G07861 PRR3
AtPRR3
Bra002512 PRR3
GSMUA Achr9G04240 PRR73
GSMUA AchrUn randomG10310 PRR73
GSMUA Achr8G01990 PRR73
Os07g0695100 PRR37
GRMZM2G005732 P37L1 constructed
GRMZM2G033962 P37L2
Sb06g014570 PRR37
Si033274m PRR37
BRADI1G16490 PRR37
BRADI1G65910 PRR73
Si034368m PRR73
Sb01g038820 PRR73
GRMZM2G095727 P73L
Os03g0284100 PRR73
SELMODRAFT 450936 PRR7b
SELMODRAFT 450934 PRR7a
Modified based on imported tree 1

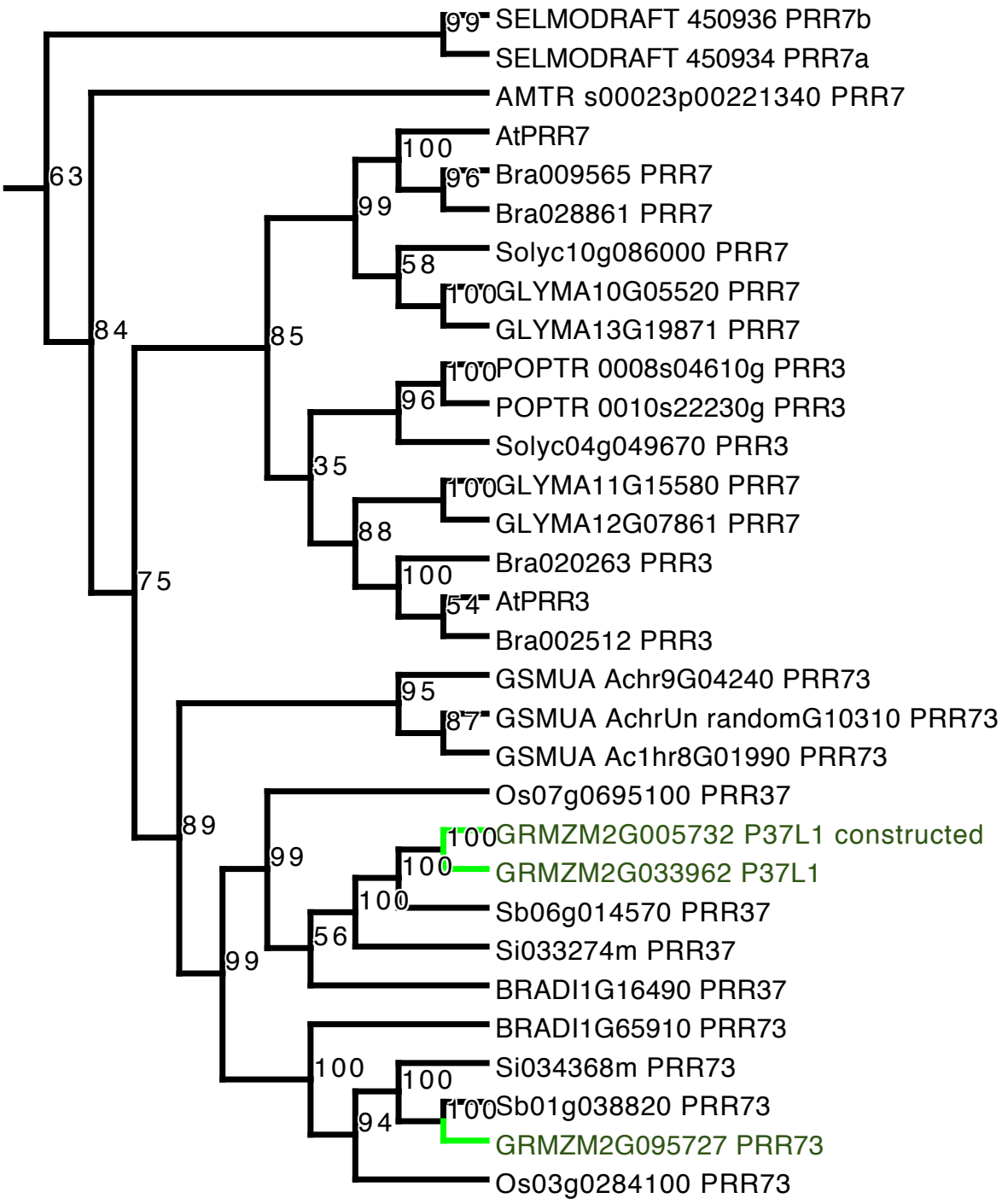

Edited, based on Imported tree 1

Figure 4.9 (this page and previous page). PRR3/7/37/73 protein subtree (see Supplemental Figure 4.2.B). Maize gene branches are highlighted in green, as are maize genes. On this page, numbers indicate percentage bootstrap values from 1000 rapid bootstrap inferences. On previous page, numbers indicate estimated branch lengths.

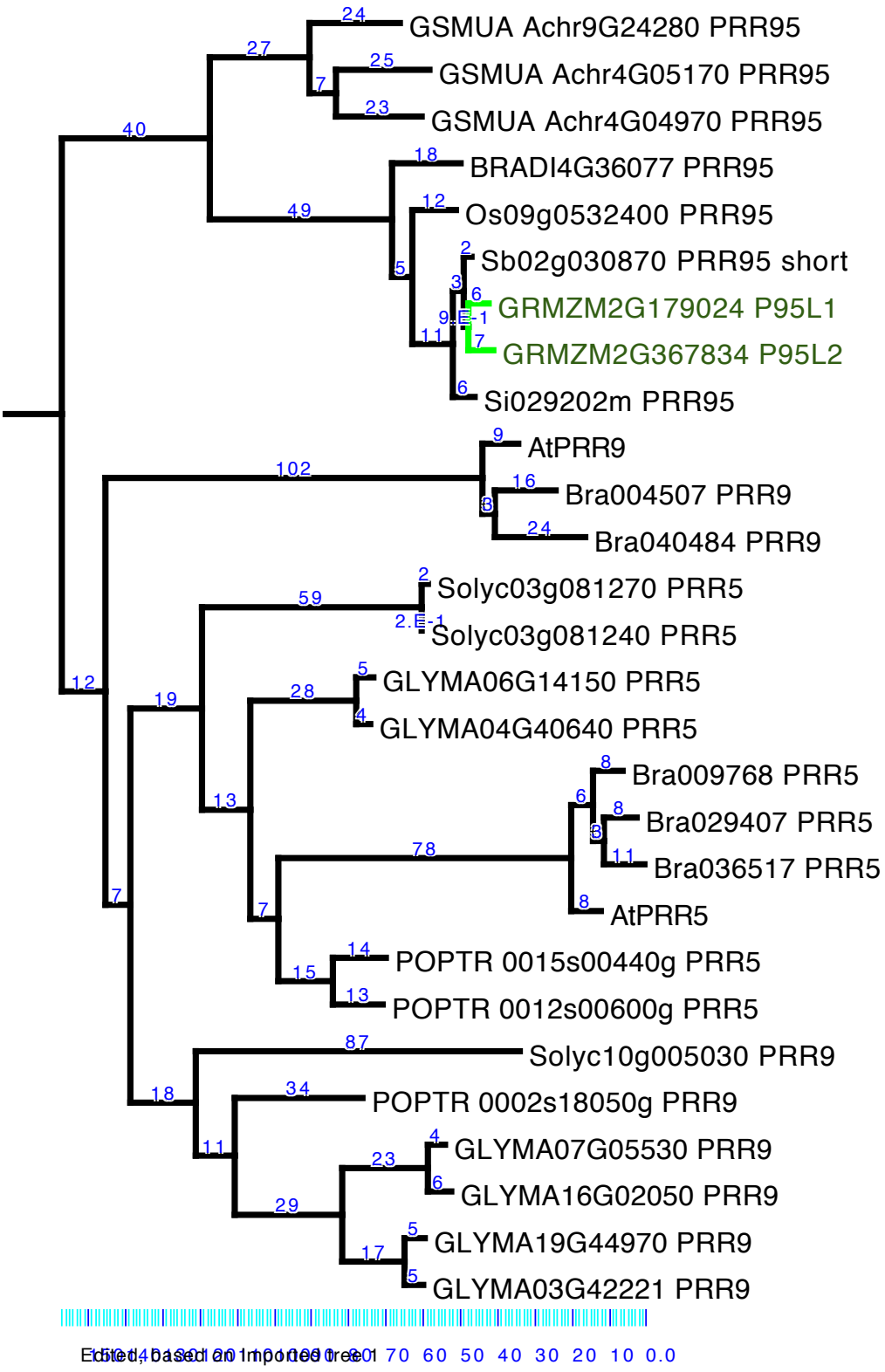
GSMUA Achr9G24280 PRR95
GSMUA Achr4G05170 PRR95
GSMUA Achr4G04970 PRR95
BRADI4G36077 PRR95
Os09g0532400 PRR95
Sb02g030870 PRR95 short
GRMZM2G179024 P95L1
GRMZM2G367834 P95L2
Si029202m PRR95
AtPRR9
Bra004507 PRR9
Bra040484 PRR9
Solyc03g081270 PRR5
Solyc03g081240 PRR5
GLYMA06G14150 PRR5
GLYMA04G40640 PRR5
Bra009768 PRR5
Bra029407 PRR5
Bra036517 PRR5
AtPRR5
POPTR 0015s00440g PRR5
POPTR 0012s00600g PRR5
Solyc10g005030 PRR9
POPTR 0002s18050g PRR9
GLYMA07G05530 PRR9
GLYMA16G02050 PRR9
GLYMA19G44970 PRR9
GLYMA03G42221 PRR9
Edited, based on imported tree
80 70 60 50 40 30 20 10 0.0

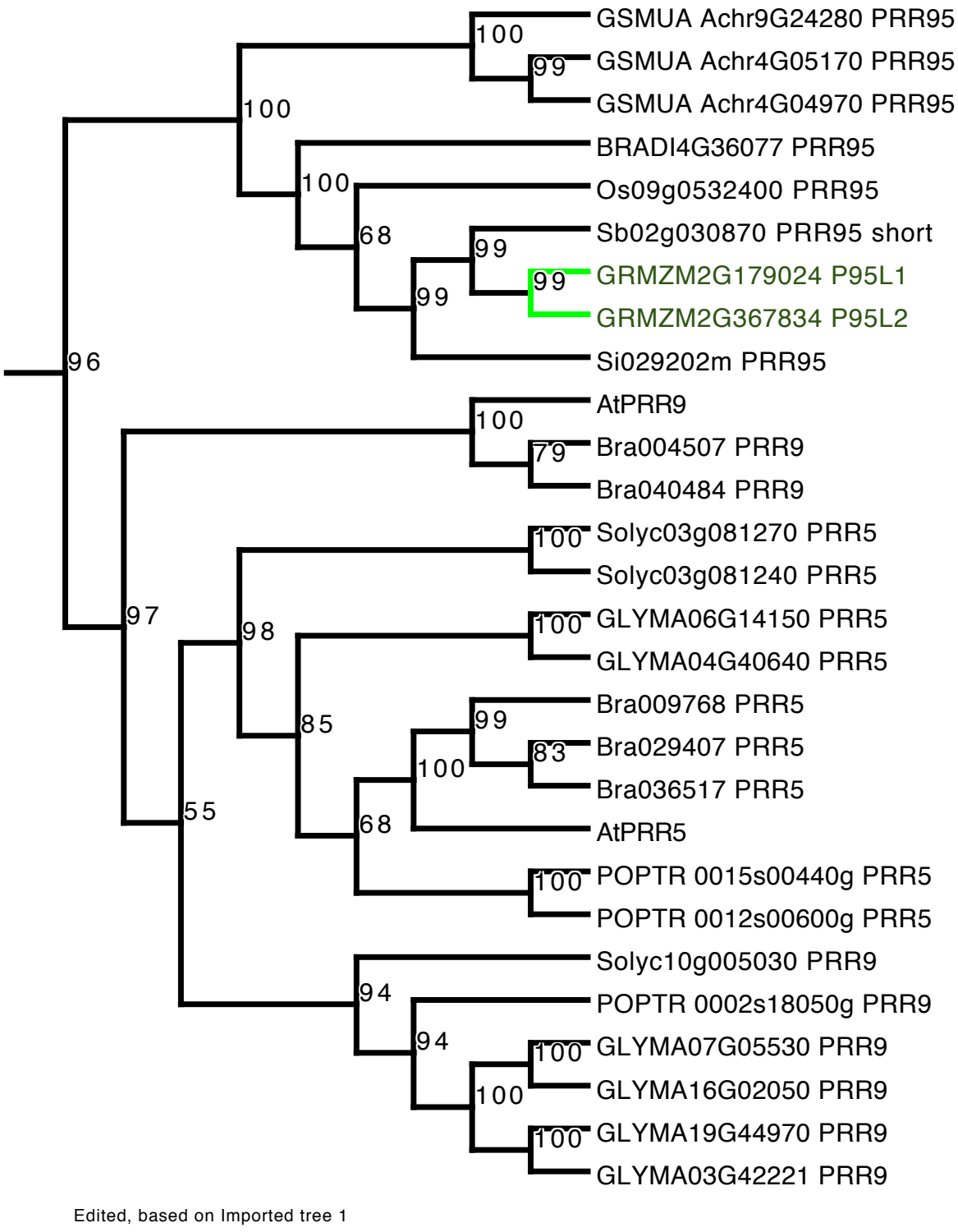

Edited, based on Imported tree 1

Figure 4.10 (this page and previous page). PRR9/5/95 protein subtree (see Supplemental Figure 4.2.B). Maize gene branches are highlighted in green, as are maize genes. On this page, numbers indicate percentage bootstrap values from 1000 rapid bootstrap inferences. On previous page, numbers indicate estimated branch lengths.

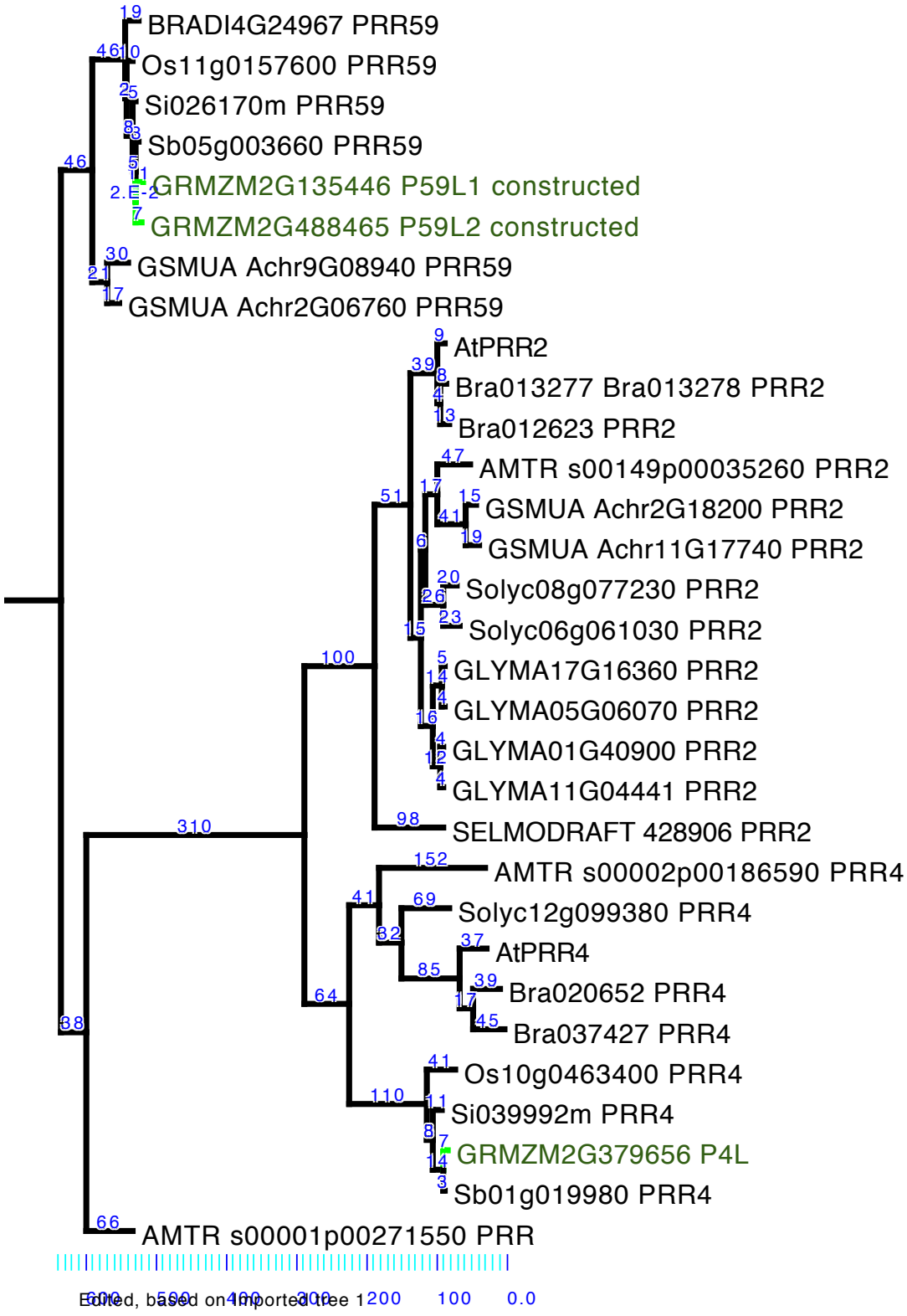
BRADI4G24967 PRR59
Os11g0157600 PRR59
Si026170m PRR59
Sb05g003660 PRR59
GRMZM2G135446 P59L1 constructed
GRMZM2G488465 P59L2 constructed
GSMUA Achr9G08940 PRR59
GSMUA Achr2G06760 PRR59
AtPRR2
Bra013277 Bra013278 PRR2
Bra012623 PRR2
AMTR s00149p00035260 PRR2
GSMUA Achr2G18200 PRR2
GSMUA Achr11G17740 PRR2
Solyc08g077230 PRR2
Solyc06g061030 PRR2
GLYMA17G16360 PRR2
GLYMA05G06070 PRR2
GLYMA01G40900 PRR2
GLYMA11G04441 PRR2
SELMODRAFT 428906 PRR2
AMTR s00002p00186590 PRR4
Solyc12g099380 PRR4
AtPRR4
Bra020652 PRR4
Bra037427 PRR4
Os10g0463400 PRR4
Si039992m PRR4
GRMZM2G379656 P4L
Sb01g019980 PRR4
AMTR s00001p00271550 PRR
Edited, based on Imported tree 1

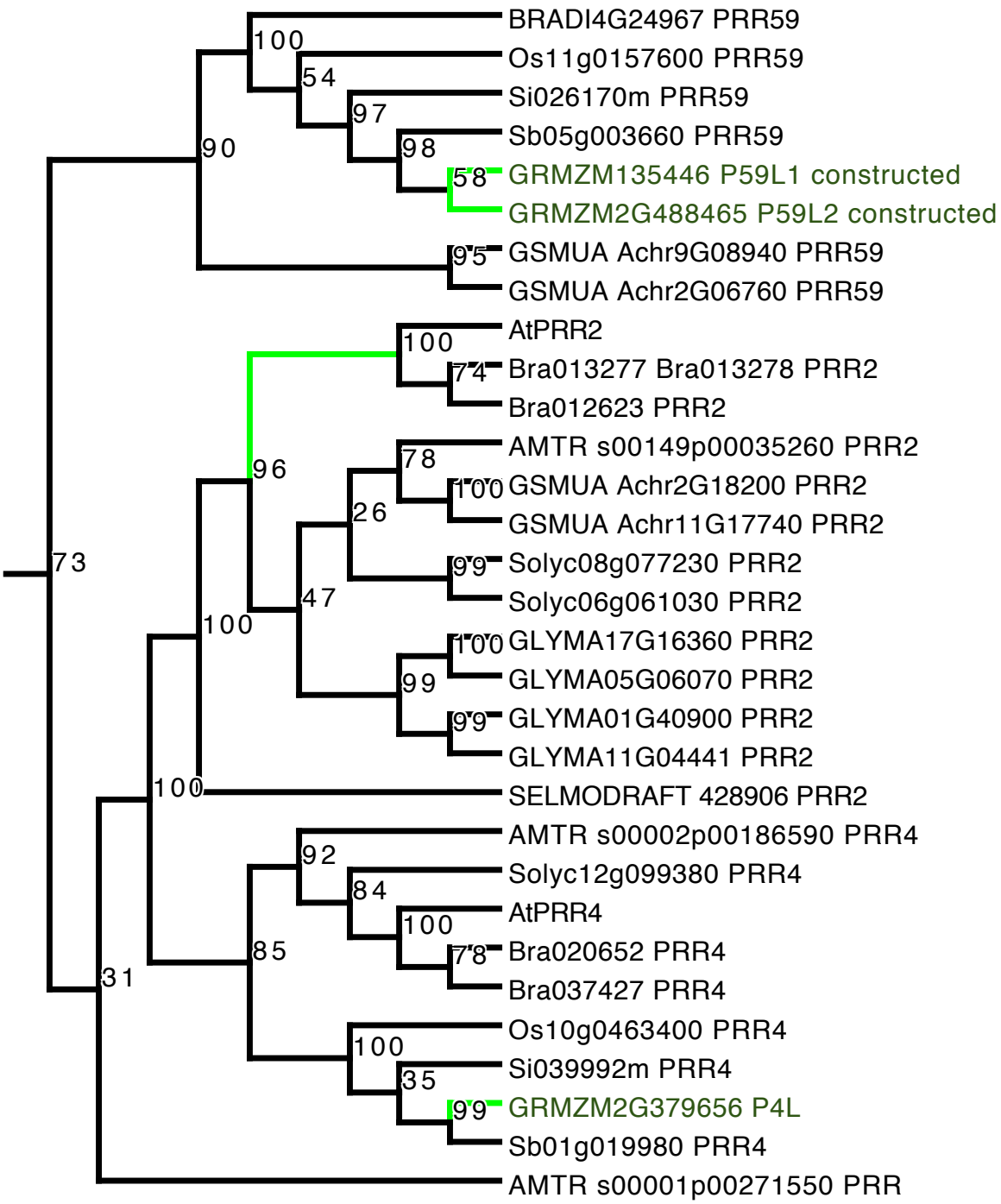

Edited, based on Imported tree 1

Figure 4.11 (this page and previous page). PRR59 and PRR2/4 protein subtree (see Supplemental Figure 4.2.B). Maize gene branches are highlighted in green, as are maize genes. On this page, numbers indicate percentage bootstrap values from 1000 rapid bootstrap inferences. On previous page, numbers indicate estimated branch lengths.

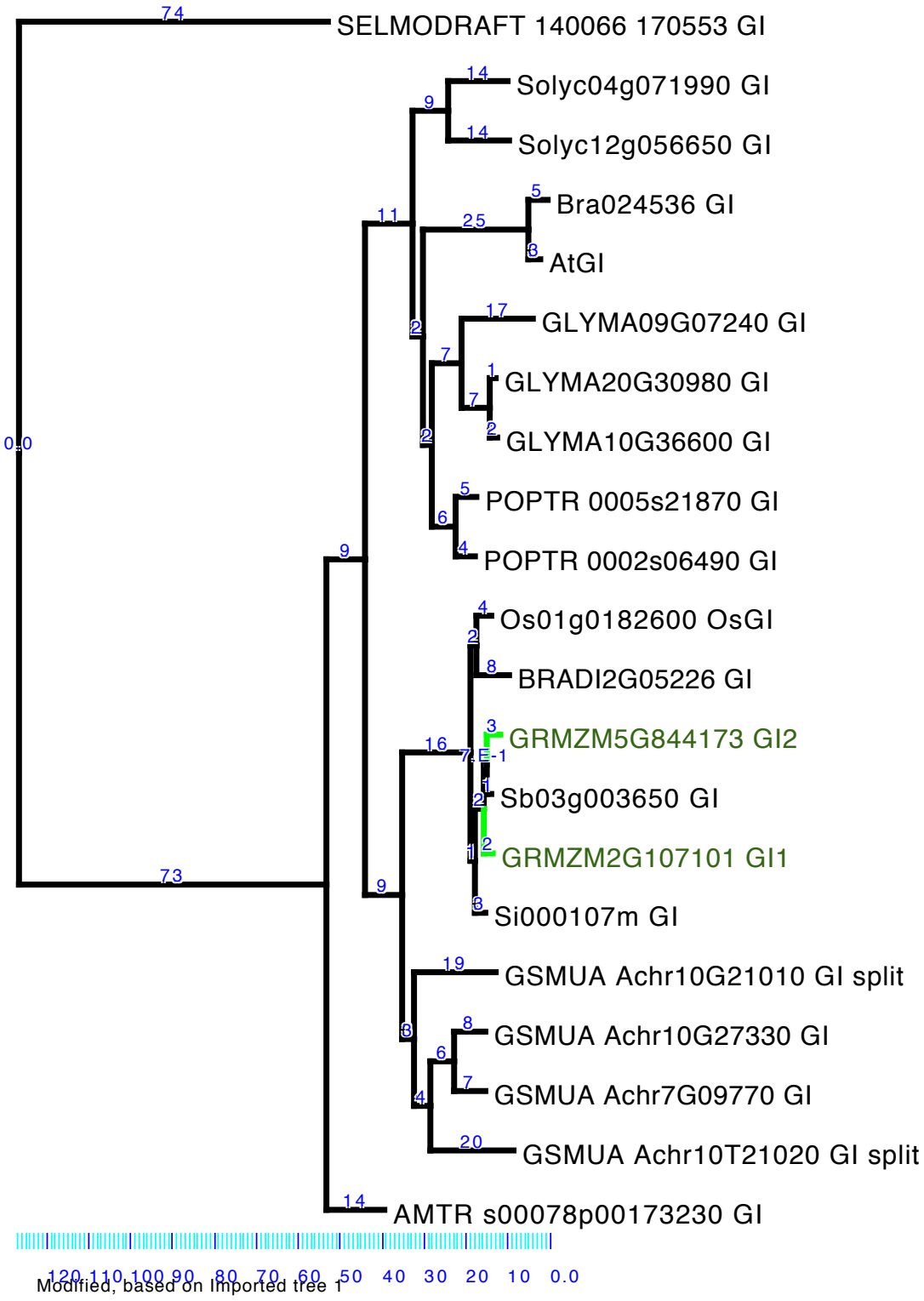
74
SELMODRAFT 140066 170553 GI
14
Solyc04g071990 GI
9
14
Solyc12g056650 GI
5
Bra024536 GI
11
25
8
AtGI
17
GLYMA09G07240 GI
2
7
1
GLYMA20G30980 GI
7
2
GLYMA10G36600 GI
0.0
5
POPTR 0005s21870 GI
6
4
POPTR 0002s06490 GI
9
4
Os01g0182600 OsGI
2
8
BRADI2G05226 GI
3
GRMZM5G844173 GI2
16
7
E-1
1
Sb03g003650 GI
2
1
2
GRMZM2G107101 GI1
73
9
3
Si000107m GI
19
GSMUA Achr10G21010 GI split
3
8
GSMUA Achr10G27330 GI
6
7
GSMUA Achr7G09770 GI
4
20
GSMUA Achr10T21020 GI split
14
AMTR s00078p00173230 GI
120 110 100 90 80 70 60 50 40 30 20 10 0.0
Modified, based on Imported tree 1

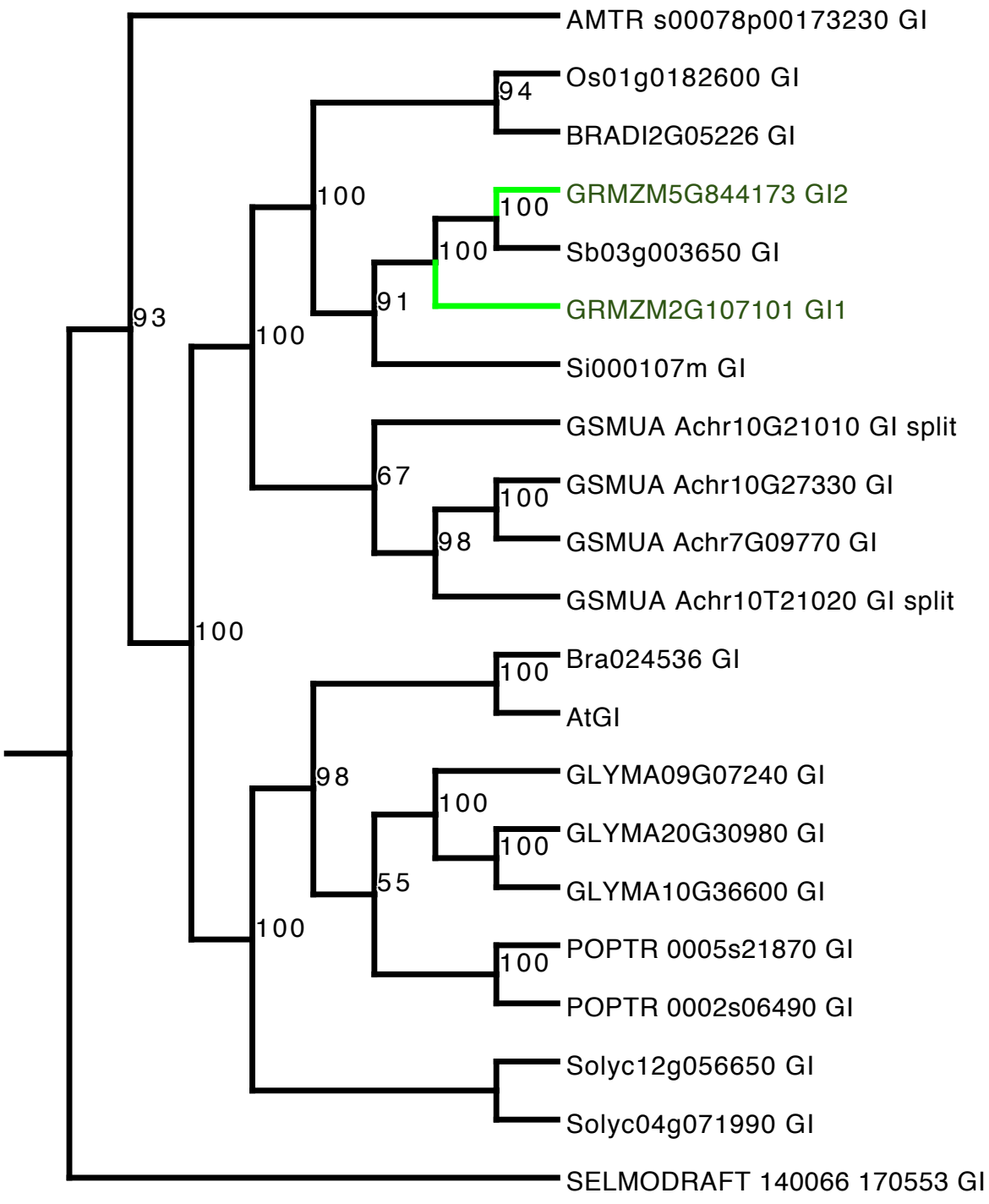

Figure 4.12 (this page and previous page). GI protein tree. Maize gene branches are highlighted in green, as are maize genes. On this page, numbers indicate percentage bootstrap values from 1000 rapid bootstrap inferences. On previous page, numbers indicate estimated branch lengths.

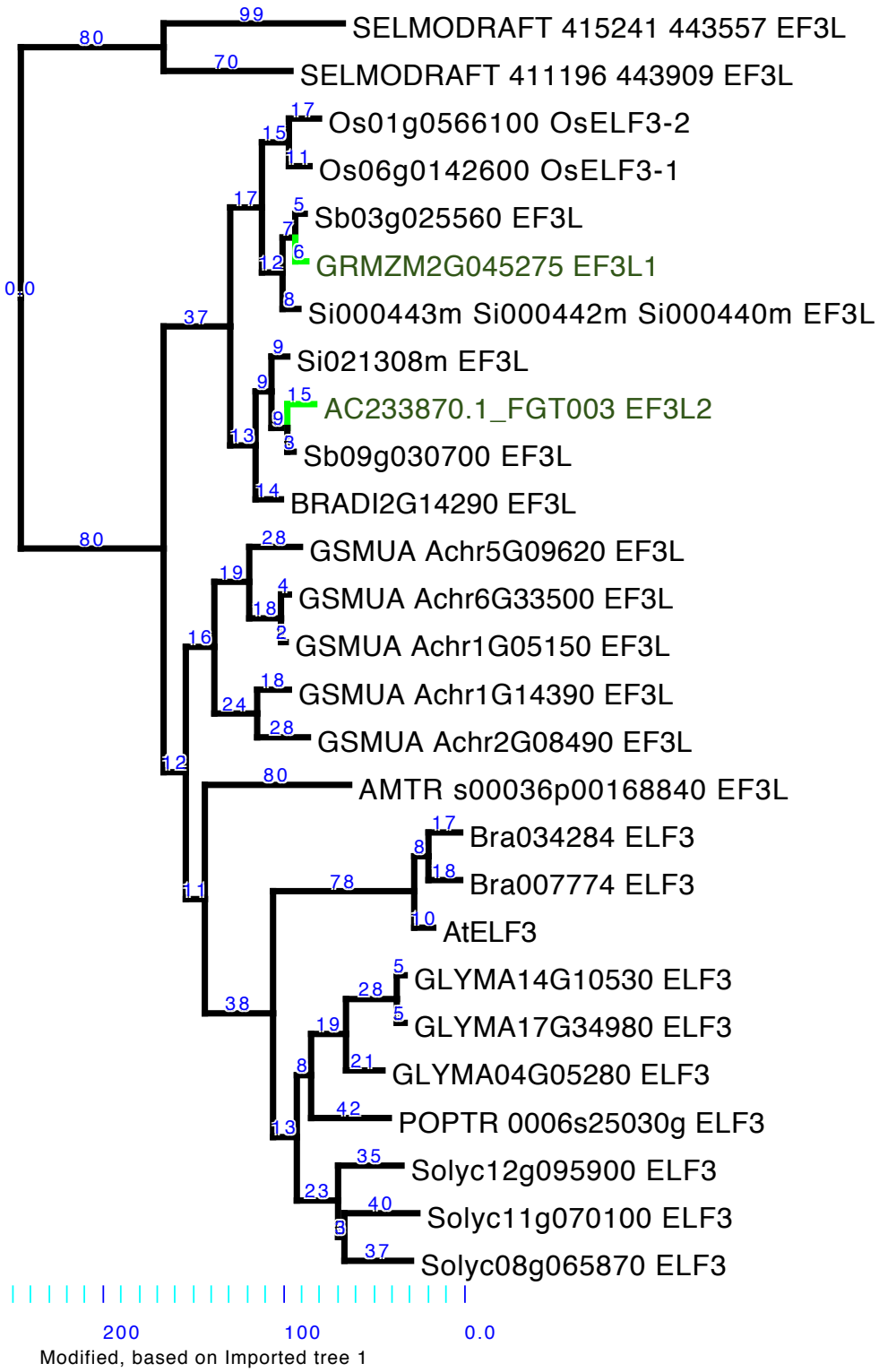
SELMODRAFT 415241 443557 EF3L
SELMODRAFT 411196 443909 EF3L
Os01g0566100 OsELF3-2
Os06g0142600 OsELF3-1
Sb03g025560 EF3L
GRMZM2G045275 EF3L1
Si000443m Si000442m Si000440m EF3L
Si021308m EF3L
AC233870.1_FGT003 EF3L2
Sb09g030700 EF3L
BRADI2G14290 EF3L
GSMUA Achr5G09620 EF3L
GSMUA Achr6G33500 EF3L
GSMUA Achr1G05150 EF3L
GSMUA Achr1G14390 EF3L
GSMUA Achr2G08490 EF3L
AMTR s00036p00168840 EF3L
Bra034284 ELF3
Bra007774 ELF3
AtELF3
GLYMA14G10530 ELF3
GLYMA17G34980 ELF3
GLYMA04G05280 ELF3
POPTR 0006s25030g ELF3
Solyc12g095900 ELF3
Solyc11g070100 ELF3
Solyc08g065870 ELF3
200
100
0.0
Modified, based on Imported tree 1

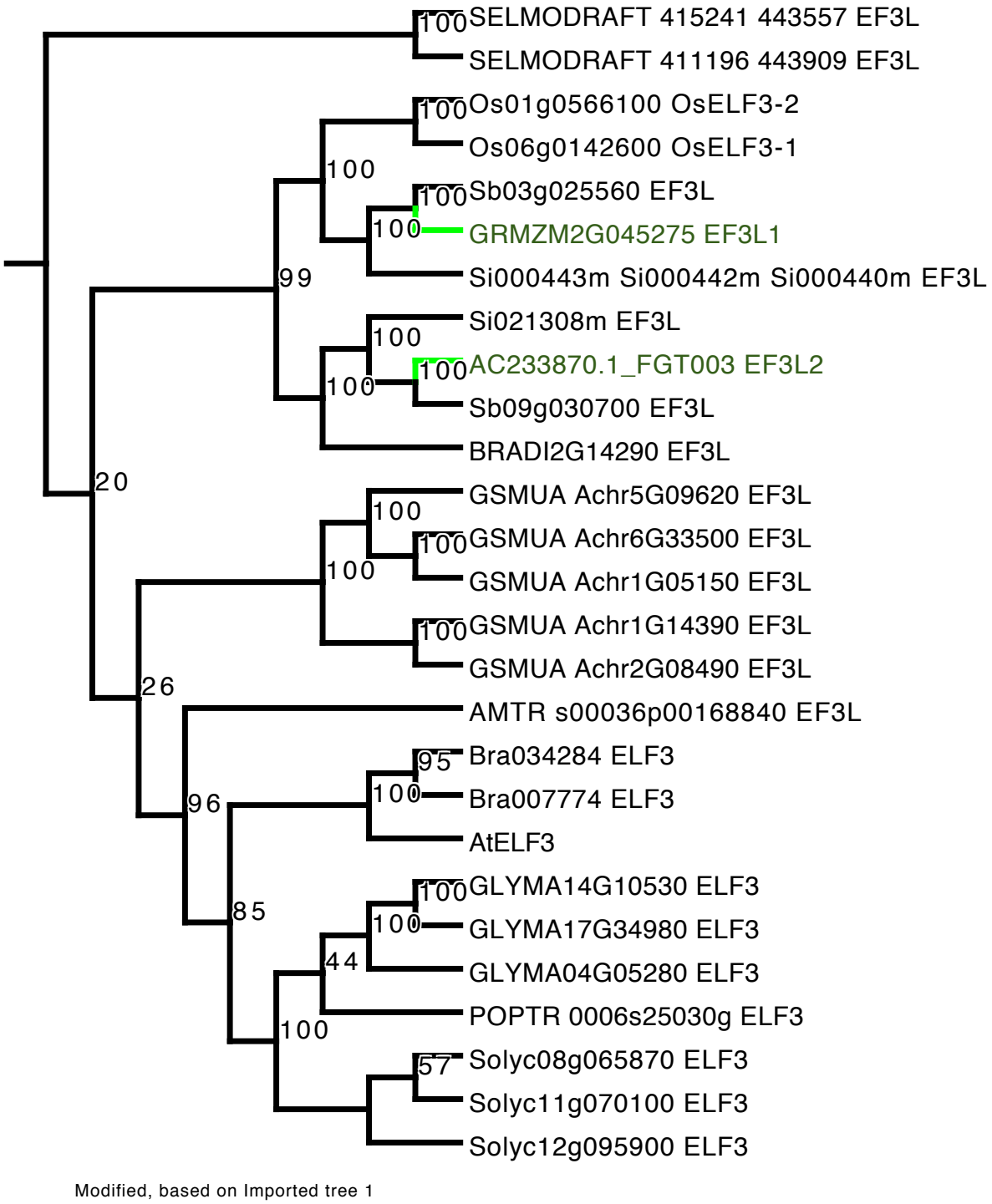

Figure 4.13 (this page and previous page). ELF3 protein tree. Maize gene branches are highlighted in green, as are maize genes. On this page, numbers indicate percentage bootstrap values from 1000 rapid bootstrap inferences. On previous page, numbers indicate estimated branch lengths.

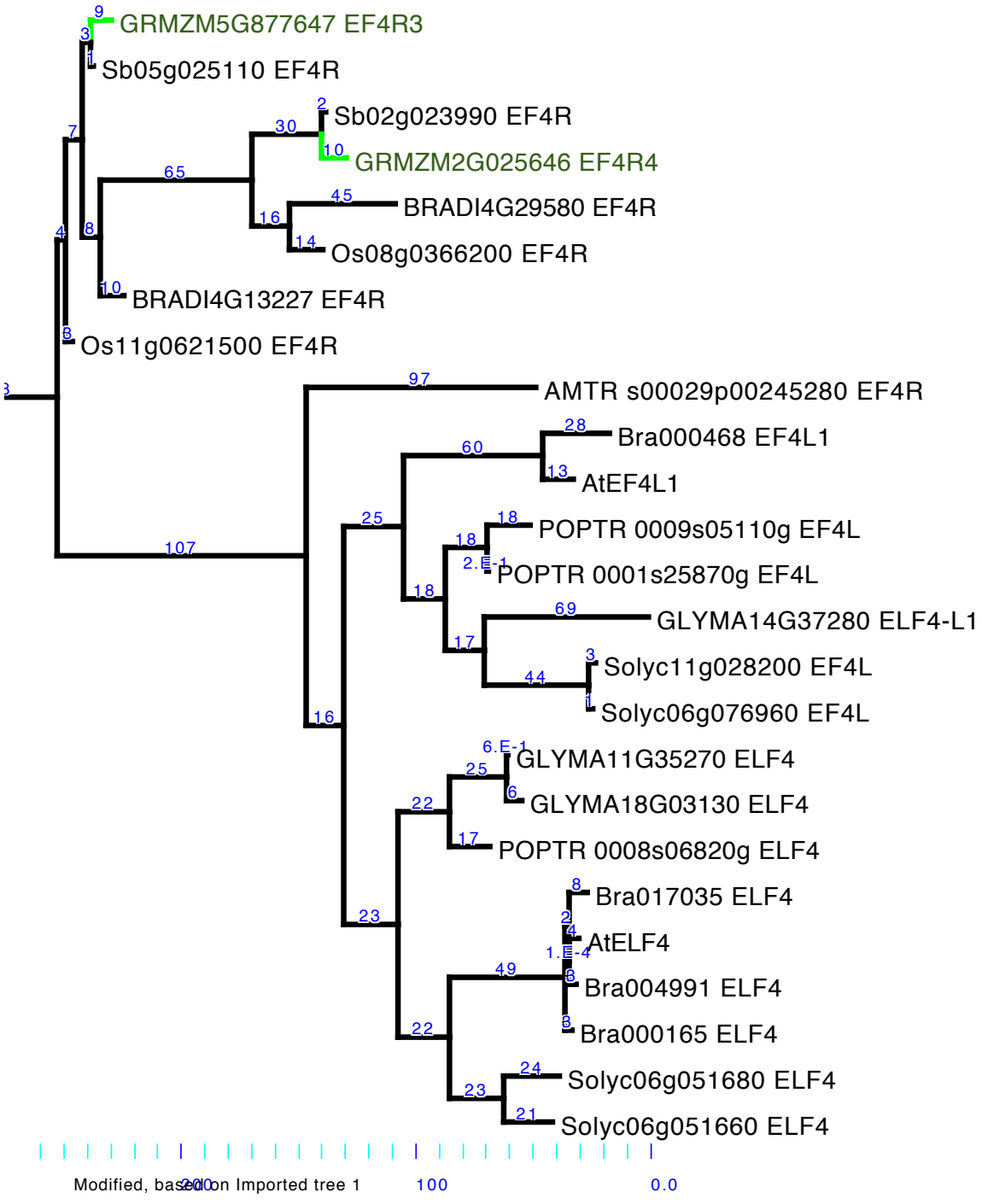
GRMZM5G877647 EF4R3
Sb05g025110 EF4R
Sb02g023990 EF4R
GRMZM2G025646 EF4R4
BRADI4G29580 EF4R
Os08g0366200 EF4R
BRADI4G13227 EF4R
Os11g0621500 EF4R
AMTR s00029p00245280 EF4R
Bra000468 EF4L1
AtEF4L1
POPTR 0009s05110g EF4L
POPTR 0001s25870g EF4L
GLYMA14G37280 ELF4-L1
Solyc11g028200 EF4L
Solyc06g076960 EF4L
GLYMA11G35270 ELF4
GLYMA18G03130 ELF4
POPTR 0008s06820g ELF4
Bra017035 ELF4
AtELF4
Bra004991 ELF4
Bra000165 ELF4
Solyc06g051680 ELF4
Solyc06g051660 ELF4
Modified, based on Imported tree 1
200
100
0.0

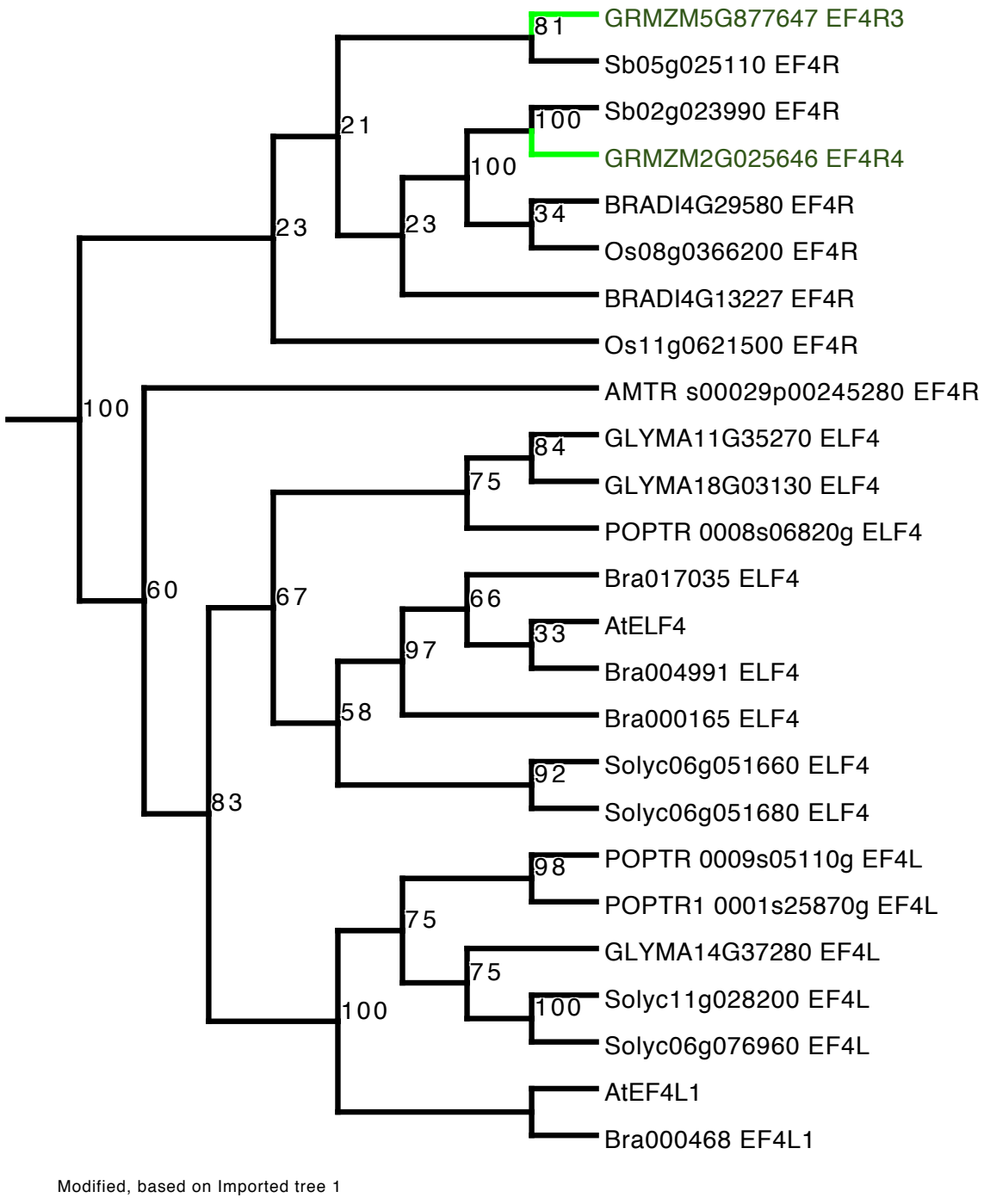

Modified, based on Imported tree 1

Figure 4.14 (this page and previous page). EF4R and ELF4/EF4L1 protein subtree (see Supplemental Figure 4.2.C). Maize gene branches are highlighted in green, as are maize genes. On this page, numbers indicate percentage bootstrap values from 1000 rapid bootstrap inferences. On previous page, numbers indicate estimated branch lengths.

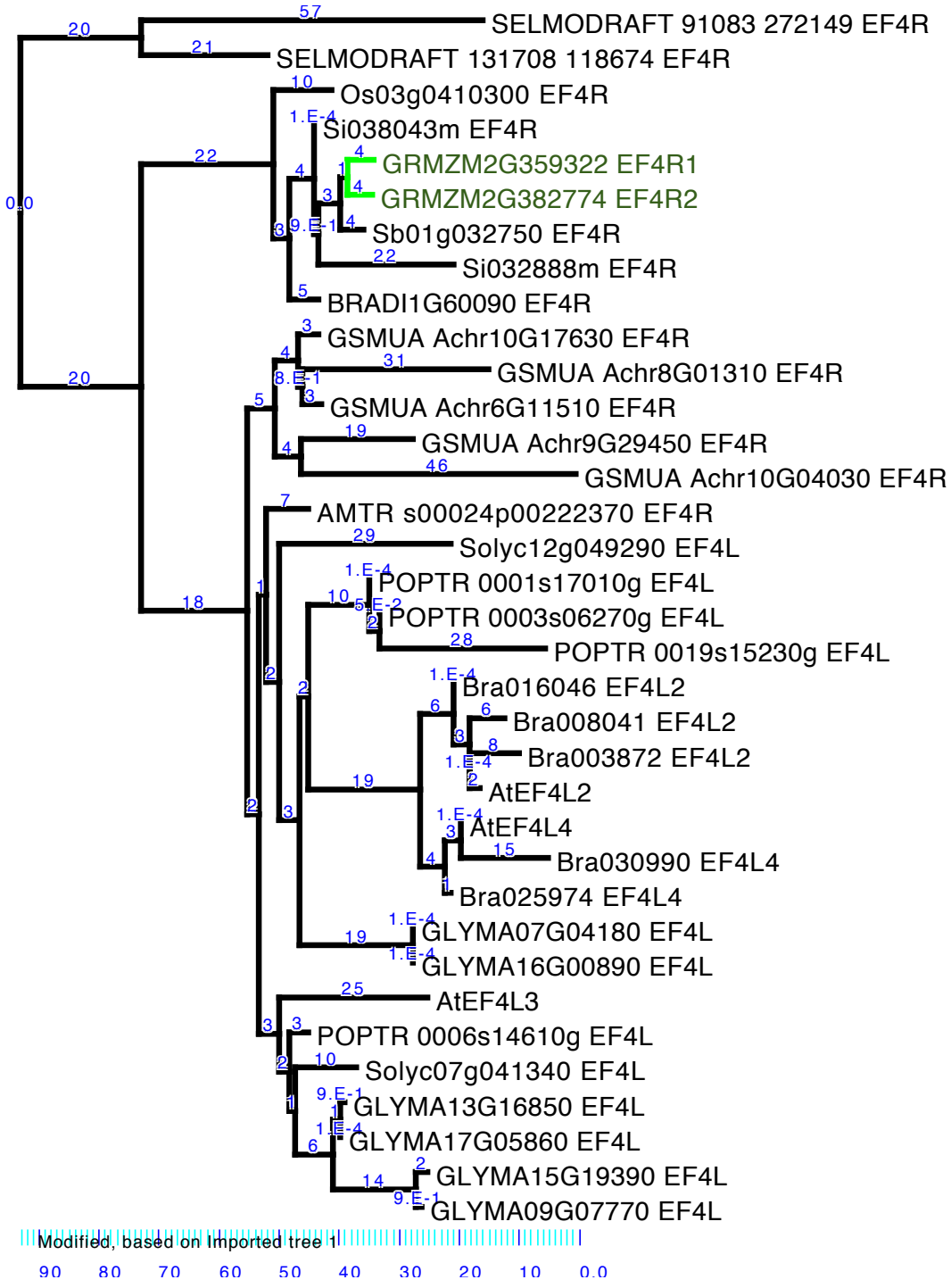
SELMODRAFT 91083 272149 EF4R
SELMODRAFT 131708 118674 EF4R
Os03g0410300 EF4R
Si038043m EF4R
GRMZM2G359322 EF4R1
GRMZM2G382774 EF4R2
Sb01g032750 EF4R
Si032888m EF4R
BRADI1G60090 EF4R
GSMUA Achr10G17630 EF4R
GSMUA Achr8G01310 EF4R
GSMUA Achr6G11510 EF4R
GSMUA Achr9G29450 EF4R
GSMUA Achr10G04030 EF4R
AMTR s00024p00222370 EF4R
Solyc12g049290 EF4L
POPTR 0001s17010g EF4L
POPTR 0003s06270g EF4L
POPTR 0019s15230g EF4L
Bra016046 EF4L2
Bra008041 EF4L2
Bra003872 EF4L2
AtEF4L2
AtEF4L4
Bra030990 EF4L4
Bra025974 EF4L4
GLYMA07G04180 EF4L
GLYMA16G00890 EF4L
AtEF4L3
POPTR 0006s14610g EF4L
Solyc07g041340 EF4L
GLYMA13G16850 EF4L
GLYMA17G05860 EF4L
GLYMA15G19390 EF4L
GLYMA09G07770 EF4L
Modified, based on Imported tree 1
90 80 70 60 50 40 30 20 10 0.0

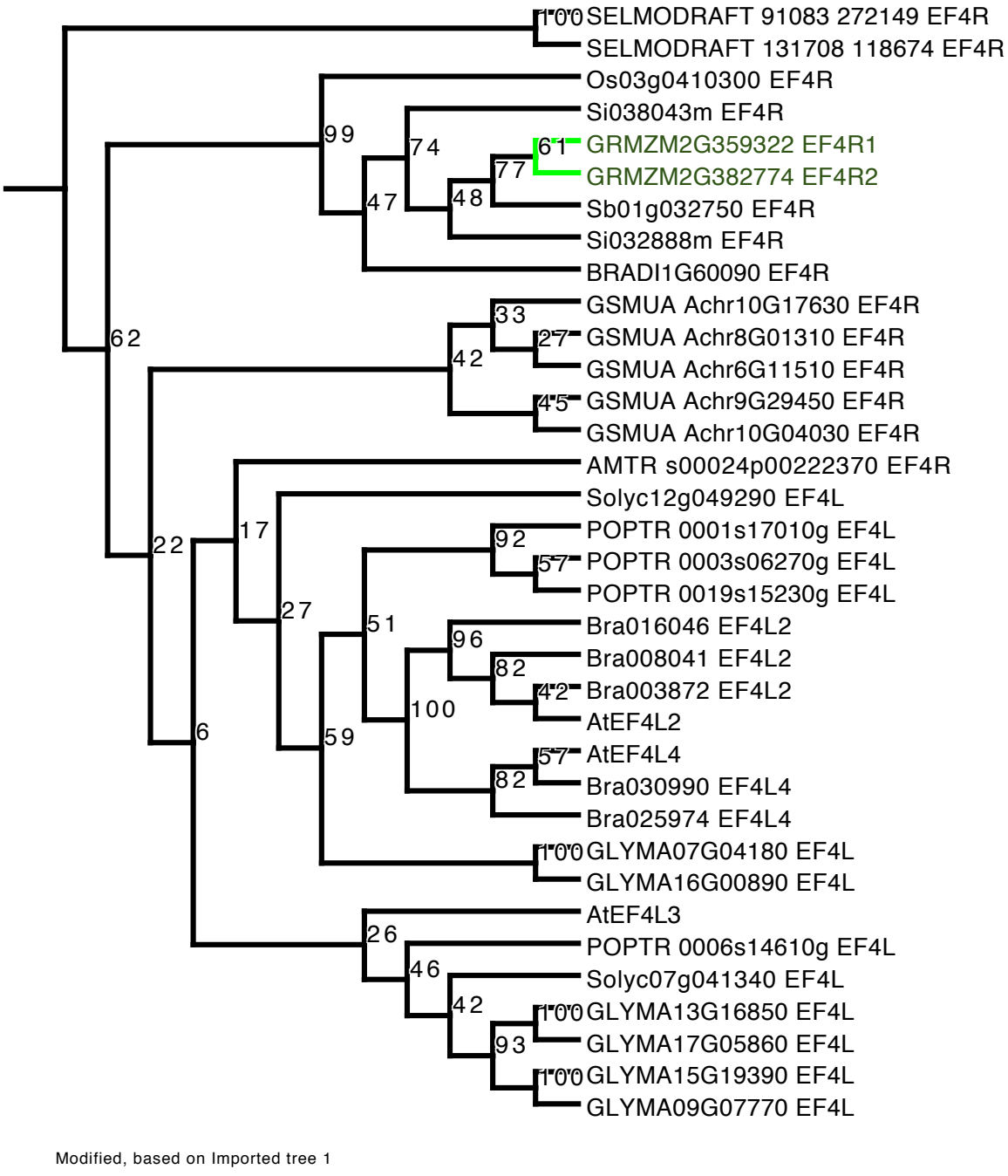

Figure 4.15 (this page and previous page). EF4R and EF4L2/3/4 protein subtree (see Supplemental Figure 4.2.C). Maize gene branches are highlighted in green, as are maize genes. On this page, numbers indicate percentage bootstrap values from 1000 rapid bootstrap inferences. On previous page, numbers indicate estimated branch lengths.

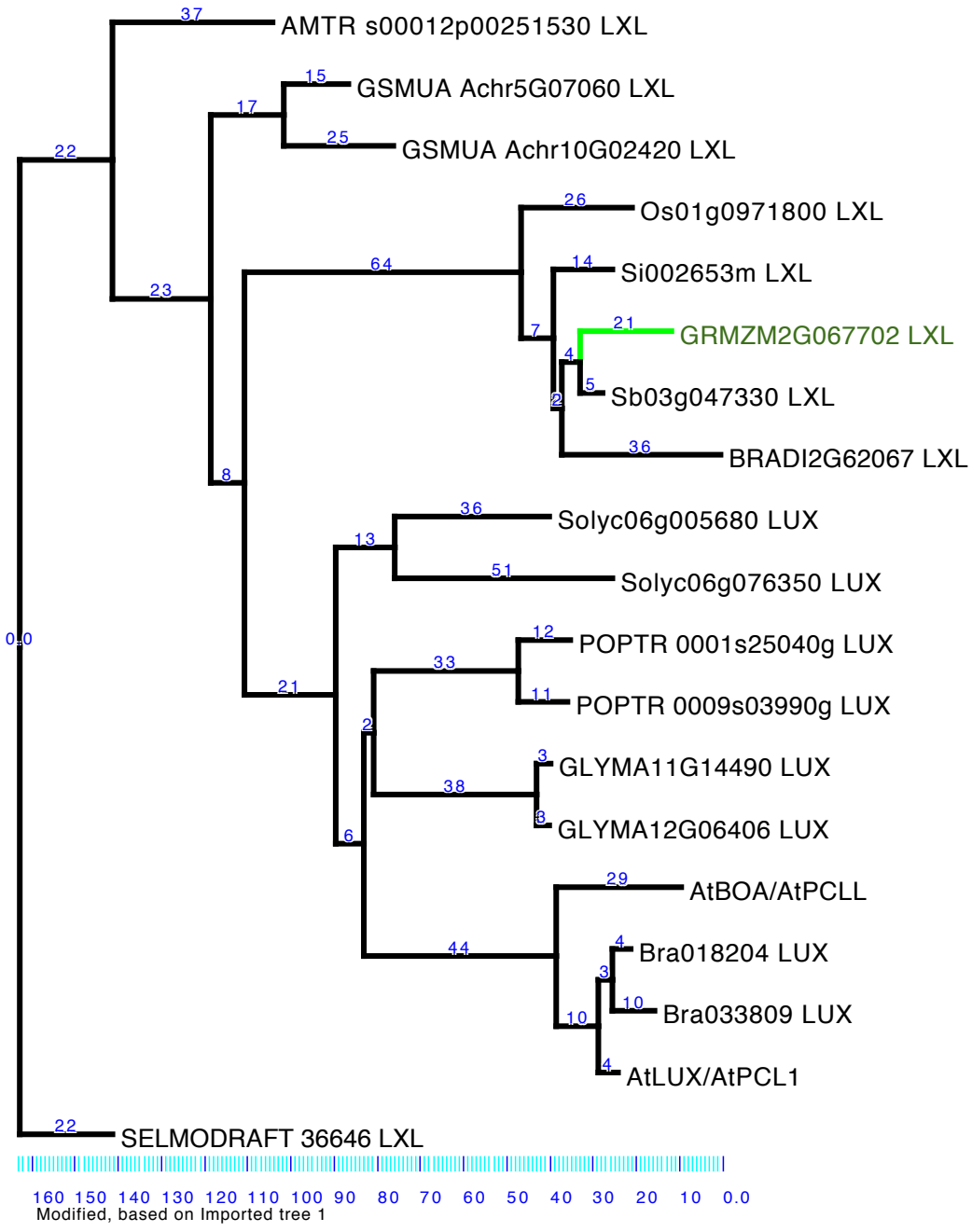
AMTR s00012p00251530 LXL
GSMUA Achr5G07060 LXL
GSMUA Achr10G02420 LXL
Os01g0971800 LXL
Si002653m LXL
GRMZM2G067702 LXL
Sb03g047330 LXL
BRADI2G62067 LXL
Solyc06g005680 LUX
Solyc06g076350 LUX
POPTR 0001s25040g LUX
POPTR 0009s03990g LUX
GLYMA11G14490 LUX
GLYMA12G06406 LUX
AtBOA/AtPCLL
Bra018204 LUX
Bra033809 LUX
AtLUX/AtPCL1
SELMODRAFT 36646 LXL
160 150 140 130 120 110 100 90 80 70 60 50 40 30 20 10 0.0
Modified, based on Imported tree 1

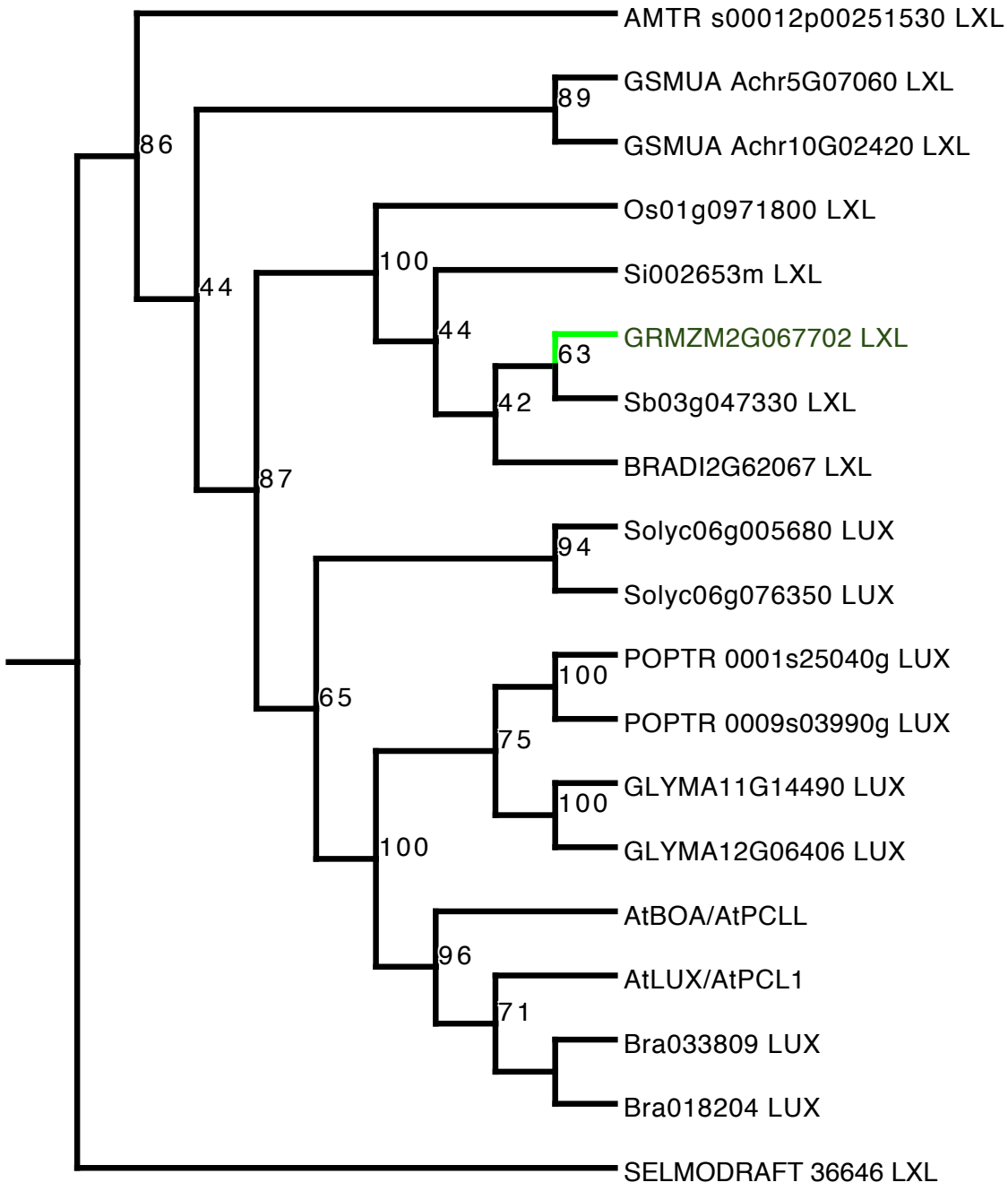

Edited, based on Imported tree 1

Figure 4.16 (this page and previous page). LUX protein tree. Maize gene branches are highlighted in green, as are maize genes. On this page, numbers indicate percentage bootstrap values from 1000 rapid bootstrap inferences. On previous page, numbers indicate estimated branch lengths.

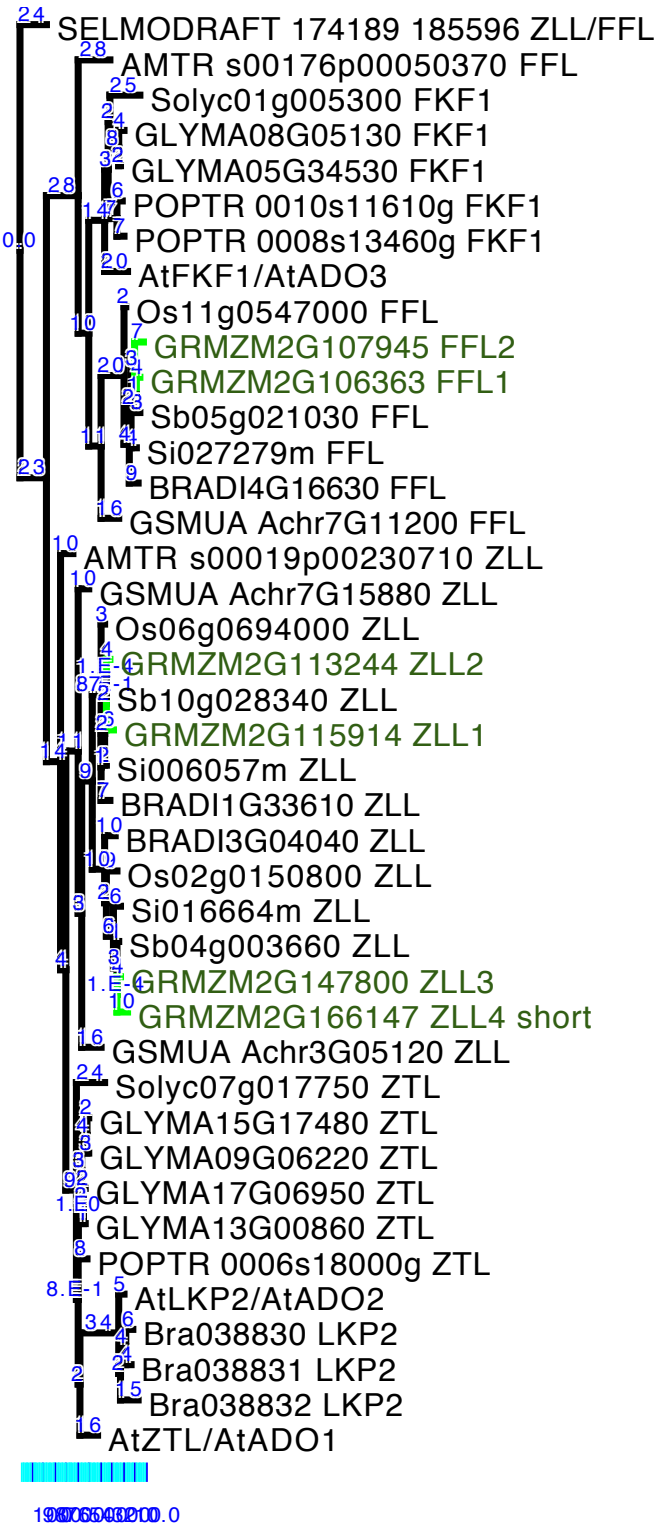

Modified, based on Imported tree 1

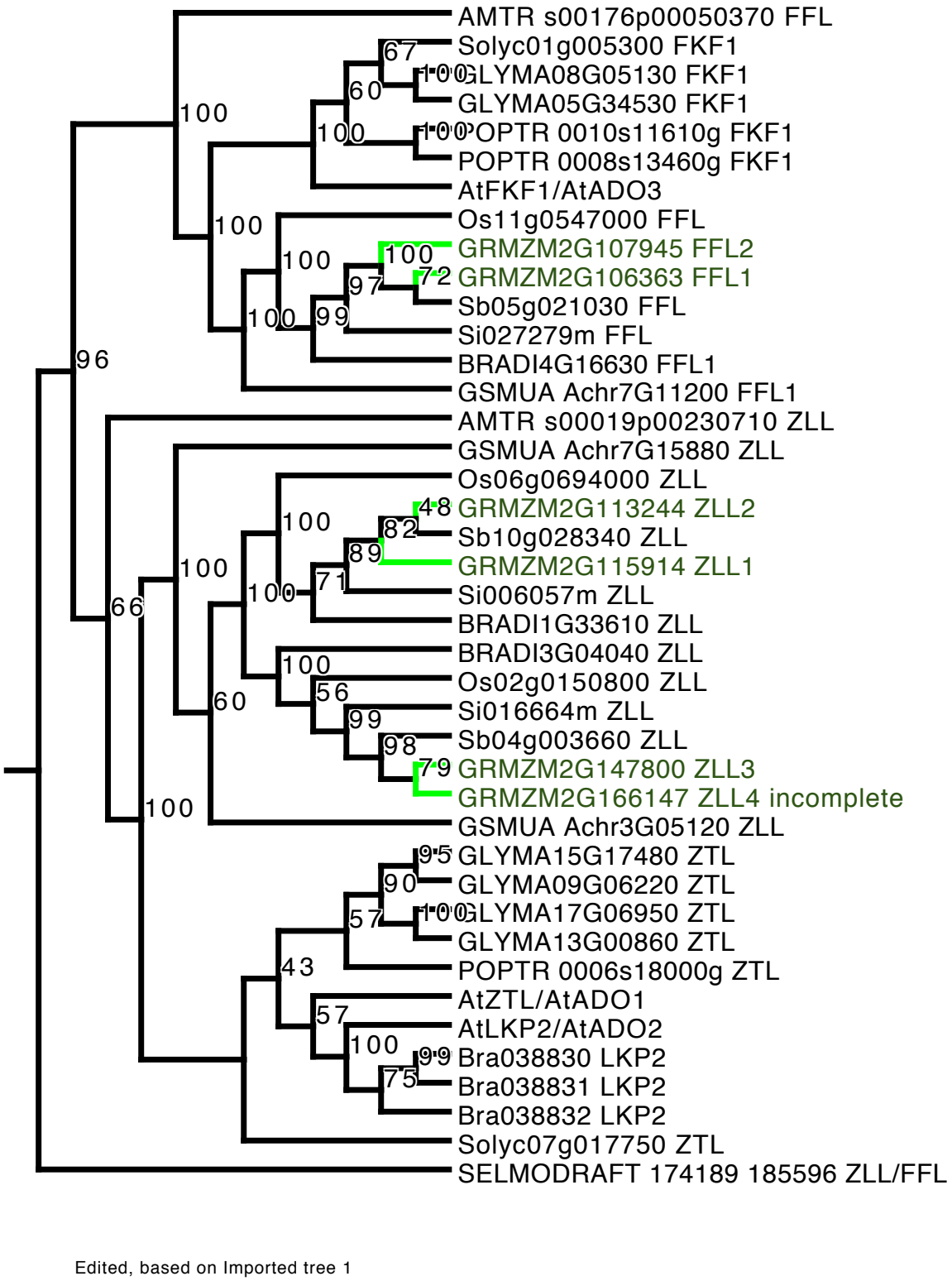

Figure 4.17 (this page and previous page). ZTL, LKP2, and FKF1 protein tree. Maize gene branches are highlighted in green, as are maize genes. On this page, numbers indicate percentage bootstrap values from 1000 rapid bootstrap inferences. On previous page, numbers indicate estimated branch lengths.

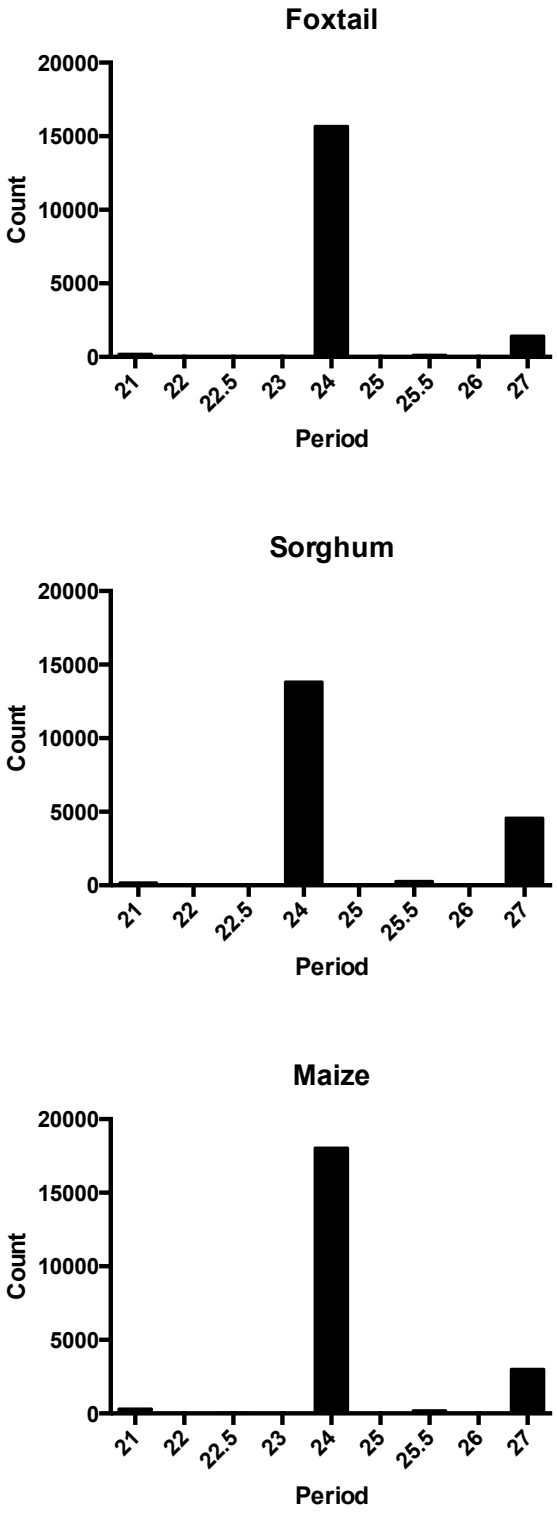

Figure 4.18. Estimated periods of the filtered rhythmic data sets according to JTK-cycle.

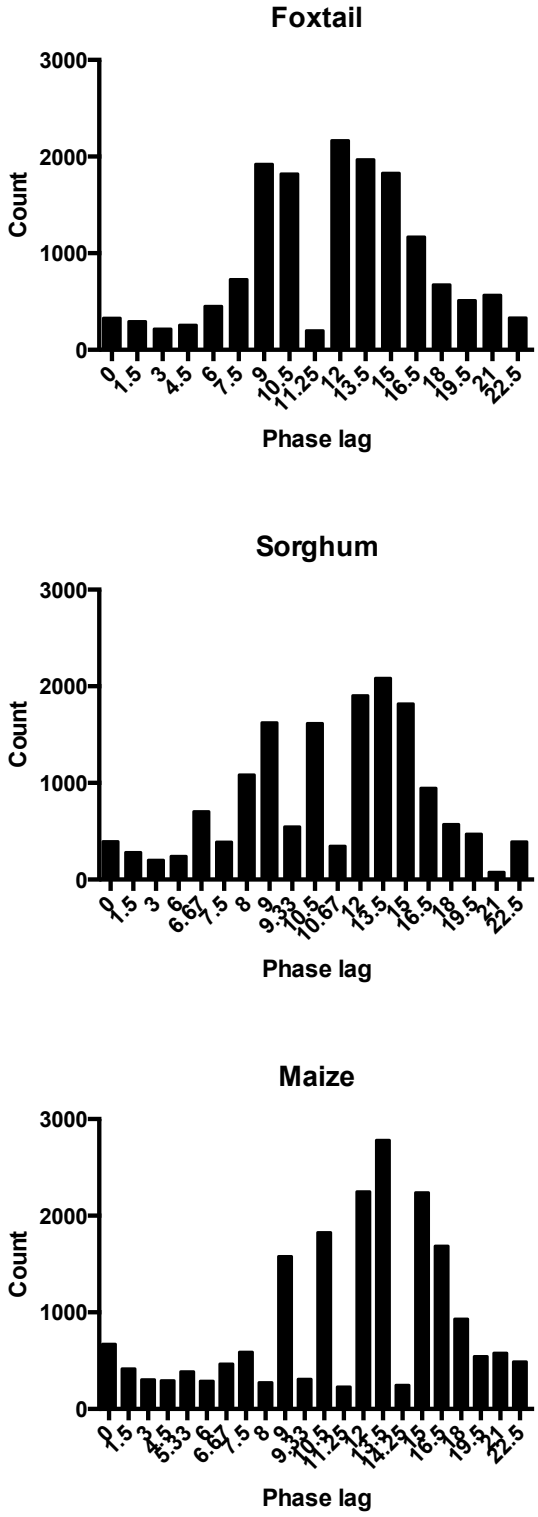

Figure 4.19. Phases of the filtered rhythmic data sets according to JTK-cycle, and adjusted for a 24 hour period. Many more phase bins were called by JTK, but only those that represented 1/100th or more of the total rhythmic gene set were graphed.

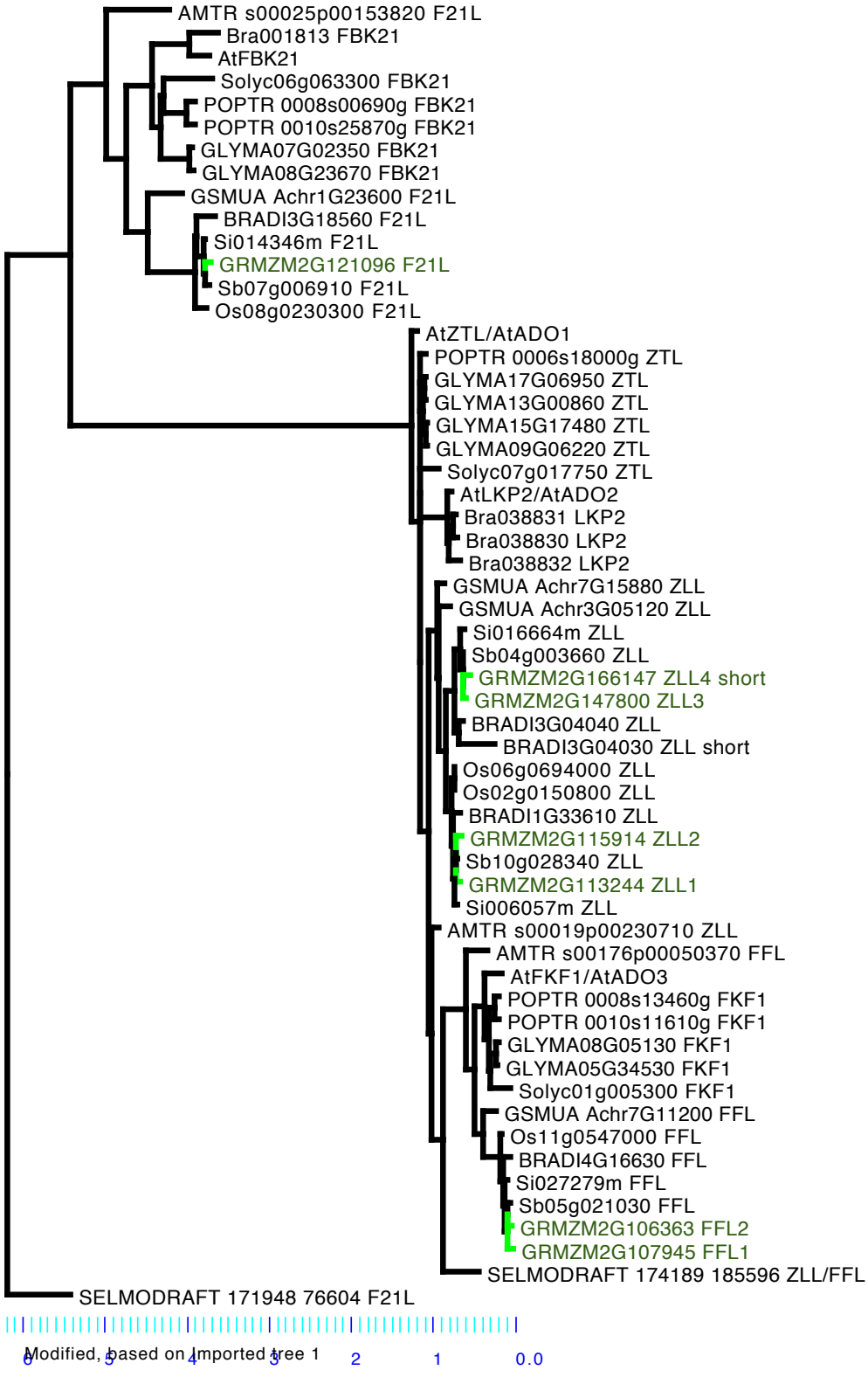
AMTR s00025p00153820 F21L
Bra001813 FBK21
AtFBK21
Solyc06g063300 FBK21
POPTR 0008s00690g FBK21
POPTR 0010s25870g FBK21
GLYMA07G02350 FBK21
GLYMA08G23670 FBK21
GSMUA Achr1G23600 F21L
BRADI3G18560 F21L
Si014346m F21L
GRMZM2G121096 F21L
Sb07g006910 F21L
Os08g0230300 F21L
AtZTL/AtADO1
POPTR 0006s18000g ZTL
GLYMA17G06950 ZTL
GLYMA13G00860 ZTL
GLYMA15G17480 ZTL
GLYMA09G06220 ZTL
Solyc07g017750 ZTL
AtLKP2/AtADO2
Bra038831 LKP2
Bra038830 LKP2
Bra038832 LKP2
GSMUA Achr7G15880 ZLL
GSMUA Achr3G05120 ZLL
Si016664m ZLL
Sb04g003660 ZLL
GRMZM2G166147 ZLL4 short
GRMZM2G147800 ZLL3
BRADI3G04040 ZLL
BRADI3G04030 ZLL short
Os06g0694000 ZLL
Os02g0150800 ZLL
BRADI1G33610 ZLL
GRMZM2G115914 ZLL2
Sb10g028340 ZLL
GRMZM2G113244 ZLL1
Si006057m ZLL
AMTR s00019p00230710 ZLL
AMTR s00176p00050370 FFL
AtFKF1/AtADO3
POPTR 0008s13460g FKF1
POPTR 0010s11610g FKF1
GLYMA08G05130 FKF1
GLYMA05G34530 FKF1
Solyc01g005300 FKF1
GSMUA Achr7G11200 FFL
Os11g0547000 FFL
BRADI4G16630 FFL
Si027279m FFL
Sb05g021030 FFL
GRMZM2G106363 FFL2
GRMZM2G107945 FFL1
SELMODRAFT 174189 185596 ZLL/FFL
SELMODRAFT 171948 76604 F21L
Modified, based on Imported tree 1
6
5
4
3
2
1
0.0

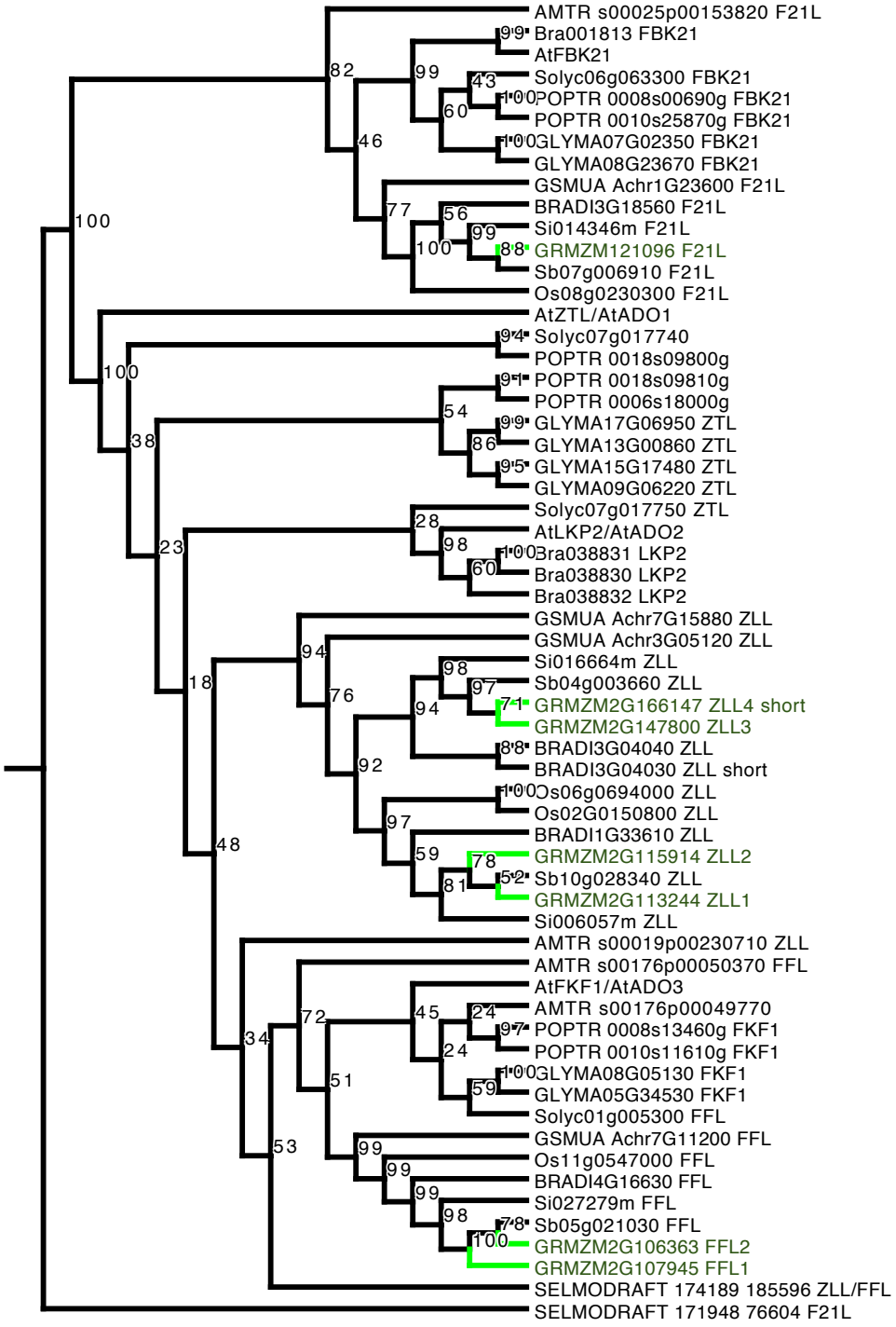

Figure 4.20 (this page and previous page). ZTL, LKP2, FKF1, and FBK21 tree. Maize gene branches are highlighted in green, as are maize genes. On this page, numbers indicate percentage bootstrap values from 1000 rapid bootstrap inferences. On previous page, numbers indicate estimated branch lengths.

Tables

AT number	Protein name	Size (aa)	Protein domains (Prosite/Pfam)	Uniprot
AT1G01060	LATE ELONGATED HYPOCOTYL (LHY)	645	Myb-type HTH DNA-binding domain/ Myb DNA-binding domain	Q6R0H1
AT2G46830	CIRCADIAN CLOCK ASSOCIATED 1 (CCA1)	608	Myb-type HTH DNA-binding domain/Myb DNA-binding domain	P92973
AT5G17300	REVEILLE1 (RVE1)	387	Myb-type HTH DNA-binding domain/Myb DNA-binding domain	F4KGY6
AT5G37260	REVEILLE2 (RVE2)	287	Myb-type HTH DNA-binding domain/Myb DNA-binding domain	F4K5X6
AT5G02840	REVEILLE4 (RVE4)	293	Myb-type HTH DNA-binding domain/Myb DNA-binding domain	Q6R0G4
AT4G01280	REVEILLE5 (RVE5)	303	Myb-type HTH DNA-binding domain/Myb DNA-binding domain	C0SVG5
AT5G52660	REVEILLE6 (RVE6)	331	Myb-type HTH DNA-binding domain/Myb DNA-binding domain	Q8H0W3
AT1G18330	REVEILLE7 (RVE7)	372	Myb-type HTH DNA-binding domain/Myb DNA-binding domain	B3H5A8
AT3G09600	REVEILLE8 (RVE8)	298	Myb-type HTH DNA-binding domain/Myb DNA-binding domain	Q8RWU3
AT5G61380	TIMING OF CAB EXPRESSION 1 (TOC1)/PRR1	618	Response regulator receiver domain, CCT motif	Q9LKL2
AT5G60100	PSEUDO-RESPONSE REGULATOR 3 (PRR3)	522	Response regulator receiver domain, CCT motif	F4JXG7
AT5G49240	PSEUDO-RESPONSE REGULATOR 4 (PRR4)	292	Response regulator receiver domain	Q9FJ16
AT5G24470	PSEUDO-RESPONSE REGULATOR 5 (PRR5)	667	Response regulator receiver domain, CCT motif	Q6LA42
AT5G02810	PSEUDO-RESPONSE REGULATOR 7 (PRR7)	727	Response regulator receiver domain, CCT motif	Q93WK5
AT2G46790	PSEUDO-RESPONSE REGULATOR 9 (PRR9)	468	Response regulator receiver domain, CCT motif	Q8L500
AT1G22770	GIGANTEA (GI)	1173	No domains detected	Q9SQI2
AT2G25930	EARLY FLOWERING 3 (ELF3)	695	No domains detected	O82804
AT2G40080	EARLY FLOWERING 4 (ELF4)	111	No domains detected/DUF1313	O04211
AT2G29950	ELF4-like 1 (EF4L1)	125	No domains detected/DUF1313	O80877
AT1G72630	ELF4-like 2 (EF4L2)	119	No domains detected/DUF1313	Q94BS8
AT2G06255	ELF4-like 3 (EF4L3)	109	No domains detected/DUF1313	Q8S8F5
AT1G17455	ELF4-like 4 (EF4L4)	114	No domains detected/DUF1313	Q570U6
AT3G46640	LUX ARRHYTHMO (LUX)/PHYTOCLOCK 1	324	Myb-type HTH DNA-binding domain/Myb DNA-binding domain	F4J959

AT number	Protein name	Size (aa)	Protein domains (Prosite/Pfam)	Uniprot
	(PCL1)			
AT5G59570	BROTHER OF LUX ARRHYTHMO (BOA)	398	Myb-type HTH DNA-binding domain/Myb DNA-binding domain	F4J959
AT5G57360	ZEITLUPE (ZTL)/ADAGIO 1 (ADO1)	626	PAS repeat, F-box domain/PAS domain, F-box-like, Kelch 4, Kelch 3, Kelch 3	F4KAN2
AT2G18915	LOV KELCH PROTEIN 2 (LKP2)/ADAGIO 2 (ADO2)	611	PAS repeat/PAS domain,F-box-like, Kelch 4, Kelch 3, Kelch 3, Kelch 2	Q8W420
AT1G68050	FLAVIN-BINDING, KELCH REPEAT, F BOX 1 (FKF1)/ADAGIO 3 (ADO3)	619	PAS repeat/PAS domain, Kelch 4, Kelch 3, Kelch 3, Kelch 2	Q9C9W9

Table 4.1. Arabidopsis clock and clock-associated proteins. Size is in amino acids (aa), and protein domain results are from Prosite (before the /) and Pfam (after the /).

Species	% of genes that are rhythmic	Paper
Dicots		
Glycine max	35.5% in diurnal conditions; 40% under drought stress	Rodrigues et al. 2015
Populus trichocarpa	~15% in circadian conditions; ~30% in diurnal conditions; 60.9% total (all conditions combined)	Filichkin et al. 2011
Carica papaya	30-55% of time-of-day specific promoter elements conserved	Zdepski et al. 2008
Monocots		
Oryza sativa	~15% in circadian conditions; ~30% in diurnal conditions; 59.5% total (all conditions combined)	Filichkin et al. 2011
Saccharum spp.	54% under photocycles	Hotta et al. 2013
Zea mays	~25% under diurnal and free-running conditions	Hayes et al 2010; Khan et al. 2010

Table 4.2. Percentages of rhythmic genes reported in other species. See the listed papers for further details.

GRMZM number	Protein name	Size (aa)	Protein domains (Prosite/Pfam)	UniProt
GRMZM2G175265 + GRMZM2G474769^	LHY-LIKE 1 (LYL1)	718	Myb-type HTH DNA-binding domain/Myb-like DNA-binding domain	K7TLS4 + K7UFK5
GRMZM2G014902	LHY-LIKE 2 (LYL2)	720	Myb-type HTH DNA-binding domain/Myb-like DNA-binding domain	K7U156
GRMZM2G145041	RVE2-LIKE (RE2L)	432	Myb-type HTH DNA-binding domain/Myb-like DNA-binding domain	B6SW63
GRMZM2G135052	RVE6-LIKE 1 (RE6L1)	277	Myb-type HTH DNA-binding domain/Myb-like DNA-binding domain	K7VFQ6
GRMZM2G170148	RVE6-LIKE 2 (RE6L2)	310	Myb-type HTH DNA-binding domain/Myb-like DNA-binding domain	B4FU12
GRMZM2G057408	RVE6-LIKE 3 (RE6L3)	336	Myb-type HTH DNA-binding domain/Myb-like DNA-binding domain	C0PCQ5
GRMZM5G833032	RVE6-LIKE 4 (RE6L4)	293	Myb-type HTH DNA-binding domain/Myb-like DNA-binding domain	B4FKM3
GRMZM2G118693	RVE6-LIKE 5 (RE6L5)	284	Myb-type HTH DNA-binding domain/Myb-like DNA-binding domain	B4G188
GRMZM2G029850	RVE7-LIKE 1 (RE7L1)	441	Myb-type HTH DNA-binding domain/Myb-like DNA-binding domain	C0HJ55
GRMZM2G170322	RVE7-LIKE 2 (RE7L2)	464	Myb-type HTH DNA-binding domain/No domains found	B4FFA6
GRMZM2G421256	RVE7-LIKE 3 (RE7L3)	344	Myb-type HTH DNA-binding domain/Myb-like DNA-binding domain	C0HI52
GRMZM2G181030	RVE7-LIKE 4 (RE7L4)	453	Myb-type HTH DNA-binding domain/Myb-like DNA-binding domain	B4FVU9
GRMZM2G115070	RVE8-LIKE 2 (RE8L2)	186	Myb-type HTH DNA-binding domain/Myb-like DNA-binding domain	B6SQ50
GRMZM2G415077	RVE8-LIKE 1 (RE8L1)	171	Myb-type HTH DNA-binding domain/Myb-like DNA-binding domain	B6UG21

GRMZM number	Protein name	Size (aa)	Protein domains (Prosite/Pfam)	UniProt
GRMZM2G148453^	TOC1-LIKE 1 (T1L1)	517	Response regulator receiver domain, CCT motif	A0A096SH15
GRMZM2G020081	TOC1-LIKE 2 (T1L2)	523	Response regulator receiver domain, CCT motif	F1DJY9
GRMZM2G145058*	TOC1-LIKE 3 (T1L3)	387	Response regulator receiver domain/no domains detected	A0A096SEN6
GRMZM2G365688*	TOC1-LIKE 4 (T1L4)	776	IQ motif/ATPase family	A0A096TFA9
GRMZM2G066638*	TOC1-LIKE 5 (T1L5)	576	Response regulator receiver domain, myosin motor domain, IQ motif/Myosin head (motor domain), IQ calmodulin-binding motif	A0A096SYW0
GRMZM2G174083*	TOC1-LIKE 6 (T1L6)	576	Response regulator receiver domain, myosin motor domain, IQ domain/Myosin head (motor domain), IQ calmodulin-binding motif	A0A096SYW0
GRMZM2G005732^	PRR37-LIKE 1 (P37L1)	740	CCT motif, Response regulator receiver domain	A0A096PTA7
GRMZM2G033962	PRR37-LIKE 2 (P37L2)	657	Response regulator receiver domain, CCT motif	Z0A096QBI8
GRMZM2G379656*	PRR4-LIKE (P4L)	145	Myb-type HTH DNA-binding domain/No domains detected	A0A096THR1
GRMZM2G488465^	PRR59-LIKE 2 (P59L2)	509	Response regulator receiver domain, CCT motif	K7UBT8
GRMZM2G135446^	PRR59-LIKE 1 (P59L1)	637	Response regulator receiver domain, CCT motif	B4FPX9
GRMZM2G095727	PRR73-LIKE (P73L)	766	Response regulator receiver domain, CCT motif	B8A2Q1
GRMZM2G179024	PRR95-LIKE 1 (P95L1)	629	Response regulator receiver domain, CCT motif	B4FWH6
GRMZM2G367834	PRR95-LIKE 2 (P95L2)	596	Response regulator receiver domain, CCT motif	A0A096TFQ0
GRMZM2G107101	GIGANTEA 1 (GI1)	1162	No domains found	B1H3M2
GRMZM5G844173	GIGANTEA 2 (GI2)	1160	No domains found	A0A096UBI9
GRMZM2G045275	ELF3-LIKE 1 (EF3L1)	756	Ribosome-binding factor A signature/No domains found	C0PGT6
AC233870.1_FG003	ELF3-LIKE 2	647	Ribosome-binding factor A	K7V8A5

GRMZM number	Protein name	Size (aa)	Protein domains (Prosite/Pfam)	UniProt
	(EF3L2)		signature/No domains found	
GRMZM2G382774	ELF4-RELATED 1 (EF4R1)	124	No domains found/DUF1313	B6SXG0
GRMZM2G359322	ELF4-RELATED 2 (EF4R2)	118	No domains found/DUF1313	B6SH35
GRMZM5G877647	ELF4-RELATED 3 (EF4R3)	129	No domains found/DUF1313	B7ZZS3
GRMZM2G025646	ELF4-RELATED 4 (EF4R4)	143	No domains found/DUF1313	B4FX35
GRMZM2G067702	LUX-LIKE (LXL)	219	Myb-type HTH DNA-binding domain/Myb-like DNA-binding domain	K7V8Y4
GRMZM2G115914	ZTL-LIKE 1 (ZLL1)	408	F-box domain/F-box-like, Kelch 4, Kelch 3, Kelch 3, Kelch 2	A0A096RVXY
GRMZM2G113244	ZTL-LIKE 2 (ZLL2)	630	PAS repeat/PAS domain, F-box-like, Kelch 4, Kelch 3, Kelch 3	K7UHC1
GRMZM2G147800	ZTL-LIKE 3 (ZLL3)	609	PAS repeat/PAS domain, F-box-like, Kelch 4, Kelch 3, Kelch 3, Kelch 4	A0A096SGM0
GRMZM2G166147*	ZTL-LIKE 4 (ZLL4)	108	No domains found/Kelch 4	K7V775
GRMZM2G106363	FKF1-LIKE 1 (FFL1)	618	PAS repeat/PAS domain, F-box domain, Kelch 4, Kelch 3, Kelch 3, Kelch 2	C0PGG9
GRMZM2G107945	FKF1-LIKE 2 (FFL2)	609	PAS repeat/PAS domain, F-box domain, Kelch 4, Kelch 3, Kelch 3	A0A096RQI5

Table 4.3. Maize clock and clock-associated proteins. Size is in amino acids (aa), and protein domain results are from Prosite (before the /) and Pfam (after the /). A * by the GRMZM number indicates that the protein appears to be a fragment or may be incomplete, while a ^ indicates that a more complete protein was constructed and used in tree building.

Genes	Maize 1 gene	Maize 2 gene	Sorghum	Setaria
*lyl1/2**	1.5	-1.5	-1.5	-1.5
re2l	21		3	1.5
re6l1	21		0	0
re6l2/3	not rhythmic	not rhythmic	not rhythmic	18
re6l4/5	21	1.5	1.5	0
re7l1/2	18	-3.33	1.5	1.5
re7l3/4	16.5	1.5	-1.5	-3
re8l1/2	not expressed	not expressed	not expressed	not expressed
t1l1/2	12	-3	-1.5	-3
*t1l3**	9			
*t1l4**	12			
*t1l5**	12			
*t1l6**	12			
*p37l1/2**	4.5	-3.17	-4.5	not rhythmic
p4l	not expressed		not expressed	not expressed
p59l1/2	7.5	1.5	0.75	0
p73l	4.5		1.5	0
p95l1/2	6	1.5	0	0
gi1/2	7.5	1.5	1.5	0
ef3l1	20.25		0.75	-0.75
ef3l2	15		1.5	-1.5
ef4r1/2	7.5	not rhythmic	1.5	0
ef4r3		10.5	not rhythmic	not rhythmic
ef4r4	13.5		-3	not rhythmic
lxl		10.5	1.5	0
zll1/2	not rhythmic	10.5	6	6
zll3/4	0	not rhythmic	0	-9
ffl1/2	8.25	0.75	-0.75	-0.75

Table 4.4. Phasing of maize paralogs and their orthologs according to JTK-cycle analysis. All phases were expressed relative to that of the maize subgenome 1 (Maize 1) gene, unless that gene was not present or not rhythmic. Green boxes and values represent reference phases, red boxes indicate non-rhythmic genes or genes that have FPKMs <10 throughout the timecourse (not expressed), and hatched boxes indicate no gene. Negative phase shifts are colored in blues, while positive phase shifts are colored in yellows. The * by *lyl1/2* indicates that the phase estimate for GRMZM2G474769 was used instead of the one for GRMZM2G175265. The ^ indicates that there is uncertainty as to which subgenome these genes are on. Note that the Setaria ortholog of *zll3/4* in fact has an estimated phase of 15, but it was adjusted to the peak nearer to 0 so as not to skew the coloring scheme too much.

GRMZM number	Gene name	Working name	Subgenome	Maize paralog
GRMZM2G175265 + GRMZM2G474769	*lhy-like 1 (lyl1)*	*lhy1*	1*	GRMZM2G014902
GRMZM2G014902	*lhy-like 2 (lyl2)*	*lhy2*	2	GRMZM2G175265 + GRMZM2G474769
GRMZM2G145041	*rve2-like (re2l)*		1	No gene
GRMZM2G135052	*rve6-like 1 (re6l1)*		1	No gene
GRMZM2G170148	*rve6-like 2 (re6l2)*		1	GRMZM2G057408
GRMZM2G057408	*rve6-like 3 (re6l3)*		2	GRMZM2G170148
GRMZM5G833032	*rve6-like 4 (re6l4)*		1	GRMZM2G118693
GRMZM2G118693	*rve6-like 5 (re6l5)*		2	GRMZM5G833032
GRMZM2G029850	*rve7-like 1 (re7l1)*		1	GRMZM2G170322
GRMZM2G170322	*rve7-like 2 (re7l2)*		2	GRMZM2G029850
GRMZM2G421256	*rve7-like 3 (re7l3)*		1	GRMZM2G181030
GRMZM2G181030	*rve7-like 4 (re7l4)*		2	GRMZM2G421256
GRMZM2G115070	*rve8-like 2 (re8l2)*		?	Local duplicate of re8l2
GRMZM2G415077	*rve8-like 1 (re8l1)*		?	Local duplicate of re8l1
GRMZM2G148453	*toc1-like 1 (t1l1)*	*toc1b*	1	GRMZM2G020081
GRMZM2G020081	*toc1-like 2 (t1l2)*	*toc1a*	2	GRMZM2G148453
GRMZM2G145058	*toc1-like 3 (t1l3)*		?	?
GRMZM2G365688	*toc1-like 4 (t1l4)*		?	?
GRMZM2G066638	*toc1-like 5 (t1l5)*		?	Duplicate of t1l6
GRMZM2G174083	*toc1-like 6 (t1l6)*		?	Duplicate of t1l5
GRMZM2G005732	*prr37-like 1 (p37l1)*		?	GRMZM2G033962
GRMZM2G033962	*prr37-like 2 (p37l2)*		?	GRMZM2G005732
GRMZM2G379656	*prr4-like (p4l)*		1	No gene
GRMZM2G488465	*prr59-like 2 (p59l2)*		probably 1	GRMZM2G135446
GRMZM2G135446	*prr59-like 1 (p59l1)*		2	GRMZM2G488465
GRMZM2G095727	*prr73-like (p73l)*	*prr73*	2	No gene
GRMZM2G179024	*prr95-like 1 (p95l1)*		1	GRMZM2G367834
GRMZM2G367834	*prr95-like 2 (p95l2)*		2	GRMZM2G179024
GRMZM2G107101	*gigantea 1 (gi1)*		2	GRMZM5G844173
GRMZM5G844173	*gigantea 2 (gi2)*		1	GRMZM2G107101
GRMZM2G045275	*elf3-like 1 (ef3l1)*	*elf3a*	1	No gene
AC233870.1_FG003	*elf3-like 2 (ef3l2)*	*elf3b*	1	No gene
GRMZM2G382774	*elf4-related 1 (ef4r1)*	*elf4a*	1	GRMZM2G359322
GRMZM2G359322	*elf4-related 2 (ef4r2)*	*elf4b*	2	GRMZM2G382774
GRMZM5G877647	*elf4-related 3*		2	No gene

GRMZM number	Gene name	Working name	Subgenome	Maize paralog
	(ef4r3)			
GRMZM2G025646	*elf4-related 4 (ef4r4)*		1	No gene
GRMZM2G067702	*lux-like (lxl)*		2	No gene
GRMZM2G115914	*ztl-like 1 (zll1)*	*ztl3*	1	GRMZM2G113244
GRMZM2G113244	*ztl-like 2 (zll2)*	*ztl4*	2	GRMZM2G115914
GRMZM2G147800	*ztl-like 3 (zll3)*	*ztl1*	1	GRMZM2G166147
GRMZM2G166147	*ztl-like 4 (zll4)*	*ztl2*	2	GRMZM2G147800
GRMZM2G106363	*fkf1-like 1 (ffl1)*		1	GRMZM2G107945
GRMZM2G107945	*fkf1-like 2 (ffl2)*		2	GRMZM2G106363

Table 4.5. Maize circadian clock and clock-associated genes, the subgenomes on which they are located, and their paralogs. Working name indicates the designation that was used for these genes during experiment, and under which genes are identified in previous chapters. The * indicates that GRMZM2G474769 is on maize subgenome 1.

Supplemental Figures

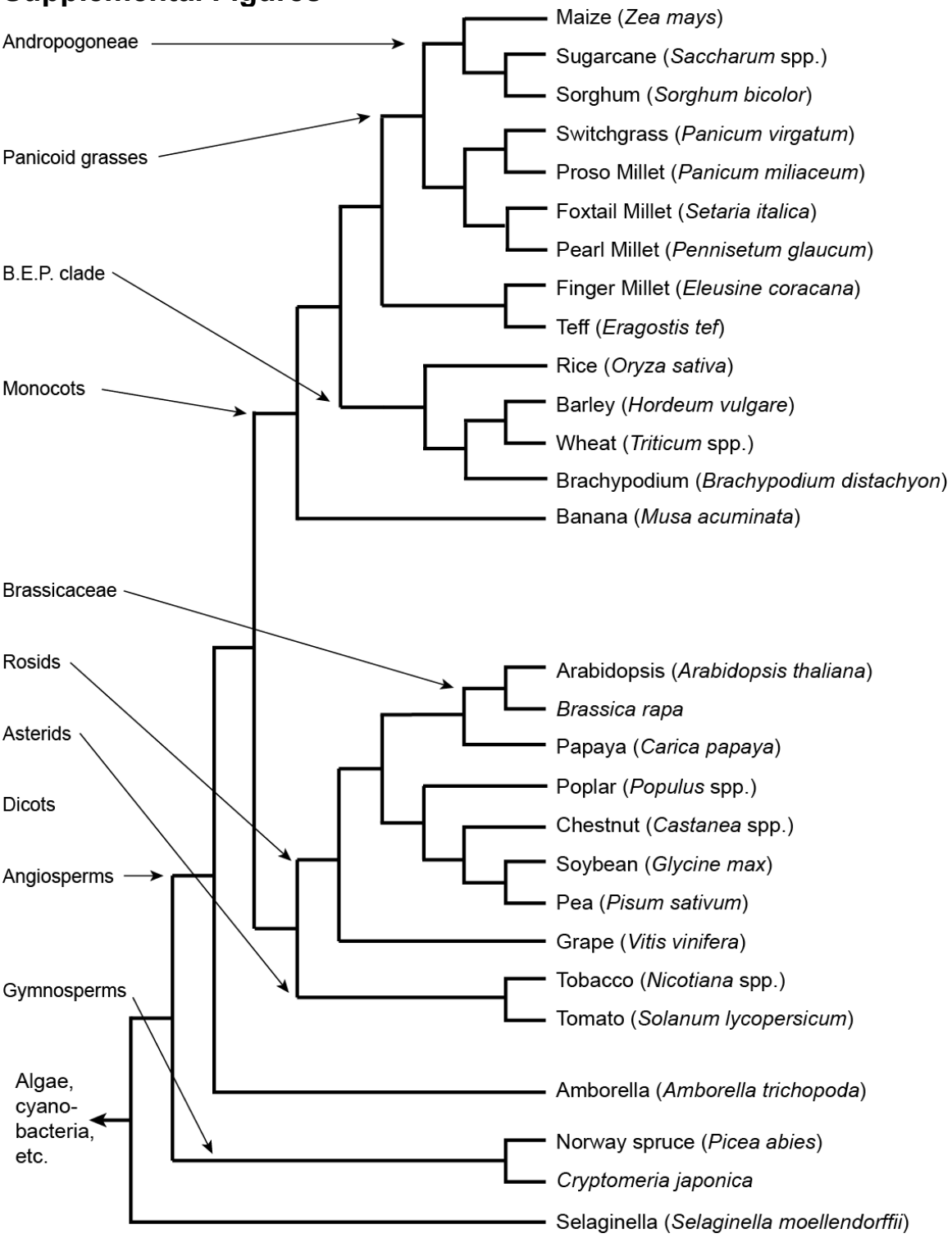

Supplemental Figure 4.1. Land plant phylogeny adapted from New grass phylogeny report (2012) and the Angiosperm Phylogeny website (www.mobot.org/MOBOT/research/APweb/).

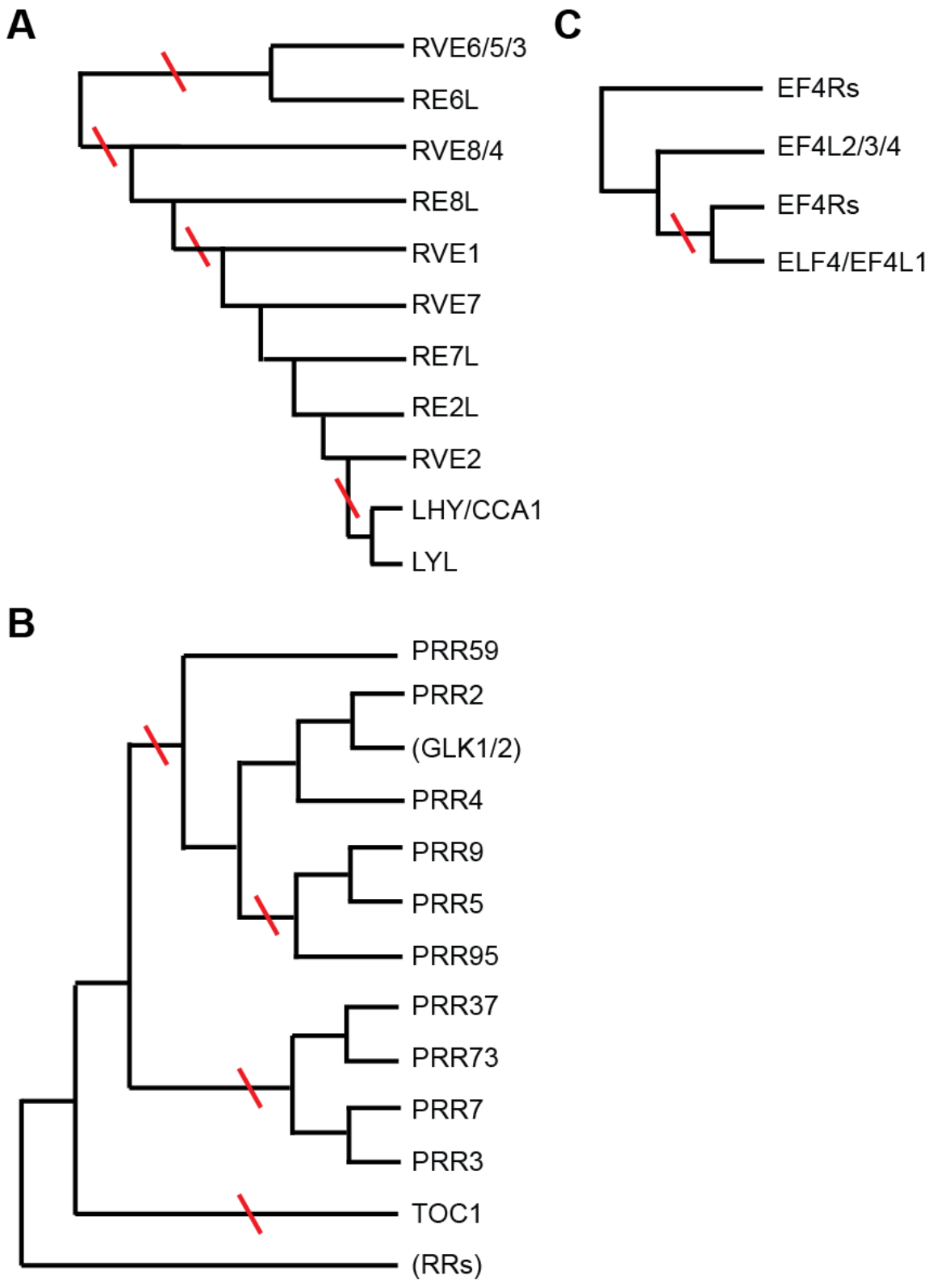

Supplemental Figure 4.2. Large protein trees were constructed for each gene family, and then subtrees were extracted from the larger tree (red slashes indicate locations at

which subtrees were cut out). **A)** The *RVE/LHY* gene family has four subtrees; one of the *RVE6* groups, one of the *RVE8* groups, one of the *RVE1*, *RVE7*, and *RVE2* groups, and one of the *LHY* group. Note that there is low bootstrap support for many of these groupings, and so the true tree topology could be quite different. **B)** The *PRR* gene family has four subtrees; one of *PRR59* and *PRR2/4*, one of *PRR9/5/95*, one of *PRR3/7/37/73*, and one of *TOC1*. Parentheses around groups indicate they were not included in the tree. **C)** The *ELF4/EF4L* family has two subtrees; one of one *EF4R* groups and the *EF4L2/3/4* group, and one of the other *EF4R* group and the *ELF4/EF4L1* group.

References

Abegg, F.A. (1936). A genetic factor for the annual habit in beets and linkage relationship.

Acevedo, A., Williamson, J.D., and Scandalios, J.G. (1991). Photoregulation of the Cat2 and Cat3 catalase genes in pigmented and pigment-deficient maize: the circadian regulation of Cat3 is superimposed on its quasi-constitutive expression in maize leaves. Genetics *127*, 601–607.

Alabadí, D., Oyama, T., Yanovsky, M.J., Harmon, F.G., Más, P., and Kay, S.A. (2001). Reciprocal regulation between TOC1 and LHY/CCA1 within the Arabidopsis circadian clock. Science *293*, 880–883.

Alonso, J.M., Stepanova, A.N., Leisse, T.J., Kim, C.J., Chen, H., Shinn, P., Stevenson, D.K., Zimmerman, J., Barajas, P., Cheuk, R., et al. (2003). Genome-wide insertional mutagenesis of Arabidopsis thaliana. Science *301*, 653–657.

Andrés, F., and Coupland, G. (2012). The genetic basis of flowering responses to seasonal cues. Nat. Rev. Genet. *13*, 627–639.

Araki, T., and Komeda, Y. (1993). Analysis of the role of the late-flowering locus, GI, in the flowering of Arabidopsis thaliana. Plant J. *3*, 231–239.

Araus, J.L., Serret, M.D., and Edmeades, G.O. (2012). Phenotyping maize for adaptation to drought. Front. Physiol. *3*, 305.

Aukerman, M.J., and Sakai, H. (2003). Regulation of flowering time and floral organ identity by a MicroRNA and its APETALA2-like target genes. Plant Cell *15*, 2730–2741.

Baldwin, I.T., and Meldau, S. (2013). Just in time: circadian defense patterns and the optimal defense hypothesis. Plant Signal. Behav. *8*, e24410.

Ballerini, E.S., and Kramer, E.M. (2011). In the Light of Evolution: A Reevaluation of Conservation in the CO-FT Regulon and Its Role in Photoperiodic Regulation of Flowering Time. Front. Plant Sci. *2*, 81.

Beadle, G. (1939). Teosinte and the origin of maize. J. Hered. *30*, 245–247.

Beales, J., Turner, A., Griffiths, S., Snape, J.W., and Laurie, D.A. (2007). A pseudo-response regulator is misexpressed in the photoperiod insensitive Ppd-D1a mutant of wheat (Triticum aestivum L.). Theor. Appl. Genet. *115*, 721–733.

Bell, G.D.H., and Bauer, A.B. (1942). Experiments on growing sugar beet under continuous illumination. J. Agric. Sci. *32*, 112.

Bendix, C., Mendoza, J.M., Stanley, D.N., Meeley, R., and Harmon, F.G. (2013). The circadian clock-associated gene gigantea1 affects maize developmental transitions. Plant, Cell Environ. *36*, 1379–1390.

Benz, B.F. (2001). Archaeological evidence of teosinte domestication from Guilá Naquitz, Oaxaca. Proc. Natl. Acad. Sci. U. S. A. *98*, 2104–2106.

Bernard, R.L. (1971). Two Major Genes for Time of Flowering and Maturity in Soybeans. Crop Sci. *11*, 242.

Bhardwaj, V., Meier, S., Petersen, L.N., Ingle, R.A., and Roden, L.C. (2011). Defence responses of Arabidopsis thaliana to infection by Pseudomonas syringae are regulated by the circadian clock. PLoS One *6*, e26968.

Black, M.M., Stockum, C., Dickson, J.M., Putterill, J., and Arcus, V.L. (2011). Expression , purification and characterisation of GIGANTEA : A circadian clock-controlled regulator of photoperiodic flowering in plants. Protein Expr. Purif. *76*, 197–204.

Bläsing, O.E., Gibon, Y., Günther, M., Höhne, M., Morcuende, R., Osuna, D., Thimm, O., Usadel, B., Scheible, W.-R., and Stitt, M. (2005). Sugars and circadian regulation make major contributions to the global regulation of diurnal gene expression in Arabidopsis. Plant Cell *17*, 3257–3281.

Boldt, R., and Scandalios, J.G. (1995). Circadian regulation of the Cat3 catalase gene in maize (Zea mays L.): entrainment of the circadian rhythm of Cat3 by different light treatments. Plant J. *7*, 989–999.

Bonato, E.R., and Vello, N.A. (1999). E6, a dominant gene conditioning early flowering and maturity in soybeans. Genet. Mol. Biol. *22*, 229–232.

Borlaug, N.E. (1983). Contributions of conventional plant breeding to food production. Science *219*, 689–693.

Börner, A., Buck-Sorlin, G.H., Hayes, P.M., Malyshev, S., and Korzun, V. (2002). Molecular mapping of major genes and quantitative trait loci determining flowering time in response to photoperiod in barley. Plant Breed. *121*, 129–132.

Boudry, P., Wieber, R., Saumitou-Laprade, P., Pillen, K., Van Dijk, H., and Jung, C. (1994). Identification of RFLP markers closely linked to the bolting gene B and their significance for the study of the annual habit in beets (Beta vulgaris L.). Theor. Appl. Genet. *88*, 852–858.

Brock, M.T., Tiffin, P., and Weinig, C. (2007). Sequence diversity and haplotype associations with phenotypic responses to crowding: GIGANTEA affects fruit set in

Arabidopsis thaliana. Mol. Ecol. *16*, 3050–3062.

Buckler, E.S., Holland, J.B., Bradbury, P.J., Acharya, C.B., Brown, P.J., Browne, C., Ersoz, E., Flint-Garcia, S., Garcia, A., Glaubitz, J.C., et al. (2009). The genetic architecture of maize flowering time. Science *325*, 714–718.

Buzzell, R.I. (2011). Inheritance of a soybean flowering response to fluorescent-daylength conditions. Can. J. Genet. Cytol.

Callaway, E. (2014). Domestication: The birth of rice. Nature *514*, S58–S59.

Campoli, C., Shtaya, M., Davis, S.J., and von Korff, M. (2012). Expression conservation within the circadian clock of a monocot: natural variation at barley Ppd-H1 affects circadian expression of flowering time genes, but not clock orthologs. BMC Plant Biol. *12*, 97.

Campoli, C., Pankin, A., Drosse, B., Casao, C.M., Davis, S.J., and von Korff, M. (2013). HvLUX1 is a candidate gene underlying the early maturity 10 locus in barley: phylogeny, diversity, and interactions with the circadian clock and photoperiodic pathways. New Phytol. *199*, 1045–1059.

Cao, S., Ye, M., and Jiang, S. (2005). Involvement of GIGANTEA gene in the regulation of the cold stress response in Arabidopsis. Plant Cell Rep. *24*, 683–690.

Carbonell-Bejerano, P., Rodríguez, V., Royo, C., Hernáiz, S., Moro-González, L.C., Torres-Viñals, M., and Martínez-Zapater, J.M. (2014). Circadian oscillatory transcriptional programs in grapevine ripening fruits. BMC Plant Biol. *14*, 78.

Carre, I.A., and Kay, S.A. (1995). Multiple DNA-Protein Complexes at a Circadian-Regulated Promoter Element. Plant Cell *7*, 2039–2051.

Chandraratna, M.F. (1953). A Gene for Photoperiod Sensitivity in Rice linked with Apiculus Colour. Nature *171*, 1162–1163.

Chaudhury, A., Okada, K., Raikhel, N., Shinozaki, K., and Sundaresan, V. (1999). A weed reaches new heights down under. Plant Cell *11*, 1817–1826.

Chaves, I., Pokorny, R., Byrdin, M., Hoang, N., Ritz, T., Brettel, K., Essen, L.-O., van der Horst, G.T.J., Batschauer, A., and Ahmad, M. (2011). The cryptochromes: blue light photoreceptors in plants and animals. Annu. Rev. Plant Biol. *62*, 335–364.

Chaw, S.-M., Chang, C.-C., Chen, H.-L., and Li, W.-H. (2004). Dating the monocot-dicot divergence and the origin of core eudicots using whole chloroplast genomes. J. Mol. Evol. *58*, 424–441.

Chen, J., Källman, T., Ma, X., Gyllenstrand, N., Zaina, G., Morgante, M., Bousquet, J.,

Eckert, A., Wegrzyn, J., Neale, D., et al. (2012). Disentangling the roles of history and local selection in shaping clinal variation of allele frequencies and gene expression in Norway spruce (Picea abies). Genetics *191*, 865–881.

Chen, M., Chory, J., and Fankhauser, C. (2004). Light Signal Transduction in Higher Plants. Annu. Rev. Genet. *38*, 87–117.

Chow, B.Y., Helfer, A., Nusinow, D.A., and Kay, S.A. (2012). ELF3 recruitment to the PRR9 promoter requires other Evening Complex members in the Arabidopsis circadian clock. Plant Signal. Behav. *7*, 170–173.

Chuck, G., Meeley, R., Irish, E., Sakai, H., and Hake, S. (2007). The maize tasselseed4 microRNA controls sex determination and meristem cell fate by targeting Tasselseed6/indeterminate spikelet1. Nat. Genet. *39*, 1517–1521.

Clough, S.J., and Bent, A.F. (1998). Floral dip: a simplified method for Agrobacterium-mediated transformation of Arabidopsis thaliana. Plant J. *16*, 735–743.

Cober, E.R., and Voldeng, H.D. (2001). A New Soybean Maturity and Photoperiod-Sensitivity Locus Linked to and. Crop Sci. *41*, 698.

Cober, E.R., Molnar, S.J., Charette, M., and Voldeng, H.D. (2010). A New Locus for Early Maturity in Soybean. Crop Sci. *50*, 524.

Coluccio, M.P., Sanchez, S.E., Kasulin, L., Yanovsky, M.J., and Botto, J.F. (2011). Genetic mapping of natural variation in a shade avoidance response: ELF3 is the candidate gene for a QTL in hypocotyl growth regulation. J. Exp. Bot. *62*, 167–176.

Corbesier, L., Vincent, C., Jang, S., Fornara, F., Fan, Q., Searle, I., Giakountis, A., Farrona, S., Gissot, L., Turnbull, C., et al. (2007). FT protein movement contributes to long-distance signaling in floral induction of Arabidopsis. Science *316*, 1030–1033.

Covington, M.F., and Harmer, S.L. (2007). The Circadian Clock Regulates Auxin Signaling and Responses in Arabidopsis. PLoS Biol. *5*, e222.

Covington, M.F., Maloof, J.N., Straume, M., Kay, S.A., and Harmer, S.L. (2008). Global transcriptome analysis reveals circadian regulation of key pathways in plant growth and development. Genome Biol. *9*, R130.

Crepy, M., Yanovsky, M.J., and Casal, J.J. (2007). Blue Rhythms Between GIGANTEA and Phytochromes. Plant Signal. Behav. *2*, 530–532.

Curtis, I.S., Nam, H.G., Yun, J.Y., and Seo, K.H. (2002). Expression of an antisense GIGANTEA (GI) gene fragment in transgenic radish causes delayed bolting and flowering. Transgenic Res. *11*, 249–256.

Dalchau, N., Baek, S.J., Briggs, H.M., Robertson, F.C., Dodd, A.N., Gardner, M.J., Stancombe, M.A., Haydon, M.J., Stan, G.-B., Gonçalves, J.M., et al. (2011). The circadian oscillator gene GIGANTEA mediates a long-term response of the Arabidopsis thaliana circadian clock to sucrose. Proc. Natl. Acad. Sci. U. S. A. *108*, 5104–5109.

Dally, N., Xiao, K., Holtgräwe, D., and Jung, C. (2014). The B2 flowering time locus of beet encodes a zinc finger transcription factor. Proc. Natl. Acad. Sci. U. S. A. *111*, 10365–10370.

Danilevskaya, O.N., Meng, X., Hou, Z., Ananiev, E. V, and Simmons, C.R. (2008). A genomic and expression compendium of the expanded PEBP gene family from maize. Plant Physiol. *146*, 250–264.

David, K.M., Armbruster, U., Tama, N., and Putterill, J. (2006). Arabidopsis GIGANTEA protein is post-transcriptionally regulated by light and dark. FEBS Lett. *580*, 1193–1197.

Demarsy, E., and Fankhauser, C. (2009). Higher plants use LOV to perceive blue light. Curr. Opin. Plant Biol. *12*, 69–74.

Deng, W., Clausen, J., Boden, S., Oliver, S.N., Casao, M.C., Ford, B., Anderssen, R.S., and Trevaskis, B. (2015). Dawn and Dusk Set States of the Circadian Oscillator in Sprouting Barley (Hordeum vulgare) Seedlings. PLoS One *10*, e0129781.

Dijk, H. Van, Boudry, P., McCombre, H., and Vernet, P. (1997). Flowering time in wild beet (Beta vulgaris ssp. maritima) along a latitudinal cline. Acta Oecologica *18*, 47–60.

Dixon, L.E., Knox, K., Kozma-Bognar, L., Southern, M.M., Pokhilko, A., and Millar, A.J. (2011). Temporal repression of core circadian genes is mediated through EARLY FLOWERING 3 in Arabidopsis. Curr. Biol. *21*, 120–125.

Dodd, A.N., Salathia, N., Hall, A., Kévei, E., Tóth, R., Nagy, F., Hibberd, J.M., Millar, A.J., and Webb, A.A.R. (2005). Plant circadian clocks increase photosynthesis, growth, survival, and competitive advantage. Science *309*, 630–633.

Doi, K., Izawa, T., Fuse, T., Yamanouchi, U., Kubo, T., Shimatani, Z., Yano, M., and Yoshimura, A. (2004). Ehd1, a B-type response regulator in rice, confers short-day promotion of flowering and controls FT-like gene expression independently of Hd1. Genes Dev. *18*, 926–936.

Doyle, M.R., Davis, S.J., Bastow, R.M., McWatters, H.G., Kozma-Bognár, L., Nagy, F., Millar, A.J., and Amasino, R.M. (2002). The ELF4 gene controls circadian rhythms and flowering time in Arabidopsis thaliana. Nature *419*, 74–77.

Dubois, P.G., and Brutnell, T.P. (2011). Topology of a maize field: distinguishing the influence of end-of-day far-red light and shade avoidance syndrome on plant height.

Plant Signal. Behav. *6*, 467–470.

Dunford, R.P., Griffiths, S., Christodoulou, V., and Laurie, D.A. (2005). Characterisation of a barley (Hordeum vulgare L.) homologue of the Arabidopsis flowering time regulator GIGANTEA. Theor. Appl. Genet. *110*, 925–931.

Duvick, D.N. (2001). Biotechnology in the 1930s: the development of hybrid maize. Nat. Rev. Genet. *2*, 69–74.

Earley, K.W., Haag, J.R., Pontes, O., Opper, K., Juehne, T., Song, K., and Pikaard, C.S. (2006). Gateway-compatible vectors for plant functional genomics and proteomics. Plant J. *45*, 616–629.

Egli, M. (2014). Intricate protein-protein interactions in the cyanobacterial circadian clock. J. Biol. Chem. *289*, 21267–21275.

Eimert, K., Wang, S.M., Lue, W.I., and Chen, J. (1995). Monogenic Recessive Mutations Causing Both Late Floral Initiation and Excess Starch Accumulation in Arabidopsis. Plant Cell *7*, 1703–1712.

Eisenberg, D., Schwarz, E., Komaromy, M., and Wall, R. (1984). Analysis of membrane and surface protein sequences with the hydrophobic moment plot. J. Mol. Biol. *179*, 125–142.

Emerson, R.A. (1924). Control of flowering in teosinte: Short-Day treatment brings early flowers. J. Hered. *15*, 41–48.

Evans, M.M., and Poethig, R.S. (1995). Gibberellins promote vegetative phase change and reproductive maturity in maize. Plant Physiol. *108*, 475–487.

Facella, P., Lopez, L., Carbone, F., Galbraith, D.W., Giuliano, G., and Perrotta, G. (2008). Diurnal and circadian rhythms in the tomato transcriptome and their modulation by cryptochrome photoreceptors. PLoS One *3*, e2798.

Fan, G., Dong, Y., Deng, M., Zhao, Z., Niu, S., and Xu, E. (2014). Plant-pathogen interaction, circadian rhythm, and hormone-related gene expression provide indicators of phytoplasma infection in Paulownia fortunei. Int. J. Mol. Sci. *15*, 23141–23162.

Farinas, B., and Mas, P. (2011). Functional implication of the MYB transcription factor RVE8/LCL5 in the circadian control of histone acetylation. Plant J. *66*, 318–329.

Farré, E.M., and Kay, S.A. (2007). PRR7 protein levels are regulated by light and the circadian clock in Arabidopsis. Plant J. *52*, 548–560.

Farré, E.M., and Liu, T. (2013). The PRR family of transcriptional regulators reflects the complexity and evolution of plant circadian clocks. Curr. Opin. Plant Biol. *16*, 621–629.

Farré, E.M., Harmer, S.L., Harmon, F.G., Yanovsky, M.J., and Kay, S.A. (2005). Overlapping and distinct roles of PRR7 and PRR9 in the Arabidopsis circadian clock. Curr. Biol. *15*, 47–54.

Faure, S., Turner, A.S., Gruszka, D., Christodoulou, V., Davis, S.J., von Korff, M., and Laurie, D.A. (2012). Mutation at the circadian clock gene EARLY MATURITY 8 adapts domesticated barley (Hordeum vulgare) to short growing seasons. Proc. Natl. Acad. Sci. U. S. A. *109*, 8328–8333.

Filichkin, S.A., Breton, G., Priest, H.D., Dharmawardhana, P., Jaiswal, P., Fox, S.E., Michael, T.P., Chory, J., Kay, S.A., and Mockler, T.C. (2011). Global profiling of rice and poplar transcriptomes highlights key conserved circadian-controlled pathways and cis-regulatory modules. PLoS One *6*, e16907.

Flis, A., Fernández, A.P., Zielinski, T., Mengin, V., Sulpice, R., Stratford, K., Hume, A., Pokhilko, A., Southern, M.M., Seaton, D.D., et al. (2015). Defining the robust behaviour of the plant clock gene circuit with absolute RNA timeseries and open infrastructure. Open Biol. *5*.

Fogelmark, K., and Troein, C. (2014). Rethinking transcriptional activation in the Arabidopsis circadian clock. PLoS Comput. Biol. *10*, e1003705.

Fornara, F., de Montaigu, A., Sánchez-Villarreal, A., Takahashi, Y., Ver Loren van Themaat, E., Huettel, B., Davis, S.J., and Coupland, G. (2015). The GI-CDF module of Arabidopsis affects freezing tolerance and growth as well as flowering. Plant J. *81*, 695–706.

Fowler, S., Lee, K., Onouchi, H., Samach, A., Richardson, K., Morris, B., Coupland, G., and Putterill, J. (1999). GIGANTEA: a circadian clock-controlled gene that regulates photoperiodic flowering in Arabidopsis and encodes a protein with several possible membrane-spanning domains. EMBO J. *18*, 4679–4688.

Fu, C., Yang, X.O., Chen, X., Chen, W., Ma, Y., Hu, J., and Li, S. (2009). OsEF3, a homologous gene of Arabidopsis ELF3, has pleiotropic effects in rice. Plant Biol. (Stuttg). *11*, 751–757.

Fujiwara, S., Wang, L., Han, L., Suh, S.-S., Salomé, P.A., McClung, C.R., and Somers, D.E. (2008). Post-translational regulation of the Arabidopsis circadian clock through selective proteolysis and phosphorylation of pseudo-response regulator proteins. J. Biol. Chem. *283*, 23073–23083.

Fukushima, A., Kusano, M., Nakamichi, N., Kobayashi, M., and Hayashi, N. (2009). Impact of clock-associated Arabidopsis pseudo-response regulators in metabolic coordination. Proc. Natl. Acad. Sci. U.S.A. *106*, 7251–7256.

Galinat, W. (1983). The origin of maize as shown by key morphological traits of its ancestor, teosinte.

Galinat, W.C., and Naylor, A.W. (1951). Relation of Photoperiod to Inflorescence Proliferation in Zea mays L. Am. J. Bot. *38*, 38–47.

Galvão, V.C., Horrer, D., Küttner, F., and Schmid, M. (2012). Spatial control of flowering by DELLA proteins in Arabidopsis thaliana. Development *139*, 4072–4082.

Garner, W.W., and Allard, H.A. (1920). Effect of the Relative Length of Day and Night and Other Factors of the Environment on Growth and Reproduction in Plants. J. Agric. Res. *XVIII*, 553–606.

Garner, W.W., and Allard, H.A. (1922). Photoperiodism, the response of the plant to relative length of day and night. Science *55*, 582–583.

Garner, W.W., and Allard, H.A. (1923). Further studies in photoperiodism, the response of the plant to relative length of day and night. J. Agric. Res. *XXIII*, 871–920.

Gaut, B.S., and Doebley, J.F. (1997). DNA sequence evidence for the segmental allotetraploid origin of maize. Proc. Natl. Acad. Sci. U. S. A. *94*, 6809–6814.

Gawroński, P., Ariyadasa, R., Himmelbach, A., Poursarebani, N., Kilian, B., Stein, N., Steuernagel, B., Hensel, G., Kumlehn, J., Sehgal, S.K., et al. (2014). A distorted circadian clock causes early flowering and temperature-dependent variation in spike development in the Eps-3Am mutant of einkorn wheat. Genetics *196*, 1253–1261.

Gendron, J.M., Pruneda-Paz, J.L., Doherty, C.J., Gross, A.M., Kang, S.E., and Kay, S.A. (2012). Arabidopsis circadian clock protein, TOC1, is a DNA-binding transcription factor. Proc. Natl. Acad. Sci. U. S. A. *109*, 3167–3172.

Golembeski, G.S., Kinmonth-Schultz, H.A., Song, Y.H., and Imaizumi, T. (2014). Photoperiodic flowering regulation in Arabidopsis thaliana. Adv. Bot. Res. *72*, 1–28.

Goodspeed, D., Chehab, E.W., Min-Venditti, A., Braam, J., and Covington, M.F. (2012). Arabidopsis synchronizes jasmonate-mediated defense with insect circadian behavior. Proc. Natl. Acad. Sci. U. S. A. *109*, 4674–4677.

Goodspeed, D., Liu, J.D., Chehab, E.W., Sheng, Z., Francisco, M., Kliebenstein, D.J., and Braam, J. (2013). Postharvest circadian entrainment enhances crop pest resistance and phytochemical cycling. Curr. Biol. *23*, 1235–1241.

Gould, P.D., Ugarte, N., Domijan, M., Costa, M., Foreman, J., Macgregor, D., Rose, K., Griffiths, J., Millar, A.J., Finkenstädt, B., et al. (2013). Network balance via CRY signalling controls the Arabidopsis circadian clock over ambient temperatures. Mol. Syst. Biol. *9*, 650.

Graf, A., Schlereth, A., Stitt, M., and Smith, A.M. (2010). Circadian control of carbohydrate availability for growth in Arabidopsis plants at night. Proc. Natl. Acad. Sci. *107*, 9458–9463.

Green, R.M., and Tobin, E.M. (1999). Loss of the circadian clock-associated protein 1 in Arabidopsis results in altered clock-regulated gene expression. Proc. Natl. Acad. Sci. U. S. A. *96*, 4176–4179.

Green, R.M., Tingay, S., Wang, Z.-Y., and Tobin, E.M. (2002). Circadian rhythms confer a higher level of fitness to Arabidopsis plants. Plant Physiol. *129*, 576–584.

Greenup, A., Peacock, W.J., Dennis, E.S., and Trevaskis, B. (2009). The molecular biology of seasonal flowering-responses in Arabidopsis and the cereals. Ann. Bot. *103*, 1165–1172.

Grundy, J., Stoker, C., and Carré, I.A. (2015). Circadian regulation of abiotic stress tolerance in plants. Front. Plant Sci. *6*, 648.

Gutiérrez, R.A., Stokes, T.L., Thum, K., Xu, X., Obertello, M., Katari, M.S., Tanurdzic, M., Dean, A., Nero, D.C., McClung, C.R., et al. (2008). Systems approach identifies an organic nitrogen-responsive gene network that is regulated by the master clock control gene CCA1. Proc. Natl. Acad. Sci. U. S. A. *105*, 4939–4944.

Habte, E., Müller, L.M., Shtaya, M., Davis, S.J., and von Korff, M. (2014). Osmotic stress at the barley root affects expression of circadian clock genes in the shoot. Plant. Cell Environ. *37*, 1321–1327.

Hake, S., and Bennetzen, J.L. (2009). Handbook of Maize: Genetics and Genomics (Springer Science & Business Media).

Harmer, S.L. (2009). The Circadian System in Higher Plants. Annu. Rev. Plant Biol. *60*, 357–377.

Harmer, S.L., Hogenesch, J.B., Straume, M., Chang, H.S., Han, B., Zhu, T., Wang, X., Kreps, J.A., and Kay, S.A. (2000). Orchestrated transcription of key pathways in Arabidopsis by the circadian clock. Science *290*, 2110–2113.

Hayama, R., Yokoi, S., Tamaki, S., Yano, M., and Shimamoto, K. (2003). Adaptation of photoperiodic control pathways produces short-day flowering in rice. Nature *422*, 719–722.

Haydon, M.J., Mielczarek, O., Robertson, F.C., Hubbard, K.E., and Webb, A.A.R. (2013). Photosynthetic entrainment of the Arabidopsis thaliana circadian clock. Nature *502*, 689–692.

Hayes, K.R., Beatty, M., Meng, X., Simmons, C.R., Habben, J.E., and Danilevskaya,

O.N. (2010). Maize global transcriptomics reveals pervasive leaf diurnal rhythms but rhythms in developing ears are largely limited to the core oscillator. PLoS One *5*, e12887.

Hazen, S.P., Schultz, T.F., Pruneda-Paz, J.L., Borevitz, J.O., Ecker, J.R., and Kay, S.A. (2005). LUX ARRHYTHMO encodes a Myb domain protein essential for circadian rhythms. Proc. Natl. Acad. Sci. U. S. A. *102*, 10387–10392.

Hecht, V., Knowles, C.L., Vander Schoor, J.K., Liew, L.C., Jones, S.E., Lambert, M.J.M., and Weller, J.L. (2007). Pea LATE BLOOMER1 is a GIGANTEA ortholog with roles in photoperiodic flowering, deetiolation, and transcriptional regulation of circadian clock gene homologs. Plant Physiol. *144*, 648–661.

Hecht, V., Laurie, R.E., Vander Schoor, J.K., Ridge, S., Knowles, C.L., Liew, L.C., Sussmilch, F.C., Murfet, I.C., Macknight, R.C., and Weller, J.L. (2011). The pea GIGAS gene is a FLOWERING LOCUS T homolog necessary for graft-transmissible specification of flowering but not for responsiveness to photoperiod. Plant Cell *23*, 147–161.

Helfer, A., Nusinow, D.A., Chow, B.Y., Gehrke, A.R., Bulyk, M.L., and Kay, S.A. (2011). LUX ARRHYTHMO encodes a nighttime repressor of circadian gene expression in the Arabidopsis core clock. Curr. Biol. *21*, 126–133.

Herrero, E., Kolmos, E., Bujdoso, N., Yuan, Y., Wang, M., Berns, M.C., Uhlworm, H., Coupland, G., Saini, R., Jaskolski, M., et al. (2012). EARLY FLOWERING4 recruitment of EARLY FLOWERING3 in the nucleus sustains the Arabidopsis circadian clock. Plant Cell *24*, 428–443.

Hicks, K.A., Millar, A.J., Carré, I.A., Somers, D.E., Straume, M., Meeks-Wagner, D.R., and Kay, S.A. (1996). Conditional circadian dysfunction of the Arabidopsis early-flowering 3 mutant. Science *274*, 790–792.

Hicks, K.A., Albertson, T.M., and Wagner, D.R. (2001). EARLY FLOWERING3 encodes a novel protein that regulates circadian clock function and flowering in Arabidopsis. Plant Cell *13*, 1281–1292.

Hoffman, D.E., Jonsson, P., Bylesjö, M., Trygg, J., Antti, H., Eriksson, M.E., and Moritz, T. (2010). Changes in diurnal patterns within the Populus transcriptome and metabolome in response to photoperiod variation. Plant. Cell Environ. *33*, 1298–1313.

Holm, K., Källman, T., Gyllenstrand, N., Hedman, H., and Lagercrantz, U. (2010). Does the core circadian clock in the moss Physcomitrella patens (Bryophyta) comprise a single loop? BMC Plant Biol. *10*, 109.

Hong, S., Kim, S.A., Guerinot, M. Lou, and McClung, C.R. (2013). Reciprocal interaction

of the circadian clock with the iron homeostasis network in Arabidopsis. Plant Physiol. *161*, 893–903.

Hsu, P.Y., and Harmer, S.L. (2012). Circadian phase has profound effects on differential expression analysis. PLoS One *7*, e49853.

Hsu, P.Y., and Harmer, S.L. (2014). Wheels within wheels: the plant circadian system. Trends Plant Sci. *19*, 240–249.

Hsu, P.Y., Devisetty, U.K., and Harmer, S.L. (2013). Accurate timekeeping is controlled by a cycling activator in Arabidopsis. Elife *2*, e00473.

Huang, W., Pérez-García, P., Pokhilko, A., Millar, A.J., Antoshechkin, I., Riechmann, J.L., and Mas, P. (2012). Mapping the core of the Arabidopsis circadian clock defines the network structure of the oscillator. Science *336*, 75–79.

Hufford, M.B., Xu, X., van Heerwaarden, J., Pyhäjärvi, T., Chia, J.-M., Cartwright, R.A., Elshire, R.J., Glaubitz, J.C., Guill, K.E., Kaeppler, S.M., et al. (2012). Comparative population genomics of maize domestication and improvement. Nat. Genet. *44*, 808–811.

Hughes, M.E., Hogenesch, J.B., and Kornacker, K. (2010). JTK_CYCLE: an efficient nonparametric algorithm for detecting rhythmic components in genome-scale data sets. J. Biol. Rhythms *25*, 372–380.

Huijser, P., and Schmid, M. (2011). The control of developmental phase transitions in plants. Development *138*, 4117–4129.

Huq, E., Tepperman, J.M., and Quail, P.H. (2000). GIGANTEA is a nuclear protein involved in phytochrome signaling in Arabidopsis. Proc. Natl. Acad. Sci. U. S. A. *97*, 9789–9794.

Ibañez, C., Ramos, A., Acebo, P., Contreras, A., Casado, R., Allona, I., and Aragoncillo, C. (2008). Overall alteration of circadian clock gene expression in the chestnut cold response. PLoS One *3*, e3567.

Ibáñez, C., Kozarewa, I., Johansson, M., Ogren, E., Rohde, A., and Eriksson, M.E. (2010). Circadian clock components regulate entry and affect exit of seasonal dormancy as well as winter hardiness in Populus trees. Plant Physiol. *153*, 1823–1833.

Iltis, H.H. (1983). From teosinte to maize: the catastrophic sexual transmutation. Science *222*, 886–894.

Ito, S., Song, Y.H., and Imaizumi, T. (2012). LOV domain-containing F-box proteins: light-dependent protein degradation modules in Arabidopsis. Mol. Plant *5*, 573–582.

Izawa, T. (2012). Physiological significance of the plant circadian clock in natural field conditions. Plant. Cell Environ. *35*, 1729–1741.

Izawa, T., Mihara, M., Suzuki, Y., Gupta, M., Itoh, H., Nagano, A.J., Motoyama, R., Sawada, Y., Yano, M., Hirai, M.Y., et al. (2011). Os-GIGANTEA confers robust diurnal rhythms on the global transcriptome of rice in the field. Plant Cell *23*, 1741–1755.

Jacobsen, S.E., and Olszewski, N.E. (1993). Mutations at the SPINDLY locus of Arabidopsis alter gibberellin signal transduction. Plant Cell *5*, 887–896.

Jaeger, K.E., and Wigge, P.A. (2007). FT protein acts as a long-range signal in Arabidopsis. Curr. Biol. *17*, 1050–1054.

James, A.B., Syed, N.H., Bordage, S., Marshall, J., Nimmo, G.A., Jenkins, G.I., Herzyk, P., Brown, J.W.S., and Nimmo, H.G. (2012). Alternative splicing mediates responses of the Arabidopsis circadian clock to temperature changes. Plant Cell *24*, 961–981.

Jang, K., Lee, H.G., Jung, S.-J., Paek, N.-C., and Seo, P.J. (2015). The E3 Ubiquitin Ligase COP1 Regulates Thermosensory Flowering by Triggering GI Degradation in Arabidopsis. Sci. Rep. *5*, 12071.

Jang, S., Marchal, V., Panigrahi, K.C.S., Wenkel, S., Soppe, W., Deng, X.-W., Valverde, F., and Coupland, G. (2008). Arabidopsis COP1 shapes the temporal pattern of CO accumulation conferring a photoperiodic flowering response. EMBO J. *27*, 1277–1288.

Jiang, B., Nan, H., Gao, Y., Tang, L., Yue, Y., Lu, S., Ma, L., Cao, D., Sun, S., Wang, J., et al. (2014). Allelic combinations of soybean maturity Loci E1, E2, E3 and E4 result in diversity of maturity and adaptation to different latitudes. PLoS One *9*, e106042.

Jiménez-Gómez, J.M., Wallace, A.D., and Maloof, J.N. (2010). Network analysis identifies ELF3 as a QTL for the shade avoidance response in Arabidopsis. PLoS Genet. *6*, e1001100.

Johansson, M., and Staiger, D. (2015). Time to flower: interplay between photoperiod and the circadian clock. J. Exp. Bot. *66*, 719–730.

Jones, D.T. (1999). Protein secondary structure prediction based on position-specific scoring matrices. J. Mol. Biol. *292*, 195–202.

Jung, C., Pillen, K., Frese, L., Fähr, S., and Melchinger, A.E. (1993). Phylogenetic relationships between cultivated and wild species of the genusBeta revealed by DNA “fingerprinting”. Theor. Appl. Genet. *86*, 449–457.

Jung, J.-H., Seo, Y.-H., Seo, P.J., Reyes, J.L., Yun, J., Chua, N.-H., and Park, C.-M. (2007). The GIGANTEA-regulated microRNA172 mediates photoperiodic flowering independent of CONSTANS in Arabidopsis. Plant Cell *19*, 2736–2748.

Kabsch, W., and Sander, C. (1983). Dictionary of protein secondary structure: pattern recognition of hydrogen-bonded and geometrical features. Biopolymers *22*, 2577–2637.

Karayekov, E., Sellaro, R., Legris, M., Yanovsky, M.J., and Casal, J.J. (2013). Heat shock-induced fluctuations in clock and light signaling enhance phytochrome B-mediated Arabidopsis deetiolation. Plant Cell *25*, 2892–2906.

Karlgren, A., Gyllenstrand, N., Källman, T., and Lagercrantz, U. (2013). Conserved function of core clock proteins in the gymnosperm Norway spruce (Picea abies L. Karst). PLoS One *8*, e60110.

Keller, S.R., Levsen, N., Olson, M.S., and Tiffin, P. (2012). Local adaptation in the flowering-time gene network of balsam poplar, Populus balsamifera L. Mol. Biol. Evol. *29*, 3143–3152.

Khan, S., Rowe, S.C., and Harmon, F.G. (2010). Coordination of the maize transcriptome by a conserved circadian clock. BMC Plant Biol. *10*, 126.

Khanna, R., Kikis, E.A., and Quail, P.H. (2003). EARLY FLOWERING 4 functions in phytochrome B-regulated seedling de-etiolation. Plant Physiol. *133*, 1530–1538.

Kiba, T., Henriques, R., Sakakibara, H., and Chua, N.-H. (2007). Targeted degradation of PSEUDO-RESPONSE REGULATOR5 by an SCFZTL complex regulates clock function and photomorphogenesis in Arabidopsis thaliana. Plant Cell *19*, 2516–2530.

Kikis, E.A., Khanna, R., and Quail, P.H. (2005). ELF4 is a phytochrome-regulated component of a negative-feedback loop involving the central oscillator components CCA1 and LHY. Plant J. *44*, 300–313.

Kim, J., Geng, R., Gallenstein, R.A., and Somers, D.E. (2013a). The F-box protein ZEITLUPE controls stability and nucleocytoplasmic partitioning of GIGANTEA. Development *140*, 4060–4069.

Kim, J.A., Yang, T.-J., Kim, J.S., Park, J.Y., Kwon, S.-J., Lim, M.-H., Jin, M., Lee, S.C., Lee, S.I., Choi, B.-S., et al. (2007a). Isolation of circadian-associated genes in Brassica rapa by comparative genomics with Arabidopsis thaliana. Mol. Cells *23*, 145–153.

Kim, J.A., Kim, J.S., Hong, J.K., Lee, Y.-H., Choi, B.-S., Seol, Y.-J., and Jeon, C.H. (2012). Comparative mapping, genomic structure, and expression analysis of eight pseudo-response regulator genes in Brassica rapa. Mol. Genet. Genomics *287*, 373–388.

Kim, T., Kim, W.Y., Fujiwara, S., Kim, J., Cha, J.-Y., Park, J.H., Lee, S.Y., and Somers, D.E. (2011). HSP90 functions in the circadian clock through stabilization of the client F-box protein ZEITLUPE. Proc. Natl. Acad. Sci. U. S. A. *108*, 16843–16848.

Kim, W.-Y., Fujiwara, S., Suh, S.-S., Kim, J., Kim, Y., Han, L., David, K., Putterill, J., Nam, H.G., and Somers, D.E. (2007b). ZEITLUPE is a circadian photoreceptor stabilized by GIGANTEA in blue light. Nature *449*, 356–360.

Kim, W.-Y., Ali, Z., Park, H.J., Park, S.J., Cha, J.-Y., Perez-Hormaeche, J., Quintero, F.J., Shin, G., Kim, M.R., Qiang, Z., et al. (2013b). Release of SOS2 kinase from sequestration with GIGANTEA determines salt tolerance in Arabidopsis. Nat. Commun. *4*, 1352.

Kim, Y., Lim, J., Yeom, M., Kim, H., Kim, J., Wang, L., Kim, W.Y., Somers, D.E., and Nam, H.G. (2013c). ELF4 regulates GIGANTEA chromatin access through subnuclear sequestration. Cell Rep. *3*, 671–677.

King, W.M., and Murfet, I.C. (1985). Flowering in Pisum : A Sixth Locus , Dne. Ann. Bot. *60*, 835–846.

Kobayashi, Y., Kaya, H., Goto, K., Iwabuchi, M., and Araki, T. (1999). A pair of related genes with antagonistic roles in mediating flowering signals. Science *286*, 1960–1962.

Kojima, S., Takahashi, Y., Kobayashi, Y., Monna, L., Sasaki, T., Araki, T., and Yano, M. (2002). Hd3a, a rice ortholog of the Arabidopsis FT gene, promotes transition to flowering downstream of Hd1 under short-day conditions. Plant Cell Physiol. *43*, 1096–1105.

Kolmos, E., Nowak, M., Werner, M., Fischer, K., Schwarz, G., Mathews, S., Schoof, H., Nagy, F., Bujnicki, J.M., and Davis, S.J. (2009). Integrating ELF4 into the circadian system through combined structural and functional studies. HFSP J. *3*, 350–366.

Koo, B.-H., Yoo, S.-C., Park, J.-W., Kwon, C.-T., Lee, B.-D., An, G., Zhang, Z., Li, J., Li, Z., and Paek, N.-C. (2013). Natural variation in OsPRR37 regulates heading date and contributes to rice cultivation at a wide range of latitudes. Mol. Plant *6*, 1877–1888.

Koornneef, M., Hanhart, C.J., and van der Veen, J.H. (1991). A genetic and physiological analysis of late flowering mutants in Arabidopsis thaliana. Mol. Gen. Genet. *229*, 57–66.

Koornneef, M., Alonso-Blanco, C., Peeters, A.J.M., and Soppe, W. (1998). Genetic control of flowering time in Arabidopsis. Annu. Rev. Plant Physiol. Plant Mol. Biol. *49*, 345–370.

Korneli, C., Danisman, S., and Staiger, D. (2014). Differential control of pre-invasive and post-invasive antibacterial defense by the Arabidopsis circadian clock. Plant Cell Physiol. *55*, 1613–1622.

Kubota, A., Kita, S., Ishizaki, K., Nishihama, R., Yamato, K.T., and Kohchi, T. (2014).

Co-option of a photoperiodic growth-phase transition system during land plant evolution. Nat. Commun. *5*, 3668.

Kuleshov, N.N. (1933). World's Diversity of Phenotypes of Maize1. Agron. J. *25*, 688.

Kuno, N., Møller, S.G., Shinomura, T., Xu, X., Chua, N.-H., and Furuya, M. (2003). The novel MYB protein EARLY-PHYTOCHROME-RESPONSIVE1 is a component of a slave circadian oscillator in Arabidopsis. Plant Cell *15*, 2476–2488.

Kusakina, J., Rutterford, Z., Cotter, S., Martí, M.C., Laurie, D.A., Greenland, A.J., Hall, A., and Webb, A.A.R. (2015). Barley Hv CIRCADIAN CLOCK ASSOCIATED 1 and Hv PHOTOPERIOD H1 Are Circadian Regulators That Can Affect Circadian Rhythms in Arabidopsis. PLoS One *10*, e0127449.

Lai, A.G., Doherty, C.J., Mueller-Roeber, B., Kay, S.A., Schippers, J.H.M., and Dijkwel, P.P. (2012). CIRCADIAN CLOCK-ASSOCIATED 1 regulates ROS homeostasis and oxidative stress responses. Proc. Natl. Acad. Sci. U. S. A. *109*, 17129–17134.

Laurie, D.A., Pratchett, N., Snape, J.W., and Bezant, J.H. (1995). RFLP mapping of five major genes and eight quantitative trait loci controlling flowering time in a winter x spring barley (Hordeum vulgare L.) cross. Genome *38*, 575–585.

Lazakis, C.M., Coneva, V., and Colasanti, J. (2011). ZCN8 encodes a potential orthologue of Arabidopsis FT florigen that integrates both endogenous and photoperiod flowering signals in maize. J. Exp. Bot. *62*, 4833–4842.

Legnaioli, T., Cuevas, J., and Mas, P. (2009). TOC1 functions as a molecular switch connecting the circadian clock with plant responses to drought. EMBO J. *28*, 3745–3757.

Li, C., and Zhang, B. (2016). MicroRNAs in Control of Plant Development. J. Cell. Physiol. *231*, 303–313.

Li, F., Zhang, X., Hu, R., Wu, F., Ma, J., Meng, Y., and Fu, Y. (2013). Identification and molecular characterization of FKF1 and GI homologous genes in soybean. PLoS One *8*, e79036.

Li, H., Handsaker, B., Wysoker, A., Fennell, T., Ruan, J., Homer, N., Marth, G., Abecasis, G., and Durbin, R. (2009). The Sequence Alignment/Map format and SAMtools. Bioinformatics *25*, 2078–2079.

Liew, L.C., Hecht, V., Laurie, R.E., Knowles, C.L., Vander Schoor, J.K., Macknight, R.C., and Weller, J.L. (2009). DIE NEUTRALIS and LATE BLOOMER 1 contribute to regulation of the pea circadian clock. Plant Cell *21*, 3198–3211.

Liew, L.C., Hecht, V., Sussmilch, F.C., and Weller, J.L. (2014). The Pea Photoperiod

Response Gene STERILE NODES Is an Ortholog of LUX ARRHYTHMO. Plant Physiol. *165*, 648–657.

Liu, H., Wang, H., Gao, P., Xü, J., Xü, T., Wang, J., Wang, B., Lin, C., and Fu, Y.-F. (2009). Analysis of clock gene homologs using unifoliolates as target organs in soybean (Glycine max). J. Plant Physiol. *166*, 278–289.

Liu, J.-J., Sturrock, R., and Ekramoddoullah, A.K.M. (2010). The superfamily of thaumatin-like proteins: its origin, evolution, and expression towards biological function. Plant Cell Rep. *29*, 419–436.

Liu, K., Goodman, M., Muse, S., Smith, J.S., Buckler, E., and John, D. (2003). Genetic Structure and Diversity Among Maize Inbred Lines as Inferred from DNA Microsatellites.

Liu, L.-J., Zhang, Y.-C., Li, Q.-H., Sang, Y., Mao, J., Lian, H.-L., Wang, L., and Yang, H.-Q. (2008). COP1-mediated ubiquitination of CONSTANS is implicated in cryptochrome regulation of flowering in Arabidopsis. Plant Cell *20*, 292–306.

Liu, T., Carlsson, J., Takeuchi, T., Newton, L., and Farré, E.M. (2013). Direct regulation of abiotic responses by the Arabidopsis circadian clock component PRR7. Plant J. *76*, 101–114.

Liu, X.L., Covington, M.F., Fankhauser, C., Chory, J., and Wagner, D.R. (2001). ELF3 encodes a circadian clock-regulated nuclear protein that functions in an Arabidopsis PHYB signal transduction pathway. Plant Cell *13*, 1293–1304.

López-Torrejón, G., Guerra, D., Catalá, R., Salinas, J., and del Pozo, J.C. (2013). Identification of SUMO targets by a novel proteomic approach in plants(F). J. Integr. Plant Biol. *55*, 96–107.

Lou, P., Xie, Q., Xu, X., Edwards, C.E., Brock, M.T., Weinig, C., and McClung, C.R. (2011). Genetic architecture of the circadian clock and flowering time in Brassica rapa. Theor. Appl. Genet. *123*, 397–409.

Lou, P., Wu, J., Cheng, F., Cressman, L.G., Wang, X., and McClung, C.R. (2012). Preferential retention of circadian clock genes during diploidization following whole genome triplication in Brassica rapa. Plant Cell *24*, 2415–2426.

Lundqvist, U. (2009). Eighty Years of Scandinavian Barley Mutation Genetics and Ireeding.

Lyons, R., Rusu, A., Stiller, J., Powell, J., Manners, J.M., and Kazan, K. (2015). Investigating the Association between Flowering Time and Defense in the Arabidopsis thaliana-Fusarium oxysporum Interaction. PLoS One *10*, e0127699.

Makino, S., Kiba, T., Imamura, A., Hanaki, N., Nakamura, A., Suzuki, T., Taniguchi, M.,

Ueguchi, C., Sugiyama, T., and Mizuno, T. (2000). Genes encoding pseudo-response regulators: insight into His-to-Asp phosphorelay and circadian rhythm in Arabidopsis thaliana. Plant Cell Physiol. *41*, 791–803.

Marcolino-Gomes, J., Rodrigues, F.A., Fuganti-Pagliarini, R., Bendix, C., Nakayama, T.J., Celaya, B., Molinari, H.B.C., de Oliveira, M.C.N., Harmon, F.G., and Nepomuceno, A. (2014). Diurnal oscillations of soybean circadian clock and drought responsive genes. PLoS One *9*, e86402.

Martin-Tryon, E.L., Kreps, J.A., and Harmer, S.L. (2007). GIGANTEA acts in blue light signaling and has biochemically separable roles in circadian clock and flowering time regulation. Plant Physiol. *143*, 473–486.

Más, P., Kim, W.-Y., Somers, D.E., and Kay, S.A. (2003). Targeted degradation of TOC1 by ZTL modulates circadian function in Arabidopsis thaliana. Nature *426*, 567–570.

Matos, D. a., Cole, B.J., Whitney, I.P., MacKinnon, K.J.M., Kay, S. a., and Hazen, S.P. (2014). Daily changes in temperature, not the circadian clock, regulate growth rate in Brachypodium distachyon. PLoS One *9*, 1–9.

Matsubara, K., Ogiso-Tanaka, E., Hori, K., Ebana, K., Ando, T., and Yano, M. (2012). Natural variation in Hd17, a homolog of Arabidopsis ELF3 that is involved in rice photoperiodic flowering. Plant Cell Physiol. *53*, 709–716.

Matsushika, A., Makino, S., Kojima, M., and Mizuno, T. (2000). Circadian waves of expression of the APRR1/TOC1 family of pseudo-response regulators in Arabidopsis thaliana: insight into the plant circadian clock. Plant Cell Physiol. *41*, 1002–1012.

Mayer, K.F.X., Martis, M., Hedley, P.E., Simková, H., Liu, H., Morris, J.A., Steuernagel, B., Taudien, S., Roessner, S., Gundlach, H., et al. (2011). Unlocking the barley genome by chromosomal and comparative genomics. Plant Cell *23*, 1249–1263.

McBlain, B.A., and Bernard, R.L. (1987). A new gene affecting the time of flowering and maturity in soybeans. J. Hered. *78*, 160–162.

McWatters, H.G., Kolmos, E., Hall, A., Doyle, M.R., Amasino, R.M., Gyula, P., Nagy, F., Millar, A.J., and Davis, S.J. (2007). ELF4 is required for oscillatory properties of the circadian clock. Plant Physiol. *144*, 391–401.

Meeley, B., and Briggs, S. (1995). Reverse genetics for maize. Maize Genet. Coop. Newsl.

Mendoza, J., Bendix, C., Meeley, R., and Harmon, F.G. (2012). The homeologous Zea mays gigantea genes : characterization of expression and novel mutant alleles.

Meng, X., Muszynski, M.G., and Danilevskaya, O.N. (2011). The FT-like ZCN8 Gene Functions as a Floral Activator and Is Involved in Photoperiod Sensitivity in Maize. Plant Cell *23*, 942–960.

Michael, T.P., and McClung, C.R. (2003). Enhancer trapping reveals widespread circadian clock transcriptional control in Arabidopsis. Plant Physiol. *132*, 629–639.

Michael, T.P., Salome, P.A., and McClung, C.R. (2003). Two Arabidopsis circadian oscillators can be distinguished by differential temperature sensitivity. Proc. Natl. Acad. Sci. U. S. A. *100*, 6878–6883.

Michael, T.P., Mockler, T.C., Breton, G., McEntee, C., Byer, A., Trout, J.D., Hazen, S.P., Shen, R., Priest, H.D., Sullivan, C.M., et al. (2008). Network Discovery Pipeline Elucidates Conserved Time-of-Day–Specific cis-Regulatory Modules. PLoS Genet. *4*, e14.

Miller, G., Suzuki, N., Ciftci-Yilmaz, S., and Mittler, R. (2010). Reactive oxygen species homeostasis and signalling during drought and salinity stresses. Plant. Cell Environ. *33*, 453–467.

Miller, T.A., Muslin, E.H., and Dorweiler, J.E. (2008). A maize CONSTANS-like gene, conz1, exhibits distinct diurnal expression patterns in varied photoperiods. Planta *227*, 1377–1388.

Ming, R., Hou, S., Feng, Y., Yu, Q., Dionne-Laporte, A., Saw, J.H., Senin, P., Wang, W., Ly, B. V, Lewis, K.L.T., et al. (2008). The draft genome of the transgenic tropical fruit tree papaya (Carica papaya Linnaeus). Nature *452*, 991–996.

Mishra, P., and Panigrahi, K.C. (2015). GIGANTEA - an emerging story. Front. Plant Sci. *6*, 8.

Mittler, R., Vanderauwera, S., Gollery, M., and Van Breusegem, F. (2004). Reactive oxygen gene network of plants. Trends Plant Sci. *9*, 490–498.

Miwa, K., Serikawa, M., Suzuki, S., Kondo, T., and Oyama, T. (2006). Conserved expression profiles of circadian clock-related genes in two Lemna species showing long-day and short-day photoperiodic flowering responses. Plant Cell Physiol. *47*, 601–612.

Miyazaki, Y., Abe, H., Takase, T., Kobayashi, M., and Kiyosue, T. (2015). Overexpression of LOV KELCH protein 2 confers dehydration tolerance and is associated with enhanced expression of dehydration-inducible genes in Arabidopsis thaliana. Plant Cell Rep. *34*, 843–852.

Mizoguchi, T., Wright, L., Fujiwara, S., Cremer, F., Lee, K., Onouchi, H., Mouradov, A.,

Fowler, S., Kamada, H., Putterill, J., et al. (2005). Distinct roles of GIGANTEA in promoting flowering and regulating circadian rhythms in Arabidopsis. Plant Cell *17*, 2255–2270.

Mizuno, T., and Nakamichi, N. (2005). Pseudo-Response Regulators (PRRs) or True Oscillator Components (TOCs). Plant Cell Physiol. *46*, 677–685.

Mizuno, N., Nitta, M., Sato, K., and Nasuda, S. (2012). A wheat homologue of PHYTOCLOCK 1 is a candidate gene conferring the early heading phenotype to einkorn wheat. Genes Genet. Syst. *87*, 357–367.

Müller, N.A., Wijnen, C.L., Srinivasan, A., Ryngajllo, M., Ofner, I., Lin, T., Ranjan, A., West, D., Maloof, J.N., Sinha, N.R., et al. (2015). Domestication selected for deceleration of the circadian clock in cultivated tomato. Nat. Genet. *advance on*.

Mullet, J., Morishige, D., McCormick, R., Truong, S., Hilley, J., McKinley, B., Anderson, R., Olson, S.N., and Rooney, W. (2014). Energy sorghum--a genetic model for the design of C4 grass bioenergy crops. J. Exp. Bot. *65*, 3479–3489.

Murakami, M., Ashikari, M., Miura, K., Yamashino, T., and Mizuno, T. (2003). The evolutionarily conserved OsPRR quintet: rice pseudo-response regulators implicated in circadian rhythm. Plant Cell Physiol. *44*, 1229–1236.

Murakami, M., Matsushika, A., Ashikari, M., Yamashino, T., and Mizuno, T. (2005). Circadian-associated rice pseudo response regulators (OsPRRs): insight into the control of flowering time. Biosci. Biotechnol. Biochem. *69*, 410–414.

Murakami, M., Tago, Y., Yamashino, T., and Mizuno, T. (2007). Comparative overviews of clock-associated genes of Arabidopsis thaliana and Oryza sativa. Plant Cell Physiol. *48*, 110–121.

Murashige, T., and Skoog, F. (1962). A Revised Medium for Rapid Growth and Bio Assays with Tobacco Tissue Cultures. Physiol. Plant. *15*, 473–497.

Murfet, I.C. (1971). Flowering in Pisum. Three distinct phenotypic classes determined by the interaction of a dominant early and a dominant late gene. Heredity (Edinb). *26*, 243–257.

Murfet, I.C. (1973). Flowering in Pisum. Hr, a gene for high response to photoperiod. Heredity (Edinb). *31*, 157–164.

Murphy, R.L., Klein, R.R., Morishige, D.T., Brady, J.A., Rooney, W.L., Miller, F.R., Dugas, D. V, Klein, P.E., and Mullet, J.E. (2011). Coincident light and clock regulation of pseudoresponse regulator protein 37 (PRR37) controls photoperiodic flowering in sorghum. Proc. Natl. Acad. Sci. U. S. A. *108*, 16469–16474.

Nagano, A.J., Sato, Y., Mihara, M., Antonio, B.A., Motoyama, R., Itoh, H., Nagamura, Y., and Izawa, T. (2012). Deciphering and prediction of transcriptome dynamics under fluctuating field conditions. Cell *151*, 1358–1369.

Nagel, D.H., and Kay, S.A. (2012). Complexity in the wiring and regulation of plant circadian networks. Curr. Biol. *22*, R648–R657.

Nakamichi, N., Kita, M., Niinuma, K., Ito, S., Yamashino, T., Mizoguchi, T., and Mizuno, T. (2007). Arabidopsis clock-associated pseudo-response regulators PRR9, PRR7 and PRR5 coordinately and positively regulate flowering time through the canonical CONSTANS-dependent photoperiodic pathway. Plant Cell Physiol. *48*, 822–832.

Nakamichi, N., Fukushima, A., Kusano, M., Sakakibara, H., Mizuno, T., and Saito, K. (2009a). Linkage between circadian clock and tricarboxylic acid cycle in Arabidopsis. Plant Signal. Behav. *4*, 660–662.

Nakamichi, N., Kusano, M., Fukushima, A., Kita, M., Ito, S., Yamashino, T., Saito, K., Sakakibara, H., and Mizuno, T. (2009b). Transcript profiling of an Arabidopsis PSEUDO RESPONSE REGULATOR arrhythmic triple mutant reveals a role for the circadian clock in cold stress response. Plant Cell Physiol. *50*, 447–462.

Nakamichi, N., Kiba, T., Henriques, R., Mizuno, T., Chua, N.-H., and Sakakibara, H. (2010). PSEUDO-RESPONSE REGULATORS 9, 7, and 5 are transcriptional repressors in the Arabidopsis circadian clock. Plant Cell *22*, 594–605.

Nakamichi, N., Kiba, T., Kamioka, M., Suzuki, T., Yamashino, T., Higashiyama, T., Sakakibara, H., and Mizuno, T. (2012). Transcriptional repressor PRR5 directly regulates clock-output pathways. Proc. Natl. Acad. Sci. U. S. A. *109*, 17123–17128.

Nefissi, R., Natsui, Y., Miyata, K., Oda, A., Hase, Y., Nakagawa, M., Ghorbel, A., and Mizoguchi, T. (2011). Double loss-of-function mutation in EARLY FLOWERING 3 and CRYPTOCHROME 2 genes delays flowering under continuous light but accelerates it under long days and short days: an important role for Arabidopsis CRY2 to accelerate flowering time in continuous lig. J. Exp. Bot. *62*, 2731–2744.

Nelson, D.C., Flematti, G.R., Riseborough, J.-A., Ghisalberti, E.L., Dixon, K.W., and Smith, S.M. (2010). Karrikins enhance light responses during germination and seedling development in Arabidopsis thaliana. Proc. Natl. Acad. Sci. U. S. A. *107*, 7095–7100.

Ng, D.W.-K., Miller, M., Yu, H.H., Huang, T.-Y., Kim, E.-D., Lu, J., Xie, Q., McClung, C.R., and Chen, Z.J. (2014). A Role for CHH Methylation in the Parent-of-Origin Effect on Altered Circadian Rhythms and Biomass Heterosis in Arabidopsis Intraspecific Hybrids. Plant Cell *26*, 2430–2440.

Nguyen, C. V, Vrebalov, J.T., Gapper, N.E., Zheng, Y., Zhong, S., Fei, Z., and

Giovannoni, J.J. (2014). Tomato GOLDEN2-LIKE transcription factors reveal molecular gradients that function during fruit development and ripening. Plant Cell *26*, 585–601.

Ni, Z., Kim, E.-D., Ha, M., Lackey, E., Liu, J., Zhang, Y., Sun, Q., and Chen, Z.J. (2009). Altered circadian rhythms regulate growth vigour in hybrids and allopolyploids. Nature *457*, 327–331.

Nose, M., and Watanabe, A. (2014). Clock genes and diurnal transcriptome dynamics in summer and winter in the gymnosperm Japanese cedar (Cryptomeria japonica (L.f.) D.Don). BMC Plant Biol. *14*, 308.

Nozue, K., Covington, M.F., Duek, P.D., Lorrain, S., Fankhauser, C., Harmer, S.L., and Maloof, J.N. (2007). Rhythmic growth explained by coincidence between internal and external cues. Nature *448*, 358–361.

Nusinow, D.A., Helfer, A., Hamilton, E.E., King, J.J., Imaizumi, T., Schultz, T.F., Farré, E.M., and Kay, S.A. (2011). The ELF4-ELF3-LUX complex links the circadian clock to diurnal control of hypocotyl growth. Nature *475*, 398–402.

Ohara, T., Fukuda, H., and Tokuda, I.T. (2015). An extended mathematical model for reproducing the phase response of Arabidopsis thaliana under various light conditions. J. Theor. Biol. *382*, 337–344.

Oliverio, K.A., Crepy, M., Martin-Tryon, E.L., Milich, R., Harmer, S.L., Putterill, J., Yanovsky, M.J., and Casal, J.J. (2007). GIGANTEA regulates phytochrome A-mediated photomorphogenesis independently of its role in the circadian clock. Plant Physiol. *144*, 495–502.

Olsen, K.M., and Wendel, J.F. (2013). Crop plants as models for understanding plant adaptation and diversification. Front. Plant Sci. *4*, 290.

Onai, K., and Ishiura, M. (2005). PHYTOCLOCK 1 encoding a novel GARP protein essential for the Arabidopsis circadian clock. Genes Cells *10*, 963–972.

Pajoro, A., Biewers, S., Dougali, E., Leal Valentim, F., Mendes, M.A., Porri, A., Coupland, G., Van de Peer, Y., van Dijk, A.D.J., Colombo, L., et al. (2014). The (r)evolution of gene regulatory networks controlling Arabidopsis plant reproduction: a two-decade history. J. Exp. Bot. *65*, 4731–4745.

Pankin, A., Campoli, C., Dong, X., Kilian, B., Sharma, R., Himmelbach, A., Saini, R., Davis, S.J., Stein, N., Schneeberger, K., et al. (2014). Mapping-by-sequencing identifies HvPHYTOCHROME C as a candidate gene for the early maturity 5 locus modulating the circadian clock and photoperiodic flowering in barley. Genetics *198*, 383–396.

Para, A., Farré, E.M., Imaizumi, T., Pruneda-Paz, J.L., Harmon, F.G., and Kay, S.A.

(2007). PRR3 Is a vascular regulator of TOC1 stability in the Arabidopsis circadian clock. Plant Cell *19*, 3462–3473.

Park, D.H., Somers, D.E., Kim, Y.S., Choy, Y.H., Lim, H.K., Soh, M.S., Kim, H.J., Kay, S.A., and Nam, H.G. (1999). Control of circadian rhythms and photoperiodic flowering by the Arabidopsis GIGANTEA gene. Science *285*, 1579–1582.

Park, H.J., Kim, W.-Y., and Yun, D.-J. (2013). A role for GIGANTEA: keeping the balance between flowering and salinity stress tolerance. Plant Signal. Behav. *8*, e24820.

Park, W., Li, J., Song, R., Messing, J., and Chen, X. (2002). CARPEL FACTORY, a Dicer homolog, and HEN1, a novel protein, act in microRNA metabolism in Arabidopsis thaliana. Curr. Biol. *12*, 1484–1495.

Pasam, R.K., Sharma, R., Malosetti, M., van Eeuwijk, F.A., Haseneyer, G., Kilian, B., and Graner, A. (2012). Genome-wide association studies for agronomical traits in a world wide spring barley collection. BMC Plant Biol. *12*, 16.

Penfield, S., and Hall, A. (2009). A role for multiple circadian clock genes in the response to signals that break seed dormancy in Arabidopsis. Plant Cell *21*, 1722–1732.

Pin, P.A., Benlloch, R., Bonnet, D., Wremerth-Weich, E., Kraft, T., Gielen, J.J.L., and Nilsson, O. (2010). An antagonistic pair of FT homologs mediates the control of flowering time in sugar beet. Science *330*, 1397–1400.

Pin, P.A., Zhang, W., Vogt, S.H., Dally, N., Büttner, B., Schulze-Buxloh, G., Jelly, N.S., Chia, T.Y.P., Mutasa-Göttgens, E.S., Dohm, J.C., et al. (2012). The role of a pseudo-response regulator gene in life cycle adaptation and domestication of beet. Curr. Biol. *22*, 1095–1101.

Pingali, P.L. (2012). Green revolution: impacts, limits, and the path ahead. Proc. Natl. Acad. Sci. U. S. A. *109*, 12302–12308.

Pokhilko, A., Fernández, A.P., Edwards, K.D., Southern, M.M., Halliday, K.J., and Millar, A.J. (2012). The clock gene circuit in Arabidopsis includes a repressilator with additional feedback loops. Mol. Syst. Biol. *8*, 574.

Polstein, L.R., and Gersbach, C.A. (2014). Light-inducible gene regulation with engineered zinc finger proteins. Methods Mol. Biol. *1148*, 89–107.

Putterill, J., Robson, F., Lee, K., Simon, R., and Coupland, G. (1995). The CONSTANS gene of Arabidopsis promotes flowering and encodes a protein showing similarities to zinc finger transcription factors. Cell *80*, 847–857.

Qian, H., Han, X., Peng, X., Lu, T., Liu, W., and Fu, Z. (2014). The circadian clock gene regulatory module enantioselectively mediates imazethapyr-induced early flowering in Arabidopsis thaliana. J. Plant Physiol. *171*, 92–98.

Quinby, J.R. (1966). Fourth Maturity Gene Locus in Sorghum1. Crop Sci. *6*, 516.

Quinby, J.R. (1967). The maturity genes of sorghum. In Advances in Agronomy, Volume 19, (Academic Press), pp. 267–305.

Quinby, J.R. (1974). Sorghum Improvement and the Genetics of Growth (Texas Agricultural Experiment Station).

Quinby, J.R. (1975). The Genetics of Sorghum Improvement. J. Hered. *66*, 56–62.

Quinby, J.R., and Karper, R.E. (1945). The Inheritance of Three Genes That Influence Time of Floral Initiation and Maturity Date in Milo1. Agron. J. *37*, 916.

Ramos, A., Pérez-Solís, E., Ibáñez, C., Casado, R., Collada, C., Gómez, L., Aragoncillo, C., and Allona, I. (2005). Winter disruption of the circadian clock in chestnut. Proc. Natl. Acad. Sci. U. S. A. *102*, 7037–7042.

Rawat, R., Schwartz, J., Jones, M.A., Sairanen, I., Cheng, Y., Andersson, C.R., Zhao, Y., Ljung, K., and Harmer, S.L. (2009). REVEILLE1, a Myb-like transcription factor, integrates the circadian clock and auxin pathways. Proc. Natl. Acad. Sci. U. S. A. *106*, 16883–16888.

Rawat, R., Takahashi, N., Hsu, P.Y., Jones, M.A., Schwartz, J., Salemi, M.R., Phinney, B.S., and Harmer, S.L. (2011). REVEILLE8 and PSEUDO-REPONSE REGULATOR5 form a negative feedback loop within the Arabidopsis circadian clock. PLoS Genet. *7*, e1001350.

Rédei, G.P. (1962). Supervital Mutants of Arabidopsis. Genetics *47*, 443–460.

Reed, J.W., Nagpal, P., Bastow, R.M., Solomon, K.S., Dowson-Day, M.J., Elumalai, R.P., and Millar, A.J. (2000). Independent action of ELF3 and phyB to control hypocotyl elongation and flowering time. Plant Physiol. *122*, 1149–1160.

Renny-Byfield, S., and Wendel, J.F. (2014). Doubling down on genomes: polyploidy and crop plants. Am. J. Bot. *101*, 1711–1725.

Riboni, M., Galbiati, M., Tonelli, C., and Conti, L. (2013). GIGANTEA enables drought escape response via abscisic acid-dependent activation of the florigens and SUPPRESSOR OF OVEREXPRESSION OF CONSTANS. Plant Physiol. *162*, 1706–1719.

Richardson, A.D., Duigan, S.P., and Berlyn, G.P. (2002). An evaluation of noninvasive

methods to estimate foliar chlorophyll content. New Phytol. *153*, 185–194.

Rodrigues, F.A., Fuganti-Pagliarini, R., Marcolino-Gomes, J., Nakayama, T.J., Molinari, H.B.C., Lobo, F.P., Harmon, F.G., and Nepomuceno, A.L. (2015). Daytime soybean transcriptome fluctuations during water deficit stress. BMC Genomics *16*, 505.

Rodríguez-Falcón, M., Bou, J., and Prat, S. (2006). Seasonal control of tuberization in potato: conserved elements with the flowering response. Annu. Rev. Plant Biol. *57*, 151–180.

Rooney, W.L., and Aydin, S. (1999). Genetic Control of a Photoperiod-Sensitive Response in Sorghum bicolor (L.) Moench. Crop Sci. *39*, 397.

Rubio, V., and Deng, X.W. (2007). Plant science. Standing on the shoulders of GIGANTEA. Science *318*, 206–207.

Rutitzky, M., Ghiglione, H.O., Curá, J.A., Casal, J.J., and Yanovsky, M.J. (2009). Comparative genomic analysis of light-regulated transcripts in the Solanaceae. BMC Genomics *10*, 60.

Saito, H., Ogiso-Tanaka, E., Okumoto, Y., Yoshitake, Y., Izumi, H., Yokoo, T., Matsubara, K., Hori, K., Yano, M., Inoue, H., et al. (2012). Ef7 encodes an ELF3-like protein and promotes rice flowering by negatively regulating the floral repressor gene Ghd7 under both short- and long-day conditions. Plant Cell Physiol. *53*, 717–728.

Sakuraba, Y., Jeong, J., Kang, M.-Y., Kim, J., Paek, N.-C., and Choi, G. (2014). Phytochrome-interacting transcription factors PIF4 and PIF5 induce leaf senescence in Arabidopsis. Nat. Commun. *5*, 4636.

Salomé, P.A., and McClung, C.R. (2005). PSEUDO-RESPONSE REGULATOR 7 and 9 are partially redundant genes essential for the temperature responsiveness of the Arabidopsis circadian clock. Plant Cell *17*, 791–803.

Salomé, P.A., Weigel, D., and McClung, C.R. (2010). The role of the Arabidopsis morning loop components CCA1, LHY, PRR7, and PRR9 in temperature compensation. Plant Cell *22*, 3650–3661.

Salvi, S., Sponza, G., Morgante, M., Tomes, D., Niu, X., Fengler, K.A., Meeley, R., Ananiev, E. V, Svitashev, S., Bruggemann, E., et al. (2007). Conserved noncoding genomic sequences associated with a flowering-time quantitative trait locus in maize. Proc. Natl. Acad. Sci. U. S. A. *104*, 11376–11381.

Sanchez, S.E., Petrillo, E., Beckwith, E.J., Zhang, X., Rugnone, M.L., Hernando, C.E., Cuevas, J.C., Godoy Herz, M.A., Depetris-Chauvin, A., Simpson, C.G., et al. (2010). A methyl transferase links the circadian clock to the regulation of alternative splicing.

Nature *468*, 112–116.

Sarker, A. (1999). Inheritance and linkage relationship of days to flower and morphological loci in lentil (Lens culinaris Medikus subsp. culinaris). J. Hered. *90*, 270–275.

Satbhai, S.B., Yamashino, T., Okada, R., Nomoto, Y., Mizuno, T., Tezuka, Y., Itoh, T., Tomita, M., Otsuki, S., and Aoki, S. (2011). Pseudo-response regulator (PRR) homologues of the moss Physcomitrella patens: insights into the evolution of the PRR family in land plants. DNA Res. *18*, 39–52.

Sawa, M., and Kay, S.A. (2011). GIGANTEA directly activates Flowering Locus T in Arabidopsis thaliana. Proc. Natl. Acad. Sci. U. S. A. *108*, 11698–11703.

Sawa, M., Nusinow, D.A., Kay, S.A., and Imaizumi, T. (2007). FKF1 and GIGANTEA complex formation is required for day-length measurement in Arabidopsis. Science *318*, 261–265.

Sawers, R.J.H., Linley, P.J., Farmer, P.R., Hanley, N.P., Costich, D.E., Terry, M.J., and Brutnell, T.P. (2002). Elongated mesocotyl1, a phytochrome-deficient mutant of maize. Plant Physiol. *130*, 155–163.

Schaffer, R., Ramsay, N., Samach, A., Corden, S., Putterill, J., Carré, I.A., and Coupland, G. (1998). The late elongated hypocotyl mutation of Arabidopsis disrupts circadian rhythms and the photoperiodic control of flowering. Cell *93*, 1219–1229.

Schnable, J.C., and Freeling, M. (2011). Genes identified by visible mutant phenotypes show increased bias toward one of two subgenomes of maize. PLoS One *6*, e17855.

Schnable, P.S., and Springer, N.M. (2013). Progress toward understanding heterosis in crop plants. Annu. Rev. Plant Biol. *64*, 71–88.

Schnable, J.C., Springer, N.M., and Freeling, M. (2011). Differentiation of the maize subgenomes by genome dominance and both ancient and ongoing gene loss. Proc. Natl. Acad. Sci. U. S. A. *108*, 4069–4074.

Schwechheimer, C. (2008). Understanding gibberellic acid signaling--are we there yet? Curr. Opin. Plant Biol. *11*, 9–15.

Seki, M., Chono, M., Matsunaka, H., Fujita, M., Oda, S., Kubo, K., Kiribuchi-Otobe, C., Kojima, H., Nishida, H., and Kato, K. (2011). Distribution of photoperiod-insensitive alleles Ppd-B1a and Ppd-D1a and their effect on heading time in Japanese wheat cultivars. Breed. Sci. *61*, 405–412.

Serikawa, M., Miwa, K., Kondo, T., and Oyama, T. (2008). Functional conservation of clock-related genes in flowering plants: overexpression and RNA interference analyses

of the circadian rhythm in the monocotyledon Lemna gibba. Plant Physiol. *146*, 1952–1963.

Shaw, L.M., Turner, A.S., and Laurie, D.A. (2012). The impact of photoperiod insensitive Ppd-1a mutations on the photoperiod pathway across the three genomes of hexaploid wheat (Triticum aestivum). Plant J. *71*, 71–84.

Shaw, L.M., Turner, A.S., Herry, L., Griffiths, S., and Laurie, D.A. (2013). Mutant alleles of Photoperiod-1 in wheat (Triticum aestivum L.) that confer a late flowering phenotype in long days. PLoS One *8*, e79459.

Sheehan, M.J., Kennedy, L.M., Costich, D.E., and Brutnell, T.P. (2007). Subfunctionalization of PhyB1 and PhyB2 in the control of seedling and mature plant traits in maize. Plant J. *49*, 338–353.

Shim, J.S., and Imaizumi, T. (2015). Circadian clock and photoperiodic response in Arabidopsis: from seasonal flowering to redox homeostasis. Biochemistry *54*, 157–170.

Shin, J., Park, E., and Choi, G. (2007). PIF3 regulates anthocyanin biosynthesis in an HY5-dependent manner with both factors directly binding anthocyanin biosynthetic gene promoters in Arabidopsis. Plant J. *49*, 981–994.

Shrestha, R., Gómez-Ariza, J., Brambilla, V., and Fornara, F. (2014). Molecular control of seasonal flowering in rice, arabidopsis and temperate cereals. Ann. Bot. *114*, 1445–1458.

Simossis, V.A., and Heringa, J. (2005). PRALINE: a multiple sequence alignment toolbox that integrates homology-extended and secondary structure information. Nucleic Acids Res. *33*, W289–W294.

Smith, C.W., and Frederiksen, R.A. (2000). History of cultivar development in the United States. In Sorghum: Origin, History, Technology, and Production, pp. 191–223.

Somers, D.E., Schultz, T.F., Milnamow, M., and Kay, S.A. (2000). ZEITLUPE encodes a novel clock-associated PAS protein from Arabidopsis. Cell *101*, 319–329.

Song, Y.H., Ito, S., and Imaizumi, T. (2013). Flowering time regulation: photoperiod- and temperature-sensing in leaves. Trends Plant Sci. *18*, 575–583.

Song, Y.H., Estrada, D.A., Johnson, R.S., Kim, S.K., Lee, S.Y., MacCoss, M.J., and Imaizumi, T. (2014). Distinct roles of FKF1, Gigantea, and Zeitlupe proteins in the regulation of Constans stability in Arabidopsis photoperiodic flowering. Proc. Natl. Acad. Sci. U. S. A. *111*, 17672–17677.

Sothern, R.B., Tseng, T.-S., Orcutt, S.L., Olszewski, N.E., and Koukkari, W.L. (2002). GIGANTEA and SPINDLY genes linked to the clock pathway that controls circadian

characteristics of transpiration in Arabidopsis. Chronobiol. Int. *19*, 1005–1022.

Strable, J., and Scanlon, M.J. (2009). Maize (Zea mays): a model organism for basic and applied research in plant biology. Cold Spring Harb. Protoc. *2009*, pdb.emo132.

Strayer, C., Oyama, T., Schultz, T.F., Raman, R., Somers, D.E., Más, P., Panda, S., Kreps, J.A., and Kay, S.A. (2000). Cloning of the Arabidopsis clock gene TOC1, an autoregulatory response regulator homolog. Science *289*, 768–771.

Suárez-López, P., Wheatley, K., Robson, F., Onouchi, H., Valverde, F., and Coupland, G. (2001). CONSTANS mediates between the circadian clock and the control of flowering in Arabidopsis. Nature *410*, 1116–1120.

Swigonová, Z., Lai, J., Ma, J., Ramakrishna, W., Llaca, V., Bennetzen, J.L., and Messing, J. (2004). Close split of sorghum and maize genome progenitors. Genome Res. *14*, 1916–1923.

Takase, T., Ishikawa, H., Murakami, H., Kikuchi, J., Sato-Nara, K., and Suzuki, H. (2011). The circadian clock modulates water dynamics and aquaporin expression in Arabidopsis roots. Plant Cell Physiol. *52*, 373–383.

Takata, N., Saito, S., Saito, C.T., and Uemura, M. (2010). Phylogenetic footprint of the plant clock system in angiosperms: evolutionary processes of pseudo-response regulators. BMC Evol. Biol. *10*, 126.

Takeuchi, T., Newton, L., Burkhardt, A., Mason, S., and Farre, E.M. (2014). Light and the circadian clock mediate time-specific changes in sensitivity to UV-B stress under light/dark cycles. J. Exp. Bot. *65*, 6003–6012.

Taylor, S.A., and Murfet, I.C. (1996). Flowering in Pisum: Identification of a new ppd allele and its physiological action as revealed by grafting. Physiol. Plant. *97*, 719–723.

Thines, B., and Harmon, F.G. (2010). Ambient temperature response establishes ELF3 as a required component of the core Arabidopsis circadian clock. Proc. Natl. Acad. Sci. U. S. A. *107*, 3257–3262.

Trapnell, C., Williams, B.A., Pertea, G., Mortazavi, A., Kwan, G., van Baren, M.J., Salzberg, S.L., Wold, B.J., and Pachter, L. (2010). Transcript assembly and quantification by RNA-Seq reveals unannotated transcripts and isoform switching during cell differentiation. Nat. Biotechnol. *28*, 511–515.

Tseng, T.-S., Salomé, P.A., McClung, C.R., and Olszewski, N.E. (2004). SPINDLY and GIGANTEA interact and act in Arabidopsis thaliana pathways involved in light responses, flowering, and rhythms in cotyledon movements. Plant Cell *16*, 1550–1563.

Turck, F., Fornara, F., and Coupland, G. (2008). Regulation and identity of florigen:

FLOWERING LOCUS T moves center stage. Annu. Rev. Plant Biol. *59*, 573–594.

Turner, A., Beales, J., Faure, S., Dunford, R.P., and Laurie, D.A. (2005). The pseudo-response regulator Ppd-H1 provides adaptation to photoperiod in barley. Science *310*, 1031–1034.

Vlăduţu, C., McLaughlin, J., and Phillips, R.L. (1999). Fine mapping and characterization of linked quantitative trait loci involved in the transition of the maize apical meristem from vegetative to generative structures. Genetics *153*, 993–1007.

Wang, Z.Y., and Tobin, E.M. (1998). Constitutive expression of the CIRCADIAN CLOCK ASSOCIATED 1 (CCA1) gene disrupts circadian rhythms and suppresses its own expression. Cell *93*, 1207–1217.

Wang, G., Schmalenbach, I., von Korff, M., Léon, J., Kilian, B., Rode, J., and Pillen, K. (2010). Association of barley photoperiod and vernalization genes with QTLs for flowering time and agronomic traits in a BC2DH population and a set of wild barley introgression lines. Theor. Appl. Genet. *120*, 1559–1574.

Wang, L., Si, Y., Dedow, L.K., Shao, Y., Liu, P., and Brutnell, T.P. (2011a). A low-cost library construction protocol and data analysis pipeline for Illumina-based strand-specific multiplex RNA-seq. PLoS One *6*, e26426.

Wang, P., Fouracre, J., Kelly, S., Karki, S., Gowik, U., Aubry, S., Shaw, M.K., Westhoff, P., Slamet-Loedin, I.H., Quick, W.P., et al. (2013). Evolution of GOLDEN2-LIKE gene function in C(3) and C (4) plants. Planta *237*, 481–495.

Wang, W., Barnaby, J.Y., Tada, Y., Li, H., Tör, M., Caldelari, D., Lee, D., Fu, X.-D., and Dong, X. (2011b). Timing of plant immune responses by a central circadian regulator. Nature *470*, 110–114.

Wang, X., Wang, Q., Nguyen, P., and Lin, C. (2014). Cryptochrome-mediated light responses in plants. Enzym. *35*, 167–189.

Wang, Z.Y., Kenigsbuch, D., Sun, L., Harel, E., Ong, M.S., and Tobin, E.M. (1997). A Myb-related transcription factor is involved in the phytochrome regulation of an Arabidopsis Lhcb gene. Plant Cell *9*, 491–507.

Warren, C.R. (2008). Rapid Measurement of Chlorophylls with a Microplate Reader. J. Plant Nutr. *31*, 1321–1332.

Watanabe, S., Xia, Z., Hideshima, R., Tsubokura, Y., Sato, S., Yamanaka, N., Takahashi, R., Anai, T., Tabata, S., Kitamura, K., et al. (2011). A map-based cloning strategy employing a residual heterozygous line reveals that the GIGANTEA gene is involved in soybean maturity and flowering. Genetics *188*, 395–407.

Watanabe, S., Harada, K., and Abe, J. (2012). Genetic and molecular bases of photoperiod responses of flowering in soybean. Breed. Sci. *61*, 531–543.

Weller, J.L., and Ortega, R. (2015). Genetic control of flowering time in legumes. Front. Plant Sci. *6*, 207.

Weller, J.L., Liew, L.C., Hecht, V.F.G., Rajandran, V., Laurie, R.E., Ridge, S., Wenden, B., Vander Schoor, J.K., Jaminon, O., Blassiau, C., et al. (2012). A conserved molecular basis for photoperiod adaptation in two temperate legumes. Proc. Natl. Acad. Sci. U. S. A. *109*, 21158–21163.

Wong, A.C.S., Hecht, V.F.G., Picard, K., Diwadkar, P., Laurie, R.E., Wen, J., Mysore, K., Macknight, R.C., and Weller, J.L. (2014). Isolation and functional analysis of CONSTANS-LIKE genes suggests that a central role for CONSTANS in flowering time control is not evolutionarily conserved in Medicago truncatula. Front. Plant Sci. *5*, 486.

Worland, A.J., Börner, A., Korzun, V., Li, W.M., Petrovíc, S., and Sayers, E.J. (1998). The influence of photoperiod genes on the adaptability of European winter wheats. Euphytica *100*, 385–394.

Wu, T.D., and Nacu, S. (2010). Fast and SNP-tolerant detection of complex variants and splicing in short reads. Bioinformatics *26*, 873–881.

Xie, Q., Wang, P., Liu, X., Yuan, L., Wang, L., Zhang, C., Li, Y., Xing, H., Zhi, L., Yue, Z., et al. (2014). LNK1 and LNK2 are transcriptional coactivators in the Arabidopsis circadian oscillator. Plant Cell *26*, 2843–2857.

Xie, Q., Lou, P., Hermand, V., Aman, R., Park, H.J., Yun, D.-J., Kim, W.Y., Salmela, M.J., Ewers, B.E., Weinig, C., et al. (2015). Allelic polymorphism of GIGANTEA is responsible for naturally occurring variation in circadian period in Brassica rapa. Proc. Natl. Acad. Sci. U. S. A. *112*, 3829–3834.

Xue, W., Xing, Y., Weng, X., Zhao, Y., Tang, W., Wang, L., Zhou, H., Yu, S., Xu, C., Li, X., et al. (2008). Natural variation in Ghd7 is an important regulator of heading date and yield potential in rice. Nat. Genet. *40*, 761–767.

Yang, L., Li, B., Zheng, X., Li, J., Yang, M., Dong, X., He, G., An, C., and Deng, X.W. (2015a). Salicylic acid biosynthesis is enhanced and contributes to increased biotrophic pathogen resistance in Arabidopsis hybrids. Nat. Commun. *6*, 7309.

Yang, Y., Peng, Q., Chen, G.-X., Li, X.-H., and Wu, C.-Y. (2013). OsELF3 is involved in circadian clock regulation for promoting flowering under long-day conditions in rice. Mol. Plant *6*, 202–215.

Yang, Y.-X., Wang, M.-M., Yin, Y.-L., Onac, E., Zhou, G.-F., Peng, S., Xia, X.-J., Shi, K.,

Yu, J.-Q., and Zhou, Y.-H. (2015b). RNA-seq analysis reveals the role of red light in resistance against Pseudomonas syringae pv. tomato DC3000 in tomato plants. BMC Genomics *16*, 120.

Yano, M., Katayose, Y., Ashikari, M., Yamanouchi, U., Monna, L., Fuse, T., Baba, T., Yamamoto, K., Umehara, Y., Nagamura, Y., et al. (2000). Hd1, a major photoperiod sensitivity quantitative trait locus in rice, is closely related to the Arabidopsis flowering time gene CONSTANS. Plant Cell *12*, 2473–2484.

Yant, L., Mathieu, J., Dinh, T.T., Ott, F., Lanz, C., Wollmann, H., Chen, X., and Schmid, M. (2010). Orchestration of the floral transition and floral development in Arabidopsis by the bifunctional transcription factor APETALA2. Plant Cell *22*, 2156–2170.

Yasumura, Y., Moylan, E.C., and Langdale, J.A. (2005). A conserved transcription factor mediates nuclear control of organelle biogenesis in anciently diverged land plants. Plant Cell *17*, 1894–1907.

Yon, F., Seo, P.-J., Ryu, J.Y., Park, C.-M., Baldwin, I.T., and Kim, S.-G. (2012). Identification and characterization of circadian clock genes in a native tobacco, Nicotiana attenuata. BMC Plant Biol. *12*, 172.

Yu, C.-P., Chen, S.C.-C., Chang, Y.-M., Liu, W.-Y., Lin, H.-H., Lin, J.-J., Chen, H.J., Lu, Y.-J., Wu, Y.-H., Lu, M.-Y.J., et al. (2015). Transcriptome dynamics of developing maize leaves and genomewide prediction of cis elements and their cognate transcription factors. Proc. Natl. Acad. Sci. U. S. A. *112*, E2477–E2486.

Yu, J.-W., Rubio, V., Lee, N.-Y., Bai, S., Lee, S.-Y., Kim, S.-S., Liu, L., Zhang, Y., Irigoyen, M.L., Sullivan, J.A., et al. (2008). COP1 and ELF3 control circadian function and photoperiodic flowering by regulating GI stability. Mol. Cell *32*, 617–630.

Yuan, Q., Saito, H., Okumoto, Y., Inoue, H., Nishida, H., Tsukiyama, T., Teraishi, M., and Tanisaka, T. (2009). Identification of a novel gene ef7 conferring an extremely long basic vegetative growth phase in rice. Theor. Appl. Genet. *119*, 675–684.

Zagotta, M.T., Hicks, K.A., Jacobs, C.I., Young, J.C., Hangarter, R.P., and Meeks-Wagner, D.R. (1996). The Arabidopsis ELF3 gene regulates vegetative photomorphogenesis and the photoperiodic induction of flowering. Plant J. *10*, 691–702.

Zakhrabekova, S., Gough, S.P., Braumann, I., Müller, A.H., Lundqvist, J., Ahmann, K., Dockter, C., Matyszczak, I., Kurowska, M., Druka, A., et al. (2012). Induced mutations in circadian clock regulator Mat-a facilitated short-season adaptation and range extension in cultivated barley. Proc. Natl. Acad. Sci. U. S. A. *109*, 4326–4331.

Zanoni, U., and Dudley, J.W. (1989). Comparison of Different Methods of Identifying Inbreds Useful for Improving Elite Maize Hybrids. Crop Sci. *29*, 577.

Zdepski, A., Wang, W., Priest, H.D., Ali, F., Alam, M., Mockler, T.C., and Michael, T.P. (2008). Conserved Daily Transcriptional Programs in Carica papaya. Trop. Plant Biol. *1*, 236–245.

Zhai, H., Lü, S., Wang, Y., Chen, X., Ren, H., Yang, J., Cheng, W., Zong, C., Gu, H., Qiu, H., et al. (2014). Allelic variations at four major maturity E genes and transcriptional abundance of the E1 gene are associated with flowering time and maturity of soybean cultivars. PLoS One *9*, e97636.

Zhang, C., Xie, Q., Anderson, R.G., Ng, G., Seitz, N.C., Peterson, T., McClung, C.R., McDowell, J.M., Kong, D., Kwak, J.M., et al. (2013). Crosstalk between the circadian clock and innate immunity in Arabidopsis. PLoS Pathog. *9*, e1003370.

Zhang, C., Gao, L., Sun, J., Jia, J., and Ren, Z. (2014). Haplotype variation of Green Revolution gene Rht-D1 during wheat domestication and improvement. J. Integr. Plant Biol. *56*, 774–780.

Zhang, X., Chen, Y., Wang, Z.-Y., Chen, Z., Gu, H., and Qu, L.-J. (2007). Constitutive expression of CIR1 (RVE2) affects several circadian-regulated processes and seed germination in Arabidopsis. Plant J. *51*, 512–525.

Zhao, J., Huang, X., Ouyang, X., Chen, W., Du, A., Zhu, L., Wang, S., Deng, X.W., and Li, S. (2012). OsELF3-1, an ortholog of Arabidopsis early flowering 3, regulates rice circadian rhythm and photoperiodic flowering. PLoS One *7*, e43705.

Zhong, H.H. (1998). Imbibition, but Not Release from Stratification, Sets the Circadian Clock in Arabidopsis Seedlings. PLANT CELL ONLINE *10*, 2005–2018.

von Zitzewitz, J., Szucs, P., Dubcovsky, J., Yan, L., Francia, E., Pecchioni, N., Casas, A., Chen, T.H.H., Hayes, P.M., and Skinner, J.S. (2005). Molecular and structural characterization of barley vernalization genes. Plant Mol. Biol. *59*, 449–467.

Zoltowski, B.D., and Imaizumi, T. (2014). Structure and Function of the ZTL/FKF1/LKP2 Group Proteins in Arabidopsis. Enzym. *35*, 213–239.

(2012). New grass phylogeny resolves deep evolutionary relationships and discovers C4 origins. New Phytol. *193*, 304–312.